

## University of Groningen

### Between adaptation and virulence

Palma Medina, Laura Marcela

**IMPORTANT NOTE: You are advised to consult the publisher's version (publisher's PDF) if you wish to cite from it. Please check the document version below.**

*Document Version*

Publisher's PDF, also known as Version of record

*Publication date:*

2019

[Link to publication in University of Groningen/UMCG research database](#)

*Citation for published version (APA):*

Palma Medina, L. M. (2019). *Between adaptation and virulence: A proteomics view on Staphylococcus aureus infections*. [Thesis fully internal (DIV), University of Groningen]. University of Groningen.

**Copyright**

Other than for strictly personal use, it is not permitted to download or to forward/distribute the text or part of it without the consent of the author(s) and/or copyright holder(s), unless the work is under an open content license (like Creative Commons).

The publication may also be distributed here under the terms of Article 25fa of the Dutch Copyright Act, indicated by the "Taverne" license. More information can be found on the University of Groningen website: <https://www.rug.nl/library/open-access/self-archiving-pure/taverne-amendment>.

**Take-down policy**

If you believe that this document breaches copyright please contact us providing details, and we will remove access to the work immediately and investigate your claim.

Downloaded from the University of Groningen/UMCG research database (Pure): <http://www.rug.nl/research/portal>. For technical reasons the number of authors shown on this cover page is limited to 10 maximum.

**Between adaptation and virulence:**

**A proteomics view on  
*Staphylococcus aureus*  
infections**

**LAURA MARCELA PALMA MEDINA**

The work described in this thesis was conducted at the Department of Medical Microbiology, University Medical Center Groningen, the Netherlands and at the Center for Functional Genomics of Microbes, University Medicine Greifswald, Germany.

The studies presented in this thesis were financially supported by the Graduate School of Medical Sciences of the University of Groningen and Deutsche Forschungsgemeinschaft Grant GRK1870.



The printing of this thesis was financially supported by the Graduate School of Medical Sciences, University of Groningen, University Medical Center Groningen, the Netherlands.

Printed by Ipskamp Printing, Enschede, the Netherlands

ISBN: 978-94-034-1824-7 (print)

ISBN: 978-94-034-1823-0 (digital)

Copyright © 2018 Laura Marcela Palma Medina.

All rights reserved. No part of this thesis may be reproduced, stored in a retrieval system, or transmitted in any form or by any means, without prior written permission of the author.



university of  
 groningen

UNIVERSITÄT GREIFSWALD  
Wissen lockt. Seit 1456



# **Between adaptation and virulence: A proteomics view on *Staphylococcus aureus* infections**

## **PhD Thesis**

to obtain the degree of PhD at the  
University of Groningen  
on the authority of the  
Rector Magnificus Prof. E. Sterken  
and in accordance with  
the decision by the College of Deans

and

to obtain the degree of PhD at the  
University of Greifswald

Double PhD degree

This thesis will be defended in public on

Monday 8 July 2019 at 11.00 hours

by

**Laura Marcela Palma Medina**

born on 27 September 1988  
in Ibagué, Colombia

**Supervisor(s):**

Prof. J.M. van Dijl  
Prof. U. Völker

**Assessment committee:**

Prof. F. Götz  
Prof. S. Hammerschmidt  
Prof. M. Heinemann  
Prof. O.P. Kuipers

**Paranymphs:**

Marines du Teil Espina  
Marina López Álvarez  
Elisa J.M. Raineri



*I can appreciate the beauty of a flower. At the same time, I see much more about the flower... I could imagine the cells in there, the complicated actions inside, which also have a beauty. I mean it's not just beauty at this dimension, at one centimeter; there's also beauty at smaller dimensions, the inner structure, also the processes... All kinds of interesting questions which the science, knowledge, only adds to the excitement, the mystery, and the awe of a flower.*

- Richard Feynman





# Table of Contents

---

## Chapter 1

Introduction and scope ..... 1

## Chapter 2

Metabolic cross-talk between human bronchial epithelial cells and internalized *Staphylococcus aureus* as a driver for infection ..... 45

## Chapter 3

Distinct adaptive responses of *Staphylococcus aureus* upon infection of bronchial epithelium during different stages of regeneration..... 91

## Chapter 4

Signatures of cytoplasmic proteins in the exoproteome distinguish community and hospital-associated methicillin-resistant *Staphylococcus aureus* USA300 lineages. 125

## Chapter 5

Metabolic niche adaptation of community- and hospital-associated methicillin-resistant *Staphylococcus aureus*..... 165

## Chapter 6

Summary and future perspectives ..... 191

## Chapter 7

Nederlandse samenvatting ..... 201

Appendices ..... 213

---



# Chapter 1

## **Introduction and scope**

---



## Why studying bacterial pathogenesis?

The presence of microorganisms that live in the human body has been acknowledged since the end of the 19<sup>th</sup> century. Nonetheless, it has been only from the beginning of the 21<sup>st</sup> century that efforts to expand our knowledge about the microbiota have gained higher priority, a development that has been enabled by technological advances in genome sequencing. The communities of microorganisms inhabiting our bodies, as well as the bodies of other multicellular organisms, comprise a multitude bacterial species, fungi, parasites, and viruses which, importantly, have evolved together with us. Consequently, the resulting commensal and symbiotic relationships have had an influence on the development and functioning of host systems, like the gastro-intestinal tract or the immune system. However, even though most of these microorganisms are commensals, or have mutualistic relationships with the host, some of them can cause disease under certain conditions.

Disease-causing microorganisms are often transmittable and therefore do not only have an impact on one individual but can potentially affect whole communities. Therefore, diminishing the impact and prevalence of such pathogens is of utmost importance. In this regard, understanding the molecular mechanisms that allow microorganisms to adapt to and harm the host would shed light on potential opportunities to develop treatments.

In particular, opportunistic bacterial pathogens like *Staphylococcus aureus* have evolved features that increase their chances of survival and spreading, while being challenged by the host immune system or antibiotic therapies. These bacterial adaptations are not only geared towards the production of molecules that have a negative impact on the host, but also to hiding from our immune defenses, granting access to scarce resources or optimizing their use. Consequently, *S. aureus*

evolved into a pathogen that is renowned for its virulence and high capacity to develop resistance to physical and chemical insults. For this reason, most research on *S. aureus* has been focused on the mechanisms this bacterium employs for infection and antibiotic resistance. In contrast, relatively little is known about its role as a commensal (1). Gaps of knowledge in this area are mainly related to the great flexibility of *S. aureus* to adapt, genetically or metabolically, to the many distinct niches in the human body. Of note, although the adaptations that *S. aureus* displays under limiting conditions have been widely studied *in vitro*, its adaptive behavior *in vivo* received relatively little attention. This relates to the fact that the conditions to which the bacteria need to respond *in vivo* are complex and frequently changing. This makes the pathogen's responses equally complex and dynamic, reflecting the continuous communication between host and pathogen. Understanding and perhaps being able to predict the course of these dynamic interactions is not only an intriguing scientific challenge, but also a necessity for the development of new and more sustainable antimicrobial therapies.

## *Staphylococcus aureus*

*S. aureus* is a Gram-positive and facultative anaerobic bacterium commonly found as a human commensal in the anterior nares, throat, and on the skin (2). Although this bacterium is part of our microbiota, it is better known for being the causative agent of several diseases ranging from mild skin infections or food poisoning, to life-threatening conditions, like sepsis or necrotizing pneumonia. More importantly, its capability to swiftly develop resistances to antibiotics makes this bacterium a public health threat in the community, as well as in hospitals (3).

The first report on *S. aureus* dates back to 1880, when the surgeon Sir Alexander Ogston observed the presence of spherical microorganisms while studying purulent infections. His illustrations depict cocci that grew in clusters, looking like "roe of fish". This observation led him to subsequently coin the name

*Staphylococcus* for this microorganism (4). However, it was not until 1884 that Friedrich Julius Rosenbach distinguished *S. aureus* from the closely related *Staphylococcus epidermidis*, based on the golden color of its colonies (hence the term *aureus*). *S. epidermidis*, on the other hand, was temporarily called *albus*, due to the white color of its colonies (5).

The outstanding capability of *S. aureus* to develop resistances against antibiotics was noticed promptly after their introduction as a common treatment of infections. During the first half of the 20<sup>th</sup> century, in fact, *S. aureus* infections were still considered highly fatal. It was only around 1940 that these infections started to be treated with penicillin, reducing the mortality rates. However, *S. aureus* isolates that developed resistance to this antibiotic were noticed shortly after the discovery of penicillin (6), and within a few years, penicillin resistant lineages had emerged in the clinic (7). Later on, methicillin was introduced as treatment for staphylococcal infection, but resistant strains (all defined as methicillin resistant *Staphylococcus aureus*, or MRSA) emerged already in 1961, only one year after its introduction (8). During the 1970s and 1980s there were several MRSA outbreaks worldwide, but these were limited to hospital settings (9). In response to the increasing incidence of MRSA infections, vancomycin started to become more frequently used, leading to the appearance of strains that were tolerant to this antibiotic in 1997 (10).

Nowadays, as penicillin resistance is commonly found in *S. aureus* strains, methicillin and related  $\beta$ -lactam antibiotics have been used as the recommended treatment for infections caused by this bacterium. Consequently, the worldwide incidence of MRSA has increased over time and many countries have reported a prevalence of methicillin resistance in 50% or more of the clinical *S. aureus* isolates (11, 12). Of note, the high capability to develop resistance to antibiotics is common among *Staphylococcus* species, but none of these is equally aggressive as *S. aureus*,



which makes MRSA a major concern for our health and wellbeing (13). Congruently, infections caused by resistant *S. aureus* lead to higher morbidity and mortality rates (3, 14).

*S. aureus* is capable of acquiring resistance to antibiotics through several processes, which include mutations in the core genome, as well as the acquisition of exogenous resistance genes carried by plasmids and other mobile genetic elements. These mechanisms started to become better understood after publication of the first whole genome sequences of two isolates of this bacterium in 2001 (15). Specifically, the latter study was carried out using two MRSA isolates, N315 and Mu50, thereby unveiling the genetic background of staphylococcal resistance, as well as the major role of horizontal gene transfer in spreading resistance between staphylococci. Importantly, this study also represents the first report on the presence of multiple virulence genes in this bacterium.

Although *S. aureus* is generally acknowledged for its role as a pathogen, carriage of this bacterium is generally asymptomatic. The 'harmless' commensal state of *S. aureus* was acknowledged in the mid-1940's, when the nose was identified as its most common niche (16). In fact, approximately 20% of the human population can be classified as recurrent carriers, while another 30% are regarded as temporal carriers of *S. aureus* in the anterior nares (17, 18). The carriers were shown to be more prone to develop nosocomial infections caused by *S. aureus*, and it has actually been reported that 80% of bacteremia cases are caused by the endogenous strain of the patient (19, 20). Of note, carriers not only have a higher risk of *S. aureus* infection, but they also transmit *S. aureus* to other individuals in the population (21). In the last 20 years, MRSA strains have adapted to spread among the community, causing infections in healthy individuals and displaying a more virulent behavior. Since *S. aureus* represents a general and serious threat for the human population, efforts have been undertaken to develop vaccines against this

pathogen but, unfortunately, none of the tested candidates has so far passed the stage of clinical trials (22, 23).

## Epidemiology

The aforementioned capability of *S. aureus* to develop resistance to antibiotics has enabled this bacterium to prevail in the population and to spread around the world in the 'antibiotic era', turning this bacterium into one of the major public-health threats. One of the first documented drug-resistant lineages that have rapidly spread to different countries was the strain 80/81. The pandemic caused by this clone lasted from 1954 to 1957, starting in Australia and expanding to several countries, including the USA and the UK, where this clone was responsible for several outbreaks (24). At that time, the incidence of *S. aureus*-caused infections was 3 per 100.000 person-years but increased to approximately 20 per 100.000 person-years during the next 30 years. This rise has been attributed to nosocomial infections, acquired after invasive medical interventions. Nowadays, the rate of *S. aureus* infections appears to be stable, but the actual incidence varies over time and is dependent on geographical location. Of note, less affluent regions of the world exhibit higher rates of the infections caused by *S. aureus* than the wealthier regions (25).

Today, MRSA is one of the most commonly identified pathogens around the globe including America, Europe, North Africa, and the Middle east (24). Infections caused by MRSA strains are no longer restricted to hospital settings and even healthy individuals are at risk of developing an infection. Of note, some individuals within the human population are particularly susceptible to develop *S. aureus* bacteremia, including babies within the first year of life, adults over 70 years old, HIV- infected individuals, intravenous drug users, and hemodialysis patients (25).

Especially since the emergence of community-associated (CA) MRSA strains, the burden of *S. aureus* infections has risen in many countries (21, 26). The first report on CA *S. aureus* came from Australia in the early 1990's, concerning patients from a remote population who had limited access to large hospitals (27). By the end of the same decade, the first CA strain from the US was isolated from healthy children that did not exhibit the commonly known risk factors (28). Subsequently, CA-MRSA has been reported to spread in very diverse communities including native Americans, islanders in the Pacific, athletes, prisoners, military personnel and individuals in day care centers (21).

Since their very first discovery, CA-MRSA isolates displayed a more virulent behavior than the HA-MRSA isolates (29, 30). In particular, CA *S. aureus* has a high capacity to produce sepsis and fatal infections like necrotizing pneumonia, purpura fulminans and post-viral Toxic Shock Syndrome (TSS). HA-MRSA is more commonly associated with respiratory infections, while CA-MRSA, on the other hand, is more often associated with skin and soft tissue infections. Enhanced virulence has been linked to the capacity of CA-MRSA lineages to kill neutrophils more rapidly and, therefore, neutralize this first line of immune defense (31–33). This also explains the more pronounced inflammation and tissue damage that are usually associated with infections caused by CA strains (34).

Identification of the virulence factors that are most representative for each group and the differences in their virulence potential is still a matter of debate. It has been suggested, however, that toxins like the Phenol-soluble Modulins (PSMs) or LukSF (produced by the Pantone-Valentine leukocidin [PVL] genes) are responsible for the increased virulence of CA-MRSA (31, 35, 36). One of the strongest arguments for this hypothesis is the higher prevalence of the PVL genes in most of the CA isolates compared to HA isolates (29, 37). Nevertheless, conflicting results regarding the real contribution of PVL to either the fitness or virulence of CA-

MRSA isolates have led to the hypothesis that additional factors may contribute to the CA phenotype.

The discrimination between HA- and CA-MRSA infections has conventionally been based on the time span between admission of a patient into a healthcare institution and the detection of a MRSA-positive culture. In general, a pathogen is considered CA if it is detected within the first 48 h after a patient's admission to a healthcare institution and if this patient has not been hospitalized within the two years prior to the detection of this patient's MRSA carriage. If it is detected after 48 h of hospitalization, the pathogen is labeled as HA. In special cases, where a patient presents particular risk factors associated to health care centers, the causative infectious agent is considered HA community onset, even if the infection is detected during the first 48 h after admission. Nonetheless, molecular characterization of HA- and CA-MRSA isolates has shown that the two groups are no longer restricted to their original locations, but rather they are migrating from the hospital into the community and *vice versa*. In consequence, the preferred characterization of clinical isolates should not only take into account clinical data, but also a molecular characterization (38).

## Molecular typing

In order to grasp the genetic variability of *S. aureus*, different methods for classification of strains have been implemented over time. These methodologies have expanded our understanding of the evolution of *S. aureus*, the spreading of this bacterium worldwide and the association of different pathologies with different genetic backgrounds. There are several classical methods to classify the different strains of *S. aureus*: two gel-based methods: Pulsed-Field Gel Electrophoresis (PFGE) and Multiple-Locus Variable Number Tandem Repeat Fingerprinting (MLVF), and three sequence-based: *spa* typing, Multilocus Sequence Typing (MLST), and multiple-locus variable-number tandem-repeat

analysis (MLVA; [Sabat et al., 2012](#)). Another method, SCC*mec* typing, is utilized only for classification of MRSA strains (12, 40). However, advancements in sequencing technologies have increased their availability in hospital settings, and currently whole-genome sequencing emerges as an efficient method for epidemiological identification of *S. aureus* isolates (41, 42).

PFGE has been one of the most frequently used methods for characterization of isolates during outbreaks. This gel-based typing method compares isolates based on their banding pattern after digestion of genomic DNA with the restriction enzyme SmaI and separation of the resulting fragments on agarose gels with alternating current directions (43). Although commonly used, this method is labor-intensive and achieving good reproducibility between laboratories is challenging (44). Strains classified by this method are clustered by 80% of similarity and the resulting clusters are designated "USA" according to the Centers for Disease Control and Prevention guidelines (45). The second gel-based typing method, MLVF, is particularly useful in a local setting but, like PFGE, it doesn't produce data that are portable among laboratories. The MLVF technique is based on the gel banding pattern of PCR fragments derived from five staphylococcal variable number tandem repeat loci (*sdrCDE*, *clfA*, *clfB*, *sspA*, and *spa*). Unfortunately, it is not possible to relate the respective DNA banding patterns to the number of repeats per locus (46).

MLST is a sequence-based technique where single nucleotide variations in seven housekeeping genes (*pta*, *tpi*, *yqiL*, *acrC*, *aroE*, *glpF*, *gmk*) are examined. The allelic variation in each locus is used to designate a sequence type (ST) to the investigated strains (47). Although this method is relatively expensive and labor-intensive, its main advantage lies in its good reproducibility and the portability of data between laboratories using an online database for comparisons (48). Up until very recently, MLST has been the most commonly used method to assess

evolutionary relationships between *S. aureus* lineages. In particular, isolates that show identity in 5 out of the 7 sequenced genes are clustered in so-called clonal complexes (49). MLST classification is often paired with SCC*mec* typing for a more refined identification of MRSA isolates (48). *Spa* typing is also based on sequence analysis of variable number tandem repeats, but in this case only the *spa* gene is targeted. *Spa* typing is widely used due to its low cost and higher discriminatory power compared to MLST (48). Moreover, this typing technique does not only take into account the number of repeat variations, but also point mutations found within the *spa* gene (50). MLVA was developed to overcome limitations of PFGE, MLST, and *spa* typing. It is as discriminatory as PFGE and produces portable data that can be readily interpreted, similar to data obtained by MLST and *spa* typing.

SCC*mec* typing is a technique used to differentiate MRSA isolates based on the Staphylococcal Cassette Chromosome *mec*, which carries the *mecA* gene, its regulator genes, and the so-called *ccr* recombinase genes. Importantly, the *mecA* gene is responsible for the methicillin resistance by encoding an additional penicillin-binding protein (PBP2A) that does not bind  $\beta$ -lactam antibiotics (Katayama et al., 2000). Currently, at least 7 types of SCC*mec* (I to VII) can be differentiated by the respective combinations of *mec* and *ccr* genes and additional resistance genes (24, 51).

All the afore-mentioned typing methods have proven to be useful for the identification and distinction of *S. aureus* isolates. However, most clinically relevant isolates of *S. aureus* belong to a limited number of lineages, and often the classical typing methods are not sufficient for detailed differentiation (52). Moreover, these techniques are laborious and time-consuming. Consequently, whole-genome sequencing is becoming increasingly popular for rapid identification and characterization of pathogens in clinical settings. Although sequencing of 16S rRNA genes has been widely used for the assignment of

bacterial isolates to pathogen species, it does not provide further details on the specific nature of the investigated microorganism. Therefore, the characterization of clinical isolates of *S. aureus* nowadays involves whole-genome sequencing. In recent years, the availability of this method in clinical microbiology laboratories has rapidly increased. Nonetheless, so far there is no standard methodology for sample preparation and sequence data analysis, which poses a great challenge for the implementation of this method in routine clinical diagnostics (53, 54).

## The 'toolbox' of *S. aureus* for infection

### Virulence factors

The virulence potential of *S. aureus* is mostly determined by its capability to produce proteinaceous and non-proteinaceous molecules that help this pathogen to colonize and invade host tissues, get access to the host's resources, or hide from the immune response of the host. These virulence factors disturb the normal function of host cells and may severely affect the host organism. Additionally, some virulence factors are responsible for triggering specific and sometimes excessive immune responses. In general, virulence factors can be distinguished by their subcellular or extracellular localization. Proteins that are linked to the surface of the pathogen are mostly involved in adhesion to extracellular matrixes or binding to other host molecules, while secreted proteins target the host's primary barriers, disrupt cell membranes and neutralize, modulate or allow to evade immune cells (55, 56).

### *Surface virulence factors*

Proteins that are anchored to the cell wall of *S. aureus* can be classified into 4 classes of proteins based on their structure, namely: i, the microbial surface components recognizing adhesive matrix molecules (MSCRAMMs); ii, the near iron transporter (NEAT) motif family; iii, the G5-E bundle family; and iv, the

three-helical bundle family. Regardless of their classification, all these proteins have a secretory signal peptide at the N-terminus and a sorting signal peptide at their C-terminus (57). These proteins can be regarded as genuine virulence factors, since mutant strains defective in any of these cell wall-associated proteins were shown to be attenuated in infection models, or cause decreased bacterial loads (58–61). Alternatively, they were shown to promote nasal colonization (62–64).

The MSCRAMMs form the largest group of surface proteins in *S. aureus*. They are characterized by the presence of two IgG-fold domains close to their N-terminus. In general, these proteins help the bacteria to colonize host tissues by attaching them to molecules from the host's extracellular matrix, like collagen, fibronectin, or fibrinogen (65). The MSCRAMMs thus include fibronectin-binding proteins A and B (FnbpAB), clumping factors A and B (ClfAB), a collagen-binding protein (Cna), and the Serine-aspartate repeat-containing proteins C, D, and E (SdrC, SdrD and SdrE). Moreover, some MSCRAMMs have secondary functions as exemplified by Fnbps which supports biofilm formation in some *S. aureus* strains (McCourt et al., 2014), or ClfA and Cna which can bind to complement factors thereby interfering with the complement system (66, 67). Importantly, the Fnbps are key for the internalization process into non-professional phagocytic cells, as they bind to the fibronectin located on the host cell membranes and trigger the signal for endocytic uptake (68).

The iron-regulated surface determinant proteins (IsdA, IsdB, IsdC, and IsdH) are part of the NEAT motif family. These proteins are renowned for their role in iron acquisition. Similar to other surface-associated proteins, they also bind to fibronectin and fibrinogen and, therefore, they participate in the internalization process by non-professional phagocytes (69). Nevertheless, being key components of the iron uptake pathway, they play a pivotal role in intracellular survival (70,



71). Lastly, the IsdABCH proteins are involved in immune evasion, but the molecular mechanisms to achieve this are still unclear (63, 72).

In *S. aureus*, the G5-E repeat ‘family’ consists only of the surface protein G (SasG), which is present only in a subset of *S. aureus* isolates. This protein plays a main role in adhesion to the nasal epithelium and has been associated with biofilm formation. Nevertheless, neither the respective molecular mechanisms, nor the ligands of this protein have been identified so far (57, 73).

Lastly, the Staphylococcal protein A (Spa) has three helical bundles in its N-terminal region that have affinity for the Fc part of immunoglobulins, especially IgG. Thus, Spa protects *S. aureus* from opsonization and, consequently, limits phagocytosis by cells of the host’s immune system (74, 75). In addition to its role in immune evasion, Spa also shows affinity to the tumor necrosis factor receptor 1 (TNFR1). This leads to increased production and release of cytokines and recruitment of polymorphonuclear leukocytes (PMNs). Therefore, Spa also acts as a pro-inflammatory molecule that increases tissue damage during the infection process (76, 77).

In addition to the proteins that are anchored to the surface of the bacterium the capsule of *S. aureus* is also a potent virulence factor, due to its role as a bacterial defense mechanism against the host immune responses. In particular, the capsule inhibits recognition of the bacteria by phagocytic cells and therefore prevents phagocytosis and killing by the immune system. The gene clusters involved in production of capsule polysaccharides are prevalent in 90% of the *S. aureus* isolates with types 5 and 8 being present in most of the clinical isolates (78).

### *Secreted virulence factors*

*S. aureus* produces several virulence factors that are released into the extracellular milieu. In general, these factors are involved in the evasion of and interference

with the host immune system or cause direct damage to host cells and tissues. Secreted proteins that play a role in adhesion or immune evasion apply similar modes of action as the afore-mentioned surface proteins. In particular, the fibrinogen-binding protein (Efb) and staphylococcal coagulase (Coa) bind to fibrinogen to protect the bacteria from phagocytosis and to start the coagulation cascade, respectively (79). Other secreted *S. aureus* proteins like the immunoglobulin G (IgG)-binding protein (Sbi), the staphylococcal complement inhibitor (SCIN), the chemotaxis inhibitory protein of staphylococci (CHIPS), and a variety of superantigens (SAg) modulate immune responses. Sbi is a protein that works similar to Spa and, accordingly, it prevents opsonization and has a proinflammatory effect (80). The SCIN and CHIPS proteins are encoded by the same gene cluster and both have a major impact on the activity of the complement system, which is part of the host's innate immune system. While SCIN binds to the C3 convertase and prevents activation of the complement system, CHIPS binds to the neutrophil receptors that are related to chemotaxis (81–83).

Contrary to the secreted proteins that serve to evade or attenuate the host's immune system, the main function of SAGs is to trigger stronger immune reactions. These proteins, including the toxic shock syndrome toxin-1 (TSST-1), activate and stimulate T-cells leading to their proliferation, excessive cytokine production and ultimately to host cell death (84). The SAGs were initially mostly linked to food poisoning (85), but subsequent research demonstrated their role in the development of infectious endocarditis, dermatitis, necrotizing pneumonia and kidney abscesses (86–88).

Besides proteins that manipulate the immune system, other secreted proteins from *S. aureus* induce lysis of host cells, enable the destruction of tissue and spreading of the bacteria to other tissues. Many of these secreted toxins are known as pore-forming toxins.

$\alpha$ -Hemolysin (Hla) is one of the major virulence factors of *S. aureus*. This pore-forming and pro-inflammatory protein is mainly regulated by the accessory gene regulator (Agr) quorum-sensing system, and contributes to abscess formation during skin infection in animal models (31, 89). Hla interacts with A Disintegrin and Metalloprotease 10 (ADAM10), which is indispensable for the structural modifications of Hla that lead to the formation of a cytolytic pore in the host cell's membrane (90). In addition to this mechanism of host cell lysis, Hla also potentiates the natural cleavage function of ADAM10 towards membrane proteins like e-cadherin, thereby promoting the disruption of tight junctions (89).

Other relevant staphylococcal pore forming proteins are the bicomponent leukotoxins, namely gamma hemolysin (Hlg), leukocidins (Luk)AB (or LukGH), LukED, and the afore-mentioned leukocidin PVL (LukSF). The lysis process caused by these toxins is host-receptor dependent, specifically involving integrin, C5aR1 or CD45 receptors (91–93). Studies have shown that LukAB and LukED play a major role in murine sepsis and renal abscess models (94, 95). Importantly, LukAB contributes to the lysis of PMNs after the pathogen has been phagocytized (91). LukSF, on the other hand, has been proposed to influence other host processes, like mitochondrial functions, leading to the induction of apoptosis (96). Nonetheless, the precise roles of this protein remain to be clarified.

Several studies that compared the impact of PVL proteins, using wild-type *S. aureus* strains and isogenic mutants, showed no significant differences in virulence, neutrophil survival or cytotoxicity in human epithelial cells (Summarized by David and Daum, 2010). Nevertheless, recent studies have highlighted some variables that have not been considered previously and that could explain the mixed results obtained while studying the impact of PVL on virulence. Although all *lukSF* genes are very similar, there is a distinctive substitution at the nucleotide 527 that distinguishes two variants of the PVL

protein termed R and H. These two variants show different geographical distribution and are distinctively associated to CA- or HA-MRSA (97–99). Moreover, the effects of PVL vary in a host-specific manner, and they have different affinity for particular targets depending on the infected organ. In this regard, it is noteworthy that PVL displays high specificity to human and rabbit neutrophils, while their affinity for the respective receptors in murine and monkey neutrophils is low. Therefore, mice are not an appropriate model to measure the impact of PVL on virulence (100). In this regard, there may actually be more variables to consider, such as the diversity in expression rates in different staphylococcal isolates and host systems (101).

The PSM proteins represent another class of cytolytic toxins produced by bacteria of the *Staphylococcus* genus, including *S. aureus* and *S. epidermidis* (102). Although these proteins are not exclusive to these species, only strains capable of colonizing epithelial surfaces produce them, indicating an evolutionary connection to the colonization site. In particular, *S. aureus* produces seven PSMs: four PSM $\alpha$ , two PSM $\beta$  and one PSM $\delta$  (delta hemolysin). All these peptides have a similar structure and amphiphilic nature, but not all are as effective as virulence factors. In this respect, virulent strains commonly produce higher amounts of PSM $\alpha$  peptides and lower amounts of PSM $\beta$  peptides (36). Of note, PSMs have potent surfactant properties and, accordingly, they have been implicated in staphylococcal spreading over wet surfaces (103).

The importance of PSMs in virulence is linked to their different roles in the host-pathogen interaction. First, they are capable of disrupting host cells by membrane perturbation in a receptor-independent manner. This independence of host receptor proteins makes them relevant in a broad spectrum of diseases (104). Secondly, they trigger inflammatory responses like chemotaxis and priming of neutrophils, and they induce cytokine expression by interaction with the formyl

peptide receptor 2 (FPR2; Kretschmer et al., 2010). Interestingly, this interaction is inhibited by the *S. aureus*-protein FPR2/ALS-inhibitory protein (FLIPr), thereby modulating the host's immune response (106). Thirdly, PSMs take part in shaping the biofilm structure and bacterial detachment from the biofilm, resulting in dissemination and bacterial spreading during infection. Due to their amphiphilic nature, these proteins are capable of opening channels, which allows the diffusion of nutrients into deeper layers of the biofilm. Since excess production of PSMs leads to detachment of the biofilm structure, their production is tightly regulated and varies within a biofilm (107, 108). Lastly, the production of PSM $\alpha$  has been recently linked to excretion of cytoplasmic proteins by inducing damage of the bacterial membrane. This disruption event is not specific for trafficking of proteins, but also prompts the release of other molecules as lipids and ATP into the extracellular milieu (109). Importantly, secretion of cytoplasmic proteins has been proposed as a potential virulence mechanism employed by numerous bacterial species, including *S. aureus* (110, 111).

In summary, *S. aureus* produces a wide range of proteins that are actively involved in the interactions between the pathogen and its host, and that are required for growth, propagation and survival of the pathogen during infection. These different virulence factors that are located at the cell surface or are secreted, modulate the environmental cues in an infection setting to favor different outcomes. Since these proteins affect directly the responses of the host, they are tightly regulated by the pathogen.

## Regulators

The adaptability of *S. aureus* to different environments is not only a consequence of its genetic variability and capability to acquire exogenous DNA, but its ability to respond appropriately to chemical and physical stimuli is also highly relevant

for the management of available resources. When it comes to the adaptation to different niches, the bacteria must optimize the consumption of the available nutrients, balancing the production of proteins that are required for survival and fitness (112). During an infection setting, these adaptations will include the production of virulence factors to access the limiting amounts of nutrients, but also activation of pathways to optimally use them. These changes in gene expression are coordinated by a network of regulators that is tightly interconnected (113). Some of the respective regulators directly control the production of virulence factors, while others are indirectly related to virulence by controlling central metabolic pathways.

One of the key challenges that *S. aureus* has to face during infection or colonization is the variable abundance of resources, like carbon and oxygen, which affects the central carbon metabolism and therefore the provision of energy and metabolic precursors (114). The main regulators that are involved in adaptation to conditions with restrictive resources are the catabolite control protein A (CcpA), catabolite control protein E (CcpE) and the GTP-sensing pleiotropic repressor CodY. All of these regulators control the transcription of genes that encode proteins to optimize energy production from alternative sources. In resource-rich environments, these regulators will prevent excessive energy consumption for unnecessary tasks (112).

The activity of CcpA is modulated by the availability of diverse compounds including simple sugars, disaccharides or alcoholic derivatives of them (115). CcpA binds to DNA sequences denominated catalytic responsive elements (CRE), which are located upstream of its target genes. Although it has been determined that CcpA has a low intrinsic affinity to CRE, its affinity is enhanced by the corepressor histidine-containing protein (HPr) in the phosphorylated state (116, 117). This corepressor is an indicator of the availability of carbon sources, because its phosphorylation state depends on the abundance of glycolytic intermediates

(115). Besides its regulatory role in the expression of genes involved in the catabolism of alternative carbon sources, CcpA also has a direct effect on virulence by controlling the expression of Hla, Spa, and TSST-1 (118, 119). Another direct regulator of central carbon metabolism is CcpE, whose activity is modulated by the presence of citrate. CcpE is a positive regulator of the expression of genes encoding proteins involved in the TCA cycle, and it also has been shown that its inactivation enhances bacterial virulence (120, 121).

A third metabolic regulator, CodY, is mainly required for the activation of the TCA cycle, but it also regulates the expression of genes for proteins involved in amino acid biosynthesis (112). The cofactors of this regulator are guanosine-5'-triphosphate (GTP) and the branched-chain amino acids (BCAAs), which increase the affinity of CodY for its target sequences. A low abundance of GTP signals stress conditions or nutrient deprivation (112, 122), while the abundance of BCAAs in the extracellular milieu serves as an indicator for the availability of carbon, nitrogen and sulfur. Diminished quantities of these cofactors trigger the derepression of CodY-regulated genes involved in alternative energy-generating pathways (123, 124). Interestingly, CodY mutants do not only increase the production of enzymes related to biosynthesis and transport of amino acids and other nutrients, but also lead to increased production of virulence factors or proteins used to adequately respond to stress conditions. In this regard, some genes encoding virulence factors, like *hla* or *capA*, have been found to be directly regulated by CodY, but this regulator indirectly affects the expression of more virulence factors by repressing Agr (125, 126).

The afore-mentioned regulators mainly respond to the availability of carbon or nitrogen sources. However, basic cellular functions are also affected by the availability of oxygen. This molecule is, in fact, the main electron acceptor during aerobic respiration, and without it, *S. aureus* is forced to use alternative metabolic

pathways like fermentation. One of the first effects of a lack of oxygen is a disbalance in the redox state of the cell which, in turn, triggers the major regulator redox-dependent transcriptional repressor (Rex) (112). This protein senses the NADH/NAD<sup>+</sup> ratio by binding either of these two molecules and regulating the expression of several proteins that play a role in maintaining the redox state. Rex-NADH derepresses the synthesis of proteins from the fermentative pathway, electron transport chain, anaerobic metabolism and regulators of nitrogen metabolism, including the two-component regulatory system SrrAB (127). Additional to the regulation by Rex, the SrrAB system also responds to the levels of oxygen and nitric oxide in the environment, sensing the reduction of menaquinone (128). The genes regulated by this system are related to cytochrome assembly, anaerobic metabolism, iron-sulfur cluster repair and NO detoxification (129).

As described above, the metabolic changes caused by nutrient scarcity lead to changes in the expression of virulence factors. This is mainly connected to the regulation of the Agr system, which has been by far the most studied regulatory system involved in staphylococcal virulence (112, 125). This quorum-sensing system is simultaneously regulated by at least 15 other proteins, among them the afore-mentioned CcpA, CodY and SrrAB regulators (126). The Agr system comprises two loci that are transcribed from two divergent promoters. The P2 promoter is located upstream of the *agrA*, *agrB*, *agrC* and *agrD* genes encoding the Agr system. AgrA is a transcriptional regulator that binds to cognate promoter regions and modulates their activity. This binding is dependent on AgrA phosphorylation, which is carried out by AgrC, a membrane protein stimulated by the abundance of the auto-inducing peptide (AIP) in the extracellular environment. AgrD is the precursor of the AIP, which is processed by the membrane protein AgrB. On the other hand, the P3 promoter regulates the expression of Hld, a virulence factor, and RNAIII, a small regulatory RNA



molecule that serves as one of the major regulators of *S. aureus* (130, 131). Currently, more than 174 genes are known to be regulated by Agr, and expression of at least 60 of them is modulated by RNAIII. Upregulation of the Agr system leads to high-level production of toxins like PSMs, Hla, LukSF and LukDE, and reductions in the level of surface proteins like Spa (128). Since Agr regulates most of the known virulence factor genes, it is essential for virulence. This has been corroborated by the generation of mutants of this system and verified in different infection models (132–136). Through the regulation of Agr by metabolic regulators like CcpA, CodY and SrrAB, the production of virulence factors is connected to the environment of *S. aureus*. On top of this, Agr expression is also modulated by additional transcriptional regulatory systems, such as the staphylococcal accessory regulator SarA and alternative sigma factor SigB.

SarA belongs to the SarA family of regulatory proteins, comprising 11 proteins that, notably, are also related to the regulation of the Agr system. In particular, the SarA protein plays an important role in its activation during early stages of bacterial growth (137). Nonetheless, the connection of SarA to the production of virulence factors is not only due to its positive effect on Agr, but it also serves to activate the expression of fibronectin-binding proteins, all hemolysins, and TSST-1 (128, 138–140). Interestingly, SarA also negatively influences the levels of other proteins related to virulence and fitness, like Spa, IsaB, proteases, and the superoxide dismutases (141–143). Thus, SarA is also a principal regulator of virulence, as was demonstrated through the use of mutants in infection models (144–146). The *sarA* gene is controlled by three promoters that are recognized by the sigma factors SigA and SigB (139), and negatively regulated by SarA and SarR, another protein belonging to the same family (147, 148).

Sigma factors are the initiation factors that define the specific binding of RNA polymerase to particular promoters. SigB is an alternative sigma factor which

responds to environmental cues. Its relevance for virulence is underpinned by its influence on the Agr and SarA regulatory systems. Further, the *sigB* gene is part of an operon that also encodes several Rsb proteins responsible for the regulation of SigB activity (Rsb, regulation of sigma B). In brief, the RsbW protein binds SigB under non-stress conditions, thereby preventing its association with target promoters. At the same time RsbW is a kinase that phosphorylates and thereby inactivates its antagonist protein RsbV. Under appropriate stress conditions, the phosphatase RsbU dephosphorylates RsbV, which then binds RsbW, concomitantly releasing SigB from its inhibition by RsbW. The liberated SigB is then able to bind to RNA polymerase and stimulate transcription of SigB-dependent genes (149). Stressful conditions that activate this regulator in shake flask cultures *in vitro* are heat shock and alkaline stress, but also the transition of *S. aureus* into the stationary phase. SigB influences expression of around 200 genes that encode proteins involved in membrane transport, biofilm formation, cell internalization, persistence and virulence (150). Importantly, SigB is also required for intracellular replication and the intracellular persistence of so-called small colony variants of *S. aureus* (SCVs; Pfortner et al., 2014; Tuchscherer et al., 2015).

So far, the complex regulatory network of *S. aureus* has mostly been studied in parts, elucidating the target genes of each known regulator and the influence of different environmental conditions on their expression. Many genes are not regulated by a single regulator but, instead, they are influenced by several of them. Importantly, the specific combination of conditions encountered during the infectious process could promote different interactions between the different nodes of the regulatory network, giving rise to specific *S. aureus* phenotypes that are advantageous to this bacterium. Therefore, it is imperative to study the expression level of bacterial proteins during colonization or infection in a comprehensive manner, taking into account the different regulatory events, in

order to expand our understanding of the contribution of these systems to human health and disease.

## *S. aureus and the host epithelium*

During the course of an infection, *S. aureus* encounters several challenges posed by the host's primary defenses. This network of pathways, cells, and effector molecules may protect the host from reinfection by invasive pathogens and prevent the development of diseases. One of the first lines in the host defense consists of a tight membrane of cells that acts as a physical barrier, preventing the invasion of the pathogen into deeper-seated tissues, and triggering the recruitment of components of the second line of defense, the innate immune system. Although the innate immune system comprises several types of cells, each with a specific function, altogether they adopt a few key strategies to deal with an invasive pathogen. These strategies include phagocytosis, production of antimicrobial peptides, and production or induction of the complement system. The interactions between the pathogen and different cells of the human body are dependent on the nature of the respective host cells and they are highly dynamic. In fact, the continuous communication between a host cell and an infective agent will determine the outcome of an infection.

One immune evasion mechanism of *S. aureus* consists of using the interior compartments of host cells as temporary hideouts that will prevent direct encounters with immune system effectors. Initially, it was thought that *S. aureus* was only capable of internalizing into phagocytic cells, like neutrophils (153). Nonetheless, recent evidence shows that *S. aureus* can be internalized also by non-professional phagocytic cells, where it can persist for long periods of time (152, 154, 155). After *S. aureus* engages non-phagocytic cells through the binding of Fnbp to fibronectin on the host cell surface, the pathogen will activate, through

different mechanisms, the phagocytic pathway. Initially the bacterium will reside inside an endosome, which needs to fuse with a lysosome to kill and degrade the internalized bacterium thanks to the presence of antimicrobial peptides, acidification of the compartment, production of reactive oxygen species, and the presence of highly potent degradative enzymes. Nonetheless, *S. aureus* is capable of manipulating this process, thereby avoiding clearance. In this regard, this pathogen can initiate the autophagocytic pathway, in which it will be encapsulated by a secondary membrane, or it may escape into the cytosol. Regardless of these optional escape routes, *S. aureus* will aim for growth and survival either by consuming the host's resources intracellularly, or by inducing host cell lysis to spread to and propagate in other tissues of the host (156).

## Scope and outline of the thesis

The goal of the PhD research described in this dissertation was to expand the understanding of the adaptive mechanisms employed by *S. aureus* to adjust to and survive the diverse conditions encountered in infection-relevant niches of the human body. Particular adaptations of *S. aureus* may consist of changes in the production of virulence factors that allow the bacteria to colonize and spread into host tissues, as well as metabolic adaptations that determine the fitness of the pathogen. Such adaptations are mostly studied separately in the invading bacteria and the respective host cell system. By contrast, this thesis describes a series of investigations where a combined approach was followed. In particular, adaptive responses in infecting bacteria and their host cells were monitored through proteomics, and subsequently the correlations of these responses and their physiological consequences were evaluated. The first two experimental chapters of this thesis focus on the adaptations of *S. aureus* upon a successful infection of bronchial epithelial cells, while the two subsequent experimental chapters describe the differences in the exo- and cytosolic proteomes of closely related MRSA

isolates with a different epidemiological history, linking the outcomes to their predominant modes of infection.

**Chapter 1** of this thesis presents a general introduction on the genetic and epidemiological diversity of *S. aureus*, emphasizing this pathogen's virulence factors and regulators that define the infection process. In addition, a general overview on the molecular interactions of *S. aureus* with cells of the human host is provided. **Chapter 2** covers the interaction between *S. aureus* and bronchial epithelial cells over four days post-infection. This extended period of observation allowed a comparative investigation of the metabolic pathways employed by *S. aureus* in the two subpopulations that it presents during infection and the occupation of different intracellular compartments. Importantly, the detected changes in the expression of metabolic pathways were simultaneously studied and correlated to the changes in the host cell proteome, offering a comprehensive picture of the dynamic interactions that occur between host and pathogen during infection. In this respect it should be noticed that pulmonary infections by *S. aureus* are highly prominent in patients with lung-related illnesses causing lesions in the epithelial lining. Therefore, in the studies described in **chapter 3**, proteomics was employed to study the adaptations of *S. aureus* during internalization within epithelial cell layers displaying two subsequent regenerative stages that occur after injury. In particular, this chapter is focused on those changes in the bacterial cytosolic proteome that occur during the first hours after internalization.

Taking into account the diversity of *S. aureus* lineages and strains, the lung epithelial model of infection employed for the studies described in chapter 2 was used to study interactions with clinical isolates of MRSA. The differences in the proteome of certain closely related *S. aureus* strains isolated in Denmark were, therefore, evaluated in experiments described in **chapters 4 and 5**. These studies include twelve isolates from two distinctive epidemiological groups, namely

community- (CA) and hospital-associated (HA) MRSA isolates. Specifically, **chapter 4** reports on the exoproteomes of these isolates and correlates the outcomes with their behavior upon infection of lung epithelial cells. Since the behavior of the investigated MRSA strains upon infection is also determined by their fitness, the cytosolic proteomes of a selection of these isolates were also investigated as described in **chapter 5**.

Altogether, the studies described in this thesis emphasize critical metabolic adaptations as drivers of the course of infection. The specific results of the present PhD research that have led to this important conclusion are summarized and discussed in **chapter 6**.

## References

1. Sugimoto, S., Iwamoto, T., Takada, K., Okuda, K.-I., Tajima, A., Iwase, T., and Mizunoe, Y. (2013) *Staphylococcus epidermidis* Esp degrades specific proteins associated with *Staphylococcus aureus* biofilm formation and host-pathogen interaction. *J. Bacteriol.* 195, 1645–1655
2. Lowy, F. D. (1998) *Staphylococcus aureus* Infections. *N. Engl. J. Med.* 339, 520–532
3. World Health Organization (2014) WHO | Antimicrobial resistance: global report on surveillance 2014. *WHO*,
4. Ogston, A. (1881) Report upon Micro-Organisms in Surgical Diseases. *Br Med J* 1, 369–375
5. Rosenbach, F. J. (1884) *Mikro-organismen bei den Wund-Infektions-Krankheiten des Menschen* (Wiesbaden J.F. Bergmann)
6. Abraham, E. P., and Chain, E. (1940) An Enzyme from Bacteria able to Destroy Penicillin. *Nature* 146, 837
7. Barber, M. (1947) Staphylococcal Infection due to Penicillin-resistant Strains. *Br Med J* 2, 863–865
8. Jevons, M. P. (1961) “Celbenin” - resistant Staphylococci. *Br Med J* 1, 124–125

9. Peacock, J. E., Marsik, F. J., and Wenzel, R. P. (1980) Methicillin-resistant *Staphylococcus aureus*: introduction and spread within a hospital. *Ann. Intern. Med.* 93, 526–532
10. Hiramatsu, K., Aritaka, N., Hanaki, H., Kawasaki, S., Hosoda, Y., Hori, S., Fukuchi, Y., and Kobayashi, I. (1997) Dissemination in Japanese hospitals of strains of *Staphylococcus aureus* heterogeneously resistant to vancomycin. *The Lancet* 350, 1670–1673
11. Stefani, S., and Varaldo, P. E. (2003) Epidemiology of methicillin-resistant staphylococci in Europe. *Clin. Microbiol. Infect.* 9, 1179–1186
12. Stefani, S., Chung, D. R., Lindsay, J. A., Friedrich, A. W., Kearns, A. M., Westh, H., and Mackenzie, F. M. (2012) Methicillin-resistant *Staphylococcus aureus* (MRSA): global epidemiology and harmonisation of typing methods. *Int. J. Antimicrob. Agents* 39, 273–282
13. Otto, M. (2012) MRSA virulence and spread. *Cell. Microbiol.* 14, 1513–1521
14. de Kraker, M. E. A., Davey, P. G., Grundmann, H., and BURDEN study group (2011) Mortality and hospital stay associated with resistant *Staphylococcus aureus* and *Escherichia coli* bacteremia: estimating the burden of antibiotic resistance in Europe. *PLoS Med.* 8, e1001104
15. Kuroda, M., Ohta, T., Uchiyama, I., Baba, T., Yuzawa, H., Kobayashi, I., Cui, L., Oguchi, A., Aoki, K., Nagai, Y., Lian, J., Ito, T., Kanamori, M., Matsumaru, H., Maruyama, A., Murakami, H., Hosoyama, A., Mizutani-Ui, Y., Takahashi, N. K., Sawano, T., Inoue, R., Kaito, C., Sekimizu, K., Hirakawa, H., Kuhara, S., Goto, S., Yabuzaki, J., Kanehisa, M., Yamashita, A., Oshima, K., Furuya, K., Yoshino, C., Shiba, T., Hattori, M., Ogasawara, N., Hayashi, H., and Hiramatsu, K. (2001) Whole genome sequencing of methicillin-resistant *Staphylococcus aureus*. *The Lancet* 357, 1225–1240
16. Williams, R. E. O. (1963) HEALTHY CARRIAGE OF *STAPHYLOCOCCUS AUREUS*: ITS PREVALENCE AND IMPORTANCE1. *Bacteriol. Rev.* 27, 56–71
17. van Belkum, A., Verkaik, N. J., de Vogel, C. P., Boelens, H. A., Verveer, J., Nouwen, J. L., Verbrugh, H. A., and Wertheim, H. F. L. (2009) Reclassification of *Staphylococcus aureus* Nasal Carriage Types. *J. Infect. Dis.* 199, 1820–1826

18. Wertheim, H. F., Melles, D. C., Vos, M. C., van Leeuwen, W., van Belkum, A., Verbrugh, H. A., and Nouwen, J. L. (2005) The role of nasal carriage in *Staphylococcus aureus* infections. *Lancet Infect. Dis.* 5, 751–762
19. von Eiff, C., Becker, K., Machka, K., Stammer, H., and Peters, G. (2001) Nasal carriage as a source of *Staphylococcus aureus* bacteremia. Study Group. *N. Engl. J. Med.* 344, 11–16
20. Wertheim, H. F., Vos, M. C., Ott, A., van Belkum, A., Voss, A., Kluytmans, J. A., van Keulen, P. H., Vandenbroucke-Grauls, C. M., Meester, M. H., and Verbrugh, H. A. (2004) Risk and outcome of nosocomial *Staphylococcus aureus* bacteraemia in nasal carriers versus non-carriers. *The Lancet* 364, 703–705
21. Chambers, H. F., and DeLeo, F. R. (2009) Waves of resistance: *Staphylococcus aureus* in the antibiotic era. *Nat. Rev. Microbiol.* 7, 629–641
22. Daum, R. S., and Spellberg, B. (2012) Progress toward a *Staphylococcus aureus* vaccine. *Clin. Infect. Dis. Off. Publ. Infect. Dis. Soc. Am.* 54, 560–567
23. Redi, D., Raffaelli, C. S., Rossetti, B., De Luca, A., and Montagnani, F. (2018) *Staphylococcus aureus* vaccine preclinical and clinical development: current state of the art. *New Microbiol.* 41, 208–213
24. Grundmann, H., Aires-de-Sousa, M., Boyce, J., and Tiemersma, E. (2006) Emergence and resurgence of methicillin-resistant *Staphylococcus aureus* as a public-health threat. *The Lancet* 368, 874–885
25. Tong, S. Y. C., Davis, J. S., Eichenberger, E., Holland, T. L., and Fowler, V. G. (2015) *Staphylococcus aureus* Infections: Epidemiology, Pathophysiology, Clinical Manifestations, and Management. *Clin. Microbiol. Rev.* 28, 603–661
26. Turner, N. A., Sharma-Kuinkel, B. K., Maskarinec, S. A., Eichenberger, E. M., Shah, P. P., Carugati, M., Holland, T. L., and Fowler, V. G. (2019) Methicillin-resistant *Staphylococcus aureus*: an overview of basic and clinical research. *Nat. Rev. Microbiol.* 17, 203
27. Udo, E. E., Pearman, J. W., and Grubb, W. B. (1993) Genetic analysis of community isolates of methicillin-resistant *Staphylococcus aureus* in Western Australia. *J. Hosp. Infect.* 25, 97–108
28. Herold, B. C., Immergluck, L. C., Maranan, M. C., Lauderdale, D. S., Gaskin, R. E., Boyle-Vavra, S., Leitch, C. D., and Daum, R. S. (1998)



Community-Acquired Methicillin-Resistant *Staphylococcus aureus* in Children With No Identified Predisposing Risk. *JAMA* 279, 593–598

29. David, M. Z., and Daum, R. S. (2010) Community-Associated Methicillin-Resistant *Staphylococcus aureus*: Epidemiology and Clinical Consequences of an Emerging Epidemic. *Clin. Microbiol. Rev.* 23, 616–687
30. DeLeo, F. R., Otto, M., Kreiswirth, B. N., and Chambers, H. F. (2010) Community-associated methicillin-resistant *Staphylococcus aureus*. *Lancet* 375, 1557–1568
31. Kobayashi, S. D., Malachowa, N., Whitney, A. R., Braughton, K. R., Gardner, D. J., Long, D., Wardenburg, J. B., Schneewind, O., Otto, M., and DeLeo, F. R. (2011) Comparative Analysis of USA300 Virulence Determinants in a Rabbit Model of Skin and Soft Tissue Infection. *J. Infect. Dis.* 204, 937–941
32. Surewaard, B., de Haas, C., Vervoort, F., Rigby, K., DeLeo, F., Otto, M., van Strijp, J., and Nijland, R. (2013) Staphylococcal alpha-Phenol Soluble Modulins contribute to neutrophil lysis after phagocytosis. *Cell. Microbiol.* 15, 1427–1437
33. Voyich, J. M., Braughton, K. R., Sturdevant, D. E., Whitney, A. R., Saïd-Salim, B., Porcella, S. F., Long, R. D., Dorward, D. W., Gardner, D. J., Kreiswirth, B. N., Musser, J. M., and DeLeo, F. R. (2005) Insights into Mechanisms Used by *Staphylococcus aureus* to Avoid Destruction by Human Neutrophils. *J. Immunol.* 175, 3907–3919
34. Greenlee-Wacker, M. C., Kremserová, S., and Nauseef, W. M. (2017) Lysis of human neutrophils by community-associated methicillin-resistant *Staphylococcus aureus*. *Blood* 129, 3237–3244
35. Li, M., Cheung, G. Y. C., Hu, J., Wang, D., Joo, H.-S., DeLeo, F. R., and Otto, M. (2010) Comparative Analysis of Virulence and Toxin Expression of Global Community-Associated Methicillin-Resistant *Staphylococcus aureus* Strains. *J. Infect. Dis.* 202, 1866–1876
36. Wang, R., Braughton, K. R., Kretschmer, D., Bach, T.-H. L., Queck, S. Y., Li, M., Kennedy, A. D., Dorward, D. W., Klebanoff, S. J., Peschel, A., DeLeo, F. R., and Otto, M. (2007) Identification of novel cytolytic peptides as key virulence determinants for community-associated MRSA. *Nat. Med.* 13, 1510–1514

37. Hu, Q., Cheng, H., Yuan, W., Zeng, F., Shang, W., Tang, D., Xue, W., Fu, J., Zhou, R., Zhu, J., Yang, J., Hu, Z., Yuan, J., Zhang, X., Rao, Q., Li, S., Chen, Z., Hu, X., Wu, X., and Rao, X. (2015) Pantone-Valentine Leukocidin (PVL)-Positive Health Care-Associated Methicillin-Resistant *Staphylococcus aureus* Isolates Are Associated with Skin and Soft Tissue Infections and Colonized Mainly by Infective PVL-Encoding Bacteriophages. *J. Clin. Microbiol.* 53, 67–72
38. Wang, S.-H., Hines, L., van Balen, J., Mediavilla, J. R., Pan, X., Hoet, A. E., Kreiswirth, B. N., Pancholi, P., and Stevenson, K. B. (2015) Molecular and Clinical Characteristics of Hospital and Community Onset Methicillin-Resistant *Staphylococcus aureus* Strains Associated with Bloodstream Infections. *J. Clin. Microbiol.* 53, 1599–1608
39. Sabat, A. J., Chlebowicz, M. A., Grundmann, H., Arends, J. P., Kampinga, G., Meessen, N. E. L., Friedrich, A. W., and van Dijk, J. M. (2012) Microfluidic-chip-based multiple-locus variable-number tandem-repeat fingerprinting with new primer sets for methicillin-resistant *Staphylococcus aureus*. *J. Clin. Microbiol.* 50, 2255–2262
40. Deurenberg, R. H., Vink, C., Kalenic, S., Friedrich, A. W., Bruggeman, C. A., and Stobberingh, E. E. (2007) The molecular evolution of methicillin-resistant *Staphylococcus aureus*. *Clin. Microbiol. Infect. Off. Publ. Eur. Soc. Clin. Microbiol. Infect. Dis.* 13, 222–235
41. Sabat, A. J., Budimir, A., Nashev, D., Sá-Leão, R., van Dijk, J. m, Laurent, F., Grundmann, H., Friedrich, A. W., and ESCMID Study Group of Epidemiological Markers (ESGEM) (2013) Overview of molecular typing methods for outbreak detection and epidemiological surveillance. *Euro Surveill. Bull. Eur. Sur Mal. Transm. Eur. Commun. Dis. Bull.* 18, 20380
42. SenGupta, D. J., Cummings, L. A., Hoogestraat, D. R., Butler-Wu, S. M., Shendure, J., Cookson, B. T., and Salipante, S. J. (2014) Whole-Genome Sequencing for High-Resolution Investigation of Methicillin-Resistant *Staphylococcus aureus* Epidemiology and Genome Plasticity. *J. Clin. Microbiol.* 52, 2787–2796
43. Sharma-Kuinkel, B. K., Rude, T. H., and Fowler, J. V. (2016) Pulse Field Gel Electrophoresis. *Methods Mol. Biol. Clifton NJ* 1373, 117–130
44. Cookson, B. D., Robinson, D. A., Monk, A. B., Murchan, S., Deplano, A., de Ryck, R., Struelens, M. J., Scheel, C., Fussing, V., Salmenlinna, S., Vuopio-Varkila, J., Cuny, C., Witte, W., Tassios, P. T., Legakis, N. J., van Leeuwen, W., van Belkum, A., Vindel, A., Garaizar, J., Haeggman, S., Olsson-

- Liljequist, B., Ransjo, U., Muller-Premru, M., Hryniewicz, W., Rossney, A., O'Connell, B., Short, B. D., Thomas, J., O'Hanlon, S., and Enright, M. C. (2007) Evaluation of molecular typing methods in characterizing a European collection of epidemic methicillin-resistant *Staphylococcus aureus* strains: the HARMONY collection. *J. Clin. Microbiol.* 45, 1830–1837
45. McDougal, L. K., Steward, C. D., Killgore, G. E., Chaitram, J. M., McAllister, S. K., and Tenover, F. C. (2003) Pulsed-field gel electrophoresis typing of oxacillin-resistant *Staphylococcus aureus* isolates from the United States: establishing a national database. *J. Clin. Microbiol.* 41, 5113–5120
46. Glasner, C., Sabat, A. J., Dreisbach, A., Larsen, A. R., Friedrich, A. W., Skov, R. L., and van Dijl, J. M. (2013) Rapid and high-resolution distinction of community-acquired and nosocomial *Staphylococcus aureus* isolates with identical pulsed-field gel electrophoresis patterns and spa types. *Int. J. Med. Microbiol.* 303, 70–75
47. Enright, M. C., Day, N. P. J., Davies, C. E., Peacock, S. J., and Spratt, B. G. (2000) Multilocus Sequence Typing for Characterization of Methicillin-Resistant and Methicillin-Susceptible Clones of *Staphylococcus aureus*. *J. Clin. Microbiol.* 38, 1008–1015
48. Chua, K. Y. L., Howden, B. P., Jiang, J.-H., Stinear, T., and Peleg, A. Y. (2014) Population genetics and the evolution of virulence in *Staphylococcus aureus*. *Infect. Genet. Evol.* 21, 554–562
49. Feil, E. J., Li, B. C., Aanensen, D. M., Hanage, W. P., and Spratt, B. G. (2004) eBURST: inferring patterns of evolutionary descent among clusters of related bacterial genotypes from multilocus sequence typing data. *J. Bacteriol.* 186, 1518–1530
50. Shopsin, B., Gomez, M., Montgomery, S. O., Smith, D. H., Waddington, M., Dodge, D. E., Bost, D. A., Riehman, M., Naidich, S., and Kreiswirth, B. N. (1999) Evaluation of Protein A Gene Polymorphic Region DNA Sequencing for Typing of *Staphylococcus aureus* Strains. *J. Clin. Microbiol.* 37, 3556–3563
51. Chlebowicz, M. A., van Dijl, J. M., and Buist, G. (2011) Considerations for the Distinction of ccrC-Containing Staphylococcal Cassette Chromosome mec Elements. *Antimicrob. Agents Chemother.* 55, 1823–1824
52. Durand, G., Javerliat, F., Bes, M., Veyrieras, J.-B., Guigon, G., Mugnier, N., Schicklin, S., Kaneko, G., Santiago-Allexant, E., Bouchiat, C., Martins-Simões, P., Laurent, F., Van Belkum, A., Vandenesch, F., and Tristan, A.

- (2018) Routine Whole-Genome Sequencing for Outbreak Investigations of *Staphylococcus aureus* in a National Reference Center. *Front. Microbiol.* 9, 511
53. Couto, N., Schuele, L., Raangs, E. C., Machado, M. P., Mendes, C. I., Jesus, T. F., Chlebowicz, M., Rosema, S., Ramirez, M., Carriço, J. A., Autenrieth, I. B., Friedrich, A. W., Peter, S., and Rossen, J. W. (2018) Critical steps in clinical shotgun metagenomics for the concomitant detection and typing of microbial pathogens. *Sci. Rep.* 8, 13767
  54. Cunningham, S. A., Chia, N., Jeraldo, P. R., Quest, D. J., Johnson, J. A., Boxrud, D. J., Taylor, A. J., Chen, J., Jenkins, G. D., Drucker, T. M., Nelson, H., and Patel, R. (2017) Comparison of Whole-Genome Sequencing Methods for Analysis of Three Methicillin-Resistant *Staphylococcus aureus* Outbreaks. *J. Clin. Microbiol.* 55, 1946–1953
  55. Dreisbach, A., van Dijk, J. M., and Buist, G. (2011) The cell surface proteome of *Staphylococcus aureus*. *Proteomics* 11, 3154–3168
  56. Sibbald, M. J. J. B., Ziebandt, A. K., Engelmann, S., Hecker, M., de Jong, A., Harmsen, H. J. M., Raangs, G. C., Stokroos, I., Arends, J. P., Dubois, J. Y. F., and van Dijk, J. M. (2006) Mapping the Pathways to Staphylococcal Pathogenesis by Comparative Secretomics. *Microbiol. Mol. Biol. Rev.* 70, 755–788
  57. Foster, T. J., Geoghegan, J. A., Ganesh, V. K., and Höök, M. (2014) Adhesion, invasion and evasion: the many functions of the surface proteins of *Staphylococcus aureus*. *Nat. Rev. Microbiol.* 12, 49–62
  58. Brouillette, E., Grondin, G., Shkreta, L., Lacasse, P., and Talbot, B. G. (2003) *In vivo* and *in vitro* demonstration that *Staphylococcus aureus* is an intracellular pathogen in the presence or absence of fibronectin-binding proteins. *Microb. Pathog.* 35, 159–168
  59. Cheng, A. G., Kim, H. K., Burts, M. L., Krausz, T., Schneewind, O., and Missiakas, D. M. (2009) Genetic requirements for *Staphylococcus aureus* abscess formation and persistence in host tissues. *FASEB J.* 23, 3393–3404
  60. Grundmeier, M., Hussain, M., Becker, P., Heilmann, C., Peters, G., and Sinha, B. (2004) Truncation of fibronectin-binding proteins in *Staphylococcus aureus* strain Newman leads to deficient adherence and host cell invasion due to loss of the cell wall anchor function. *Infect. Immun.* 72, 7155–7163
  61. Que, Y.-A., Haefliger, J.-A., Piroth, L., François, P., Widmer, E., Entenza, J. M., Sinha, B., Herrmann, M., Francioli, P., Vaudaux, P., and Moreillon, P.

- (2005) Fibrinogen and fibronectin binding cooperate for valve infection and invasion in *Staphylococcus aureus* experimental endocarditis. *J. Exp. Med.* 201, 1627–1635
62. Burian, M., Rautenberg, M., Kohler, T., Fritz, M., Krismer, B., Unger, C., Hoffmann, W. H., Peschel, A., Wolz, C., and Goerke, C. (2010) Temporal expression of adhesion factors and activity of global regulators during establishment of *Staphylococcus aureus* nasal colonization. *J. Infect. Dis.* 201, 1414–1421
  63. Clarke, S. R., Mohamed, R., Bian, L., Routh, A. F., Kokai-Kun, J. F., Mond, J. J., Tarkowski, A., and Foster, S. J. (2007) The *Staphylococcus aureus* surface protein IsdA mediates resistance to innate defenses of human skin. *Cell Host Microbe* 1, 199–212
  64. Mulcahy, M. E., Geoghegan, J. A., Monk, I. R., O’Keeffe, K. M., Walsh, E. J., Foster, T. J., and McLoughlin, R. M. (2012) Nasal Colonisation by *Staphylococcus aureus* Depends upon Clumping Factor B Binding to the Squamous Epithelial Cell Envelope Protein Loricrin. *PLoS Pathog.* 8, e1003092
  65. Bien, J., Sokolova, O., and Bozko, P. (2011) Characterization of Virulence Factors of *Staphylococcus aureus*: Novel Function of Known Virulence Factors That Are Implicated in Activation of Airway Epithelial Proinflammatory Response. *J. Pathog.* 2011, e601905
  66. Hair, P. S., Echague, C. G., Sholl, A. M., Watkins, J. A., Geoghegan, J. A., Foster, T. J., and Cunnion, K. M. (2010) Clumping factor A interaction with complement factor I increases C3b cleavage on the bacterial surface of *Staphylococcus aureus* and decreases complement-mediated phagocytosis. *Infect. Immun.* 78, 1717–1727
  67. Kang, M., Ko, Y.-P., Liang, X., Ross, C. L., Liu, Q., Murray, B. E., and Höök, M. (2013) Collagen-binding microbial surface components recognizing adhesive matrix molecule (MSCRAMM) of Gram-positive bacteria inhibit complement activation via the classical pathway. *J. Biol. Chem.* 288, 20520–20531
  68. Edwards, A. M., Potts, J. R., Josefsson, E., and Massey, R. C. (2010) *Staphylococcus aureus* host cell invasion and virulence in sepsis is facilitated by the multiple repeats within FnBPA. *PLoS Pathog.* 6, e1000964
  69. Kim, H. K., DeDent, A., Cheng, A. G., McAdow, M., Bagnoli, F., Missiakas, D. M., and Schneewind, O. (2010) IsdA and IsdB antibodies protect mice

- against *Staphylococcus aureus* abscess formation and lethal challenge. *Vaccine* 28, 6382–6392
70. Mazmanian, S. K., Skaar, E. P., Gaspar, A. H., Humayun, M., Gornicki, P., Jelenska, J., Joachmiak, A., Missiakas, D. M., and Schneewind, O. (2003) Passage of heme-iron across the envelope of *Staphylococcus aureus*. *Science* 299, 906–909
  71. Pilpa, R. M., Robson, S. A., Villareal, V. A., Wong, M. L., Phillips, M., and Clubb, R. T. (2009) Functionally distinct NEAT (NEAr Transporter) domains within the *Staphylococcus aureus* IsdH/HarA protein extract heme from methemoglobin. *J. Biol. Chem.* 284, 1166–1176
  72. Visai, L., Yanagisawa, N., Josefsson, E., Tarkowski, A., Pezzali, I., Rooijackers, S. H. M., Foster, T. J., and Speziale, P. (2009) Immune evasion by *Staphylococcus aureus* conferred by iron-regulated surface determinant protein IsdH. *Microbiology.* 155, 667–679
  73. Corrigan, R. M., Rigby, D., Handley, P., and Foster, T. J. (2007) The role of *Staphylococcus aureus* surface protein SasG in adherence and biofilm formation. *Microbiology.* 153, 2435–2446
  74. Cedergren, L., Andersson, R., Jansson, B., Uhlén, M., and Nilsson, B. (1993) Mutational analysis of the interaction between staphylococcal protein A and human IgG1. *Protein Eng.* 6, 441–448
  75. Graille, M., Stura, E. A., Corper, A. L., Sutton, B. J., Taussig, M. J., Charbonnier, J. B., and Silverman, G. J. (2000) Crystal structure of a *Staphylococcus aureus* protein A domain complexed with the Fab fragment of a human IgM antibody: structural basis for recognition of B-cell receptors and superantigen activity. *Proc. Natl. Acad. Sci. U. S. A.* 97, 5399–5404
  76. Gómez, M. I., Lee, A., Reddy, B., Muir, A., Soong, G., Pitt, A., Cheung, A., and Prince, A. (2004) *Staphylococcus aureus* protein A induces airway epithelial inflammatory responses by activating TNFR1. *Nat. Med.* 10, 842–848
  77. Gómez, M. I., O’Seaghdha, M., Magargee, M., Foster, T. J., and Prince, A. S. (2006) *Staphylococcus aureus* Protein A Activates TNFR1 Signaling through Conserved IgG Binding Domains. *J. Biol. Chem.* 281, 20190–20196
  78. Luong, T., Sau, S., Gomez, M., Lee, J. C., and Lee, C. Y. (2002) Regulation of *Staphylococcus aureus* Capsular Polysaccharide Expression by *agr* and *sarA*. *Infect. Immun.* 70, 444–450

79. Ko, Y.-P., Kang, M., Ganesh, V. K., Ravirajan, D., Li, B., and Höök, M. (2016) Coagulase and Efb of *Staphylococcus aureus* Have a Common Fibrinogen Binding Motif. *mBio* 7, e01885-15
80. Gonzalez, C. D., Ledo, C., Gai, C., Garófalo, A., and Gómez, M. I. (2015) The Sbi Protein Contributes to *Staphylococcus aureus* Inflammatory Response during Systemic Infection. *PLOS ONE* 10, e0131879
81. Ricklin, D., Tzekou, A., Garcia, B. L., Hammel, M., McWhorter, W. J., Sfyroera, G., Wu, Y.-Q., Holers, V. M., Herbert, A. P., Barlow, P. N., Geisbrecht, B. V., and Lambris, J. D. (2009) A Molecular Insight into Complement Evasion by the Staphylococcal Complement Inhibitor Protein Family. *J. Immunol.* 183, 2565–2574
82. Rooijackers, S. H. M., Ruyken, M., Roon, J. V., Kessel, K. P. M. V., Strijp, J. A. G. V., and Wamel, W. J. B. V. (2006) Early expression of SCIN and CHIPS drives instant immune evasion by *Staphylococcus aureus*. *Cell. Microbiol.* 8, 1282–1293
83. Rooijackers, S. H. M., Wu, J., Ruyken, M., van Domselaar, R., Planken, K. L., Tzekou, A., Ricklin, D., Lambris, J. D., Janssen, B. J. C., van Strijp, J. A. G., and Gros, P. (2009) Structural and functional implications of the complement convertase stabilized by a staphylococcal inhibitor. *Nat. Immunol.* 10, 721–727
84. Proft, T., and Fraser, J. D. (2003) Bacterial superantigens. *Clin. Exp. Immunol.* 133, 299–306
85. Ferry, T., Thomas, D., Genestier, A.-L., Bes, M., Lina, G., Vandenesch, F., and Etienne, J. (2005) Comparative Prevalence of Superantigen Genes in *Staphylococcus aureus* Isolates Causing Sepsis With and Without Septic Shock. *Clin. Infect. Dis.* 41, 771–777
86. Mölne, L., and Tarkowski, A. (2000) An experimental model of cutaneous infection induced by superantigen-producing *Staphylococcus aureus*. *J. Invest. Dermatol.* 114, 1120–1125
87. Salgado-Pabón, W., Breshears, L., Spaulding, A. R., Merriman, J. A., Stach, C. S., Horswill, A. R., Peterson, M. L., and Schlievert, P. M. (2013) Superantigens Are Critical for *Staphylococcus aureus* Infective Endocarditis, Sepsis, and Acute Kidney Injury. *mBio* 4, e00494-13
88. Wilson, G. J., Seo, K. S., Cartwright, R. A., Connelley, T., Chuang-Smith, O. N., Merriman, J. A., Guinane, C. M., Park, J. Y., Bohach, G. A., Schlievert, P.

- M., Morrison, W. I., and Fitzgerald, J. R. (2011) A novel core genome-encoded superantigen contributes to lethality of community-associated MRSA necrotizing pneumonia. *PLoS Pathog.* 7, e1002271
89. Inoshima, I., Inoshima, N., Wilke, G. A., Powers, M. E., Frank, K. M., Wang, Y., and Bubeck-Wardenburg, J. (2011) A *Staphylococcus aureus* pore-forming toxin subverts the activity of ADAM10 to cause lethal infection in mice. *Nat. Med.* 17, 1310–1314
90. Wilke, G. A., and Wardenburg, J. B. (2010) Role of a disintegrin and metalloprotease 10 in *Staphylococcus aureus*  $\alpha$ -hemolysin-mediated cellular injury. *Proc. Natl. Acad. Sci. U. S. A.* 107, 13473–13478
91. DuMont, A. L., Yoong, P., Day, C. J., Alonzo, F., McDonald, W. H., Jennings, M. P., and Torres, V. J. (2013) *Staphylococcus aureus* LukAB cytotoxin kills human neutrophils by targeting the CD11b subunit of the integrin Mac-1. *Proc. Natl. Acad. Sci. U. S. A.* 110, 10794–10799
92. Spaan, A. N., Henry, T., van Rooijen, W. J. M., Perret, M., Badiou, C., Aerts, P. C., Kemmink, J., de Haas, C. J. C., van Kessel, K. P. M., Vandenesch, F., Lina, G., and van Strijp, J. A. G. (2013) The staphylococcal toxin Panton-Valentine Leukocidin targets human C5a receptors. *Cell Host Microbe* 13, 584–594
93. Tromp, A. T., Van Gent, M., Abrial, P., Martin, A., Jansen, J. P., De Haas, C. J. C., Van Kessel, K. P. M., Bardoel, B. W., Kruse, E., Bourdonnay, E., Boettcher, M., McManus, M. T., Day, C. J., Jennings, M. P., Lina, G., Vandenesch, F., Van Strijp, J. A. G., Lebbink, R. J., Haas, P.-J. A., Henry, T., and Spaan, A. N. (2018) Human CD45 is an F-component-specific receptor for the staphylococcal toxin Panton-Valentine leukocidin. *Nat. Microbiol.* 3, 708–717
94. Alonzo, F., Benson, M. A., Chen, J., Novick, R. P., Shopsin, B., and Torres, V. J. (2012) *Staphylococcus aureus* leucocidin ED contributes to systemic infection by targeting neutrophils and promoting bacterial growth *in vivo*. *Mol. Microbiol.* 83, 423–435
95. Dumont, A. L., Nygaard, T. K., Watkins, R. L., Smith, A., Kozhaya, L., Kreiswirth, B. N., Shopsin, B., Unutmaz, D., Voyich, J. M., and Torres, V. J. (2011) Characterization of a new cytotoxin that contributes to *Staphylococcus aureus* pathogenesis. *Mol. Microbiol.* 79, 814–825
96. Genestier, A.-L., Michallet, M.-C., Prévost, G., Bellot, G., Chalabreysse, L., Peyrol, S., Thivolet, F., Etienne, J., Lina, G., Vallette, F. M., Vandenesch, F.,



- and Genestier, L. (2005) *Staphylococcus aureus* Panton-Valentine leukocidin directly targets mitochondria and induces Bax-independent apoptosis of human neutrophils. *J. Clin. Invest.* 115, 3117–3127
97. Dumitrescu, O., Tristan, A., Meugnier, H., Bes, M., Gouy, M., Etienne, J., Lina, G., and Vandenesch, F. (2008) Polymorphism of the *Staphylococcus aureus* Panton-Valentine Leukocidin Genes and Its Possible Link with the Fitness of Community-Associated Methicillin-Resistant *S. aureus*. *J. Infect. Dis.* 198, 792–794
  98. John, J. F., and Lindsay, J. A. (2008) Clones and drones: do variants of Panton-Valentine leukocidin extend the reach of community-associated methicillin-resistant *Staphylococcus aureus*? *J. Infect. Dis.* 197, 175–178
  99. O'Hara, F. P., Guex, N., Word, J. M., Miller, L. A., Becker, J. A., Walsh, S. L., Scangarella, N. E., West, J. M., Shawar, R. M., and Amrine-Madsen, H. (2008) A Geographic Variant of the *Staphylococcus aureus* Panton-Valentine Leukocidin Toxin and the Origin of Community-Associated Methicillin-Resistant *S. aureus* USA300. *J. Infect. Dis.* 197, 187–194
  100. Löffler, B., Hussain, M., Grundmeier, M., Brück, M., Holzinger, D., Varga, G., Roth, J., Kahl, B. C., Proctor, R. A., and Peters, G. (2010) *Staphylococcus aureus* panton-valentine leukocidin is a very potent cytotoxic factor for human neutrophils. *PLoS Pathog.* 6, e1000715
  101. Varshney, A. K., Martinez, L. R., Hamilton, S. M., Bryant, A. E., Levi, M. H., Gialanella, P., Stevens, D. L., and Fries, B. C. (2010) Augmented production of Panton-Valentine leukocidin toxin in methicillin-resistant and methicillin-susceptible *Staphylococcus aureus* is associated with worse outcome in a murine skin infection model. *J. Infect. Dis.* 201, 92–96
  102. Periasamy, S., Chatterjee, S. S., Cheung, G. Y. C., and Otto, M. (2012) Phenol-soluble modulins in staphylococci. *Commun. Integr. Biol.* 5, 275–277
  103. Tsompanidou, E., Denham, E. L., Becher, D., Jong, A. de, Buist, G., Oosten, M. van, Manson, W. L., Back, J. W., Dijk, J. M. van, and Dreisbach, A. (2013) Distinct Roles of Phenol-Soluble Modulins in Spreading of *Staphylococcus aureus* on Wet Surfaces. *Appl Env. Microbiol.* 79, 886–895
  104. Cheung, G. Y. C., Joo, H.-S., Chatterjee, S. S., and Otto, M. (2014) Phenol-soluble modulins – critical determinants of staphylococcal virulence. *FEMS Microbiol. Rev.* 38, 698–719

105. Kretschmer, D., Gleske, A.-K., Rautenberg, M., Wang, R., Köberle, M., Bohn, E., Schöneberg, T., Rabiet, M.-J., Boulay, F., Klebanoff, S. J., van Kessel, K. A., van Strijp, J. A., Otto, M., and Peschel, A. (2010) Human formyl peptide receptor 2 senses highly pathogenic *Staphylococcus aureus*. *Cell Host Microbe* 7, 463–473
106. Prat, C., Bestebroer, J., de Haas, C. J. C., van Strijp, J. A. G., and van Kessel, K. P. M. (2006) A new staphylococcal anti-inflammatory protein that antagonizes the formyl peptide receptor-like 1. *J. Immunol.* 177, 8017–8026
107. Schwartz, K., Syed, A. K., Stephenson, R. E., Rickard, A. H., and Boles, B. R. (2012) Functional amyloids composed of phenol soluble modulins stabilize *Staphylococcus aureus* biofilms. *PLoS Pathog.* 8, e1002744
108. Wang, R., Khan, B. A., Cheung, G. Y. C., Bach, T.-H. L., Jameson-Lee, M., Kong, K.-F., Queck, S. Y., and Otto, M. (2011) *Staphylococcus epidermidis* surfactant peptides promote biofilm maturation and dissemination of biofilm-associated infection in mice. *J. Clin. Invest.* 121, 238–248
109. Ebner, P., Luqman, A., Reichert, S., Hauf, K., Popella, P., Forchhammer, K., Otto, M., and Götz, F. (2017) Non-classical Protein Excretion Is Boosted by PSM $\alpha$ -Induced Cell Leakage. *Cell Rep.* 20, 1278–1286
110. Ebner, P., Rinker, J., Nguyen, M. T., Popella, P., Nega, M., Luqman, A., Schitteck, B., Marco, M. D., Stevanovic, S., and Götz, F. (2016) Excreted Cytoplasmic Proteins Contribute to Pathogenicity in *Staphylococcus aureus*. *Infect. Immun.* 84, 1672–1681
111. Henderson, B., and Martin, A. (2011) Bacterial Virulence in the Moonlight: Multitasking Bacterial Moonlighting Proteins Are Virulence Determinants in Infectious Disease ▽. *Infect. Immun.* 79, 3476–3491
112. Somerville, G. A., and Proctor, R. A. (2009) At the Crossroads of Bacterial Metabolism and Virulence Factor Synthesis in Staphylococci. *Microbiol. Mol. Biol. Rev.* 73, 233–248
113. Cheung, A. L., Bayer, A. S., Zhang, G., Gresham, H., and Xiong, Y.-Q. (2004) Regulation of virulence determinants *in vitro* and *in vivo* in *Staphylococcus aureus*. *FEMS Immunol. Med. Microbiol.* 40, 1–9
114. Eisenreich, W., Heesemann, J., Rudel, T., and Goebel, W. (2015) Metabolic Adaptations of Intracellular Bacterial Pathogens and their Mammalian Host Cells during Infection (“Pathometabolism”). *Microbiol. Spectr.* 3,

115. Li, C., Sun, F., Cho, H., Yelavarthi, V., Sohn, C., He, C., Schneewind, O., and Bae, T. (2010) CcpA Mediates Proline Auxotrophy and Is Required for *Staphylococcus aureus* Pathogenesis. *J. Bacteriol.* 192, 3883–3892
116. Deutscher, J., Küster, E., Bergstedt, U., Charrier, V., and Hillen, W. (1995) Protein kinase-dependent HPr/CcpA interaction links glycolytic activity to carbon catabolite repression in Gram-positive bacteria. *Mol. Microbiol.* 15, 1049–1053
117. Schumacher, M. A., Allen, G. S., Diel, M., Seidel, G., Hillen, W., and Brennan, R. G. (2004) Structural Basis for Allosteric Control of the Transcription Regulator CcpA by the Phosphoprotein HPr-Ser46-P. *Cell* 118, 731–741
118. Seidl, K., Stucki, M., Ruegg, M., Goerke, C., Wolz, C., Harris, L., Berger-Bächli, B., and Bischoff, M. (2006) *Staphylococcus aureus* CcpA Affects Virulence Determinant Production and Antibiotic Resistance. *Antimicrob. Agents Chemother.* 50, 1183–1194
119. Seidl, K., Bischoff, M., and Berger-Bächli, B. (2008) CcpA Mediates the Catabolite Repression of *tst* in *Staphylococcus aureus*. *Infect. Immun.* 76, 5093–5099
120. Ding, Y., Liu, X., Chen, F., Di, H., Xu, B., Zhou, L., Deng, X., Wu, M., Yang, C.-G., and Lan, L. (2014) Metabolic sensor governing bacterial virulence in *Staphylococcus aureus*. *Proc. Natl. Acad. Sci. USA* 111, E4981–E4990
121. Hartmann, T., Baronian, G., Nippe, N., Voss, M., Schulthess, B., Wolz, C., Eisenbeis, J., Schmidt-Hohagen, K., Gaupp, R., Sunderkötter, C., Beisswenger, C., Bals, R., Somerville, G. A., Herrmann, M., Molle, V., and Bischoff, M. (2014) The Catabolite Control Protein E (CcpE) Affects Virulence Determinant Production and Pathogenesis of *Staphylococcus aureus*. *J. Biol. Chem.* 289, 29701–29711
122. Lemos, J. A., Nascimento, M. M., Lin, V. K., Abranches, J., and Burne, R. A. (2008) Global Regulation by (p)ppGpp and CodY in *Streptococcus mutans*. *J. Bacteriol.* 190, 5291–5299
123. Kaiser, J. C., Sen, S., Sinha, A., Wilkinson, B. J., and Heinrichs, D. E. (2016) The role of two branched-chain amino acid transporters in *Staphylococcus aureus* growth, membrane fatty acid composition and virulence. *Mol. Microbiol.* 102, 850–864

124. Pohl, K., Francois, P., Stenz, L., Schlink, F., Geiger, T., Herbert, S., Goerke, C., Schrenzel, J., and Wolz, C. (2009) CodY in *Staphylococcus aureus*: a Regulatory Link between Metabolism and Virulence Gene Expression. *J. Bacteriol.* 191, 2953–2963
125. Majerczyk, C. D., Dunman, P. M., Luong, T. T., Lee, C. Y., Sadykov, M. R., Somerville, G. A., Bodi, K., and Sonenshein, A. L. (2010) Direct targets of CodY in *Staphylococcus aureus*. *J. Bacteriol.* 192, 2861–2877
126. Roux, A., Todd, D. A., Velázquez, J. V., Cech, N. B., and Sonenshein, A. L. (2014) CodY-Mediated Regulation of the *Staphylococcus aureus* Agr System Integrates Nutritional and Population Density Signals. *J. Bacteriol.* 196, 1184–1196
127. Pagels, M., Fuchs, S., Pané-Farré, J., Kohler, C., Menschner, L., Hecker, M., McNamarra, P. J., Bauer, M. C., von Wachenfeldt, C., Liebeke, M., Lalk, M., Sander, G., von Eiff, C., Proctor, R. A., and Engelmann, S. (2010) Redox sensing by a Rex-family repressor is involved in the regulation of anaerobic gene expression in *Staphylococcus aureus*. *Mol. Microbiol.* 76, 1142–1161
128. Horn, J., Stelzner, K., Rudel, T., and Fraunholz, M. (2018) Inside job: *Staphylococcus aureus* host-pathogen interactions. *Int. J. Med. Microbiol.* 308, 607–624
129. Kinkel, T. L., Roux, C. M., Dunman, P. M., and Fang, F. C. (2013) The *Staphylococcus aureus* SrrAB two-component system promotes resistance to nitrosative stress and hypoxia. *mBio* 4, e00696-00613
130. Koenig, R. L., Ray, J. L., Maleki, S. J., Smeltzer, M. S., and Hurlburt, B. K. (2004) *Staphylococcus aureus* AgrA binding to the RNAIII-*agr* regulatory region. *J. Bacteriol.* 186, 7549–7555
131. Lina, G., Jarraud, S., Ji, G., Greenland, T., Pedraza, A., Etienne, J., Novick, R. P., and Vandenesch, F. (1998) Transmembrane topology and histidine protein kinase activity of AgrC, the *agr* signal receptor in *Staphylococcus aureus*. *Mol. Microbiol.* 28, 655–662
132. Abdelnour, A., Arvidson, S., Bremell, T., Rydén, C., and Tarkowski, A. (1993) The accessory gene regulator (*agr*) controls *Staphylococcus aureus* virulence in a murine arthritis model. *Infect. Immun.* 61, 3879–3885
133. Cheung, A. L., Eberhardt, K. J., Chung, E., Yeaman, M. R., Sullam, P. M., Ramos, M., and Bayer, A. S. (1994) Diminished virulence of a *sar*-*agr*-

- mutant of *Staphylococcus aureus* in the rabbit model of endocarditis. *J. Clin. Invest.* 94, 1815–1822
134. Cheung, G. Y. C., Wang, R., Khan, B. A., Sturdevant, D. E., and Otto, M. (2011) Role of the accessory gene regulator *agr* in community-associated methicillin-resistant *Staphylococcus aureus* pathogenesis. *Infect. Immun.* 79, 1927–1935
  135. Gillaspay, A. F., Hickmon, S. G., Skinner, R. A., Thomas, J. R., Nelson, C. L., and Smeltzer, M. S. (1995) Role of the accessory gene regulator (*agr*) in pathogenesis of staphylococcal osteomyelitis. *Infect. Immun.* 63, 3373–3380
  136. Mairpady Shambat, S., Siemens, N., Monk, I. R., Mohan, D. B., Mukundan, S., Krishnan, K. C., Prabhakara, S., Snäll, J., Kearns, A., Vandenesch, F., Svensson, M., Kotb, M., Gopal, B., Arakere, G., and Norrby-Teglund, A. (2016) A point mutation in AgrC determines cytotoxic or colonizing properties associated with phenotypic variants of ST22 MRSA strains. *Sci. Rep.* 6, 31360
  137. Ballal, A., and Manna, A. C. (2009) Expression of the *sarA* family of genes in different strains of *Staphylococcus aureus*. *Microbiology* 155, 2342–2352
  138. Andrey, D. O., Renzoni, A., Monod, A., Lew, D. P., Cheung, A. L., and Kelley, W. L. (2010) Control of the *Staphylococcus aureus* Toxic Shock *tst* Promoter by the Global Regulator SarA. *J. Bacteriol.* 192, 6077–6085
  139. Andrey, D. O., Jousselin, A., Villanueva, M., Renzoni, A., Monod, A., Barras, C., Rodriguez, N., and Kelley, W. L. (2015) Impact of the Regulators SigB, Rot, SarA and sarS on the Toxic Shock Tst Promoter and TSST-1 Expression in *Staphylococcus aureus*. *PloS One* 10, e0135579
  140. Loughran, A. J., Atwood, D. N., Anthony, A. C., Harik, N. S., Spencer, H. J., Beenken, K. E., and Smeltzer, M. S. (2014) Impact of individual extracellular proteases on *Staphylococcus aureus* biofilm formation in diverse clinical isolates and their isogenic *sarA* mutants. *MicrobiologyOpen* 3, 897–909
  141. Ballal, A., and Manna, A. C. (2009) Regulation of superoxide dismutase (*sod*) genes by SarA in *Staphylococcus aureus*. *J. Bacteriol.* 191, 3301–3310
  142. Beenken, K. E., Blevins, J. S., and Smeltzer, M. S. (2003) Mutation of *sarA* in *Staphylococcus aureus* Limits Biofilm Formation. *Infect. Immun.* 71, 4206–4211
  143. Morrison, J. M., Anderson, K. L., Beenken, K. E., Smeltzer, M. S., and Dunman, P. M. (2012) The staphylococcal accessory regulator, SarA, is an

- RNA-binding protein that modulates the mRNA turnover properties of late-exponential and stationary phase *Staphylococcus aureus* cells. *Front. Cell. Infect. Microbiol.* 2, 26
144. Gresham, H. D., Lowrance, J. H., Caver, T. E., Wilson, B. S., Cheung, A. L., and Lindberg, F. P. (2000) Survival of *Staphylococcus aureus* inside neutrophils contributes to infection. *J. Immunol.* 164, 3713–3722
  145. Loughran, A. J., Gaddy, D., Beenken, K. E., Meeker, D. G., Morello, R., Zhao, H., Byrum, S. D., Tackett, A. J., Cassat, J. E., and Smeltzer, M. S. (2016) Impact of *sarA* and Phenol-Soluble Modulins on the Pathogenesis of Osteomyelitis in Diverse Clinical Isolates of *Staphylococcus aureus*. *Infect. Immun.* 84, 2586–2594
  146. Zielinska, A. K., Beenken, K. E., Mrak, L. N., Spencer, H. J., Post, G. R., Skinner, R. A., Tackett, A. J., Horswill, A. R., and Smeltzer, M. S. (2012) *sarA*-mediated repression of protease production plays a key role in the pathogenesis of *Staphylococcus aureus* USA300 isolates. *Mol. Microbiol.* 86, 1183–1196
  147. Cheung, A. L., Nishina, K., and Manna, A. C. (2008) SarA of *Staphylococcus aureus* Binds to the *sarA* Promoter to Regulate Gene Expression. *J. Bacteriol.* 190, 2239–2243
  148. Manna, A. C., Bayer, M. G., and Cheung, A. L. (1998) Transcriptional analysis of different promoters in the *sar* locus in *Staphylococcus aureus*. *J. Bacteriol.* 180, 3828–3836
  149. Knobloch, J. K.-M., Jäger, S., Horstkotte, M. A., Rohde, H., and Mack, D. (2004) RsbU-Dependent Regulation of *Staphylococcus epidermidis* Biofilm Formation Is Mediated via the Alternative Sigma Factor  $\sigma^B$  by Repression of the Negative Regulator Gene *icaR*. *Infect. Immun.* 72, 3838–3848
  150. Guldemann, C., Boor, K. J., Wiedmann, M., and Guariglia-Oropeza, V. (2016) Resilience in the Face of Uncertainty: Sigma Factor B Fine-Tunes Gene Expression To Support Homeostasis in Gram-Positive Bacteria. *Appl. Environ. Microbiol.* 82, 4456–4469
  151. Pförtner, H., Burian, M. S., Michalik, S., Depke, M., Hildebrandt, P., Dhople, V. M., Pané-Farré, J., Hecker, M., Schmidt, F., and Völker, U. (2014) Activation of the alternative sigma factor SigB of *Staphylococcus aureus* following internalization by epithelial cells – An *in vivo* proteomics perspective. *Int. J. Med. Microbiol.* 304, 177–187

152. Tuchscher, L., Bischoff, M., Lattar, S. M., Noto Llana, M., Pförtner, H., Niemann, S., Geraci, J., Van de Vyver, H., Fraunholz, M. J., Cheung, A. L., Herrmann, M., Völker, U., Sordelli, D. O., Peters, G., and Löffler, B. (2015) Sigma Factor SigB Is Crucial to Mediate *Staphylococcus aureus* Adaptation during Chronic Infections. *PLoS Pathog* 11, e1004870
153. Thwaites, G. E., and Gant, V. (2011) Are bloodstream leukocytes Trojan Horses for the metastasis of *Staphylococcus aureus*? *Nat. Rev. Microbiol.* 9, 215
154. Sendi, P., and Proctor, R. A. (2009) *Staphylococcus aureus* as an intracellular pathogen: the role of small colony variants. *Trends Microbiol.* 17, 54–58
155. Tuchscher, L., Medina, E., Hussain, M., Völker, W., Heitmann, V., Niemann, S., Holzinger, D., Roth, J., Proctor, R. A., Becker, K., Peters, G., and Löffler, B. (2011) *Staphylococcus aureus* phenotype switching: an effective bacterial strategy to escape host immune response and establish a chronic infection. *EMBO Mol. Med.* 3, 129–141
156. Garzoni, C., and Kelley, W. L. (2009) *Staphylococcus aureus*: new evidence for intracellular persistence. *Trends Microbiol.* 17, 59–65

## Chapter 2

# **Metabolic cross-talk between human bronchial epithelial cells and internalized *Staphylococcus aureus* as a driver for infection**

---

Laura M. Palma Medina, Ann-Kristin Becker, Stephan Michalik, Harita Yedavally, Elisa J.M. Raineri, Petra Hildebrandt, Manuela Gesell Salazar, Kristin Surmann, Henrike Pförtner, Solomon A. Mekonnen, Anna Salvati, Lars Kaderali, Jan Maarten van Dijl<sup>#</sup>, Uwe Völker<sup>#</sup>

<sup>#</sup>Corresponding authors

*Molecular and Cellular Proteomics*, (2019) 18: 892-908

Supplementary Material is available at [http://bit.ly/Thesis\\_Palma\\_Medina](http://bit.ly/Thesis_Palma_Medina)





## Abstract

*Staphylococcus aureus* is infamous for causing recurrent infections of the human respiratory tract. This is a consequence of its ability to adapt to different niches, including the intracellular milieu of lung epithelial cells. To understand the dynamic interplay between epithelial cells and the intracellular pathogen, we dissected their interactions over four days by mass spectrometry. Additionally, we investigated the dynamics of infection through live cell imaging, immunofluorescence and electron microscopy. The results highlight a major role of often overlooked temporal changes in the bacterial and host metabolism, triggered by fierce competition over limited resources. Remarkably, replicating bacteria reside predominantly within membrane-enclosed compartments and induce apoptosis of the host within ~24 hours post infection. Surviving infected host cells carry a subpopulation of non-replicating bacteria in the cytoplasm that persists. Altogether, we conclude that, besides the production of virulence factors by bacteria, it is the way in which intracellular resources are used, and how host and intracellular bacteria subsequently adapt to each other that determines the ultimate outcome of the infectious process.

## Introduction

*Staphylococcus aureus* is a Gram-positive opportunistic pathogen of humans, but also a commensal of the human body. Specifically, *S. aureus* is commonly found in the anterior nares of around 30% of the human population (1). Although most *S. aureus* carriers do not present any clinical symptoms, *S. aureus* can cause a wide range of diseases such as skin and soft tissue infections, osteomyelitis, septic arthritis and pneumonia (2, 3). This pathogen has gained particular notoriety in recent years due to its prevalence in nosocomial infections and the rise of methicillin-resistant *S. aureus* (MRSA) (3–5).

Although *S. aureus* often acts as an extracellular pathogen, it can evade immune responses and antibiotic therapy by entering human cells. The latter strategy is also used by the bacteria as a mechanism to spread to other tissues and both professional as well as non-professional phagocytic cells are used for internalization (6–8). After the bacteria have been taken up by the host cells, they will initially be localized in vesicles, which subsequently might fuse with lysosomes or be engulfed by an isolation membrane due to autophagy, and the bacteria inside them may prevail or escape into the cytosol. While the internalization by host cells is potentially lethal for the bacteria, the survivors will have two options: proliferation or persistence. In the first case, the bacteria replicate intracellularly and subsequently induce lysis of the host cells. The released bacteria search for new host cells to be infected and spread into new tissues (6–8). In the second case, the persistent bacteria do not multiply, but adapt to the intracellular environment and may survive intracellularly without causing clinical symptoms for extended time periods. This pattern has been linked to relapse of infections or emergence of small colony variants (SCVs) of *S. aureus* which display reduced metabolic activity (9–11).

Despite strain-specific differences in overall virulence, all *S. aureus* strains, including laboratory strains, are capable of displaying proliferative and persistent phenotypes. While this phenomenon has been known (6), the actual adaptations either enabling active intracellular proliferation or reduced metabolic activity and persistence are still poorly understood. The precise outcome of the interplay between the bacterium and the host depends on the type of host cell involved and, perhaps most importantly, the physiological states of both parties (12, 13). The main challenge in obtaining a detailed understanding of the adaptive behavior of internalized *S. aureus* lies in the fact that it is essential to study quantitative changes over an extended period of time, not only in one of the two interacting parties but simultaneously in both of them. Previous studies have addressed these aspects only partially either by focusing on the internalized bacteria only, or over only fairly short periods of time post infection (p.i.) (11, 12, 14–17). Yet, it is important to get the ‘complete picture’ of such an infection scenario, because the invasion and destruction of lung epithelial cells is representative for some of the most serious staphylococcal diseases possible, especially necrotizing pneumonia.

The present study was designed to close the current knowledge gap on the interplay between *S. aureus* and lung epithelial cells by a time-resolved analysis of both parties over the longest possible period of time. The limits for such an analysis are set by the amount of material that can be extracted for bacteria- and host cell-specific analyses, and the parameters to be measured. This led us to a proteomics approach, where adaptations of the bronchial epithelial cell line 16HBE14o- and *S. aureus* were followed up to four days p.i. using a ‘Data Independent Acquisition’ (DIA) method. Importantly, our findings highlight dynamic adaptive changes, in both the host and the internalized pathogen, and describe the active cross-talk between them at different stages of infection. Additionally, we correlate these adaptations with the intracellular localization of the bacteria p.i. and the epithelial cells’ response. The observations suggest that,

after a period of violent conflict, both parties reach an equilibrium phase where they are apparently at peace and the bacteria have reached a persister status.

## Materials and methods

### Bacterial strains

*S. aureus* strain HG001 (18) was used to perform all experiments. The bacteria carried plasmid pJL-sar-GFP to constitutively express the green fluorescent protein (GFP; Liese et al., 2013). For the immunostaining protocols, a *spa* mutant was used to prevent unspecific binding of marker antibodies to protein A. The HG001  $\Delta spa$  strain was kindly provided by Dr. Jan Pané-Farré, University of Greifswald. Cultivation of bacteria was performed in prokaryotic minimal essential medium (pMEM): 1x MEM without sodium bicarbonate (Invitrogen, Germany) supplemented with 1x non-essential amino acids (PAN-Biotech GmbH, Germany), 4 mM L-glutamine (PAN-Biotech GmbH), 10 mM HEPES (PAN-Biotech GmbH, Germany), 2 mM L-alanine, 2 mM L-leucine, 2 mM L-isoleucine, 2 mM L-valine, 2 mM L-aspartate, 2 mM L-glutamate, 2 mM L-serine, 2 mM L-threonine, 2 mM L-cysteine, 2 mM L-proline, 2 mM L-histidine, 2 mM L-phenylalanine and 2 mM L-tryptophan (Sigma-Aldrich, Germany), adjusted to pH 7.4 and sterilized by filtration. One day before the infection of epithelial cells, bacterial overnight cultures in pMEM supplemented with 0.01% yeast extract and 10  $\mu\text{g}\cdot\text{ml}^{-1}$  erythromycin were prepared by serial dilutions ( $1\cdot 10^{-6}$  up to  $1\cdot 10^{-10}$ ) of a 100  $\mu\text{l}$  glycerol stock of a bacterial culture with an  $\text{OD}_{600}$  of 1.2. Incubation was performed at 37°C and 220 rpm. The following day, the main culture was inoculated from an overnight culture with an  $\text{OD}_{600}$  between 0.3 to 0.8. The starting  $\text{OD}_{600}$  of the main culture was set to 0.05 and it was incubated for approximately 2 h in a shaking water bath at 150 rpm and 37°C until it reached the mid-exponential phase at an  $\text{OD}_{600}$  of approximately 0.4 (Supplemental Figure S1). The bacteria

were then harvested and used for preparation of the master mix for infection as explained below in the “Internalization experiments” paragraph.

## Cell line

The human epithelial cell line 16HBE14o- is a transformed bronchial epithelial cell line originally derived from a 1-year-old heart-lung transplant patient (20). This cell line is known for its ability to form tight junctions and to differentiate. The cells were cultured at 37°C in 5% CO<sub>2</sub> in eukaryotic minimal essential medium (eMEM): 1x MEM (Biochrom AG, Germany) supplemented with 10% (v/v) fetal calf serum (FCS; Biochrom AG, Germany), 2% (v/v) L-glutamine 200 mM (PAN-Biotech GmbH, Germany) and 1% (v/v) non-essential amino acids 100x (PAN-Biotech GmbH, Germany). The splitting of cells was carried out every three days with 0.25% trypsin-EDTA (Gibco®, USA). After thawing of frozen stocks (in liquid N<sub>2</sub>) the cells were maintained for 20 additional passages. The cell lines stocks used are not authenticated.

## Experimental Design and Statistical Rationale

Four independent biological replicates of the infection set-up were used for quantification of bacterial and host cell populations, and for mass spectrometry measurements. The number of replicates was selected to ensure that at every time point there were at least three consistent measurements for every protein. The sampling of each independent infection consisted of 8 samples taken over the course of four days, including a 0 h sample which is the control condition. In total, 32 samples of the cytosolic proteome of bacteria and 32 samples of the human bronchial epithelial cell proteome were measured. To avoid measuring replicates of the same condition sequentially, the measuring order of each set of samples was determined by assigning a random number between 1 and 32 to each sample

(function sample in R version 3.4.4 (21)). Additionally, samples for imaging were collected from three independent infection experiments.

To determine changes over time in protein abundance, an empirical Bayes moderated F-test was conducted for each protein profile. This test also evaluates the similarity of the replicates. The moderated p-values were corrected for multiple testing using Benjamini and Hochberg's multiple testing correction.

## Internalization experiments

Internalization experiments were performed essentially as described by Pförtner et al. (22). Briefly, internalization was performed using a confluent 16HBE14o- cell layer seeded at a density of  $1 \cdot 10^5$  cells $\cdot$ cm $^{-2}$  in 12-well plates, three days prior to infection. The infection was carried out at a multiplicity of infection (MOI) of 25 bacteria per host cell. The master mix for infection was prepared from a mid-exponential (OD $_{600}$  of 0.4) culture of *S. aureus* HG001 diluted in eMEM, buffered with 2.9  $\mu$ l sodium hydrogen carbonate (7.5%) per ml bacterial culture added. The growth medium over the confluent epithelial layer was replaced with the master mix, and the co-culture was incubated for 1 h at 37°C in 5% CO $_2$ . Afterwards, the medium was collected (non-adherent sample) and replaced with eMEM medium containing 10  $\mu$ g $\cdot$ ml $^{-1}$  of lysostaphin (AMBI Products LLC, USA). The medium was replaced every two days.

For collection of the proteome samples, the culturing medium was aspirated, and the epithelial cell layers were treated for 5 min at 37°C with UT buffer (8 M urea, 2 M thiourea in MS-grade water) to generate samples for analysis by mass spectrometry (MS). If samples were intended for the collection of bacteria, the disruption of epithelial cells was performed for 5 min at 37°C in 0.05% sodium dodecyl sulfate (SDS). Samples were collected at 2.5 h, 6.5 h, 24 h, 48 h, 72 h, and 96 h p.i..

To monitor changes in the abundance of human and bacterial cells, counting was performed at the times of sample collection. Epithelial cells were counted upon staining with trypan blue dye using a Countess® system (Invitrogen, Germany). Quantification of intracellular bacteria and infected epithelial cells was performed with a Guava® easyCyte flow cytometer (Merck Millipore, Germany) by excitation of the GFP with a 488 nm laser and detection at 510-540 nm.

## Preparation of proteome samples

Upon disruption of epithelial cells with 0.05% SDS, two million liberated bacteria were sorted by flow cytometry using a FACSAria IIIu cell sorter (Becton Dickinson Biosciences, USA) per time point. The recognition of bacteria was carried out by excitation with a 488 nm laser and the emission was detected in the range of 515–545 nm. The bacterial cells were collected on low protein binding filter membranes with a pore size of 0.22 µm (Merck Millipore, Germany). These bacteria-containing filters were immediately placed in Eppendorf tubes that were then frozen by transferring them to a -20°C freezer for the course of the experiment and then kept at -80°C until use. The bacteria on the filter were lysed by incubation for 30 min at 37°C with 7.4 µg·ml<sup>-1</sup> lysostaphin in 50 mM ammonium bicarbonate (23). Digestion of bacterial proteins on the filter was performed overnight at 37°C with 0.1% Rapigest SF surfactant (Waters, Germany) and 0.3 µg of trypsin.

For human proteome analyses, the protein content of samples was quantified using a Bradford assay (Biorad, Germany). Four µg of protein per sample were prepared for MS measurements by reduction with 2.5 mmol·L<sup>-1</sup> dithiothreitol for 1 hour at 60°C and alkylation with 10 mmol·L<sup>-1</sup> iodoacetamide for 30 min at 37°C. Then, the samples were digested overnight with trypsin (protein:trypsin 25:1) at 37°C.



The following 16HBE14o- samples were used for the construction of the spectral library of the host: a confluent cell layer cultured in a 10 cm dish for 3 days, an apoptotic cell layer in a 10 cm dish cultured for a week, non-polarized cells cultured for 3 days over Transwells®, and lastly polarized cells cultured for 11 days over Transwells®. The last two conditions were grown over 12 mm inserts with 0.4 µm pores, and with media volumes of 400 µl on the apical side and 1300 µl on the basal side of the cultures. Furthermore, to expand the host proteome library, published reads (24) of the bronchial epithelium cell line S9 were also used. These cells are immortalized cells isolated from a patient with cystic fibrosis that were transformed with a hybrid virus adeno-12-SV40 (ATCC® number CRL-2778) (25). For the construction of the host proteome spectral library, aliquots of the different samples of whole cell lysates of 16HBE14o- in UT buffer were mixed, and then 25 µg of the extract mixture was fractionated by SDS-PAGE. The gel was partitioned into ten protein-containing pieces that were destained by 15 min washes with ammonium bicarbonate solution (200 mM) in 50% acetonitrile at 37°C and 500 rpm. Then, the gel pieces were dehydrated by incubation with acetonitrile at 37°C and 500 rpm. The supernatant was discarded afterwards. Proteins in each gel piece were in-gel digested overnight at 37°C with 20 µl of trypsin (10 ng·µl<sup>-1</sup>) and 30 µl ammonium bicarbonate solution (20 mM). Lastly, the peptides were extracted by addition of 0.1% acetic acid and incubation in an ultrasound bath for 30 min. Afterwards, the supernatant was collected, 50% acetonitrile with 0.05% acetic acid were added to the gel pieces for another 30 min incubation, and both supernatant fractions were united. Two of the supernatants of the ten SDS-PAGE fractions were mixed to generate five final samples with essentially the same protein quantity, which were then used for further processing and DDA-measurements.

The tryptic peptides derived from bacterial or human proteins were concentrated and purified using C<sub>18</sub> ZipTip columns (Merck Millipore, Germany). All samples

were resuspended in a buffer consisting of 2% acetonitrile and 0.1% acetic acid in MS-grade water. Indexed Retention Time (iRT) peptides (Biognosys AG, Switzerland) were added to the samples for feature alignment, peak calibration and signal quantification. The spike in of the samples was carried out according to the manufacturer's instructions assuring that the injected volumes have one IE (injection equivalent) of iRT peptide mix (Biognosys AG, Switzerland). The final volume of the samples and the injection volumes were set to 12  $\mu\text{l}$  and 10  $\mu\text{l}$  for *S. aureus* samples, 20  $\mu\text{l}$  and 5  $\mu\text{l}$  for 16HBE14o- samples, and 20  $\mu\text{l}$  and 4  $\mu\text{l}$  for the spectral library samples, respectively.

## Mass spectrometry measurements

Tryptic peptides were separated on an Accucore 150-C18 analytical column of 250 mm (25 cm  $\times$  75  $\mu\text{m}$ , 2,6  $\mu\text{m}$  C18 particles, 150  $\text{\AA}$  pore size, Thermo Fischer Scientific, USA) using a Dionex Ultimate 3000 nano-LC system (Thermo Fischer Scientific, Germany). Peptides were eluted at a constant temperature of 40°C and a flow rate of 300 nL/min with a 120 min linear gradient (2% to 25%) of buffer (acetonitrile in 0.1% acetic acid).

To design a spectral library MS/MS data were recorded on a Q Exactive mass spectrometer (Thermo Fischer Scientific, Germany) in data dependent mode (DDA). The MS scans were carried out in a  $m/z$  range of 300 to 1650  $m/z$ . Data was acquired with a resolution of 70,000 and an AGC target of  $3 \cdot 10^6$ . The top 10 most abundant isotope patterns with charge  $\geq 2$  from the survey scan were selected for fragmentation by high energy collisional dissociation (HCD) with a maximal injection time of 120 ms, an isolation window of 3  $m/z$ , and a normalized collision energy of 27.5 eV. Dynamic exclusion was set to 30 s. The MS/MS scans had a resolution of 17,500 and an AGC target of  $2 \cdot 10^5$ .

MS/MS analyses of samples were performed in data independent mode (DIA) on a Q Exactive Plus mass spectrometer (Thermo Fischer Scientific, Germany) following the method described by Bruderer et al. (26). Briefly, the data was acquired in the  $m/z$  range from 400 to 1220  $m/z$ , the resolution for MS and MS/MS was 35000, and the AGC target was  $5 \cdot 10^6$  for MS, and  $3 \cdot 10^6$  for MS/MS. The number of DIA isolation windows was 19 with 2  $m/z$  overlap. For further details to the instrumental setup and the parameters for LC-MS/MS analysis in DDA and DIA mode see Supplemental Tables S1 and S2.

## Immunofluorescent confocal microscopy

Time-lapse imaging was carried out with a DeltaVisionRT deconvolution microscope (GE Healthcare Europe GmbH, Germany). To perform the imaging, the actual infection experiment was carried out on a glass bottom 35-mm plate (MatTek, USA). After a change of media with lysostaphin, the plate was transferred to the microscope base under incubation conditions. Imaging of the epithelial layer was performed by light microscopy, while GFP fluorescent bacteria were observed by excitation with a 490/20 nm mercury vapor lamp and detection of fluorescence at 528/38 nm. Image acquisition was performed every 5 min for the first 48 h, then from 48 h to 72 h and finally from 92 h to 96 h. Picture processing was performed with Fiji (<http://fiji.sc/Fiji>).

Subcellular localization of microtubule-associated protein 1A/1B-light chain (LC3) and lysosomal-associated membrane protein 1 (LAMP-1) by immunofluorescence microscopy was performed using a Leica TCS SP8 Confocal laser scanning microscope (Leica Microsystems B.V., Netherlands). The cells were seeded over coverslips of 18 mm diameter three days prior to infection as described above. However, in this case a HG001  $\Delta$ spa mutant was used to avoid aspecific IgG binding. The samples were collected at 0 h, 1 h, 2.5 h, 6.5 h, 24 h, 48 h, 72 h, and 96

h by fixation with 2% para-formaldehyde (PFA) for 20 min at room temperature. Preparation of the samples for the actual microscopy was performed simultaneously after conclusion of the experiment. The samples were permeabilized with 0.5% Tween 20 for 30 min at room temperature and then nonspecific binding sites were blocked with 1% bovine serum albumin, 10% FCS in 0.07% Tween 20 for 120 min at room temperature. All antibodies were diluted in blocking solution. Primary rabbit anti-LC3B (Cat. No. 1384; Novus Biologicals, Netherlands) and mouse CD107a (LAMP-1; Cat. No. 555798; BD, Netherlands) antibodies were used at 1:500 and 1:100 dilutions, respectively. The incubation was carried out simultaneously for 1 h at room temperature in a humidified chamber. The secondary Goat anti-rabbit antibody conjugated with Alexa Fluor 594 (A11012; Invitrogen, Netherlands) and goat anti-mouse antibody conjugated with Alexa Fluor 647 (A-21236; Invitrogen, Netherlands) were used, both, at a 1:500 dilution with incubation for 1 h at room temperature. Lastly, the DNA was stained with 4',6-diamidino-2-phenylindole (DAPI), the slides were mounted with Mowiol® 4-88 mounting medium (EMD Chemical, Inc., CA, USA) and stored at -20°C until microscopic visualization.

## Transmission electron microscopy (TEM)

After the invasion assay, 16HBE14o- cells were fixed with 0.2% glutaraldehyde and 2% PFA in 0.1 M sodium cacodylate buffer (pH 7.4) for 10 min. Subsequently, the fixative solution was replaced with new fixative solution and incubation was continued for 30 min at room temperature. The cells were rinsed twice for 5 min each in 0.1 M cacodylate buffer at room temperature followed by post-fixation in 1% Osmium tetroxide/1.5% potassiumferrocyanide in 0.1M sodium cacodylate at 4°C for 30 min. The 16HBE14o- cells were then incubated with 1% tannic acid in 0.05 M of sodium cacodylate buffer for 5 min to enhance the color of the 16HBE14o- cell membranes and demonstrate the internalization of *S. aureus*. The

cells were washed with Milli-Q water, dehydrated through serial incubation in graded ethanol (30%, 50%, 70% and 100%) and lastly embedded in EPON resin (Hexion, USA). Ultrathin sections (80 nm) were cut with an UC7 ultramicrotome (Leica, Austria) and contrasted using 5% uranyl acetate for 20 min, followed by Reynolds lead citrate for 2 min. Images were recorded with a FEI CM100 transmission electron microscope operated at 80 KV using a Morada digital camera.

## Identification and quantification of proteins

Human proteins were identified using Spectronaut™ Pulsar 11 (v11.0.18108.11.30271) software (Biognosys AG, Switzerland) against a human bronchial epithelial cell line generated from data-dependent acquisition measurements of 16HBE14o- samples and 12 additional data sets of the cell line S9 that were previously published (24). The spectral library construction was based upon a Comet database search using a human protein database in a target-decoy approach using the trans-proteomic-pipeline (TPP) version 4.8.0 PHILAE (27, 28). The raw files were converted to mzML files with msconvert (Proteowizard version 3.0.11537; 31<sup>st</sup> November 2017) using a vendor peak picker on spectra with MS level 1-2. Then, the mzML files were searched with the Comet search engine (2014.02 rev. 0) against a human data base that comprised 20.217 Uniprot-reviewed entries (February 2018), 102 cRAP common contaminants entries (<https://www.thegpm.org/crap/>) and 1 entry for the concatenated iRT peptides. The target-decoy version of this database was generated by adding all reverse entries resulting in 40.640 entries in total. The target-decoy search was performed with a parent mass error of  $\pm 20$  ppm, fragment mass error of 0.01 Da, and allowing full-tryptic peptides (trypsin/P cleavage rule) with up to two internal cleavage sites. The search included fixed modification of +57.021464 for carbamidomethylated cysteine and variable modification of +15.9949 for oxidized

methionine. The search results were scored using PeptideProphet (29) and iProphet (30) with a minimal peptide length of 7 amino acids. The global protein FDR calculation of 0.01 was assessed with MAYU (31). The filtered peptide spectrum matches were used to generate the ion library in Spectronaut™ v11.0.15038.14.27660 (Asimov; Biognosys AG, Switzerland) setting the m/z mass range from 300 to 1,800, 6 to 10 fragments per peptide, removing fragments smaller than 3 amino acids, no segmented regression, and a minimum root mean square error of 0.5.

The *S. aureus* ion library used in this study was generated previously (32). Briefly, the data sets used for the construction of this library comprise samples of the cytosolic and exoproteomes of *S. aureus* HG001 and the isogenic  $\Delta$ rho mutant ST1258. This ion library was constructed with a similar protocol as the one applied for the host library. The Comet database search was based on the fasta file from AureoWiki (33). This database comprises 2,852 *S. aureus* protein entries. The final database used for the target-decoy approach contains 5,944 entries in total (including cRAP contaminants). The peptide spectral matching was performed using the trypsin/P digest rule with a number of tolerable termini (NTT) of 2, a parent mass error of  $\pm 30$  ppm, fragment mass tolerance of 0.01 Da, variable modification of +15.9949 for methionine oxidation and fixed modification of +57.021464 for carbamidomethylation (sample preparation-dependent). The generation of the ion library in Spectronaut™ v11.0.15038.14.27660 resulted in a constructed library consisting of 2,154 proteins with 38,570 tryptic peptides.

The Spectronaut DIA-MS analysis was carried out using dynamic MS1 and MS2 mass tolerance, dynamic XIC RT extraction window, automatic calibration, dynamic decoy strategy (library size factor = 0.1, minimum limit = 5000), protein Q-value cutoff of 0.01, precursor Q-value cutoff of 0.001. The search included variable modifications of +15.9949 for oxidized methionine, and if reduction and

alkylation was used, fixed modifications of +57.021464 for carbamidomethylated cysteine. A local cross run normalization was performed using complete profiles with a Q-value < 0.001. The MS2 peak area was quantified and reported. Missing values were parsed using an iRT profiling strategy with carry-over of exact peak boundaries (minimum Q-value row selection = 0.001). Only non-identified precursors were parsed with a Q-value > 0.0001. Ion values were parsed when at least 25% of the samples contained high quality measured values. The settings for the Spectronaut™ analyses are available in Supplemental Table S3. Afterwards, parsed values were filtered out again, if they were more than two-fold higher than the measured values preventing false positives due to parsing. For further analyses proteins with at least two identified peptides were taken into account. The identified proteins were annotated based on the Uniprot database and the gene names for *S. aureus* were extracted from AureoWiki (33).

## Statistical testing of changes in protein abundances over time

Peptide intensities were normalized by the mean of all time points. The time-course data of each protein were then calculated as the median of all normalized peptide data belonging to that protein. Subsequently, the protein data were analyzed using the LIMMA package version 3.34.9 (34) in R version 3.4.4 (21). First, a natural regression spline with four degrees of freedom was fitted for each protein, considering that expression changes smoothly over time. Then, a linear model (35) with eight parameters was fitted to the data, including an intercept, four spline parameters and three parameters corresponding to comparability of the four replicates. An empirical Bayes moderated F-test was conducted for each protein, which can detect very general changes over time while simultaneously testing for similarity of the replicates. Due to general differences in replicate 1 data at 6.5 h and 24 h, these 16HBE14o- cell samples were excluded for the testing only,

but not for calculating the median values. The moderated p-values were corrected for multiple testing using Benjamini and Hochberg's multiple testing correction. Finally, proteins with an adjusted p-value below  $\alpha = 0.01$  were assumed to be significantly changed during the time course of infection. For further analyses, the data were averaged over the replicates using the median for each protein and shifted to start in zero at time point 0 h.

Afterwards the time course data of all significantly changed proteins were clustered using a noise-robust soft-clustering (fuzzy c-means) implemented in the Mfuzz package version 2.38.0 (36, 37) in R version 3.4.4 (21). Since the clustering is performed in Euclidian space, the expression values of proteins were standardized for clustering only to have a standard deviation of 1, so that only the dynamics were considered. The optimal number of clusters was chosen using both a cluster validity index (minimum centroid distance) and a manual validation of biologically meaningful groupings.

## Data and Software availability

The identified peptide ions and their Q-values are included in Supplemental Tables S4 and S5. All protein annotations and median abundances are included in Supplemental Tables S6 and S7. The raw files from mass spectrometry have been deposited in MassIVE (<https://massive.ucsd.edu>) with the access codes MSV000082920 (*S. aureus*) and MSV000082923 (16HBE14o-).

## Results

*S. aureus* population displays a dormant state after 48 h p. i. in human epithelial cells.

To analyze physiological changes in *S. aureus* internalized by 16HBE14o- lung epithelial cells over an extended period of time, we applied a previously



established infection assay (22) and assessed the longest time span over which bacteria could be reproducibly isolated from the infected cells in sufficient amounts to enable proteome profiling. Pilot experiments showed that this is possible for at least 96 h, which was therefore, selected as the end point for all further analyses. During these 96 h, the fate of the infected cells and the internalized bacteria was recorded through time-lapse microscopy as shown in the three Supplemental movies and illustrated through snapshots in Figure 1A. Additionally, the abundance of the bacterial population during infection was measured by quantification of the mean fluorescence intensity (Figure 1B). These data show that the internalized bacteria do not multiply significantly during the first 8 h p.i. Subsequently, the majority of bacteria start to proliferate leading to lysis of their respective host cells. Of note, in the applied experimental setup, host cell lysis is suicidal for the bacteria due to the presence of lysostaphin in the medium. Accordingly, the liberated bacteria disappear and cannot re-infect other cells. After approximately 30 h p.i., non-replicating bacteria remain detectable within the surviving host cells until the end of the experiment at 96 h p.i. These findings were corroborated by flow cytometric counting of the bacterial numbers (Figure 1C). Notably, two distinctive bacterial phenotypes were observed over time, namely one involving high rates of intracellular bacterial replication and another one involving internalized bacteria in a dormant state. Furthermore, while the number of host cells remains essentially constant during the first 24 h p.i., this number increases during later stages (Figure 1C). The percentage of host cells that contain bacteria gradually decreases over time, starting with a maximum of ~27% at 2.5 h p.i. and ending with ~13% at 96 h p.i.

As microscopy and flow cytometry cannot reveal the intricacies of the processes occurring in host cells and internalized bacteria, we employed quantitative proteomics profiling. This approach has the advantage of quantifying many different proteins belonging to the adaptive processes in bacteria and the human

host cells with good reproducibility. Thus, changes in each protein's abundance can be followed over time and compared. Through data-independent acquisition,

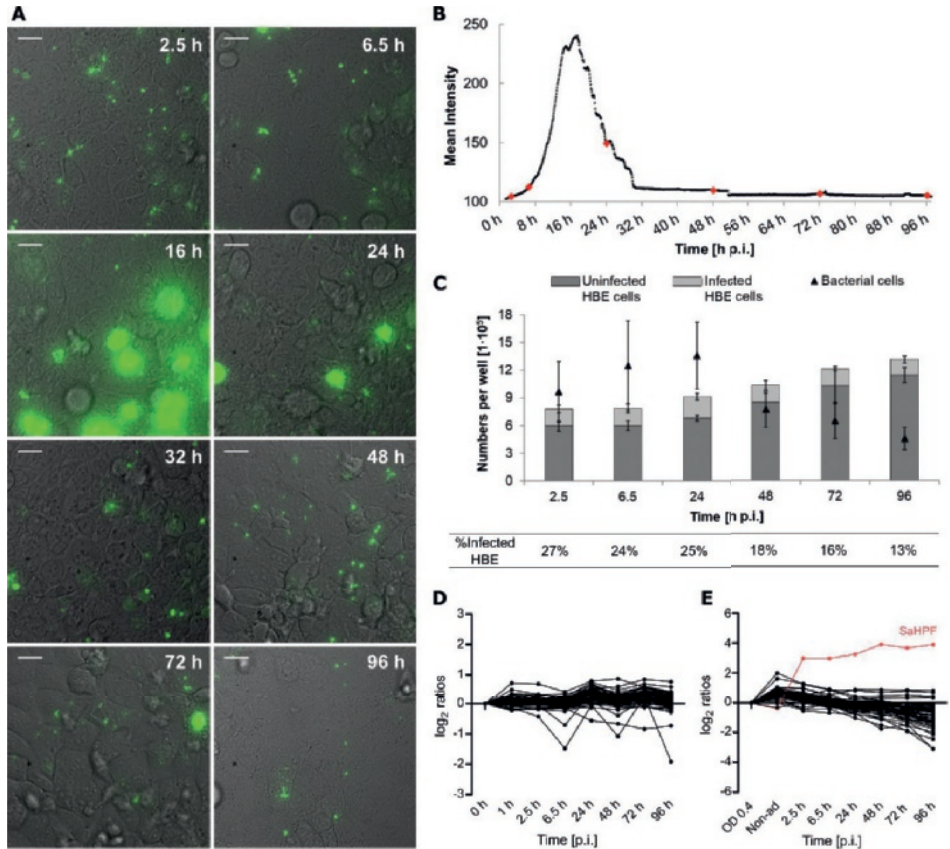


**Figure 1. After internalization two subpopulations of *S. aureus* can be distinguished by differences in replication rate.** The progression of the infection was followed by time-lapse microscopy (A; Supplemental videos; scale bar=20  $\mu$ m) and the GFP fluorescence intensity was quantified to elucidate the dynamics of the bacterial population (B). Most of the bacteria replicate intracellularly during the first day of infection, but a secondary subpopulation remains in a dormant state during the whole time of observation. The red dots indicate the time points of sample collection for further experiments. Counting of bacterial cells, and infected and uninfected host cells, as jointly presented in (C) confirmed the changes in both populations. Average values of four replicates are presented (B-C). Mass spectrometry quantification of ribosomal proteins of the host (D) or *S. aureus* (E). The list of proteins presented in the line plots is available in Supplemental Table S8. The levels of the proteins were calculated based on the mid-exponential phase or the 0 h time point as reference, for the bacteria and the host, respectively. The SaHPF protein detected in higher amounts is colored in red.

application of an in-house built *S. aureus* HG001 spectral library (24, 32) and human cell line spectral libraries, we achieved a complete data collection for 3644 human and 930 staphylococcal proteins at all time points during 96 h p.i. (Supplemental Tables S6 and S7). Since the bacterial population displays two different phenotypes with different prominence at the different stages of infection, the observed proteome dynamics describe the adaptive changes in the bacteria at each stage and the final 'shape' of the persistent bacteria. Likewise, these measurements record the influence of the intracellular bacteria on the host's physiological state over time. To determine the weight of the observed changes, the generated bacterial and host proteome data were fitted to spline lines and tested against constant linearity. This linearity test takes into account the replicates' variability, rendering it an indicator of the reliability of the observed changes. Furthermore, all proteins that show significant changes were clustered depending on their behavior over time, thereby marking the stages p.i. at which important changes take place (Supplemental Figure S2).

The differences in bacterial and host replication rates as observed by microscopy are mirrored in the abundance of the respective ribosomal proteins (Figure 1 D-E). Consistent with their unimpaired growth, the host cells do not show major regulatory changes in ribosomal protein abundance over the time course of infection. In contrast, the amounts of bacterial proteins that make up the small and large ribosomal subunits start to decrease after internalization, being detectable at substantially lowered amounts at 48 h p.i. This time point correlates with the absence of bacterial growth observed in the live cell imaging. An exception to this general trend is the '*Staphylococcus aureus* hibernation promotion factor' (SaHPF), which shows significantly increased levels right from the start of infection (Figure 1E). This protein represses translation, and therefore, it is important for survival in the stationary phase and during conditions of nutrient deprivation (38, 39).

Nutrient competition affects primarily *S. aureus*, but staphylococcal persistence triggers changes in host metabolism at 48 h p.i.

The acquisition of metabolites and their subsequent conversion to cellular constituents is a fundamental feature of all living organisms. This implies that different organisms residing in the same system are likely to compete for nutrients. Accordingly, internalized *S. aureus* will compete with the host for carbon sources. This is clearly reflected in the proteins required for central carbon metabolism, both in the bacteria and the host. At first instance, the proteins related to the bacterial glycolytic pathway remain fairly stable upon internalization displaying similar levels as encountered in exponentially growing bacteria (Figure 2). Yet, at 6.5 h p.i., the pathogen displays changes in the levels of most of the proteins related to the glucose activation phase. Correspondingly, the host presents similar changes, but only from 48 h p.i. onwards, which coincides with transition of the *S. aureus* population into a dormant state. Remarkably, during the entire course of infection, neither the pathogen nor its host regulates proteins related to the production of acetyl-CoA from pyruvate. During nutrient-rich conditions, *S. aureus* will produce acetate from acetyl-coA, thereby providing the NAD<sup>+</sup> necessary for the glycolysis process (40). Our analysis shows that, upon internalization, the bacteria repress some of the respective enzymes, but this regulation is reversed 48 h p.i., suggesting that the dormant bacteria restart the production of acetate. Proteins involved in the TCA cycle do not mirror this behavior, displaying increased levels upon internalization and remaining at a constant increased level over the whole duration of the experiment. This strategy would supply the bacteria with sufficient metabolic energy under conditions of low glucose availability. The strongest level increase takes place around 24 h p.i., which corresponds to the transition in subpopulation predominance from the

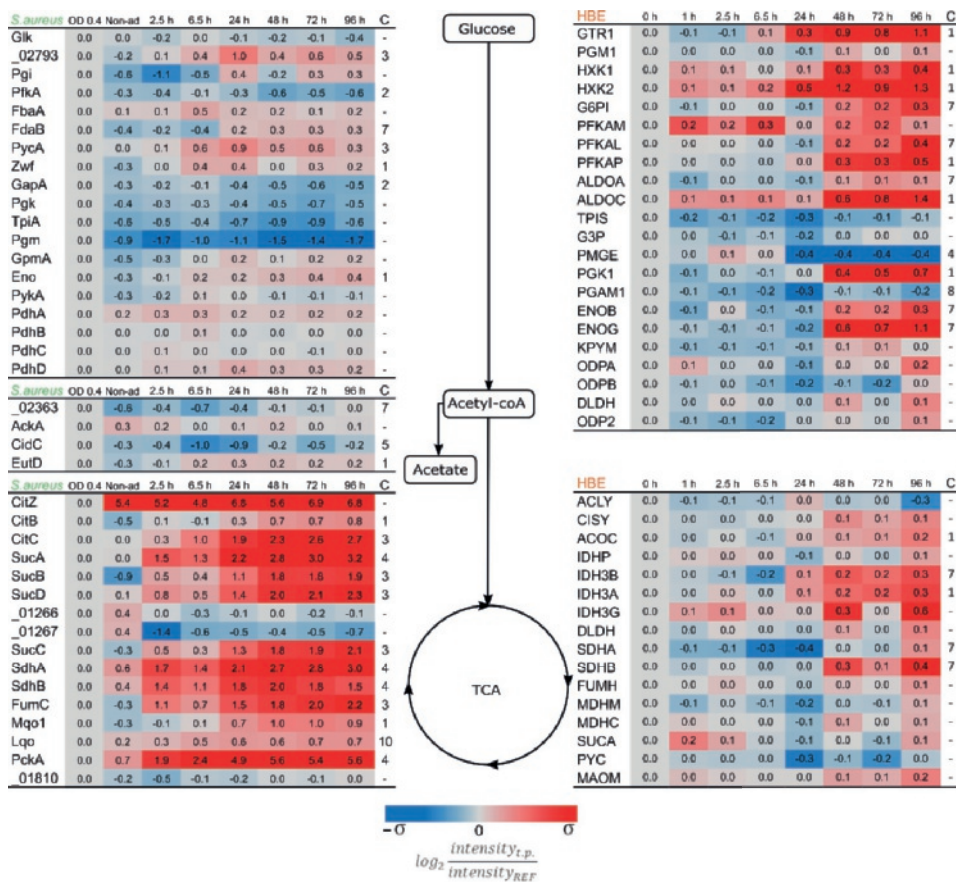


**Figure 2. Quantification of proteins related to the central carbon metabolism.** Proteins were grouped depending on their main function in the different pathways, and boxes mark selected central metabolites. The proteome data from *S. aureus* are depicted on the left side of the diagram and the proteins without assigned gene symbol are labeled according to their locus tag without the “SAOUHSC\_” identifier. The host data are shown on the right side of the diagram. Protein trends that deviate (p-value < 0.01) from constant linearity over time were fitted to clusters according to their behavior (Supplemental Figure S2). Clustering assignment is shown in the last column “C”. The color coding is based on the standard deviation of each set of data.  $\sigma_{S. aureus}$  = 2.34 and  $\sigma_{HBE}$  = 0.33. The ratios were obtained from the measurements of four biological replicates

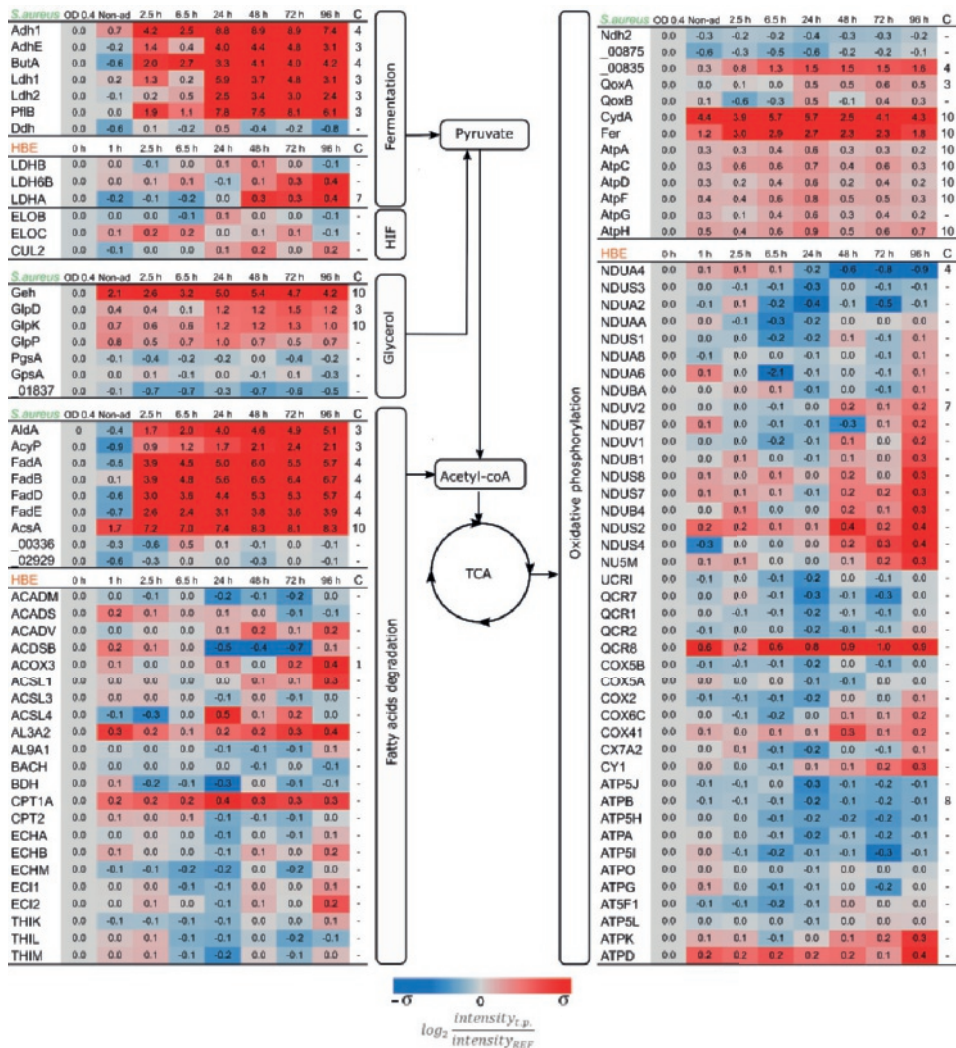
replicating to the dormant phenotype of the bacteria. The two proteins of this pathway that do not display increased levels (SAOUHSC\_01266, and SAOUHSC\_01267) are 2-oxoglutarate oxidoreductases, which participate in

reverse TCA cycle and synthesize 2-ketoglutarate. In contrast to the bacteria, most TCA cycle proteins from the human host cells show no changes in abundance, except for those involved in the metabolism of fumarate and  $\alpha$ -ketoglutarate. Of note, these compounds are key intermediates in amino acid metabolism.

After the first 2.5 h p.i., the bacteria activate pathways related to energy acquisition from alternative sources, like fatty acids, as can be inferred from the elevated levels of *S. aureus* proteins involved in the catabolism of glycerol and fatty acids (Figure 3). This increased level of fatty acid degrading enzymes becomes even stronger after the bacteria are predominantly in a dormant state, suggesting that the persistent bacteria prefer fatty acids over glycerol. This effect is not observed in the host proteome, where the levels of most proteins related to fatty acid degradation do not show major modifications.

Oxygen is a key factor limiting bacterial metabolism during infection due to the microaerobic environment they are exposed to after internalization (13, 17). This is clearly reflected by the mild increase in *S. aureus* proteins related to fermentation upon internalization (Figure 3), but the major rise takes place after 24 h p.i. On the other hand, most proteins related to the electron transport chain present a peak of upregulation at 24 h p.i., after which their abundance decreases. Conversely, the host proteome does not show major changes regarding the possible competition for oxygen. Only four proteins related to fermentation and oxidative phosphorylation present some regulation (Figure 3). In addition, the proteins Elongin-B (ELOB), Elongin-C (ELOC) and Cullin-5 (CUL2), which are involved in the degradation of the Hypoxia-Inducible Factor (HIF $\alpha$ ) remain constant over time, indicating that there is no increase in the abundance of this factor and suggesting that the host cells do not perceive a reduction of the available oxygen.

Amino acids are major alternative sources for carbon and nitrogen, which may play a role in adaptations of a pathogen to the intracellular milieu. In particular



arginine, asparagine, and tryptophan have gained interest due to their relevance in the host's and bacterial defense mechanisms (41, 42). The pathways for biosynthesis and degradation of amino acids are complex since they are interconnected. Nevertheless, the proteomics data purport that *S. aureus* employs most pathways needed for amino acid metabolism during the entire course of infection. Conversely, the host proteome is geared towards utilization of amino acids that are primarily linked to the TCA cycle (Figure 4).

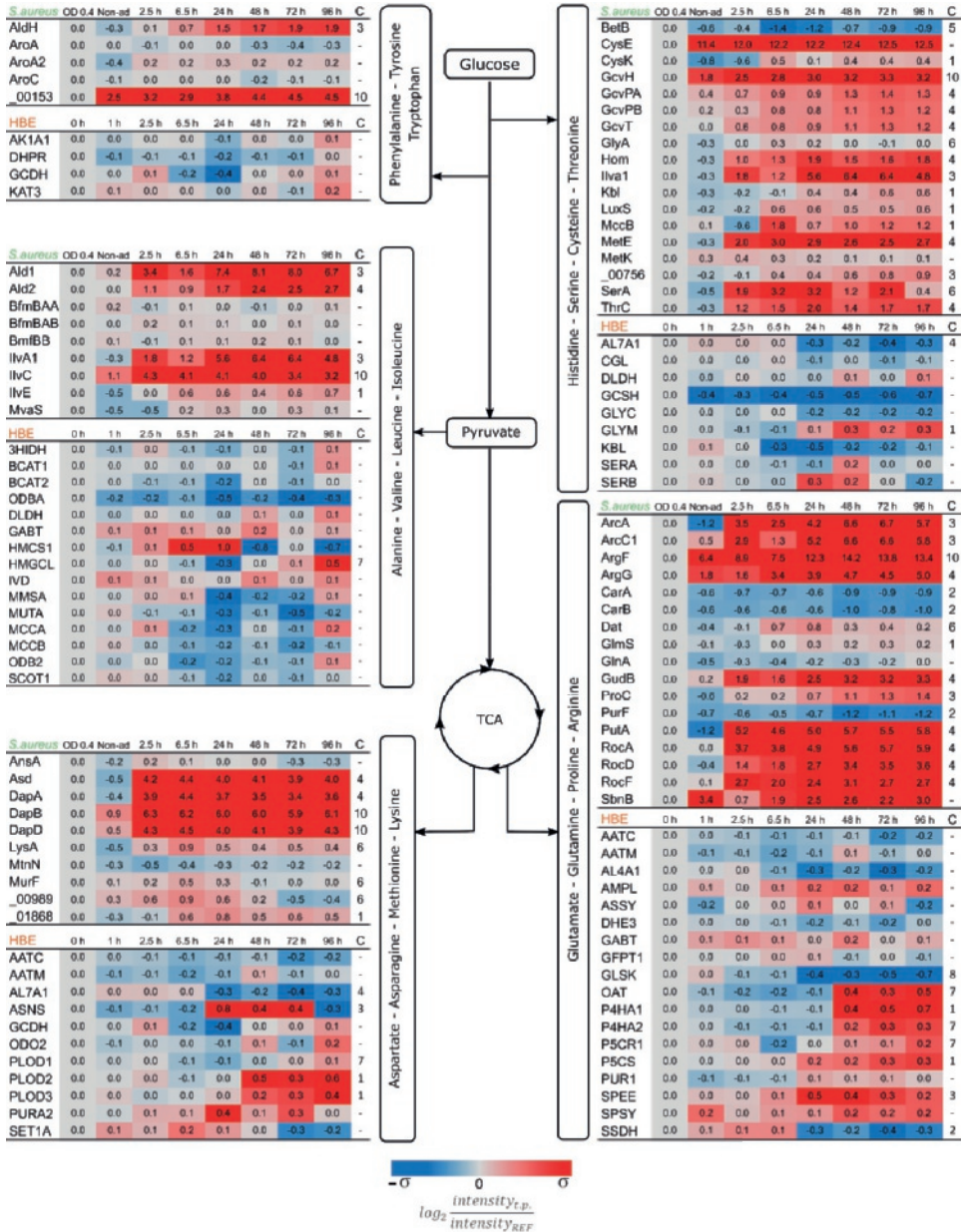
◀ **Figure 3. Proteins related to alternative carbon sources and respiration.** Assignment of proteins to pathogen (*S. aureus*) and host (HBE) is indicated on top of the respective protein groups. Due to limited carbon sources post infection, alternative pathways for energy consumption are upregulated. Substrates like glycerol and fatty acids are being consumed during intracellular conditions. Another major adjustment is related to oxygen availability which affects the pathways related to fermentation and oxidative phosphorylation. The protein quantities were derived from the mass spectrometry measurements of four biological replicates. Time trends with significant changes ( $p$ -value  $< 0.01$ ) were fitted into different clusters depending on their behavior (Supplemental Figure S2). The assigned cluster is presented in the column "C". The color coding is based on the standard deviation of each set of data.  $\sigma_{S. aureus} = 2.34$  and  $\sigma_{HBE} = 0.33$ . HIF: Hypoxia-Inducible Factor.

---

Bacterial enzymes linked to the degradation of histidine, serine, cysteine and threonine show increased levels right from the moment of internalization, even preceding the start of intracellular replication. These proteins are related directly with the generation of precursors of pyruvate and the one-carbon metabolism. Nevertheless, since there is no replication of bacteria after 48 h p.i., the degradation of histidine, serine, cysteine and threonine is most likely used to access an alternative carbon source. On the contrary, the infected host cells induce the GLYM protein at later stages of infection, which is directly related to the conversion of serine into glycine and 5,10-methylenetetrahydrofolate. The latter molecule is an indispensable building block for purine biosynthesis (43, 44). This finding is fully consistent with the continuing growth of the human cell layer once the internalized pathogen predominantly presents a state of dormancy after 48 h p.i.

Branched-chain amino acids (BCAAs; Valine, Leucine, Isoleucine) are essential for human cells and, thus, need to be ingested from the environment. Consequently, the human proteins handling these amino acids are all involved in their degradation. Only at the last time point p.i. the human proteins addressing BCAAs have slightly increased levels (Figure 4). On the other hand, the BCAAs play a crucial role in the regulation of *S. aureus* metabolism, since they serve as





cofactors for CodY. This regulator also represses the production of the IlvA1, IlvE and IlvC proteins, which have all increased abundance to participate in the biosynthesis of BCAAs (45). In parallel, the observed upregulation of the Ald1 and Ald2 proteins involved in the degradation of alanine implies that also this amino acid is used as an alternative carbon source during infection.

◀ **Figure 4. Progression of the pathways related to amino acid metabolism.** Assignment of proteins to pathogen (*S. aureus*) and host (HBE) is indicated on top of the respective protein groups. The catabolism of amino acids after infection would provide resources to compensate for the lack of carbon and nitrogen sources. Moreover, the anabolism of these molecules is likewise required for some defensive functions of either the bacteria or the host. The represented ratios are the average of four biological replicates. Proteins with significant changes (p-value <0.01) were clustered in groups depending on their general behavior and their assigned cluster is showed in column "C". The color coding is based on the standard deviation of each set of data.  $\sigma_{S. aureus}$ = 2.34 and  $\sigma_{HBE}$ = 0.33.

---

The amino acid catabolic pathways related to the TCA cycle are mostly needed to generate the intermediate molecules  $\alpha$ -ketoglutarate, oxaloacetate and fumarate. *S. aureus* increases levels of proteins from the urea cycle (RocADF; ArcAC) to degrade arginine and also to produce  $\alpha$ -ketoglutarate from glutamate (GudB). Therefore, these substrates are used to feed the TCA cycle. Of note, the degradation of arginine is carried out by two pathways. Firstly, the arginase pathway will produce glutamate (46) and presents upregulation right from the beginning of the infection (RocADF). Similarly, the arginine deaminase pathway (ArcAC), converting arginine to ornithine (47), expresses higher levels from the beginning of the infection but its highest quantities are found in the dormant bacterial population. Further, upregulated proteins associated with aspartate metabolism are dedicated to the production of lysine, as was also observed by Michalik et al. and Surmann et al. (13, 24). In contrast to the internalized bacteria, the amino acid metabolism in the infected host cells is geared towards the biosynthesis of amino acids for protein production. Specifically, the glutamate and aspartate metabolic pathways are upregulated in relation to the formation of collagen (PLOD2, PLOD3, P4HA1, P4HA2), and the synthesis of asparagine (ASNS), L-proline (OAT, P5CR1) and spermidine (SPEE). With exception of ASNS and SPEE, all of these regulatory events start to take place after 48 h p.i. with a constant increment.

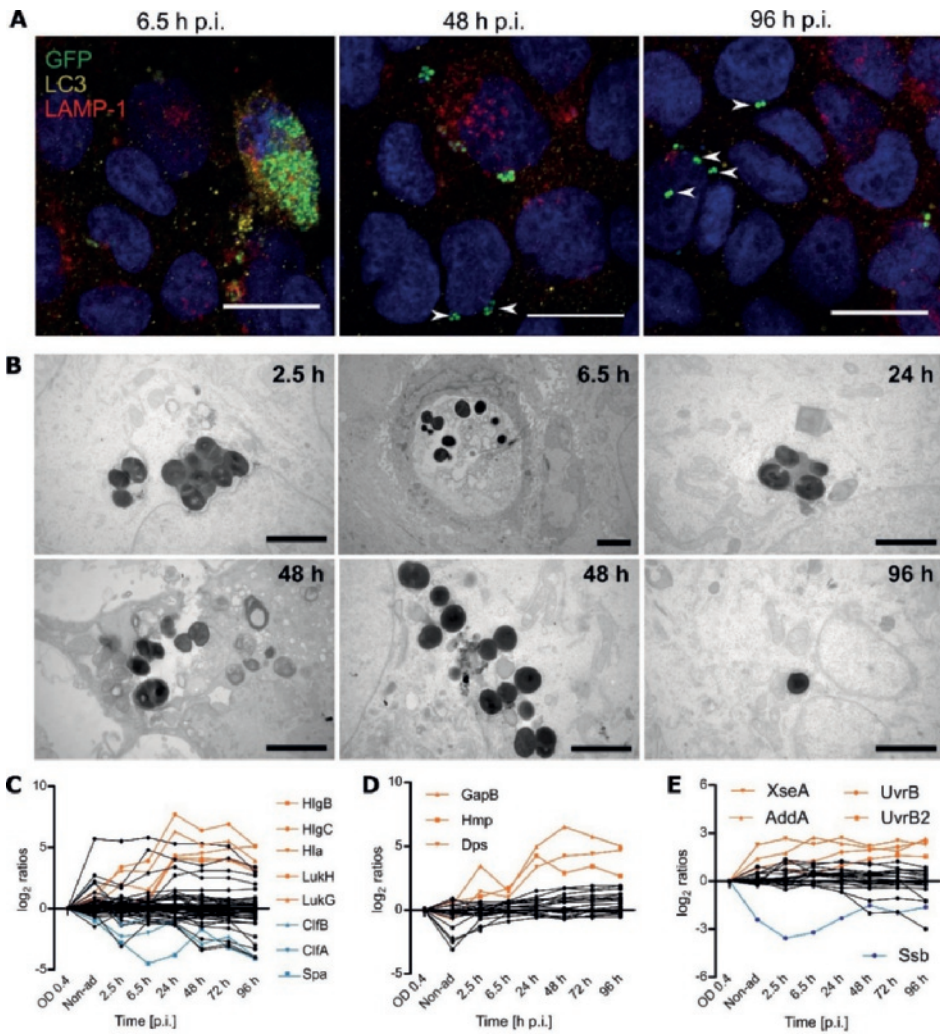
*Staphylococcus aureus* escapes degradative compartments, leading to a persistent population residing in the cytosol.

Since *S. aureus* can reside in different intracellular niches, we determined the subcellular location of the bacteria over time through confocal immunofluorescence microscopy (Figure 5A; Supplemental Figure S3). Inspection of the co-localization of the GFP-positive bacteria with LAMP-1 and LC3 revealed that, during the first 24 h p.i., most of the bacteria are located inside membranes. Specifically, the replicating population resides inside LAMP-1- or LC3-associated compartments, while individual bacteria or small bacterial clusters are detectable in the cytosol from 2.5 h p.i. with increasing frequency over time. Ultimately, at the last time points, most observed bacteria do not co-localize with the membrane markers, suggesting a cytosolic localization of the persistent subpopulation. To substantiate these findings, we performed transmission electron microscopy (Figure 5B; Supplemental Figure S4), highlighting that the replicating bacteria localize inside so-called ‘light phagosomal compartments’ or ‘dark degradative compartments’, which are possibly lysosomes, during the first 48 h p.i. Further, at 72 h and 96 h p.i. all bacteria are no longer enclosed by a membrane, ultimately showing that the persister population resides in the cytosol. Of note, all bacterial clusters found inside phagocytic membranes are located in dying host cells (Figure 5B, Supplemental Figure S4).

Considering that the escape of *S. aureus* from the vesicles relies on particular toxins (48), we inspected the possible presence of staphylococcal virulence factors. Consistent with the observed changes in the subcellular localization of bacteria, the toxins HlgB, HlgC, Hla, LukH and LukG are upregulated after 24 h p.i. (Figure 5C; Supplemental Table S8). These pore-forming proteins have been correlated

with escape and subsequent host cell lysis (48). Of note, all these toxins are regulated by the Agr and/or SaeSR systems that positively or negatively regulate many more proteins involved in pathogenesis (49). Accordingly, the surface-bound protein Spa, which is negatively regulated by Agr, is present in decreased amounts upon internalization with a minimum at 6.5 h p.i. A similar but less pronounced trend is observed for the surface-bound proteins ClfA and ClfB, the expression of which relies also on other regulators, such as the sigma factor B (SigB) in case of ClfA.

As the physicochemical conditions within different subcellular compartments differ substantially, bacteria within these compartments need to respond appropriately to different stresses. This is particularly true for lysosomes and phagosomes, which represent acidic compartments. In addition, the phagosomes are known to produce massive amounts of reactive oxygen species (ROS). Such conditions have a strong propensity to damage bacterial macromolecules, such as DNA and proteins. Indeed, the levels of many bacterial proteins involved in the prevention of oxidative damage are altered over time. These include KatA, SodA, SodM, AhpC, GapB, Hmp, and Dps (Figure 5D; Supplemental Table S8). In particular, the latter three proteins present a strong upregulation. GapB increases the production of NADPH, which is needed to keep antioxidant proteins in a reduced state to allow them to reduce ROS and keep cytoplasmic proteins in a reduced state. The nitric oxide dioxygenase Hmp is involved in NO detoxification (50), while the ferroxidase Dps prevents DNA damage by binding iron and thus inhibiting hydroxyl radical formation (51). Of note, the upregulation of these proteins is triggered at 24 h p.i., a time point at which the growing bacteria are escaping from the cells (Figure 1A, B) and the shift towards dormant/latent cells is taking place. Interestingly, the levels of these proteins remain high at later time points p.i. Similarly, proteins involved in the response to DNA damage, in particular XseA and AddA, are upregulated upon internalization (Figure 5E),



while other DNA damage-inducible proteins such as UvrB and UvrB2 are upregulated after 24 h. These observations imply that the bacteria are probably exposed to ROS and reactive nitrogen species (RNS) until 96 h p.i. and, remarkably, that this upregulation is not specifically related to the compartment in which they reside.

◀ **Figure 5. The persistent subpopulation of *S. aureus* is mostly found in the cytosolic environment of the host.** Intracellular localization of *S. aureus* was examined by colocalization with the protein markers LC3 for phagosomes, and LAMP-1 for lysosomes (A; scale bar: 20  $\mu\text{m}$ ). After internalization of *S. aureus* by the HBE cells, most of the bacterial population is located inside closed compartments. Still, the percentage of bacteria that escapes the vesicles (white arrow heads) increases over time and most of the bacteria are found in a cytosolic environment by the end of the infection. These results were corroborated by electron microscopy (B; scale bar= 2  $\mu\text{m}$ ). During the first hours of infection most bacteria are located inside degradative vesicles (dark compartments) or phagosomes (light compartments), but single bacteria escaped the closed compartments as early as 2.5 h p.i. (Supplemental Figure S4). By the end of the time of observation, at 72 h and 96 h p.i., all observed bacterial clusters are cytosolic. The displayed images are representative of different time points, additional images are provided in Supplemental Figures S3 and S4. The escape from the compartments could be induced by proteins related to pathogenesis, including toxins regulated by Agr and SaeRS (C). Moreover, this escape might have an impact on the production of stress proteins related to oxidative stress (D) and DNA repair (E). The list of proteins included in the line plots is available in the Supplemental Table S8. A selection of significantly ( $p\text{-value}<0.01$ ) regulated proteins is displayed in orange and blue. The mass spectrometry data represents the average of four biological replicates.

---

Intracellular *S. aureus* persists induce a non-apoptotic reaction of the host.

During the live cell imaging, it was observed that host cells lyse as a consequence of the replication of intracellular bacteria. This raised the question whether any indicators related to the mode of cell death could be identified. Indeed, the host cell proteome showed strong regulation of particular proteins implicated in cell death (Figure 6). Of note, most regulators involved in the so-called apoptotic and pyroptotic pathways are kinases, which require activation to perform their functions, therefore their abundance does not correlate with host responses. Consequently, we investigated the cell death mechanisms by looking at other modulators of these pathways not requiring activation. These include the BAX, BAD, DBLOH, UACA, APAF, and ACS proteins that promote the initiation of

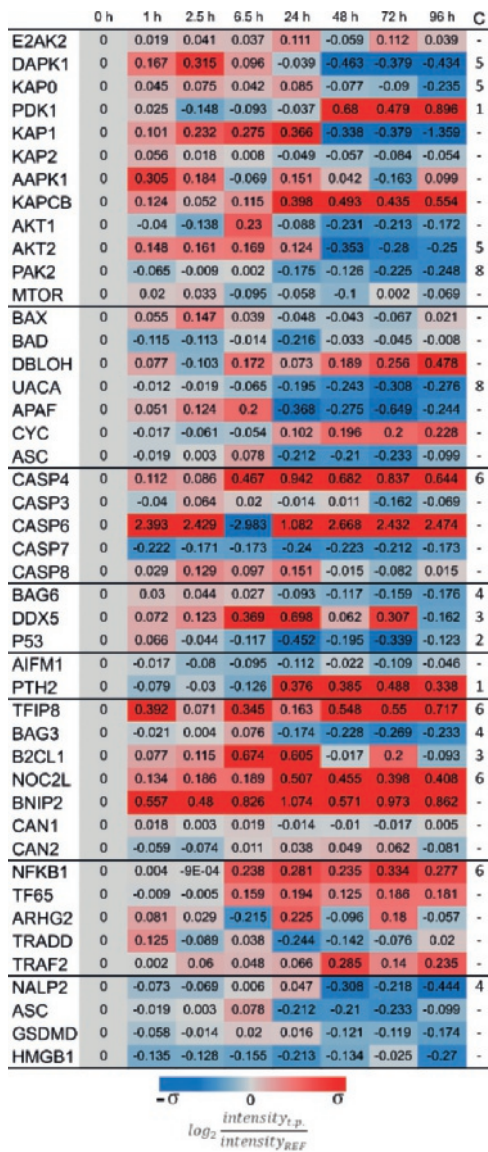


**Figure 6. Death of the host cells is not caused by induction of the classical apoptotic pathway.** Mass spectrometry data of human proteins associated with different apoptosis-related pathways are presented in the figure. From top to bottom the presented groups of proteins include: kinases, regulators of caspases, the caspases, activators of P53, proteins related to caspase-independent activation of apoptosis, anti-apoptotic proteins, proinflammatory and pro-NF- $\kappa$ B, and lastly pyroptosis. The color coding is based on the standard deviation  $\sigma_{HBE} = 0.3$

apoptosis by stimulating caspase production. However, most of these proteins present no regulation, likely leading to the observed mild abundance changes of pro-apoptotic caspases CASP3, CASP7, and CASP8. However, CASP3 and CASP8 still display moderately increased abundance at early time points until 24 h p.i., hinting at potential apoptotic events occurring during bacterial replication. CASP6, on the other hand,

is upregulated during the entire course of infection. Another pathway that can trigger apoptosis of the host cells depends on activation of P53. Its respective activators (BAG6, DDX5) are upregulated at early time points p.i., but their abundance decreases at 48 h p.i. On the other hand, anti-apoptotic proteins, such as TFIP8, 2CL1, NOC2L and BNIP2, display upregulation upon infection (Figure

6). Consistent with the latter observation, the Calpain 1 and 2 proteins, which are regulated in response to apoptosis, show no altered levels over the entire time course of infection. Lastly, it is noteworthy that CASP4 is the only caspase that shows consistent upregulation post internalization. This protein is related with the activation of the inflammasome or pyroptosis. Another protein involved in this pathway is NF- $\kappa$ B, whose upregulation appears synchronized with CASP4. Nonetheless, so-called pro-NF- $\kappa$ B proteins like TF65, ARHG2, TRADD and TRAF2 show no significant regulation. Lastly, proteins related to the activation of the inflammasome on the canonical or non-canonical pathways (52) were present at lower levels at the end of the infection, starting at 48 h p.i., indicating that these pathways are not activated. Altogether, these observations are consistent with apoptotic events that occur exclusively during the early stages of infection, when the bacteria still replicate.

## Discussion

During the infectious process, *S. aureus* has the option to evade the human immune defenses, or to invade non-professional phagocytic cells in order to hide from the host immune system and to evade antibiotic therapy. Upon internalization, the pathogen needs to adapt to the intracellular conditions so that it can survive, replicate, eventually leave the host cell and spread to other tissues. To optimise its fitness, the internalized pathogen displays population heterogeneity, where a fraction of the internalized bacterial population starts to replicate while another fraction displays low growth rates and reaches a state of dormancy (53). These two populations reflect the two main objectives of the internalized bacteria, where the replicating bacteria will ultimately disrupt epithelial cells in order to invade and infect the underlying tissue, while the dormant bacteria will persist intracellularly for an extended period of time.



Right from the moment the bacteria are internalized by a host cell, both host and pathogen need to adapt to the new situation, and then they will start to compete for resources. Importantly, such adaptations at the bacterial end are not limited to the production of virulence factors or mounting of defense mechanisms, but they also involve an optimized management of resources and the sensing of changes in the intracellular environment due to host cell adaptations (41). A clear example of this is the observed downregulation of bacterial ribosomal proteins, which relates to the formation of the alarmone ppGpp due to the induction of the stringent response upon nutrient starvation and exposure to various stresses. The ppGpp molecule is synthesized from GTP, and the resulting decrease in GTP is sensed by the CodY regulatory system of *S. aureus* (50). Of note, CodY is a major modulator of *S. aureus* central carbon and amino acid metabolism and it also influences staphylococcal virulence (54). Consistent with the idea that the observed downregulation of ribosomal proteins is a consequence of ppGpp production, we observed an upregulation of the CodY-regulated proteins PycA, AcsA, ButA, Hom, metE, SerA, ThrC, Asd, DapABD and ArgG. In this context, the activation of the *ilv-leu* operon is particularly noteworthy as this will result in the synthesis of BCAAs, which are cofactors of CodY (50). Of note, the inactivation of CodY may also result from reduced amino acid supply, and induction of the biosynthetic operons will counteract this shortage. However, high levels of BCAAs would then lead to repression again, but it remains unclear whether intracellularly such high BCAA levels are reached.

Importantly, the biological pathways in the internalized bacteria and their host cells are not isolated from each other despite their physical separation by the bacterial cell envelope. Accordingly, changes in pathway regulation at either end will impact the whole biological system. Thus, host cell homeostasis will change in response to the presence of internalized bacteria. This is exemplified by the observed optimization of glucose uptake and catabolism in the host cells from 48 h

p.i. onwards, once they predominantly carry dormant bacteria. Interestingly, this correlates with the observed shift of the bacterial intracellular localization from an encapsulated state in vesicles to a free state in the cytosol. Therefore, this re-localization event could very well be a trigger for direct competition for nutrients that has a significant impact on the host cells' energy metabolism. Similarly, under nutrient-deprived conditions, the regulation of metabolic processes plays a crucial role in the adaptation of *S. aureus* to the altered conditions intracellularly. This is underpinned by the observed upregulation of proteins that are crucial for survival of the bacteria, such as PckA, AckA, FumC, SdhA, SucC, SucA and GudB, or proteins that promote their proliferation, such as Ald1, Ald2, Pyc, AspA, Mqo1, GltA, AcnA, Icd, RocA, RocD and PutA. In fact, this observation is reminiscent of an *in vitro* study by Halsey et al. (55), who reported that under glucose restriction several of the afore-mentioned proteins have an impact on the fitness of the pathogen.

A fermentative phenotype combined with inactivation of the electron transport chain has been associated with the development of SCVs that are often observed upon intracellular persistence of *S. aureus* (40). While we did not observe the emergence of such SCVs by plating intracellular bacteria during our experimental setup, the observed changes in the bacterial proteome from 24 h p.i. onwards are indicative of a metabolic shift towards fermentation. Some of the proteins involved in bacterial electron transport become less abundant at late stages p.i compared to their levels during replication, while major proteins involved in the fermentation of pyruvate and acetate catabolism are constitutively upregulated throughout till the end of the infection. In particular, we observe a shift from terminal oxidases that require high oxygen concentrations to those that need lower concentrations, but do not pump H<sup>+</sup> anymore, which is consistent with microaerobic intracellular conditions. Further, it is known that the formation of SCVs is linked to SigB, which is an important factor for intracellular persistence

(11). Indeed, a clear role for SigB in reaching the dormancy state is indicated by changes in the abundance of 58 predominantly SigB-dependent proteins during the late stages of infection, among them Asp23, CidC, ClpL, FdhA, GapA, OpuBA and SpoVG (Supplemental Table S6). In this respect, it is noteworthy that *S. aureus* strains defective in SigB are unable to catabolize acetate (56).

Besides the changes in the central carbon metabolism of the host, the host's amino acid metabolism is also altered, altering the outcome of infection. Contrary to bacteria, which degrade amino acids mostly for the acquisition of carbon and nitrogen, the TCA-related amino acid production by the host cells is not related to an optimization of energy production but rather to the production of other molecules like purines, proline and collagen. However, some of the regulated proteins may also affect other pathways. For example, the observed asparagine synthase (ASNS) upregulation could be related to 'infection stress'. This idea would be consistent with a previous study on group A streptococcal (GAS) infection, where the pathogen was shown to induce pores in the host membranes, leading to Ca<sup>2+</sup> influx into the cytoplasm. In turn, this led to an upregulated synthesis of asparagine, which was then utilized by the pathogen (57). In our experimental setup, the ASNS abundance peaks at 24 h p.i., which correlates with the highest production of pore-forming toxins and escape of growing bacteria from the host cells, suggesting a similar regulatory mechanism as proposed for GAS.

Importantly, we observed that *S. aureus* induces its two pathways for arginine degradation right upon internalization. It has been reported that arginine depletion by the pathogen induces death of the host cell (42). Moreover, competition for arginine with the host protein iNOS reduces the production of NO, which serves in the host's antibacterial defense. Lastly, the deaminase pathway produces NH<sub>3</sub> and ATP, which supports the intracellular survival of the

bacteria. In particular, the ammonia produced increases the pH of the intracellular environment thereby preventing fusion of the endosome with the lysosome (41, 42), while the production of ATP generates a source of energy during hypoxic conditions or when the electron transport system is deficient (58). The degradation of arginine usually occurs in environments with a high proline concentration (46). Interestingly, proteins related to production of proline are upregulated in the host proteome after 48 h p.i., when the bacterial machinery for arginine catabolism becomes massively upregulated. The host cell death induced by arginine starvation is regulated by activation of AMPK, which suppresses the master regulator mTOR and could lead to autophagy (42). In this context, it is noteworthy that spermidine is implicated in autophagy as well (59), and the SPEE protein, responsible for spermidine synthesis, is part of the same host pathway that also leads to the synthesis of glutamate, glutamine, proline, and arginine. As for ASNS, the abundance of SPEE peaks at 24 h p.i., which correlates well with the localization of the bacteria in phagocytic membranes as observed by fluorescence microscopy and TEM. These results underpin a connection between host amino acid starvation and autophagy, as suggested by a recent study (60). While the roles of arginine and asparagine metabolism in infectious processes have been studied previously, the presently observed regulation of amino acid metabolism focuses additional attention on proline, glutamate, and alanine as potential modulators of infection.

Membrane-enclosed bacteria can be observed within the host cells up until 48 h p.i. as evidenced by TEM. This time-span covers the bacterial replication phase in the infectious process (i.e. until 24 h p.i.), but also non-replicating bacteria are able to escape from lysosomes and phagosomes which is most clearly evident from 48 h p.i. onwards. Consequently, once the bacteria have entered the dormant state, they will persist intracellularly in the cytosol. These findings contrast with what has been found in other models that investigated *S. aureus* infection of other

human cell types, where the cytosolic bacteria proliferated after phagosomal escape (61).

The bacterial escape from vesicles is most likely due to the production of pore-forming toxins that are regulated by SaeRS and Agr (50). The latter regulator is itself regulated by CodY, which also regulates most of the carbon resource management as described above (62). Nevertheless, some bacteria remain in vesicles until the very end of the present experiment. Together, these observations suggest that the bacteria-containing vesicles are possibly not fully functional. This intriguing idea is supported by the observed bacterial behavior, where oxidative stress and DNA-damage-induced responses are observed right from the beginning till the end of the experiment without a detectable peak. In fact, the abundance of some proteins related to these stress responses increased more strongly from 24 h p.i. onwards, when the majority of bacteria have already been liberated from vesicular captivity. A possible vesicle malfunction could be due to the aforementioned production of pore-forming toxins. The latter idea is supported by the fact that the production of these toxins seems to be reduced at the last time points of infection where the majority of intracellular bacteria are no longer enclosed in a membrane.

Lastly, our present proteome analyses reveal that apoptosis of the host cell could occur from 6.5 h until 24 h p.i., suggesting that the replicating bacteria employ this mechanism to escape from their host cells as captured by live cell imaging. In addition, we observed upregulation of Caspase 4 and NF- $\kappa$ B indicating activation of the inflammasome from 6.5 h p.i.. Nevertheless, the abundance profile of other proteins implicated in the so-called pyroptosis does not support the activation of this self-destructive pathway. This suggests that the bacterial presence, even in dormancy, somehow leads to suppression of pyroptosis, which would lead to host

cell lysis. Whether this is directly related to the bacterial actions, or indirectly to the response of the host to the bacterial presence is unclear.

Taken altogether, the present proteomics dissection of interactions between human bronchial epithelial cells and internalized *S. aureus* highlights the dynamic adaptive changes in the two interacting systems over an unprecedented period of time. This was necessary to obtain a proper understanding of the levels at which the two systems collide and eventually reach an equilibrium. Importantly, while in the past years host-pathogen interaction studies have focused attention on the roles of bacterial virulence factors and immune evasion, our present observations place dynamic host-pathogen interactions at the metabolic level in the limelight. Clearly, pore-forming toxins have a crucial role in giving the invading bacteria access to the resources that are hidden within the host cells, but it is the way in which these resources are used by the bacteria and how the host and the bacteria subsequently adapt to each other that determines the ultimate outcome of the infectious process.

## Acknowledgements

We thank Jan Pané-Farré for providing the HG001  $\Delta$ spa, Jeroen Kuipers for his assistance during the electron microscopy imaging, Dr. Muriel Mari for the support in identifying the vesicles in the microscopy images, and Giorgio Gabarrini for his comments that greatly improved the manuscript. Funding for this project was received from the Graduate School of Medical Sciences of the University of Groningen [to L.M.P.M., S.A.M., and J.M.v.D.], the Deutsche Forschungsgemeinschaft Grants GRK1870 [to L.M.P.M., S.A.M. and U.V.] and SFBTRR34 [to U.V.], and CEC MSCI-ITN grant 713482 [ALERT, to H.Y., E.J.M.R, A.M.S., and J.M.v.D.]. Part of this work has been performed at the UMCG Imaging and Microscopy Center (UMIC), which is sponsored by NWO-grants 40-00506-98-9021 (TissueFaxes) and 175-010-2009-023 (Zeiss 2p). The funders had no role in

study design, data collection and analysis, decision to publish, or preparation of the manuscript.

## Declaration of interest

The authors declare that they have no financial and non-financial competing interests in relation to the documented research.

## References

1. Wertheim, H. F., Melles, D. C., Vos, M. C., van Leeuwen, W., van Belkum, A., Verbrugh, H. A., and Nouwen, J. L. (2005) The role of nasal carriage in *Staphylococcus aureus* infections. *Lancet Infect. Dis.* 5, 751–762
2. Lowy, F. D. (1998) *Staphylococcus aureus* Infections. *N. Engl. J. Med.* 339, 520–532
3. Tong, S. Y. C., Davis, J. S., Eichenberger, E., Holland, T. L., and Fowler, V. G. (2015) *Staphylococcus aureus* Infections: Epidemiology, Pathophysiology, Clinical Manifestations, and Management. *Clin. Microbiol. Rev.* 28, 603–661
4. Breathnach, A. S. (2013) Nosocomial infections and infection control. *Medicine (Baltimore)* 41, 649–653
5. Appelbaum, P. C. (2006) MRSA—the tip of the iceberg. *Clin. Microbiol. Infect.* 12, 3–10
6. Fraunholz, M., and Sinha, B. (2012) Intracellular *Staphylococcus aureus*: Live-in and let die. *Front. Cell. Infect. Microbiol.* 2, 43
7. Garzoni, C., and Kelley, W. L. (2009) *Staphylococcus aureus*: new evidence for intracellular persistence. *Trends Microbiol.* 17, 59–65
8. Lehar, S. M., Pillow, T., Xu, M., Staben, L., Kajihara, K. K., Vandlen, R., DePalatis, L., Raab, H., Hazenbos, W. L., Hiroshi Morisaki, J., Kim, J., Park, S., Darwish, M., Lee, B.-C., Hernandez, H., Loyet, K. M., Lupardus, P., Fong, R., Yan, D., Chalouni, C., Luis, E., Khalfin, Y., Plise, E., Cheong, J., Lyssikatos, J. P., Strandh, M., Koefoed, K., Andersen, P. S., Flygare, J. A., Wah Tan, M., Brown, E. J., and Mariathasan, S. (2015) Novel antibody-antibiotic conjugate eliminates intracellular *S. aureus*. *Nature* 527, 323–328
9. Proctor, R. A., van Langevelde, P., Kristjansson, M., Maslow, J. N., and Arbeit, R. D. (1995) Persistent and relapsing infections associated with

- small-colony variants of *Staphylococcus aureus*. Clin. Infect. Dis. Off. Publ. Infect. Dis. Soc. Am. 20, 95–102
10. Seifert, H., Wisplinghoff, H., Schnabel, P., and von Eiff, C. (2003) Small Colony Variants of *Staphylococcus aureus* and Pacemaker-related Infection. Emerg. Infect. Dis. 9, 1316–1318
  11. Tuscherr, L., Bischoff, M., Lattar, S. M., Noto Llana, M., Pfortner, H., Niemann, S., Geraci, J., Van de Vyver, H., Fraunholz, M. J., Cheung, A. L., Herrmann, M., Völker, U., Sordelli, D. O., Peters, G., and Löffler, B. (2015) Sigma Factor SigB Is Crucial to Mediate *Staphylococcus aureus* Adaptation during Chronic Infections. PLoS Pathog 11, e1004870
  12. Strobel, M., Pfortner, H., Tuscherr, L., Völker, U., Schmidt, F., Kramko, N., Schnittler, H.-J., Fraunholz, M. J., Löffler, B., Peters, G., and Niemann, S. (2016) Post-invasion events after infection with *Staphylococcus aureus* are strongly dependent on both the host cell type and the infecting *S. aureus* strain. Clin. Microbiol. Infect. 22, 799–809
  13. Surmann, K., Michalik, S., Hildebrandt, P., Gierok, P., Depke, M., Brinkmann, L., Bernhardt, J., Salazar, M. G., Sun, Z., Shteynberg, D., Kusebauch, U., Moritz, R. L., Wollscheid, B., Lalk, M., Völker, U., and Schmidt, F. (2014) Comparative proteome analysis reveals conserved and specific adaptation patterns of *Staphylococcus aureus* after internalization by different types of human non-professional phagocytic host cells. Front. Microbiol. 5, 392
  14. Hecker, M., Mäder, U., and Völker, U. (2018) From the genome sequence via the proteome to cell physiology – Pathoproteomics and pathophysiology of *Staphylococcus aureus*. Int. J. Med. Microbiol. 308, 545–557
  15. Kiedrowski, M. R., Paharik, A. E., Ackermann, L. W., Shelton, A. U., Singh, S. B., Starner, T. D., and Horswill, A. R. (2016) Development of an *in vitro* colonization model to investigate *Staphylococcus aureus* interactions with airway epithelia. Cell. Microbiol. 18, 720–732
  16. Richter, E., Harms, M., Ventz, K., Nölker, R., Fraunholz, M. J., Mostertz, J., and Hochgräfe, F. (2016) Quantitative Proteomics Reveals the Dynamics of Protein Phosphorylation in Human Bronchial Epithelial Cells during Internalization, Phagosomal Escape, and Intracellular Replication of *Staphylococcus aureus*. J. Proteome Res. 15, 4369–4386



17. Surmann, K., Simon, M., Hildebrandt, P., Pfortner, H., Michalik, S., Stentzel, S., Steil, L., Dhople, V. M., Bernhardt, J., Schlüter, R., Depke, M., Gierok, P., Lalk, M., Bröker, B. M., Schmidt, F., and Völker, U. (2015) A proteomic perspective of the interplay of *Staphylococcus aureus* and human alveolar epithelial cells during infection. *J. Proteomics* 128, 203–217
18. Herbert, S., Ziebandt, A.-K., Ohlsen, K., Schäfer, T., Hecker, M., Albrecht, D., Novick, R., and Götz, F. (2010) Repair of Global Regulators in *Staphylococcus aureus* 8325 and Comparative Analysis with Other Clinical Isolates. *Infect. Immun.* 78, 2877–2889
19. Liese, J., Rooijackers, S. H. M., van Strijp, J. A. G., Novick, R. P., and Dustin, M. L. (2013) Intravital two-photon microscopy of host–pathogen interactions in a mouse model of *Staphylococcus aureus* skin abscess formation. *Cell. Microbiol.* 15, 891–909
20. Cozens, A. L., Yezzi, M. J., Kunzelmann, K., Ohrui, T., Chin, L., Eng, K., Finkbeiner, W. E., Widdicombe, J. H., and Gruenert, D. C. (1994) CFTR expression and chloride secretion in polarized immortal human bronchial epithelial cells. *Am. J. Respir. Cell Mol. Biol.* 10, 38–47
21. R Core Team (2018) R: A language and environment for statistical computing (R Foundation for Statistical Computing, Vienna, Austria.)
22. Pfortner, H., Wagner, J., Surmann, K., Hildebrandt, P., Ernst, S., Bernhardt, J., Schurmann, C., Gutjahr, M., Depke, M., Jehmlich, U., Dhople, V., Hammer, E., Steil, L., Völker, U., and Schmidt, F. (2013) A proteomics workflow for quantitative and time-resolved analysis of adaptation reactions of internalized bacteria. *Methods* 61, 244–250
23. Depke, M., Michalik, S., Rabe, A., Surmann, K., Brinkmann, L., Jehmlich, N., Bernhardt, J., Hecker, M., Wollscheid, B., Sun, Z., Moritz, R. L., Völker, U., and Schmidt, F. (2015) A peptide resource for the analysis of *Staphylococcus aureus* in host pathogen interaction studies. *Proteomics* 15, 3648–3661
24. Michalik, S., Depke, M., Murr, A., Gesell Salazar, M., Kusebauch, U., Sun, Z., Meyer, T. C., Surmann, K., Pfortner, H., Hildebrandt, P., Weiss, S., Palma Medina, L. M., Gutjahr, M., Hammer, E., Becher, D., Pribyl, T., Hammerschmidt, S., Deutsch, E. W., Bader, S. L., Hecker, M., Moritz, R. L., Mäder, U., Völker, U., and Schmidt, F. (2017) A global *Staphylococcus aureus* proteome resource applied to the *in vivo* characterization of host-pathogen interactions. *Sci. Rep.* 7, 9718

25. Zeitlin, P. L., Lu, L., Rhim, J., Cutting, G., Stetten, G., Kieffer, K. A., Craig, R., and Guggino, W. B. (1991) A Cystic Fibrosis Bronchial Epithelial Cell Line: Immortalization by Adeno-12-SV40 Infection. *Am. J. Respir. Cell Mol. Biol.* 4, 313–319
26. Bruderer, R., Bernhardt, O. M., Gandhi, T., Miladinović, S. M., Cheng, L.-Y., Messner, S., Ehrenberger, T., Zanotelli, V., Butscheid, Y., Escher, C., Vitek, O., Rinner, O., and Reiter, L. (2015) Extending the Limits of Quantitative Proteome Profiling with Data-Independent Acquisition and Application to Acetaminophen-Treated Three-Dimensional Liver Microtissues. *Mol. Cell. Proteomics* 14, 1400–1410
27. Deutsch, E. W., Mendoza, L., Shteynberg, D., Slagel, J., Sun, Z., and Moritz, R. L. (2015) Trans-Proteomic Pipeline, a standardized data processing pipeline for large-scale reproducible proteomics informatics. *Proteomics Clin. Appl.* 9, 745–754
28. Deutsch, E. W., Mendoza, L., Shteynberg, D., Farrah, T., Lam, H., Tasman, N., Sun, Z., Nilsson, E., Pratt, B., Prazen, B., Eng, J. K., Martin, D. B., Nesvizhskii, A., and Aebersold, R. (2010) A Guided Tour of the Trans-Proteomic Pipeline. *Proteomics* 10, 1150–1159
29. Keller, A., Nesvizhskii, A. I., Kolker, E., and Aebersold, R. (2002) Empirical Statistical Model To Estimate the Accuracy of Peptide Identifications Made by MS/MS and Database Search. *Anal. Chem.* 74, 5383–5392
30. Shteynberg, D., Deutsch, E. W., Lam, H., Eng, J. K., Sun, Z., Tasman, N., Mendoza, L., Moritz, R. L., Aebersold, R., and Nesvizhskii, A. I. (2011) iProphet: Multi-level Integrative Analysis of Shotgun Proteomic Data Improves Peptide and Protein Identification Rates and Error Estimates. *Mol. Cell. Proteomics* 10, M111
31. Reiter, L., Claassen, M., Schrimpf, S. P., Jovanovic, M., Schmidt, A., Buhmann, J. M., Hengartner, M. O., and Aebersold, R. (2009) Protein Identification False Discovery Rates for Very Large Proteomics Data Sets Generated by Tandem Mass Spectrometry. *Mol. Cell. Proteomics* 8, 2405–2417
32. Nagel, A., Michalik, S., Debarbouille, M., Hertlein, T., Salazar, M. G., Rath, H., Msadek, T., Ohlsen, K., Dijl, J. M. van, Völker, U., and Mäder, U. (2018) Inhibition of Rho Activity Increases Expression of SaeRS-Dependent Virulence Factor Genes in *Staphylococcus aureus*, Showing a Link between Transcription Termination, Antibiotic Action, and Virulence. *mBio* 9, e01332-18

33. Fuchs, S., Mehlan, H., Bernhardt, J., Hennig, A., Michalik, S., Surmann, K., Pané-Farré, J., Giese, A., Weiss, S., Backert, L., Herbig, A., Nieselt, K., Hecker, M., Völker, U., and Mäder, U. (2018) AureoWiki-The repository of the *Staphylococcus aureus* research and annotation community. *Int. J. Med. Microbiol.* 308, 558–568
34. Ritchie, M. E., Phipson, B., Wu, D., Hu, Y., Law, C. W., Shi, W., and Smyth, G. K. (2015) limma powers differential expression analyses for RNA-sequencing and microarray studies. *Nucleic Acids Res.* 43, e47
35. Phipson, B., Lee, S., Majewski, I. J., Alexander, W. S., and Smyth, G. K. (2016) Robust hyperparameter estimation protects against hypervariable genes and improves power to detect differential expression. *Ann. Appl. Stat.* 10, 946–963
36. Futschik, M. E., and Carlisle, B. (2005) Noise-robust soft clustering of gene expression time-course data. *J. Bioinform. Comput. Biol.* 3, 965–988
37. Kumar, L., and E. Futschik, M. (2007) Mfuzz: A software package for soft clustering of microarray data. *Bioinformatics* 2, 5–7
38. Basu, A., and Yap, M.-N. F. (2016) Ribosome hibernation factor promotes *Staphylococcal* survival and differentially represses translation. *Nucleic Acids Res.* 44, 4881–4893
39. Ueta, M., Wada, C., and Wada, A. (2010) Formation of 100S ribosomes in *Staphylococcus aureus* by the hibernation promoting factor homolog SaHPF. *Genes Cells* 15, 43–58
40. Somerville, G. A., and Proctor, R. A. (2009) At the Crossroads of Bacterial Metabolism and Virulence Factor Synthesis in *Staphylococci*. *Microbiol. Mol. Biol. Rev.* 73, 233–248
41. Ren, W., Rajendran, R., Zhao, Y., Tan, B., Wu, G., Bazer, F. W., Zhu, G., Peng, Y., Huang, X., Deng, J., and Yin, Y. (2018) Amino Acids As Mediators of Metabolic Cross Talk between Host and Pathogen. *Front. Immunol.* 9, 319
42. Xiong, L., Teng, J. L. L., Botelho, M. G., Lo, R. C., Lau, S. K. P., and Woo, P. C. Y. (2016) Arginine Metabolism in Bacterial Pathogenesis and Cancer Therapy. *Int. J. Mol. Sci.* 17, 363
43. Giardina, G., Brunotti, P., Fiascarelli, A., Cicalini, A., Costa, M. G. S., Buckle, A. M., di Salvo, M. L., Giorgi, A., Marani, M., Paone, A., Rinaldo, S.,

- Paiardini, A., Contestabile, R., and Cutruzzolà, F. (2015) How pyridoxal 5'-phosphate differentially regulates human cytosolic and mitochondrial serine hydroxymethyltransferase oligomeric state. *FEBS J.* 282, 1225–1241
44. Morscher, R. J., Ducker, G. S., Li, S. H.-J., Mayer, J. A., Gitai, Z., Sperl, W., and Rabinowitz, J. D. (2018) Mitochondrial translation requires folate-dependent tRNA methylation. *Nature* 554, 128–132
  45. Kaiser, J. C., King, A. N., Grigg, J. C., Sheldon, J. R., Edgell, D. R., Murphy, M. E. P., Brinsmade, S. R., and Heinrichs, D. E. (2018) Repression of branched-chain amino acid synthesis in *Staphylococcus aureus* is mediated by isoleucine via CodY, and by a leucine-rich attenuator peptide. *PLOS Genet.* 14, e1007159
  46. Gardan, R., Rapoport, G., and Débarbouillé, M. (1997) Role of the transcriptional activator RocR in the arginine-degradation pathway of *Bacillus subtilis*. *Mol. Microbiol.* 24, 825–837
  47. Ryan, S., Begley, M., Gahan, C. G. M., and Hill, C. (2009) Molecular characterization of the arginine deiminase system in *Listeria monocytogenes*: regulation and role in acid tolerance. *Environ. Microbiol.* 11, 432–445
  48. Jarry, T. M., Memmi, G., and Cheung, A. L. (2008) The expression of alpha-haemolysin is required for *Staphylococcus aureus* phagosomal escape after internalization in CFT-1 cells. *Cell. Microbiol.* 10, 1801–1814
  49. Geiger, T., Goerke, C., Mainiero, M., Kraus, D., and Wolz, C. (2008) The Virulence Regulator Sae of *Staphylococcus aureus*: Promoter Activities and Response to Phagocytosis-Related Signals. *J. Bacteriol.* 190, 3419–3428
  50. Horn, J., Stelzner, K., Rudel, T., and Fraunholz, M. (2018) Inside job: *Staphylococcus aureus* host-pathogen interactions. *Int. J. Med. Microbiol.* 308, 607–624
  51. Oogai, Y., Kawada-Matsuo, M., and Komatsuzawa, H. (2016) *Staphylococcus aureus* SrrAB Affects Susceptibility to Hydrogen Peroxide and Co-Existence with *Streptococcus sanguinis*. *PLOS ONE* 11, e0159768
  52. Liu, X., and Lieberman, J. (2017) in *Advances in Immunology*, ed Alt FW (Academic Press), pp 81–117.
  53. Fisher, R. A., Gollan, B., and Helaine, S. (2017) Persistent bacterial infections and persister cells. *Nat. Rev. Microbiol.* 15, 453–464

54. Pohl, K., Francois, P., Stenz, L., Schlink, F., Geiger, T., Herbert, S., Goerke, C., Schrenzel, J., and Wolz, C. (2009) CodY in *Staphylococcus aureus*: a Regulatory Link between Metabolism and Virulence Gene Expression. *J. Bacteriol.* 191, 2953–2963
55. Halsey, C. R., Lei, S., Wax, J. K., Lehman, M. K., Nuxoll, A. S., Steinke, L., Sadykov, M., Powers, R., and Fey, P. D. (2017) Amino Acid Catabolism in *Staphylococcus aureus* and the Function of Carbon Catabolite Repression. *mBio* 8, e01434-16
56. Somerville, G. A., Saïd-Salim, B., Wickman, J. M., Raffel, S. J., Kreiswirth, B. N., and Musser, J. M. (2003) Correlation of Acetate Catabolism and Growth Yield in *Staphylococcus aureus*: Implications for Host-Pathogen Interactions. *Infect. Immun.* 71, 4724–4732
57. Baruch, M., Belotserkovsky, I., Hertzog, B. B., Ravins, M., Dov, E., McIver, K. S., Le Breton, Y. S., Zhou, Y., Youting, C. C., and Hanski, E. (2014) An Extracellular Bacterial Pathogen Modulates Host Metabolism to Regulate its Own Sensing and Proliferation. *Cell* 156, 97–108
58. Makhlin, J., Kofman, T., Borovok, I., Kohler, C., Engelmann, S., Cohen, G., and Aharonowitz, Y. (2007) *Staphylococcus aureus* ArcR Controls Expression of the Arginine Deiminase Operon. *J. Bacteriol.* 189, 5976–5986
59. Minois, N. (2014) Molecular basis of the “anti-aging” effect of spermidine and other natural polyamines - a mini-review. *Gerontology* 60, 319–326
60. Bravo-Santano, N., Ellis, J. K., Mateos, L. M., Calle, Y., Keun, H. C., Behrends, V., and Letek, M. (2018) Intracellular *Staphylococcus aureus* Modulates Host Central Carbon Metabolism To Activate Autophagy. *mSphere* 3, e00374-18
61. Grosz, M., Kolter, J., Paprotka, K., Winkler, A.-C., Schäfer, D., Chatterjee, S. S., Geiger, T., Wolz, C., Ohlsen, K., Otto, M., Rudel, T., Sinha, B., and Fraunholz, M. (2014) Cytoplasmic replication of *Staphylococcus aureus* upon phagosomal escape triggered by phenol-soluble modulín  $\alpha$ . *Cell. Microbiol.* 16, 451–465
62. Roux, A., Todd, D. A., Velázquez, J. V., Cech, N. B., and Sonenshein, A. L. (2014) CodY-Mediated Regulation of the *Staphylococcus aureus* Agr System Integrates Nutritional and Population Density Signals. *J. Bacteriol.* 196, 1184–1196

## Chapter 3

# **Distinct adaptive responses of *Staphylococcus aureus* upon infection of bronchial epithelium during different stages of regeneration**

---

Laura M. Palma Medina, Ann-Kristin Becker, Stephan Michalik, Petra Hildebrandt, Manuela Gesell Salazar, Kristin Surmann, Solomon A. Mekonnen, Lars Kaderali, Jan Maarten van Dijl<sup>‡</sup>, Uwe Völker<sup>#</sup>

<sup>#</sup>Corresponding authors

Manuscript in preparation for submission to *Molecular and Cellular Proteomics*

Supplementary Material is available at [http://bit.ly/Thesis\\_Palma\\_Medina](http://bit.ly/Thesis_Palma_Medina)



## Abstract

The primary barrier that protects our lungs against infection by pathogens is a tightly sealed layer of epithelial cells. When the integrity of this barrier is disrupted as a consequence of chronic pulmonary diseases or viral insults, bacterial pathogens will gain access to underlying tissues. A major pathogen that can take advantage of such conditions is *Staphylococcus aureus*, thereby causing severe pneumonia. In this study, we investigated how *S. aureus* responds to different conditions of the human epithelium, especially non-polarization and fibrogenesis during regeneration using an *in vitro* infection model. The infective process was monitored by quantification of the epithelial cell- and bacterial populations, fluorescence microscopy and mass spectrometry. The results uncover differences in bacterial internalization and population dynamics that dictate the outcome of infection. Protein profiling reveals that, irrespective of the polarization state of the epithelial cells, the invading bacteria mount similar responses to adapt to the intracellular milieu. Remarkably, a bacterial adaptation that did depend on the state of the epithelial cells was enhanced production of nitric oxide and early upregulation of proteins for redox homeostasis when bacteria were confronted with a polarized cell layer. This is indicative of nitric oxide-dependent modulation of the cytoplasmic redox state to maintain homeostasis early during infection, even before internalization. Our present observations provide a deeper insight into how *S. aureus* takes advantage of a breached epithelial barrier, and how infected epithelial cells have limited ability to respond adequately to staphylococcal insults.



## Introduction

*Staphylococcus aureus* is an opportunistic pathogen (1) that is renowned for its ability to colonize several sites in the human body (2, 3). One of the most frequent sites of colonization is the respiratory tract, where it is commonly found as a commensal bacterium residing in the nose and throat (4, 5). However, *S. aureus* also has the potential to infect the upper and lower parts of the respiratory tract, causing severe infections, including necrotizing pneumonia (6, 7). Although these infections can occur in community or hospital settings, the development of a chronic lung infection is commonly associated with pre-existing infections by other organisms or with lung-associated diseases, like chronic obstructive pulmonary disease (COPD), cystic fibrosis (CF) or bronchiectasis (8–14).

The epithelial cell layer of the lungs is our first barrier of defense against airborne pathogenic bacteria. Nevertheless, in the aforementioned conditions, the outermost layer of the lungs gets damaged, leading to wounded patches in the epithelial membrane. After damage, the epithelial cells will pass through a process of healing that starts with migration of the epithelial cells to repopulate the created gap, followed by activation of the polarization machinery and fibrogenesis (15–17). The latter involves regulatory pathways like sonic hedgehog signaling (Shh), transforming growth factor beta (TGFB), and Wnt/Wingless/Integrated (Wnt) pathways, that are commonly deregulated in chronic lung diseases and could lead to permanent fibrosis (18–20). These pathological conditions affect several functions of the membrane, including correct localization of proteins in the cellular membrane, homogeneity of the membrane, transport gradients, direction of cell division, and the permeability of the membrane (21, 22). Consequently, the affected sites are regarded as portals for invasion of underlying tissues by *S. aureus* or other pathogens (15, 22).

To date, most studies on the mechanisms employed by *S. aureus* to breach epithelial barriers focused on model systems that mimic one particular state of the epithelial cells. On this basis, it is known that *S. aureus* weakens the epithelial layer by secreting toxins that disrupt the polarized cells, enabling the pathogen to cross the barrier and enter host cells (23, 24). Upon entry, the bacteria adapt to the intracellular milieu where they have to face nutrient scarcity and defensive host mechanisms. To do so, the bacteria activate pathways related to energy generation from the most readily available sources and balance the expression of virulence factors to take optimal advantage of their host (25–28). However, an important knowledge gap relates to the question how *S. aureus* responds to different states of the human epithelium, such as non-polarization or fibrogenesis during regeneration. Therefore, the aim of this study was to define possible differential responses of *S. aureus* to such pre-infection conditions with focus on changes at the proteome level. To this end, we devised an *in vitro* model that simulates staphylococcal infection at two different stages of epithelial regeneration. The first stage involves a layer of non-polarized cells, which mimics the earliest stage of regeneration where the bacteria have ‘easy access’ to the epithelium. The second involves a polarized host cell membrane at the stage of fibrogenesis, where the bacteria can only gain access to the cells by disruption of the tight junctions connecting the regenerating epithelial cells. The results obtained with this model reveal distinct bacterial internalization rates depending on the stage of epithelial regeneration. While the internalized bacteria displayed similar adaptations at the proteome level, the timing of these adaptations differed. Remarkably, differences are most clearly evident for proteins under control of the redox regulator Rex, where induction of Rex-regulated proteins is observed at an earlier time point when the bacteria are confronting polarized epithelial cells. Our observations show that bacteria approaching the polarized epithelial cells adapt to a physiological state that involves production and resistance to nitric oxide (NO).

## Materials and Method

### Bacterial strains and culture conditions

*S. aureus* strain HG001 (29) carrying plasmid pJL76 (Liese *et al.*, 2013; GFP codon optimized) was used for internalization experiments into epithelial cells followed by mass spectrometry analyses. For immunofluorescence microscopy, a  $\Delta spa$  mutant was used to avoid unspecific binding of the antibodies.

Cultivation of bacteria was carried out in prokaryotic minimal essential medium (pMEM): 1x MEM without sodium bicarbonate (Invitrogen, Karlsruhe, Germany) supplemented with 1x non-essential amino acids (PAN-Biotech GmbH, Aidenbach, Germany), 4 mM L-glutamine (PAN-Biotech GmbH, Germany), 10 mM HEPES (PAN-Biotech GmbH), 2 mM L-alanine, 2 mM L-leucine, 2 mM L-isoleucine, 2 mM L-valine, 2 mM L-aspartate, 2 mM L-glutamate, 2 mM L-serine, 2 mM L-threonine, 2 mM L-cysteine, 2 mM L-proline, 2 mM L-histidine, 2 mM L-phenyl alanine, and 2 mM L-tryptophan (All from Sigma-Aldrich, Schnelldorf, Germany), adjusted to pH 7.4 and sterilized through filtration.

The cultivation of the samples was performed as described previously (30). In brief, overnight cultures were done as serial dilutions in media enriched with 0.01% yeast extract. Additionally, all overnight cultures contained 10  $\mu\text{g/ml}$  erythromycin (Sigma-Aldrich) to maintain pJL76. In addition, 10  $\mu\text{g/ml}$  tetracycline (Sigma-Aldrich) was added to cultures of the  $\Delta spa$  mutant. Cultures were incubated for 16 h in an orbital shaking incubator at 37°C and 220 rpm. All main cultures for infection experiments were prepared in pMEM without yeast extract or antibiotics and inoculated with bacteria from overnight cultures in the mid-exponential phase. Incubation of the main cultures was carried out in a shaking water bath at 37°C and 150 rpm.

## Cell lines and culture conditions

The immortalized 16HBE14o- epithelial cell line is derived from transformed bronchial epithelial cells of a 1-year-old heart-lung transplant patient (31). Cultivation of the cells was carried out in eukaryotic minimal essential medium (eMEM): 1x MEM with Earle's salts with 2.2 g/l NaHCO<sub>3</sub> (Biochrom AG, Berlin, Germany) supplemented with 10% (v/v) fetal calf serum (FCS; Biochrom AG), 2% (v/v) L-glutamine 200mM (PAN-Biotech GmbH) and 1% (v/v) non-essential amino acids 100x (PAN-Biotech GmbH). The cells were cultured in 10 cm plates at 37°C and 5% CO<sub>2</sub> in a humid atmosphere and were kept for no more than 15 passages.

The seeding of the cells was done at a density of 1x10<sup>5</sup> cells/cm<sup>2</sup> over a 12 mm Transwell® polyester membrane with 0.4 µm pore size (Corning, Schnellendorf, Germany), to promote the polarization of the cell membrane. Cells were cultured for 3 and 11 days depending on the desired condition for infection. The volume of medium on the apical side was 400 µl and 1300 µl on the basal side. The medium was exchanged every second day until day eight after which the exchange was done daily.

## Measurement of transepithelial electrical resistance

Bioelectric measurements were performed with an EVOMX Volt-ohmmeter equipped with STX2 chopstick electrodes (WPI, Berlin, Germany). To measure the resistance of the cell layer, the medium of every cultured Transwell® was replaced with pre-warmed eMEM medium (500 µl and 1500 µl on the apical and basal sides, respectively) and equilibrated for 10 min at room temperature. The TEER was calculated by subtracting the blank measurement and subsequently multiplying it by the area of the Transwell®. After measurement, the medium was exchanged with pre-warmed fresh medium.

## Internalization procedure

The protocol for infection was based on the methods described by Pfortner et al. (30) with some adaptations for infection in Transwells®. The bacterial main cultures were inoculated at a starting OD<sub>600</sub> of 0.05, grown until mid-exponential phase and collected at OD<sub>600</sub> of ~0.4. Prior to infection, the number of bacterial cells was determined by flow cytometry with a Guava easyCyte™ flow cytometer (Merck Millipore, Darmstadt, Germany), using a blue 50 mW laser to excite bacterial GFP that allowed quantification of the bacteria. The same day of infection, epithelial cells were counted by detachment from the porous membrane by 5 min incubation at 37°C with 0.25% trypsin-EDTA (Gibco®, Grand Island, NY). Then, the cell solution was mixed in equal quantities with trypan blue dye, and the cell number was quantified with a Countess® (Invitrogen).

Infection of host epithelial cells with *S. aureus* was carried out by exchange of the apical media with the infection mix. This solution contained *S. aureus* diluted in eMEM to a multiplicity of infection of 25 and buffered with 2.9 µl sodium hydrogen carbonate (7.5%, PAN-Biotech GmbH) per ml of bacterial culture. Epithelial cells were exposed to the bacteria for 1 h at 37°C and 5% CO<sub>2</sub>. Afterwards, the media on the apical and basal sides were exchanged with fresh eMEM medium containing 10 µg/ml lysostaphin (AMBI Products LLC, Lawrence, NY).

Sampling for counting of 16HBE14o- cells at every time point was performed as described above and, additionally, the number of infected cells was counted in the Guava easyCyte™ flow cytometer. The collection of internalized bacteria was done by incubation with 0.05% sodium dodecyl sulfate (SDS; Carl Roth, Karlsruhe, Germany) for 5 min at 37°C, and bacterial quantification was performed using a GUAVA® easyCyte.

## Immunofluorescence staining

16HBE14o- cells were cultured over Transwell® supports for 3 or 11 days. The medium of the wells was removed, and the cells were washed with phosphate-buffered saline (PBS). Fixation of cells was done with 5% acetic acid in absolute ethanol for 10 min at room temperature. To avoid autofluorescence the supports were incubated for 15 min at room temperature with 50 mM NH<sub>4</sub>Cl. Subsequently, permeabilization of the cells and blocking of non-specific binding were carried out. To this end, cells were incubated for 30 min at room temperature with 0.2% bovine serum albumin (BSA) and 0.1% saponin in PBS, followed by overnight incubation at 4°C with 2% BSA, 0.1% saponin and 5% Neutral Goat Serum in PBS. Additional blocking was performed with 12 µg/ml of a human monoclonal antibody (1D9; van den Berg et al., 2015) diluted in the same blocking solution for 2 h at room temperature in a humidifier chamber. Thereafter, immunofluorescence staining was carried out using a rabbit polyclonal antibody against ZO-1 (40-2200; Invitrogen) in a 1:100 dilution and a goat polyclonal secondary antibody against rabbit conjugated with alexa flour® 647 (A-21244; Thermo Fisher Scientific, Landsmeer, The Netherlands) in a 1:2000 dilution. The incubation of antibodies was done separately, each for 1 h at room temperature in the humidifier chamber. The cells were washed with blocking solution between incubations. Finally, the DNA was stained with 4',6-diamidino-2-phenylindole (DAPI) by incubation for 15 min at room temperature and the slides were mounted with Mowiol® 4-88 (EMD 208 Chemical, Inc., Temecula, CA). Visualization of the samples was done in a Leica SP8 microscope at the UMCG Microscopy and Imaging Center.

## Nitric oxide and reactive oxygen species measurements

NO concentrations in the media and within epithelial cells were measured by the Griess method. In brief, the assay determines the nitrite concentrations in collected

samples. Medium fractions were collected at different time points and mixed 1:1 with the Griess reagent (G4410, Sigma Aldrich). Then, 100  $\mu$ L samples were passed to a 96-well plate and shaken for 15 min. The absorbance of the samples was measured at 540 nm. To measure intracellular NO concentrations, epithelial cells were disrupted with 1% SDS, and the measurements were done as described above. The NO concentration was determined by correlation with a standard curve of sodium nitrite on the same day of the infection.

The quantification of intracellular ROS was carried out with 2',7'-dichlorodihydrofluorescein diacetate (H<sub>2</sub>DCFDA) as an indicator. At each time point, epithelial cells were washed with PBS and then incubated with a solution of 5  $\mu$ M H<sub>2</sub>DCFDA for 1 h at 37°C in a 5% CO<sub>2</sub> incubator. Then, the epithelial cells were disrupted with 1% SDS and aliquots 150  $\mu$ L were transferred to a 96-well plate. The fluorescence was measured by excitation at 485/20, using an emission filter of 590/35. Measurements were corrected for the total protein quantity per sample, as determined with a BCA Protein Assay Kit (Thermo Fisher Scientific).

All measurements of nitrogen and reactive oxygen species were carried out in dark 96-well plates using a Synergy™ 2 multi-mode microplate reader (BioTek Instruments, Inc., Winooski, VT). All measurements were done from the bottom.

## Sample preparation for mass spectrometry

The sample preparation of human lung epithelial and bacterial samples was performed as described before in detail (26, 27).

The collection of epithelial cell samples was carried out at the beginning of the infection, and 1 h, 2.5 h, and 6.5 h p.i. by disruption with UT buffer (8 M urea, 2M thiourea in MS-grade water, Sigma-Aldrich) and immediate freezing in liquid nitrogen. Further disruption of the cells was done with 5 cycles of freeze-thawing

using liquid nitrogen and shaking at 30°C, followed by ultrasonication with a Sonopuls homogenizer (Bandelin electronic, Berlin, Germany) in 3 cycles of 3 seconds at 50% power and 1 min cooling on ice. The samples were centrifuged at maximal speed (~20000 x g) for 1 h at 4°C, the supernatant was collected, and the protein concentration of the samples was quantified using a Bradford assay (Biorad, Hercules, CA). Samples containing 4 µg of protein were prepared for mass spectrometry by reduction with 2.5 mmol/L<sup>1</sup> dithiothreitol for 1 h at 60°C and alkylation with 10mmol/L<sup>1</sup> iodoacetamide for 30 min at 37°C. Lastly, samples were digested with trypsin (1:25 trypsin:protein) at 37°C overnight and purified using C<sub>18</sub> columns (Merck Millipore).

*S. aureus* HG001 sampling for mass spectrometry involved one sample of the main culture in mid-exponential phase, collection of the non-adherent bacteria after 1 h of infection, and samples of internalized bacteria collected at 2.5 h and 6.5 h p.i. The last two samples were obtained by disruption of the host cells with 0.05% SDS for 5 min at 37°C. All samples were concentrated by centrifugation for 10 min at 10000xg and 4°C, the supernatant was removed, and the pellet was diluted in 2 ml of PBS. Subsequently, 2 million bacteria were sorted for each time point by flow cytometry using a FACSAria IIIu cell sorter (Becton Dickinson Biosciences, Franklin Lakes, NJ). Excitation of GFP was done with a 488 nm laser and the emission signal was detected in a 515-545 nm range. Afterward, the bacteria were collected on low protein binding filter membranes with a pore size of 0.22 µm (Merck Millipore). The bacterial cells were lysed on the filter by incubation with 7.4 µg·ml<sup>-1</sup> lysostaphin in 50 mM ammonium bicarbonate for 30 min at 37°C. Finally, digestion of the liberated proteins was performed with 0.3 µg of trypsin at 37°C overnight and tryptic peptides were purified using C<sub>18</sub> ZipTip columns (Merck Millipore, Germany).



Hyper Reaction Monitoring (HRM) peptides were added to all samples of epithelial cells and bacteria for peak detection, mass calibration, noise reduction and signal quantification (Biognosys AG, Schlieren, Switzerland).

## Mass spectrometry measurements and analysis.

Separation of tryptic peptides was accomplished with a Dionex Ultimate 3000 nano-LC system (Dionex/Thermo Fischer Scientific) using an Accucore 150-C18 analytical column of 250 nm (25 cm x 173 75  $\mu\text{m}$ , 2,6  $\mu\text{m}$  C18 particles, 150  $\text{\AA}$  pore size, Thermo Fischer Scientific). MS/MS measurements were performed on a QExactive (Thermo Fischer Scientific,) in data-independent mode (DIA) following the method described by Bruderer et al. (33). Supplemental Table 3 details the instrumental set-up and parameters used for the measurements.

Proteins were identified and quantified using Spectronaut™ V11.0.18108.11.30271 software (Biognosys AG) against MS databases generated from data-dependent acquisition (DDA) measurements of either *S. aureus* (34) or 16HBE14o- cells (27), under different culture conditions. The search included fixed modifications of +57.021464 by carbamidomethylation of cysteine and variable modification of +15.9949 due to oxidation of methionine. All the settings for the Spectronaut™ analyses are included in the Supplemental Table 4. A local cross run normalization was carried out to assays with Q-values < 0.001 and the reported quantifications refer to the MS2 peak area. Missing ion values were parsed when at least 25% of all samples had high quality quantifications. The parsing was performed using iRT profiling with carry-over of exact peak boundaries (minimum Q-value row selection = 0.001) and only for precursors with a Q-value > 0.0001. To prevent false positives, the parsed values were filtered out if their values were more than two-fold higher than the measured values.

## Statistical testing of changes in protein abundances over time

For further analysis, only proteins with at least two peptides were considered. Normalization of each peptide was performed based on the mean value of all time points. The final protein dynamics was calculated as the median of all corresponding normalized peptides. A linear model was fitted for every protein using the LIMMA package version 3.34.9 (35) in R version 3.4.4 (36). An empirical Bayes moderated t-test was conducted for each protein to detect significant differences between polarized and non-polarized cells. Moreover, every protein was tested individually in both conditions for changes over time by an empirical Bayes moderated F-test. All moderated p-values were corrected for multiple testing using Benjamini and Hochberg's multiple testing correction. Protein changes were assumed significant when their adjusted p-value was lower than 0.01 for the epithelial cell proteome, or lower than 0.05 for the *S. aureus* proteome.

The annotation of identified proteins was based on the Uniprot data base. For *S. aureus* the annotation was complemented with the AureoWiki data base (37), and the regulons as described by Nagel et al., 2018. The latter was used as a database to draw Voronoi tree maps using the Paver 2.1 software (DECODON GmbH, Greifswald, Germany).

## Data and Software availability

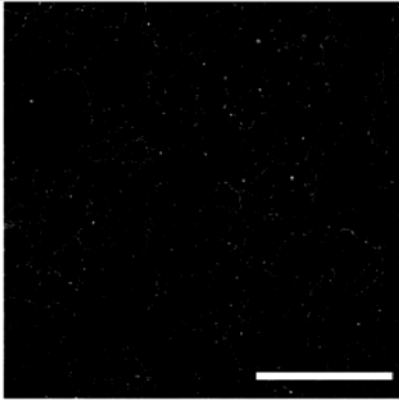
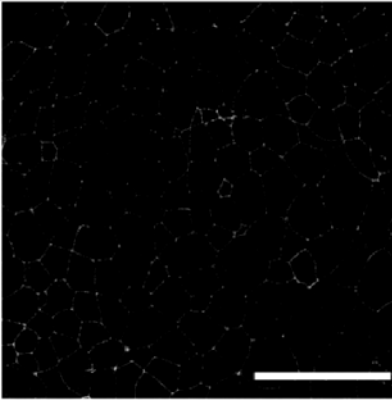
The raw files from mass spectrometry have been deposited in *MassIVE* (<https://massive.ucsd.edu>) under MSV000083271 (16HBE14o-) and MSV000083269 (*S. aureus*). The raw output files from Spectronaut™, including peptide ions and its Q-values, are included in Supplemental Tables 5 and 6. All protein annotations and median abundances are included in Supplemental Tables 1 and 2.

## Results

### Distinctive protein abundances define regenerative stages of bronchial epithelial cells

The epithelial cell line 16HBE14o- is known for its capacity to form tight junctions, polarize and differentiate (31, 38), which makes it suitable for the development of membranes with regenerating phenotypes. To obtain two cell membranes with distinctive characteristics, the cells were cultured over porous membranes under the same conditions for different time periods. The first distinctive characteristic between the membranes after three or eleven days of culturing was their polarization state (Figure 1), which was shown by measurement of trans-epithelial electrical resistance (TEER) and immunofluorescence of the tight junction protein Zonula Occludens-1 (ZO-1). A layer of 16HBE14o- cells reaches its highest resistance after fourteen days of culture (Supplemental Figure 1). To represent different regenerative states, the cell layer should display imperfect polarization and, accordingly, we decided to culture the cells for three and eleven days. Importantly, the epithelial cell layer cultured for three days reached a state of confluency, but it did not develop polarity as evidenced by a marginal increase in resistance and the absence of ZO-1 localization at the lateral sites of the cell membranes. In contrast, the cell layers cultured over eleven days displayed an at least three-fold increased electrical resistance consistent with a more organized localization of ZO-1 (Figure 1).

To further characterize the 16HBE14o- cells at different stages of polarization, their cytosolic proteome was profiled by mass spectrometry (MS). In total, the levels of 3498 proteins were quantified. Of these, 1633 proteins presented significantly different levels at the two investigated time points (Supplemental Table 1). More than half of the latter proteins related to the production of the extracellular matrix

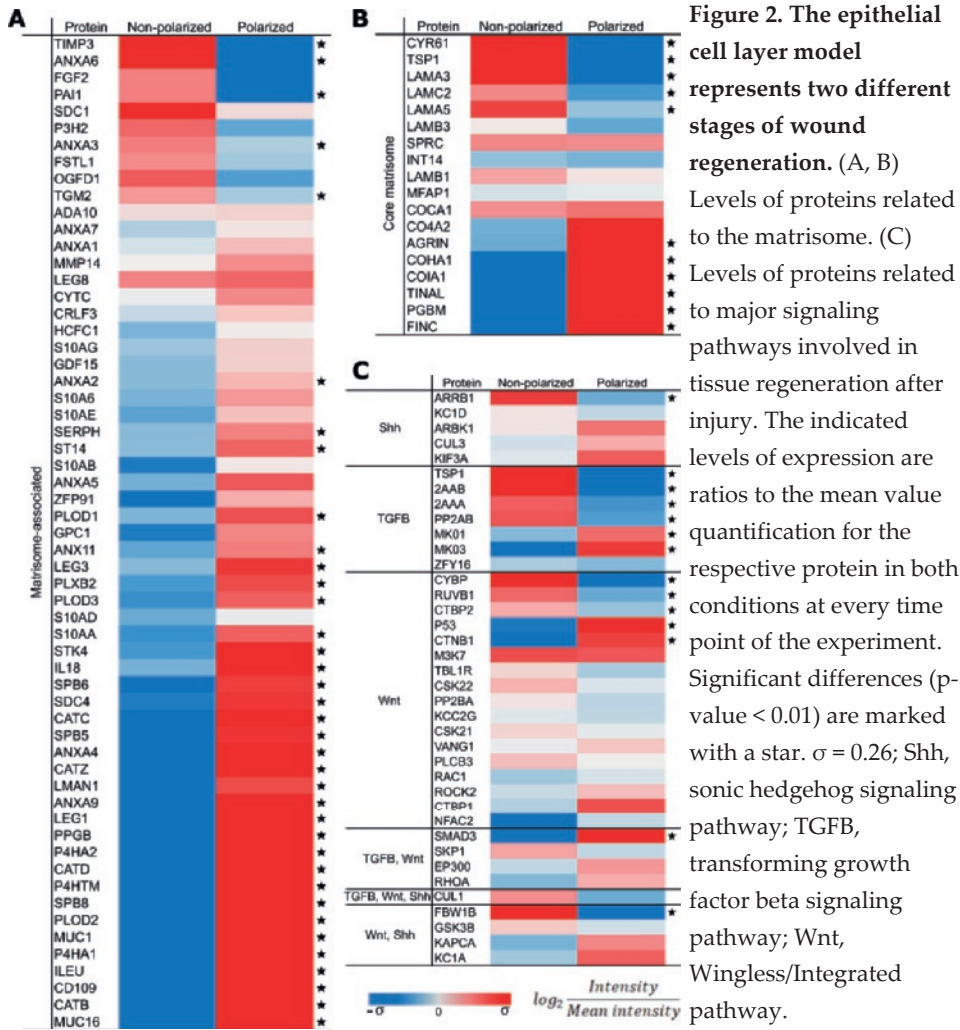
	Non-polarized	Polarized
Days of culture	3	11
TEER [ $\Omega \cdot \text{cm}^2$ ]	<40	~130
ZO-1		

**Figure 1. Epithelial cell layers with distinctive polarization states.** The cell line 16HBE14o- was cultured for 3 and 11 days in order to obtain confluent cell layers with two different polarization states. The polarization states were monitored by measurements of the TEER and by immunostaining with an antibody specific for of Zonula-Occludens 1. The micrographs present the maximum pixel value of the Z-stacks of the epithelial cell layers. Scale bar: 100  $\mu\text{m}$

(ECM), as well as pathways related to healing like TGFB, Shh, and Wnt (Figure 2). Of note, several proteins of the core matrisome (i.e. the ensemble of all ECM proteins and ECM-associated proteins) were detected at differing levels, despite the fact that most of them are secreted during ECM production (Figure 2B). Considering the observed differences in protein abundance, we conclude that the cells represent distinctive regenerative stages after three or eleven days of culturing.

The polarization state of the host membrane determines the rate of internalization of *S. aureus*

After three or eleven days of culturing, the developed epithelial cell layers were infected with *S. aureus* for one hour. Subsequently, non-internalized bacteria were



killed by the addition of lysostaphin, and the course of infection was followed by immunofluorescent confocal microscopy (Figure 3A; Supplemental Figures 2 and 3) and quantification of host and bacterial populations (Figure 3B-D). Imaging of the infection at 2.5 h post infection (p.i.) showed that the bacterial internalization in cells of a non-polarized membrane is highly effective and that the bacterial clusters distributed homogeneously over the cell layer. In contrast, the infection of cells in a polarized membrane occurred at specific sites of the cell layer where disruption of the tight junctions is evident.

Also, the progression of infection was different depending on the polarization state of the cultured cells. In non-polarized cells, the *S. aureus* population increased during the first hours of infection, leading to lysis of the host cells which became clearly evident from 24 h p.i. onwards (Figure 3B), when the bacterial population had doubled (Figure 3C). At 48 h p.i., the host cell membrane was completely disrupted as evidenced by a decrease of the TEER (Figure 3D). The

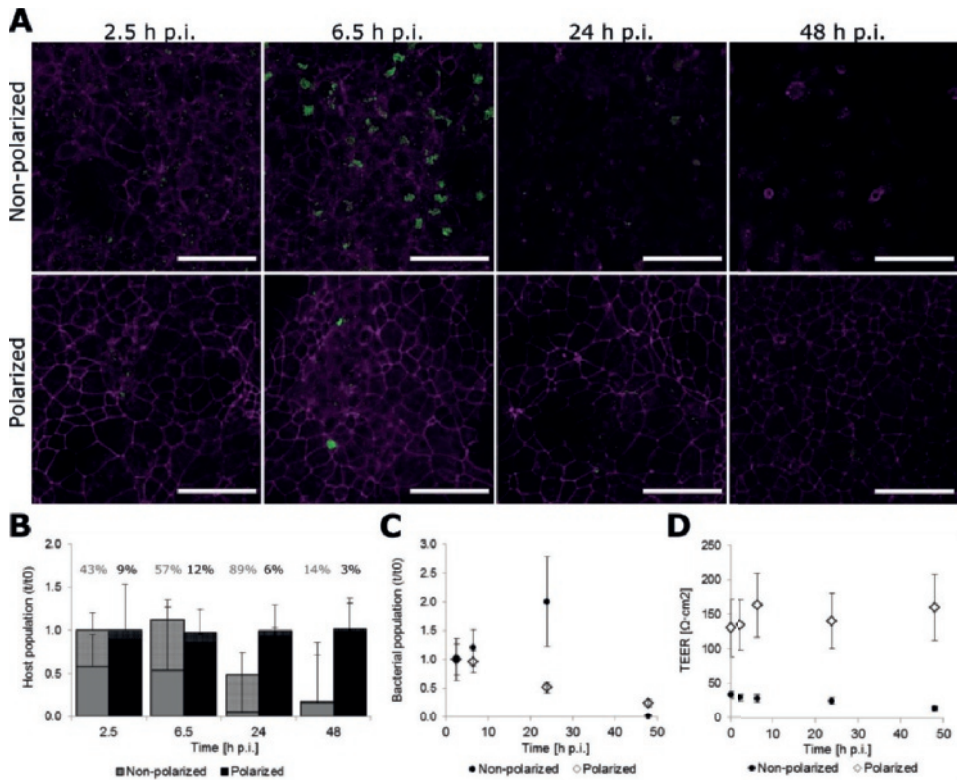


**Figure 3. Dynamics of bacterial and host populations p.i.** (A) Development of the *S. aureus* infection and integrity of the cell layer were tracked by immunofluorescence microscopy. The presented micrographs are the maximum pixel values of the Z-stacks of the infected membranes. ZO-1 is depicted in magenta and *S. aureus* in green. The individual representations of each channel are available in Supplemental Figures 2 and 3. Scale bar: 100  $\mu$ m. (B, C) Counting of the host and bacterial cell populations by flow cytometry. The complemented bars with dots and the percentages refer to the proportion of epithelial cells that contain intracellular *S. aureus*. (D) The polarity of the cell membrane was tracked during infection by TEER measurements.

bacteria internalized by polarized cells also multiplied during the first hours of infection, causing a slight decrease in the TEER at 24 h p.i.. However, in this case, the epithelial cell layer was able to overcome any damage caused by the infection and by 48 h p.i. merely 3% of the host cell population harbored bacteria.

## Bacterial proteome profiles mirror adaptations to epithelial cell layer integrity

Quantitative proteome profiling was applied to visualize the adaptations of host cells and infecting bacteria during the first 6.5 h p.i. Although the epithelial cell layers differed drastically in the initial protein abundances as mentioned above, no major changes in host cell protein dynamics were detectable upon infection with *S. aureus* (Supplemental Table 1). In contrast, the bacterial proteome was highly dynamic; of the 1108 proteins monitored, more than 50% presented significant changes during the first 6.5 h p.i. ( $p < 0.05$ ; Supplemental Table 2). Interestingly, most of these proteins displayed similar behavior in both settings of infection indicating that, by and large, the bacteria went through similar adaptive processes. However, the timing of the adaptive changes was markedly different for 67 staphylococcal proteins depending on the stage of regeneration of the infected epithelial cell layer (Supplemental Figure 4).

In order to appreciate the differences in *S. aureus* adaptation to epithelial cells at different stages of regeneration, the proteins displaying changes in level prior and during internalization were grouped according to their known regulators as described by Nagel et al., 2018. Proteins of which the level is subject to the control by CodY, Agr, Sae, Fur, Rex and SigB displayed infection-related changes in level (Figure 4). However, most clusters of proteins controlled by particular regulators did not show changes that could be related to the host cell regeneration state. This was different for proteins controlled by the redox regulator Rex, where ~50% of

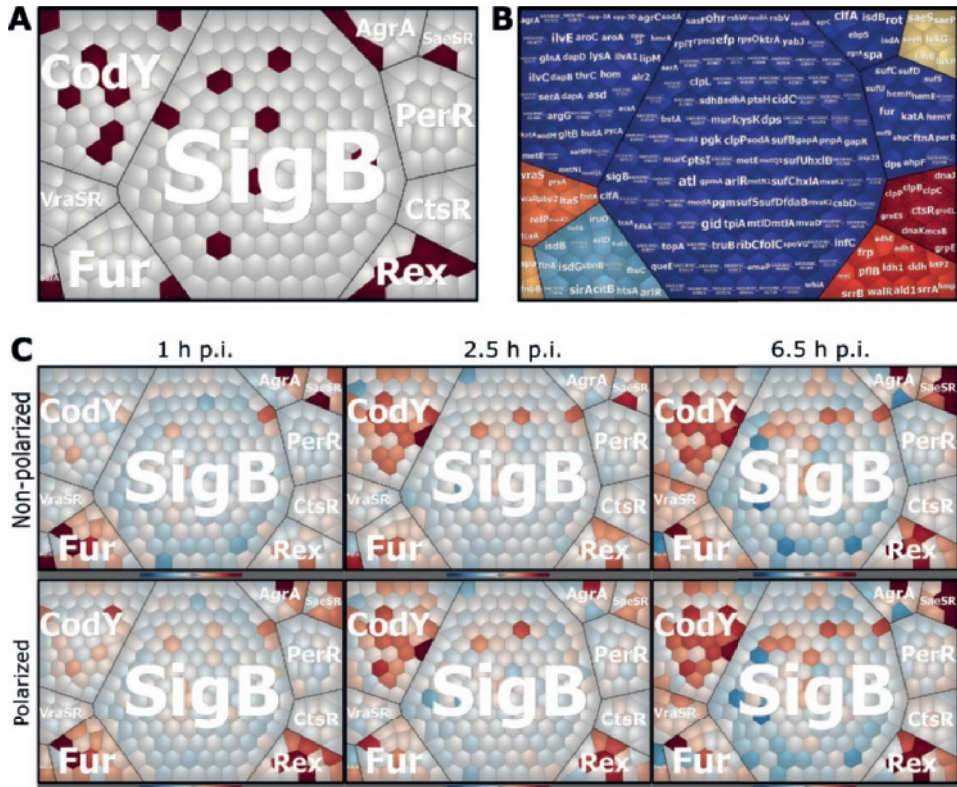
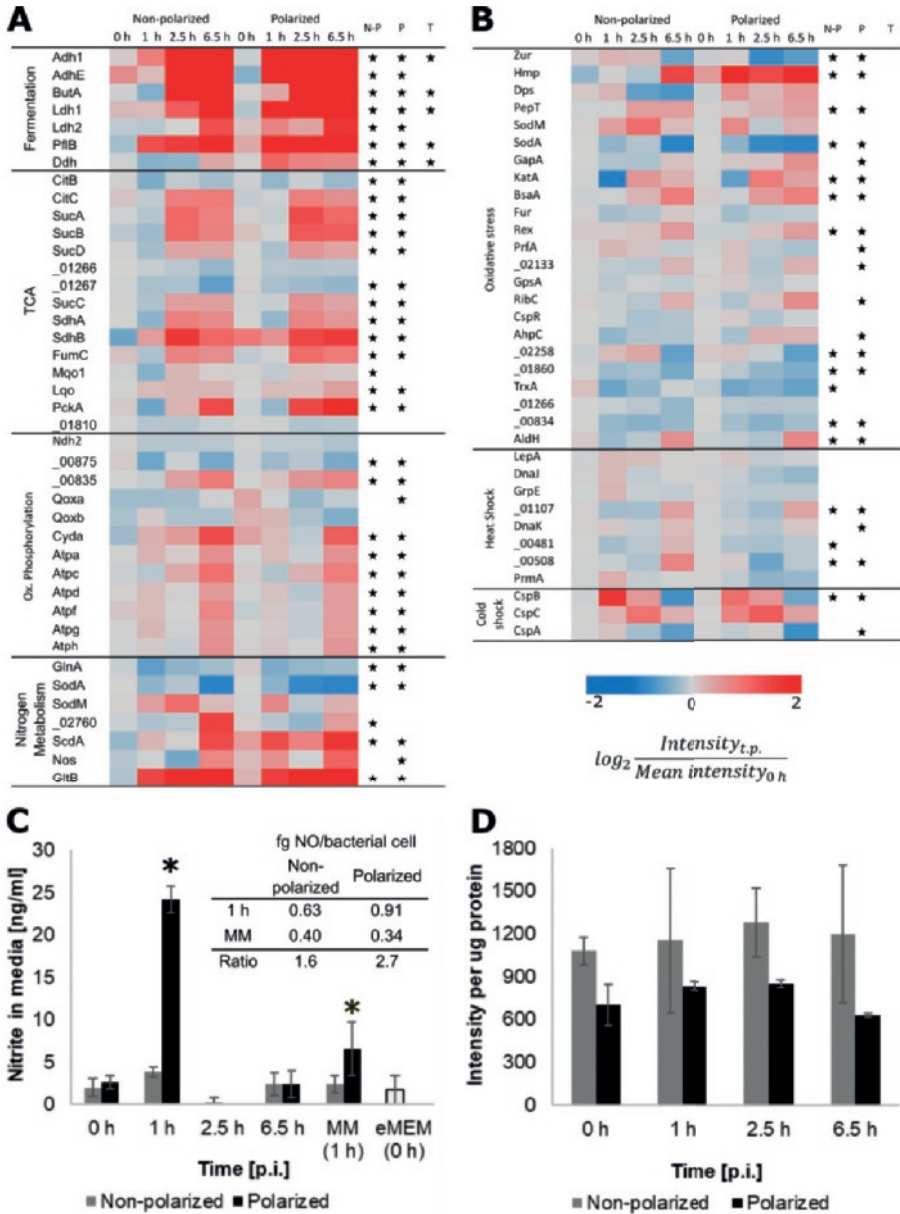


**Figure 4. Voronoi tree map representation of *S. aureus* protein levels grouped by major regulators.** (A) Proteins that displayed significantly ( $p$ -value $<0.05$ ) different dynamics during the first 6.5 h p.i. between the two infection models are highlighted in maroon. (B) Names of the proteins represented in each polygon of panel A. (C) Changes in protein amounts are presented at every time point relative to the respective protein quantities in the exponential phase. The 1 h sample represents the fraction of bacteria in the medium that was neither internalized into, nor attached to host cells after addition of the master mix.

these proteins displayed differential behavior (Figure 4), namely an earlier increase in level when the bacteria were confronted with polarized host cells. This difference in regulation became also clearly evident in a clustering of identified proteins based on metabolic pathways, where proteins related to fermentation





were found to be upregulated at earlier time points (Figure 5A). On the contrary, such a different time dependency in regulation between *S. aureus* challenged by polarized vs. non-polarized host cells was not observed for other pathways related to energy acquisition, like the TCA cycle and oxidative phosphorylation, and for

◀ **Figure 5. Central carbon and nitrogen metabolism of *S. aureus* during infection-related stress conditions.** The levels of a selection of proteins related to (A) carbon and nitrogen metabolism, and (B) stress conditions are represented in relation to the mean values of measured proteins extracted from the bacteria in exponential growth phase  $OD_{600}=0.4$ . Significant changes ( $p$ -value  $< 0.05$ ) are marked with stars in the last tree columns, which relate to changes over time during non-polarized conditions (N-P), polarized conditions (P) and the comparison of both trends (T). *S. aureus* proteins without an assigned gene symbol are labeled according to their locus tag without the "SAOUHSC\_" identifier. Additionally, (C) the concentration of nitrite in the apical media and (D) intracellular ROS were measured. The nitrate concentration in fresh eMEM media and the master mix (i.e. a solution of the *S. aureus* culture in eMEM used for infection) after 1 h incubation at 37°C were measured as controls. The measurements of NO in the basal media and intracellularly are included in Supplemental Figure 5. Measurements with significantly different levels are marked with an asterisk ( $p < 0.05$ ).

---

the majority of proteins involved in oxidative stress management (Figures 5A and 5B).

The activation of the Rex-regulated proteins is an indicator of changes in the redox state of the bacteria, which may be influenced by the concentration of nitric oxide (NO) in the environment (39). Therefore, the concentration of instable diatomic free radical NO in the medium was assessed over time by quantification of nitrite using the Griess reaction method (Figure 5C). The initial concentration of NO ( $t=0$  h) was comparable to the control (eMEM medium), showing that the epithelial cells produced very low amounts of NO, if any. However, in samples collected at 1 h p.i., where living bacteria were still abundantly present in the medium, significant amounts of NO were detectable. Of note, significant but lower nitrite concentrations were also measured in the bacterial master mixes incubated independently for 1 h (Figure 5C). Nonetheless, this increment was most clearly evident in the infection setting with polarized cells. In contrast, no nitric oxide was detectable once the non-internalized bacteria had been killed with lysostaphin, showing that living bacteria in the medium were responsible for NO production. This view was corroborated by an observed increase of the bacterial nitric oxide

synthase (Nos) during infection of polarized cells (Figure 5A), and of the flavohaemoglobin Hmp, which has NO-reductase and NO-dioxygenase activity (Figure 5B). In addition, no changes in the NO concentration were observed in basal culture medium or within the epithelial cells over the course of this experiment (Supplemental Figure 5).

To rule out the possibility that the observed changes in the bacterial metabolic pathways related to the production of reactive oxygen species (ROS) inside the epithelial cells, we also measured the intracellular ROS concentrations upon infection. Due to the regenerative state of the polarized and non-polarized epithelial cells, both of them displayed high amounts of ROS which slightly increased over time p.i.. However, unlike the NO levels, the ROS levels did not correlate with the observed activation of Rex-regulated proteins, showing that this activation must be attributed to NO production, particularly by the bacteria approaching a polarized epithelial cell barrier.

## Discussion

The epithelial cell layer in the human lung forms an important primary barrier against infection. Breaches of this barrier are dangerous as they provide easy access to pathogens that can then not only invade underlying tissues, but also cause additional damage to the epithelium by entering the respective cells from the basolateral side. Ultimately, this may lead to pneumonia, severe damage of the lungs and, in the worst case, death of the patient. Consequently, effective repair of a damaged lung epithelium is believed to be critical to avoid potentially life-threatening pulmonary infections. Despite this, it has so far not been studied in detail how different stages of regeneration of the epithelial layer determine the outcome of a bacterial infection and how these stages are reflected in the adaptive responses that take place in infecting bacteria. In the present study, we sought to improve our understanding of these interactions by establishing an infection

model where epithelial cell layers were exposed to *S. aureus* at two distinct early stages of regeneration. In this respect, it should be noted that upon lung injury, the epithelial cells will go through different stages of recovery that include inflammation and fibrogenesis phenotypes (15, 22). As shown by Schiller et al. (17), protein expression post injury is highly dynamic, and particular proteins play different roles in recovery over time. These regenerative stages were reflected in the proteins we identified in lung epithelial cells cultured for three or eleven days in our experimental set-up. In particular, the high levels of the SERPINH1, ST14, PLOD1, LGALS3, PLXB2, PLOD3, CTSZ, LGALS1, CTSA, P4HA2, CTSD, PLOD2, TINAGL1, P4HA1, CTSB, and FN1 proteins as detected in polarized 16HBE14o-cells can be regarded as a signature for fibrogenesis. Likewise, the detected low abundance of the TIMP3, THBS1, LAMA3, FGF2, LAMA5, and LAMB3 proteins is also a clear indicator for fibrinogenesis during polarization. On this basis, the non-polarized epithelial cell layer obtained after three days of culturing seems to resemble the initial migratory state of a damaged lung epithelium. In contrast, the polarized epithelial cells obtained after eleven days of culturing serves as a model for a subsequent early stage of fibrogenesis.

The dynamics of *S. aureus* infection in the two model stages of lung epithelial regeneration reflect the *in vivo* course of an infection remarkably well. As documented by microscopy, the infecting staphylococci clearly impacted on the epithelial cells during the first 6.5 h p.i., where the bacteria first broke the tight junctions in case of a polarized cell layer, and subsequently started to replicate intracellularly in both polarized and non-polarized cells. Of note, bacterial replication was substantially stronger in the non-polarized cells. Unexpectedly, this difference had no distinctive effect on the epithelial cells' proteome. Of course, in case of the polarized cells the rate of bacterial internalization is relatively low, so it is intuitive that changes in the host's proteome may have passed unnoticed. On the contrary, one might expect more severe changes in the proteome of non-

polarized epithelial cells that are virtually defenseless to the invading staphylococci. In particular, only two and nine proteins showed significantly different changes in the polarized and non-polarized epithelial set-ups, respectively, after challenge with *S. aureus* (Supplemental Table 1). Presumably, changes in the epithelial cell proteome will be more severe during later time points p.i. when the infection will probably elicit severe apoptotic reactions, but this can unfortunately not be assessed in our present experimental set-up. However, the latter view seems realistic based on the findings from our previous study, where the effects of staphylococcal internalization on submerged 16HBE14o- lung epithelial cells was studied over a period of 96 h (27).

The differential rates of *S. aureus* internalization by polarized and non-polarized epithelial cells probably reflect the fact that fibronectin, one of the major host cell anchors for *S. aureus*, is exposed exclusively at the basolateral side of polarized epithelial cells (40, 41). The fact that this protein is essentially absent from the apical cell surface severely restricts the bacterial internalization (42). *S. aureus* overcomes this challenge by disruption of tight junctions between the epithelial cells with aid of the pore-forming toxin Hla (23, 43, 44). Although, the production of Hla was not detectable in the cytosolic proteome fraction of the investigated bacteria, its presence can be inferred from the observed regulation of other proteins that are also controlled by the Agr quorum sensing system, such as ClfA and Spa (44).

While the polarized epithelial cell layer is capable of overcoming the imposed staphylococcal infection, the infected non-polarized epithelium is heading for disaster. In particular, strongly replicating internalized bacteria will almost inevitably induce massive lysis of these cells during the first day of infection (26, 27). Bacteria thus liberated from the epithelial enclosure will be released into the external milieu where, in principle, they can engage in another round of host cell

infection. However, under our present experimental conditions the latter will not be observed as the released bacteria are eliminated by lysostaphin that was added to the culture medium at 1 h p.i. Interestingly, when non-polarized epithelial cells were challenged with *S. aureus*, the percentage of infected cells increased over time as a result of lysis of non-infected cells. Possibly, this is a consequence of the release of epithelial or bacterial debris into the medium that will induce apoptosis.

Despite the observed differences in infection dynamics, the adaptations of *S. aureus* p.i. were largely similar in polarized and non-polarized epithelial cells, showing that the initial adaptations to the infection conditions do not depend on the polarization state of the host cells. Such adaptations include elevated production of proteins related to the catabolism of alternative carbon sources, the degradation of amino acids and the TCA cycle. Moreover, also the levels of proteins regulated by SaeRS and Agr, which have been linked to virulence, changed upon internalization (Supplemental Table 2). Remarkably, there were no differences in the dynamics of bacterial proteins responsive to oxidative-, heat- or cold-stress conditions between the two infection settings. The latter is consistent with the fact that no significant changes in ROS production by polarized and non-polarized cells were detectable, even though the rates of infection in both settings were strikingly different.

Remarkably, the earlier upregulation of Rex-regulated proteins in bacteria facing a polarized epithelial barrier implies a critical difference in the local conditions with potential implications for the course of infection. The Rex regulon is known to respond to changes in the NAD<sup>+</sup>/NADH ratio of the bacterial cytoplasm, which may relate to limited availability of oxygen, excessive TCA cycle activity, or increased levels of NO (39, 45). As a consequence, the bacteria will upregulate pathways for anaerobic metabolism. This behavior could have been anticipated based on the fact that NO is a signaling molecule employed in wound repair (46)

and, therefore, produced in higher quantities during illnesses that compromise the lung epithelium like asthma and COPD (47–50). In addition, NO production is a known anti-infective defense mechanism employed by human host cells (51–53). Nevertheless, a difference in NO production by the epithelial cells at different stages of regeneration was not detectable in our experimental set-up. On the contrary, we detected significant NO production by the infecting bacterial cells prior to internalization, especially when confronted with an intact epithelial cell barrier. Accordingly, the differential timing in the detection of Rex-regulated proteins must be a consequence of the bacterial NO production at 1 h p.i. Of note, once internalized, the fermentative pathways will be further upregulated as a consequence of the microaerobic environment that the bacteria are exposed to intracellularly (26–28). Importantly, the increased production of NO can be attributed to the observed upregulation of Nos production in the bacteria. The latter might be beneficial for bacterial homeostasis as it allows a modulation of membrane bioenergetics during infection. It has been shown that this is advantageous for *S. aureus* when facing an intact epithelial barrier by experiments in a murine model, where bacterial Nos-deficiency precluded long-term nasal colonization (54).

In conclusion, we explored the adaptive behavior of *S. aureus* upon close encounters with polarized and non-polarized lung epithelial cells that mimic the clinical situation of a wounded epithelium at different early regenerative stages. In the clinical context, such scenarios will be encountered in particular when the lung epithelial cell layer is damaged by common pathogens, such as influenza (12, 55). Our present observations provide a deeper insight into how the *S. aureus* bacterium can take advantage of such a breach of barrier, and how infected epithelial cells have a limited ability of responding to the staphylococcal insult especially during the very early stages of tissue regeneration. Our study also highlights the importance of early adaptations of *S. aureus*, where the production

of NO is employed in the confrontation with polarized epithelial cells to maintain bacterial homeostasis and to stay fit for infection.

## Acknowledgements

We thank Jan Pané-Farré for providing *S. aureus* HG001  $\Delta spa$ , and Rita Ferreira and Mafalda Bispo for sharing protocols for NO and ROS measurements. Funding for this project was received from the Graduate School of Medical Sciences of the University of Groningen [to L.M.P.M., S.A.M., and J.M.v.D.], the Deutsche Forschungsgemeinschaft Grants GRK1870 [to L.M.P.M., S.A.M. and U.V.] and SFBTRR34 [to U.V.]. Part of this work has been performed at the UMCG Imaging and Microscopy Center (UMIC), which is sponsored by NWO-grants 40-00506-98-9021 (TissueFaxes) and 175-010-2009-023 (Zeiss 2p). The funders had no role in study design, data collection and analysis, decision to publish, or preparation of the manuscript.

## References

1. Lowy, F. D. (1998) *Staphylococcus aureus* Infections. *N. Engl. J. Med.* 339, 520–532
2. Dastgheyb, S. S., and Otto, M. (2015) Staphylococcal adaptation to diverse physiologic niches: an overview of transcriptomic and phenotypic changes in different biological environments. *Future Microbiol.* 10, 1981–1995
3. Sollid, J. U. E., Furberg, A. S., Hanssen, A. M., and Johannessen, M. (2014) *Staphylococcus aureus*: Determinants of human carriage. *Infect. Genet. Evol.* 21, 531–541
4. Wertheim, H. F., Melles, D. C., Vos, M. C., van Leeuwen, W., van Belkum, A., Verbrugh, H. A., and Nouwen, J. L. (2005) The role of nasal carriage in *Staphylococcus aureus* infections. *Lancet Infect. Dis.* 5, 751–762
5. Krismer, B., Liebeke, M., Janek, D., Nega, M., Rautenberg, M., Hornig, G., Unger, C., Weidenmaier, C., Lalk, M., and Peschel, A. (2014) Nutrient Limitation Governs *Staphylococcus aureus* Metabolism and Niche Adaptation in the Human Nose. *PLOS Pathog.* 10, e1003862



6. Gillet, Y., Vanhems, P., Lina, G., Bes, M., Vandenesch, F., Floret, D., and Etienne, J. (2007) Factors Predicting Mortality in Necrotizing Community-Acquired Pneumonia Caused by *Staphylococcus aureus* Containing Panton-Valentine Leukocidin. *Clin. Infect. Dis.* 45, 315–321
7. Chen, J., Luo, Y., Zhang, S., Liang, Z., Wang, Y., Zhang, Y., Zhou, G., Jia, Y., Chen, L., and She, D. (2014) Community-acquired necrotizing pneumonia caused by methicillin-resistant *Staphylococcus aureus* producing Panton-Valentine leukocidin in a Chinese teenager: case report and literature review. *Int. J. Infect. Dis.* 26, 17–21
8. Zhang, Q., Illing, R., Hui, C. K., Downey, K., Carr, D., Stearn, M., Alshafi, K., Menzies-Gow, A., Zhong, N., and Fan Chung, K. (2012) Bacteria in sputum of stable severe asthma and increased airway wall thickness. *Respir. Res.* 13, 35
9. Pastacaldi, C., Lewis, P., and Howarth, P. (2011) Staphylococci and staphylococcal superantigens in asthma and rhinitis: a systematic review and meta-analysis. *Allergy* 66, 549–555
10. Papi, A., Bellettato, C. M., Braccioni, F., Romagnoli, M., Casolari, P., Caramori, G., Fabbri, L. M., and Johnston, S. L. (2006) Infections and Airway Inflammation in Chronic Obstructive Pulmonary Disease Severe Exacerbations. *Am. J. Respir. Crit. Care Med.* 173, 1114–1121
11. Wilkinson, T. M. A., Hurst, J. R., Perera, W. R., Wilks, M., Donaldson, G. C., and Wedzicha, J. A. (2006) Effect of Interactions Between Lower Airway Bacterial and Rhinoviral Infection in Exacerbations of COPD. *Chest* 129, 317–324
12. Chekabab, S. M., Silverman, R. J., Lafayette, S. L., Luo, Y., Rousseau, S., and Nguyen, D. (2015) *Staphylococcus aureus* Inhibits IL-8 Responses Induced by *Pseudomonas aeruginosa* in Airway Epithelial Cells. *PLoS ONE* 10, e0137753.
13. Shah, P. L., Mawdsley, S., Nash, K., Cullinan, P., Cole, P. J., and Wilson, R. (1999) Determinants of chronic infection with *Staphylococcus aureus* in patients with bronchiectasis. *Eur. Respir. J.* 14, 1340–1344
14. Schwerdt, M., Neumann, C., Schwartbeck, B., Kampmeier, S., Herzog, S., Görlich, D., Dübbers, A., Große-Onnebrink, J., Kessler, C., Küster, P., Schültingkemper, H., Treffon, J., Peters, G., and Kahl, B. C. (2018) *Staphylococcus aureus* in the airways of cystic fibrosis patients - A retrospective long-term study. *Int. J. Med. Microbiol. IJMM* 308, 631–639

15. Puchelle, E., Zahm, J.-M., Tournier, J.-M., and Coraux, C. (2006) Airway epithelial repair, regeneration, and remodeling after injury in chronic obstructive pulmonary disease. *Proc. Am. Thorac. Soc.* 3, 726–733
16. Wilson, M., and Wynn, T. (2009) Pulmonary fibrosis: pathogenesis, etiology and regulation. *Mucosal Immunol.* 2, 103–121
17. Schiller, H. B., Fernandez, I. E., Burgstaller, G., Schaab, C., Scheltema, R. A., Schwarzmayr, T., Strom, T. M., Eickelberg, O., and Mann, M. (2015) Time- and compartment-resolved proteome profiling of the extracellular niche in lung injury and repair. *Mol. Syst. Biol.* 11, 819
18. Fernandez, I. E., and Eickelberg, O. (2012) New cellular and molecular mechanisms of lung injury and fibrosis in idiopathic pulmonary fibrosis. *The Lancet* 380, 680–688
19. Kisseleva, T., and Brenner, D. A. (2008) Mechanisms of Fibrogenesis. *Exp. Biol. Med.* 233, 109–122
20. Kleinman, H. K., Philp, D., and Hoffman, M. P. (2003) Role of the extracellular matrix in morphogenesis. *Curr. Opin. Biotechnol.* 14, 526–532
21. Rodriguez-Boulan, E., and Macara, I. G. (2014) Organization and execution of the epithelial polarity programme. *Nat. Rev. Mol. Cell Biol.* 15, 225–242
22. Herard, A. L., Zahm, J. M., Pierrot, D., Hinrasky, J., Fuchey, C., and Puchelle, E. (1996) Epithelial barrier integrity during *in vitro* wound repair of the airway epithelium. *Am. J. Respir. Cell Mol. Biol.* 15, 624–632
23. R ath, S., Ziesemer, S., Witte, A., Konkel, A., M uller, C., Hildebrandt, P., V olker, U., and Hildebrandt, J.-P. (2013) *S. aureus* haemolysin A-induced IL-8 and IL-6 release from human airway epithelial cells is mediated by activation of p38- and Erk-MAP kinases and additional, cell type-specific signalling mechanisms. *Cell. Microbiol.* 15, 1253–1265
24. Soong, G., Martin, F. J., Chun, J., Cohen, T. S., Ahn, D. S., and Prince, A. (2011) *Staphylococcus aureus* Protein A Mediates Invasion across Airway Epithelial Cells through Activation of RhoA GTPase Signaling and Proteolytic Activity. *J. Biol. Chem.* 286, 35891–35898
25. Kiedrowski, M. R., Paharik, A. E., Ackermann, L. W., Shelton, A. U., Singh, S. B., Starner, T. D., and Horswill, A. R. (2016) Development of an *in vitro* colonization model to investigate *Staphylococcus aureus* interactions with airway epithelia. *Cell. Microbiol.* 18, 720–732

26. Michalik, S., Depke, M., Murr, A., Gesell Salazar, M., Kusebauch, U., Sun, Z., Meyer, T. C., Surmann, K., Pfortner, H., Hildebrandt, P., Weiss, S., Palma Medina, L. M., Gutjahr, M., Hammer, E., Becher, D., Pribyl, T., Hammerschmidt, S., Deutsch, E. W., Bader, S. L., Hecker, M., Moritz, R. L., Mäder, U., Völker, U., and Schmidt, F. (2017) A global *Staphylococcus aureus* proteome resource applied to the *in vivo* characterization of host-pathogen interactions. *Sci. Rep.* 7, 9718
27. Palma Medina, L. M., Becker, A.-K., Michalik, S., Yedavally, H., Raineri, E. J. M., Hildebrandt, P., Gesell Salazar, M., Surmann, K., Pfortner, H., Mekonnen, S. A., Salvati, A., Kaderali, L., van Dijk, J. M., and Völker, U. (2019) Metabolic cross-talk between human bronchial epithelial cells and internalized *Staphylococcus aureus* as a driver for infection. *Mol. Cell. Proteomics* 18, 892-908.
28. Surmann, K., Simon, M., Hildebrandt, P., Pfortner, H., Michalik, S., Stentzel, S., Steil, L., Dhople, V. M., Bernhardt, J., Schlüter, R., Depke, M., Gierok, P., Lalk, M., Bröker, B. M., Schmidt, F., and Völker, U. (2015) A proteomic perspective of the interplay of *Staphylococcus aureus* and human alveolar epithelial cells during infection. *J. Proteomics* 128, 203–217
29. Herbert, S., Ziebandt, A.-K., Ohlsen, K., Schäfer, T., Hecker, M., Albrecht, D., Novick, R., and Götz, F. (2010) Repair of Global Regulators in *Staphylococcus aureus* 8325 and Comparative Analysis with Other Clinical Isolates. *Infect. Immun.* 78, 2877–2889
30. Pfortner, H., Wagner, J., Surmann, K., Hildebrandt, P., Ernst, S., Bernhardt, J., Schurmann, C., Gutjahr, M., Depke, M., Jehmlich, U., Dhople, V., Hammer, E., Steil, L., Völker, U., and Schmidt, F. (2013) A proteomics workflow for quantitative and time-resolved analysis of adaptation reactions of internalized bacteria. *Methods* 61, 244–250
31. Cozens, A. L., Yezzi, M. J., Kunzelmann, K., Ohrui, T., Chin, L., Eng, K., Finkbeiner, W. E., Widdicombe, J. H., and Gruenert, D. C. (1994) CFTR expression and chloride secretion in polarized immortal human bronchial epithelial cells. *Am. J. Respir. Cell Mol. Biol.* 10, 38–47
32. van den Berg, S., Bonarius, H. P. J., van Kessel, K. P. M., Elsinga, G. S., Kooi, N., Westra, H., Bosma, T., van der Kooi-Pol, M. M., Koedijk, D. G. A. M., Groen, H., van Dijk, J. M., Buist, G., and Bakker-Woudenberg, I. A. J. M. (2015) A human monoclonal antibody targeting the conserved staphylococcal antigen IsaA protects mice against *Staphylococcus aureus* bacteremia. *Int. J. Med. Microbiol.* 305, 55–64

33. Bruderer, R., Bernhardt, O. M., Gandhi, T., Miladinović, S. M., Cheng, L.-Y., Messner, S., Ehrenberger, T., Zanotelli, V., Butscheid, Y., Escher, C., Vitek, O., Rinner, O., and Reiter, L. (2015) Extending the Limits of Quantitative Proteome Profiling with Data-Independent Acquisition and Application to Acetaminophen-Treated Three-Dimensional Liver Microtissues. *Mol. Cell. Proteomics* 14, 1400–1410
34. Nagel, A., Michalik, S., Debarbouille, M., Hertlein, T., Salazar, M. G., Rath, H., Msadek, T., Ohlsen, K., Dijn, J. M. van, Völker, U., and Mäder, U. (2018) Inhibition of Rho Activity Increases Expression of SaeRS-Dependent Virulence Factor Genes in *Staphylococcus aureus*, Showing a Link between Transcription Termination, Antibiotic Action, and Virulence. *mBio* 9, e01332-18
35. Ritchie, M. E., Phipson, B., Wu, D., Hu, Y., Law, C. W., Shi, W., and Smyth, G. K. (2015) limma powers differential expression analyses for RNA-seq and microarray studies. *Nucleic Acids Res.* 43, e47
36. R Core Team (2018) R: A language and environment for statistical computing (R Foundation for Statistical Computing, Vienna, Austria.)
37. Fuchs, S., Mehlan, H., Bernhardt, J., Hennig, A., Michalik, S., Surmann, K., Pané-Farré, J., Giese, A., Weiss, S., Backert, L., Herbig, A., Nieselt, K., Hecker, M., Völker, U., and Mäder, U. (2018) AureoWiki-The repository of the *Staphylococcus aureus* research and annotation community. *Int. J. Med. Microbiol.* 308, 558–568
38. Ehrhardt, C., Kneuer, C., Laue, M., Schaefer, U. F., Kim, K.-J., and Lehr, C.-M. (2003) 16HBE14o- Human Bronchial Epithelial Cell Layers Express P-Glycoprotein, Lung Resistance-Related Protein, and Caveolin-1. *Pharm. Res.* 20, 545–551
39. Somerville, G. A., and Proctor, R. A. (2009) At the Crossroads of Bacterial Metabolism and Virulence Factor Synthesis in Staphylococci. *Microbiol. Mol. Biol. Rev.* 73, 233–248
40. Matlin, K. S., Haus, B., and Zuk, A. (2003) Integrins in epithelial cell polarity: using antibodies to analyze adhesive function and morphogenesis. *Methods* 30, 235–246
41. Schoenenberger, C. A., Zuk, A., Zinkl, G. M., Kendall, D., and Matlin, K. S. (1994) Integrin expression and localization in normal MDCK cells and transformed MDCK cells lacking apical polarity. *J. Cell Sci.* 107, 527–541

42. Garzoni, C., and Kelley, W. L. (2009) *Staphylococcus aureus*: new evidence for intracellular persistence. *Trends Microbiol.* 17, 59–65
43. Monecke, S., Müller, E., Büchler, J., Stieber, B., and Ehricht, R. (2014) *Staphylococcus aureus* *In vitro* Secretion of Alpha Toxin (hla) Correlates with the Affiliation to Clonal Complexes. *PLOS ONE* 9, e100427
44. Horn, J., Stelzner, K., Rudel, T., and Fraunholz, M. (2018) Inside job: *Staphylococcus aureus* host-pathogen interactions. *Int. J. Med. Microbiol.* 308, 607–624
45. Pagels, M., Fuchs, S., Pané-Farré, J., Kohler, C., Menschner, L., Hecker, M., McNamarra, P. J., Bauer, M. C., von Wachenfeldt, C., Liebeke, M., Lalk, M., Sander, G., von Eiff, C., Proctor, R. A., and Engelmann, S. (2010) Redox sensing by a Rex-family repressor is involved in the regulation of anaerobic gene expression in *Staphylococcus aureus*. *Mol. Microbiol.* 76, 1142–1161
46. Luo, J., and Chen, A. F. (2005) Nitric oxide: a newly discovered function on wound healing. *Acta Pharmacol. Sin.* 26, 259
47. Lane, C., Knight, D., Burgess, S., Franklin, P., Horak, F., Legg, J., Moeller, A., and Stick, S. (2004) Epithelial inducible nitric oxide synthase activity is the major determinant of nitric oxide concentration in exhaled breath. *Thorax* 59, 757–760
48. Lee, W., and Thomas, P. S. (2009) Oxidative stress in COPD and its measurement through exhaled breath condensate. *Clin. Transl. Sci.* 2, 150–155
49. Liu, J., Sandrini, A., Thurston, M. C., Yates, D. H., and Thomas, P. S. (2007) Nitric oxide and exhaled breath nitrite/nitrates in chronic obstructive pulmonary disease patients. *Respir. Int. Rev. Thorac. Dis.* 74, 617–623
50. Malinovschi, A., Ludviksdottir, D., Tufvesson, E., Rolla, G., Bjermer, L., Alving, K., and Diamant, Z. (2015) Application of nitric oxide measurements in clinical conditions beyond asthma. *Eur. Clin. Respir. J.* 2,
51. Akaike, T., and Maeda, H. (2000) Nitric oxide and virus infection. *Immunology* 101, 300–308
52. Bogdan, C. (2015) Nitric oxide synthase in innate and adaptive immunity: an update. *Trends Immunol.* 36, 161–178
53. Roy, S., Sharma, S., Sharma, M., Aggarwal, R., and Bose, M. (2004) Induction of nitric oxide release from the human alveolar epithelial cell line

A549: an *in vitro* correlate of innate immune response to *Mycobacterium tuberculosis*. *Immunology* 112, 471–480

54. Kinkel, T. L., Ramos-Montañez, S., Pando, J. M., Tadeo, D. V., Strom, E. N., Libby, S. J., and Fang, F. C. (2016) An Essential Role for Bacterial Nitric Oxide Synthase in *Staphylococcus aureus* Electron Transfer and Colonisation. *Nat. Microbiol.* 2, 16224
55. Löffler, B., Niemann, S., Ehrhardt, C., Horn, D., Lanckohr, C., Lina, G., Ludwig, S., and Peters, G. (2013) Pathogenesis of *Staphylococcus aureus* necrotizing pneumonia: the role of PVL and an influenza coinfection. *Expert Rev. Anti Infect. Ther.* 11, 1041–1051



## Chapter 4

# **Signatures of cytoplasmic proteins in the exoproteome distinguish community and hospital-associated methicillin-resistant *Staphylococcus aureus* USA300 lineages**

---

Solomon A. Mekonnen, Laura M. Palma Medina, Corinna Glasner, Eleni Tsompanidou, Anne de Jong, Stefano Grasso, Marc Schaffer, Ulrike Mäder, Anders R. Larsen, Heidi Gumpert, Henrik Westh, Uwe Völker, Andreas Otto, Dörte Becher, Jan Maarten van Dijl

*Virulence* 8: 891–907 (2017)

Supplementary Material is available at [http://bit.ly/Thesis\\_Palma\\_Medina](http://bit.ly/Thesis_Palma_Medina)





## Abstract

Methicillin-resistant *Staphylococcus aureus* (MRSA) is the common name for a heterogeneous group of highly drug-resistant staphylococci. Two major MRSA classes are distinguished based on epidemiology, namely community-associated (CA) and hospital-associated (HA) MRSA. Notably, the distinction of CA- and HA-MRSA based on molecular traits remains difficult due to the high genomic plasticity of *S. aureus*. Here we sought to pinpoint global distinguishing features of CA- and HA-MRSA through a comparative genome and proteome analysis of the notorious MRSA lineage USA300. We show for the first time that CA- and HA-MRSA isolates can be distinguished by two distinct extracellular protein abundance clusters that are predictive not only for epidemiologic behavior, but also for their growth and survival within epithelial cells. This 'exoproteome profiling' also groups more distantly related HA-MRSA isolates into the HA exoproteome cluster. Comparative genome analysis suggests that these distinctive features of CA- and HA-MRSA isolates relate predominantly to the accessory genome. Intriguingly, the identified exoproteome clusters differ in the relative abundance of typical cytoplasmic proteins, suggesting that signatures of cytoplasmic proteins in the exoproteome represent a new distinguishing feature of CA- and HA-MRSA. Our comparative genome and proteome analysis focuses attention on potentially distinctive roles of 'liberated' cytoplasmic proteins in the epidemiology and intracellular survival of CA- and HA-MRSA isolates. Such extracellular cytoplasmic proteins were recently invoked in staphylococcal virulence, but their implication in the epidemiology of MRSA is unprecedented.

## Introduction

*Staphylococcus aureus* is a wide-spread commensal bacterium, but also a notoriously drug-resistant pathogen that causes a wide range of diseases, varying from mild skin infections to life-threatening invasive diseases <sup>1</sup>. About 20-30 % of the healthy human population is known to carry *S. aureus*, the anterior nares being the preferred niche <sup>2</sup>.

Since the clinical implementation of antibiotics, *S. aureus* has acquired a range of resistance traits through mutations and horizontal gene transfer. This has culminated in the emergence of methicillin-resistant *S. aureus* (MRSA), a major healthcare problem world-wide <sup>3,4</sup>. The emergence of MRSA is a particularly worrisome development since it is associated with increased morbidity and mortality, especially if very young, immune-compromised or elderly individuals are infected <sup>5,6</sup>. Moreover, no effective vaccine against MRSA is currently available <sup>7-9</sup>.

Two major classes of MRSA are currently distinguished based on their epidemiology, namely community-associated (CA) and hospital-associated (HA) MRSA. CA-MRSA is mainly a threat to healthy individuals, causing in particular skin and soft tissues infections, but also serious invasive infections such as pneumonia and osteomyelitis <sup>10-13</sup>. In contrast, HA-MRSA infections are associated with prolonged hospitalization, stay in intensive care units, hemodialysis, surgery, and long-term exposure to antibiotics <sup>14</sup>.

Molecular markers for high-confidence distinction between CA- and HA-MRSA isolates are urgently needed in the prevention and control of hospital outbreaks. Different DNA typing methods, such as pulsed-field gel electrophoresis (PFGE) and *Staphylococcus* protein A (*spa*) typing have been used to differentiate between these two classes of MRSA <sup>15</sup>. This was so far feasible, because particular *S. aureus*

lineages with distinct sequence types are associated with the CA- or HA-associated behavior. In addition, particular virulence genes (e.g. for the Panton-Valentin leukocidin; PVL), the arginine catabolic mobile element (ACME), and mobile genetic elements carrying the *mecA* gene for methicillin resistance are used to distinguish CA- and HA-MRSA<sup>11-14,16,17</sup>. However, such DNA-based typing methods do not allow easy distinction between closely related CA- and HA-MRSA lineages, because the causative molecular features have remained largely enigmatic. For instance, PFGE assigns CA-MRSA isolates with the *spa* type t008 and HA-MRSA isolates with the *spa* type t024 to the same USA300 lineage<sup>18</sup>. Likewise, *spa* typing has insufficient discriminatory power to distinguish closely related CA and HA isolates as it assigns CA-USA300 isolates with the multi-locus sequence type ST8 and more distantly related HA isolates with the sequence type ST8 to the same *spa* type t008<sup>18</sup>. Nevertheless, we have previously shown that a multiple-locus variable number tandem repeat fingerprinting (MLVF) approach may distinguish these highly related *S. aureus* isolates<sup>19</sup>.

An important challenge for the clinic is that *S. aureus* types previously regarded as CA, such as USA300 and the European ST80 clone, are becoming common hospital pathogens causing outbreaks<sup>18,20-22</sup>. Clearly, an increasing prevalence of CA-MRSA in the community makes it harder to exclude the respective lineages from hospitals, because they can be carried into the hospitals by MRSA-positive patients, healthcare workers and visitors. Furthermore, it is conceivable that these bacteria have acquired, either before or after entry into the hospital environment, properties that facilitate their spread in this setting. The latter view would be supported by the observation that the closely related USA300 isolates with *spa* types t008 and t024 display different epidemiology<sup>18</sup>.

The distinction of CA- and HA-MRSA at the molecular level is challenging, because many factors may contribute to bacterial epidemiological behavior, not in

the last place interactions with the human host. High-throughput analytical ‘omics’ approaches, especially genomics and proteomics, are particularly suitable for exploring such multi-factorial behavior since they allow the definition of feature- or condition-specific signatures <sup>23,24</sup>. Furthermore, proteomics applied to bacterial pathogens grown under infection-mimicking conditions is a powerful tool for investigating different lineage- or type-specific patterns of gene expression <sup>25</sup>. In the context of infection-related research, it is important to focus special attention on the extracellular proteome (‘exoproteome’) as it represents the main reservoir of virulence factors that are first in interacting with the human host <sup>26,27</sup>. Specifically, secreted toxins and other virulence factors of *S. aureus* contribute to tissue damage, host invasion, and evasion of the host’s immune responses <sup>28,29</sup>. Thus, proteomics has a high potential for identifying diagnostic biomarkers, and novel vaccine or drug targets <sup>30</sup>.

To obtain a better understanding of the molecular differences between CA- and HA-MRSA, the present study was aimed at a global comparative genome and exoproteome analysis of 12 MRSA isolates belonging to the USA300 lineage as defined by PFGE. As these isolates were all collected from Denmark (DK), we refer to them as the CA<sup>DK</sup> and HA<sup>DK</sup> isolates. Specifically, the CA<sup>DK</sup> group had the sequence type ST8, the *spa* type t008 and was PVL-positive, whereas the HA<sup>DK</sup> group was characterized by the sequence type ST8 and the *spa* type t024 <sup>18,21</sup>. As a control group, we also investigated the exoproteomes of three HA-MRSA isolates from the Dutch (NL) - German (DE) border region, here referred to as HA<sup>NL-DE</sup>, which have the sequence type ST8, and *spa* type t008 or t024 <sup>19</sup>. The genomes of all 15 isolates were sequenced, and their extracellular proteins were analyzed by liquid chromatography and mass spectrometry (LC-MS). In brief, CA and HA isolates could be distinguished to some extent by the accessory genome. More importantly, a principal component analysis (PCA) of the exoproteome MS data

clustered the 15 investigated isolates into two groups that match their different epidemiological behavior.

## Results

### Comparative genomic analysis

Whole genome sequence analysis was performed to determine the genomic similarities and differences of all 15 investigated isolates. A phylogenetic tree based on the core genome of the isolates showed that the six CA<sup>DK</sup>, and five of the six HA<sup>DK</sup> isolates formed two distinct clusters (Fig. 1). One HA<sup>DK</sup> isolate (D3) showed a more distant relationship with the other HA<sup>DK</sup> isolates. Furthermore, the three HA<sup>NL-DE</sup> isolates formed a separate cluster that is closer to the CA<sup>DK</sup> than the HA<sup>DK</sup> isolates. In addition to the phylogenetic analysis, a comparative analysis of the accessory genomes of the isolates was performed, which is presented as a heatmap in Figure 1. As illustrated in the heat map, the CA isolates have overall more accessory genes than the HA isolates. Perhaps more importantly, the clustering of accessory genes is indicative of a separation between the CA and HA isolates, irrespective of the geographical origin of the HA isolates. This separation is also reflected in the presence or absence of a number of known virulence genes (red lines in Fig. 1), such as the PVL-encoding genes *lukF* and *lukS* that were exclusively found in the CA isolates, and the enterotoxin-encoding genes *sea*, *sed*, *sej*, and *ser* that were only present in the investigated HA isolates (Supplementary Table 1). Of note, PVL is often used as a marker for CA-MRSA and enterotoxin genes appear to be rare in CA isolates of the USA300 lineage <sup>31</sup>, but a possible association of enterotoxin genes with HA behavior would be novel.

Both CA- and HA-MRSA isolates carried a *norA* gene that provides resistance to fluoroquinolones, and *mecA* and *blaZ* genes for  $\beta$ -lactam resistance (Supplementary Table 2). Genes potentially providing resistance to macrolides,

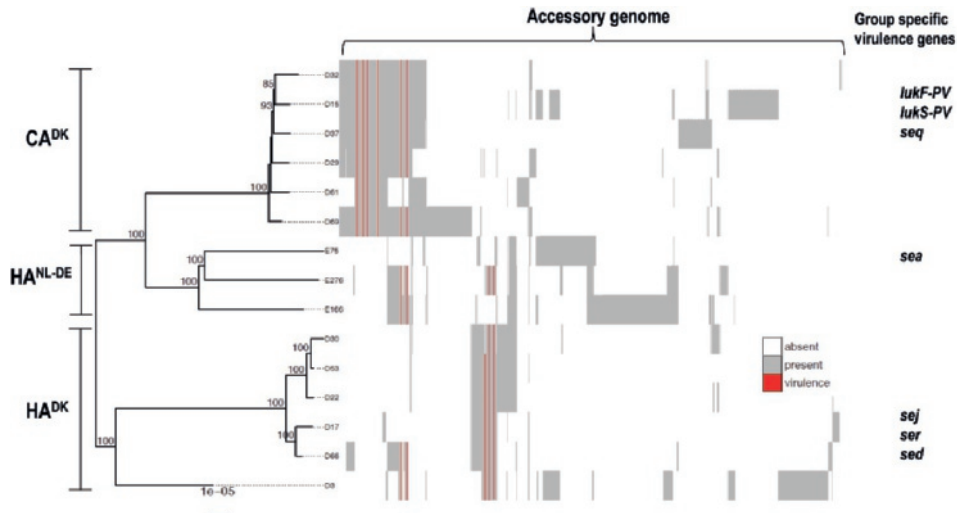


**Fig. 1. Phylogenetic tree and accessory genomes of all 15 investigated CA<sup>DK</sup>, HA<sup>DK</sup> and HA<sup>NL-DE</sup> isolates.** The tree is midpoint rooted and bootstrap support >70% is indicated on the branches. The heatmap to the right of the phylogenetic tree illustrates the accessory genome. The columns of the heatmap are hierarchically clustered based on the presence/absence of genes. Known virulence genes are indicated in red. Examples of virulence genes that are exclusively present in one of the three groups are indicated as group-specific virulence genes.

lincosamides and streptogramin B (*msr(A)*), aminoglycosides (*aph(3')-III*), and macrolides (*mph(C)*) were exclusively identified in the CA-MRSA isolates, whereas *erm(A)* and *spc* that provide resistance to macrolides and aminoglycosides, respectively, were exclusively identified among the HA-MRSA isolates (Supplementary Table 2). Altogether, the CA-MRSA isolates carried more (potential) antimicrobial resistance genes than the investigated HA-MRSA isolates.

## Unique and shared exoproteins

To characterize the exoproteomes of the 15 MRSA isolates, they were cultured in RPMI medium since a recent study showed that global gene expression profiles of *S. aureus* cells grown in RPMI or human plasma are highly similar<sup>24</sup>. Samples were withdrawn for exoproteome analyses at mid-exponential growth phase and

90 min after entry into the stationary phase. No major differences in the growth curves of the 15 MRSA were observed (data not shown). As shown by gel-free mass spectrometry, a total number of 409 unique proteins was identified from the 15 exoproteome samples of exponentially grown isolates. Similarly, a total number of 458 unique proteins was identified from the 15 exoproteome samples generated from stationary phase cultures. Proteins were considered for further analyses when they were present in at least 50 % of the isolates of a particular group, i.e. when a protein was present in three out of the six isolates in CA<sup>DK</sup> and HA<sup>DK</sup>, and in two out of three isolates in HA<sup>NL-DE</sup>. Thus, 283 and 307 unique proteins identified in the exponential or stationary phase samples, respectively, were included in the subsequent analyses (Supplementary Table 3). The majority of these proteins was shared by all three groups both in the exponential (Fig. 2a) and stationary (Fig. 2b) growth phases. Importantly, there are more proteins shared by the HA<sup>DK</sup> and HA<sup>NL-DE</sup> isolates than by the HA<sup>DK</sup> or HA<sup>NL-DE</sup> isolates and CA<sup>DK</sup> isolates. This implies that, in terms of exoprotein production, the two groups of HA isolates are more closely related with each other than the HA and CA isolates.

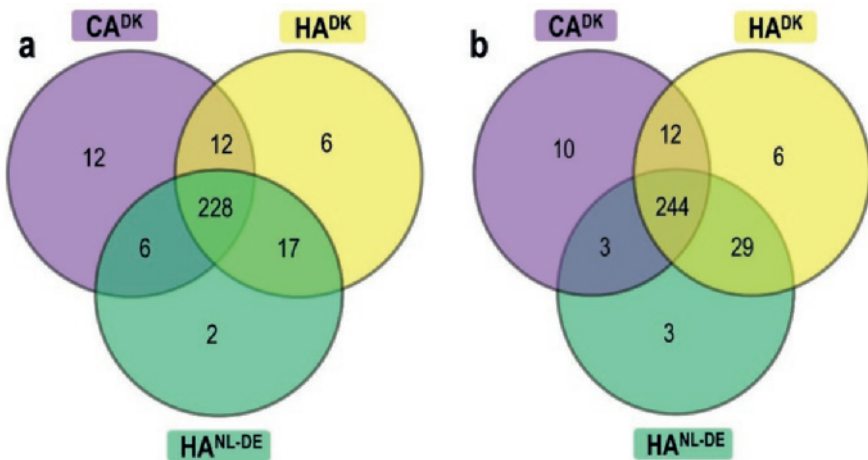


**Fig. 2. Shared and uniquely identified proteins in CA<sup>DK</sup>, HA<sup>DK</sup> and HA<sup>NL-DE</sup> *S. aureus* isolates.** The Venn diagrams relate to cells in the exponential (a) and stationary (b) growth phases. The numbers of commonly and uniquely identified proteins of the different groups of isolates are indicated.



Furthermore, unique proteins ranging from 2 to 12 proteins in the exponential growth phase, and 3 to 10 proteins from the stationary growth phase, which were specific to only one of the three groups of isolates were identified (Fig. 2a,b). Together, these data show that the majority of extracellular proteins of the CA<sup>DK</sup>, HA<sup>DK</sup> and HA<sup>NL-DE</sup> is common. Yet, a subset of the exoproteins appears to be specific for each of the three groups of isolates.

### Predicted sub-cellular localization of identified exoproteins

Bacterial exoproteomes are known to contain proteins that are actively secreted and proteins that are liberated from the cells through (auto-)lysis or other unidentified 'non-classical secretion' mechanisms <sup>27,32-37</sup>. These proteins can be distinguished through signal peptide predictions, which is relevant as most known virulence factors contain signal peptides to direct their export from the cytoplasm <sup>26</sup>. Thus, we predicted the sub-cellular localization of proteins that were identified by MS. The vast majority of the proteins identified in the exoproteomes of the isolates in the exponential and stationary growth phases were assigned to the class of cytoplasmic proteins followed by secreted proteins, lipoproteins, cytoplasmic membrane proteins and cell wall-associated proteins (Fig. 3a, b). Notably, in the exponential growth phase, the numbers of accessory exoproteins that were predicted as cytoplasmic were higher in the CA<sup>DK</sup> group than in the HA<sup>DK</sup> and HA<sup>NL-DE</sup> groups (Fig. 3c). Conversely, in the stationary phase, the numbers of accessory exoproteins predicted as cytoplasmic were higher among the HA<sup>DK</sup> and HA<sup>NL-DE</sup> groups than in the CA<sup>DK</sup> group (Fig. 3d). For exoproteins with a predicted localization in the membrane (i.e. membrane- and lipoproteins) or cell wall no major differences were observed in the three groups, irrespective of the growth phase (data not shown). Lastly, higher numbers of predicted secretory proteins were identified in growth media of the HA group than the CA group in

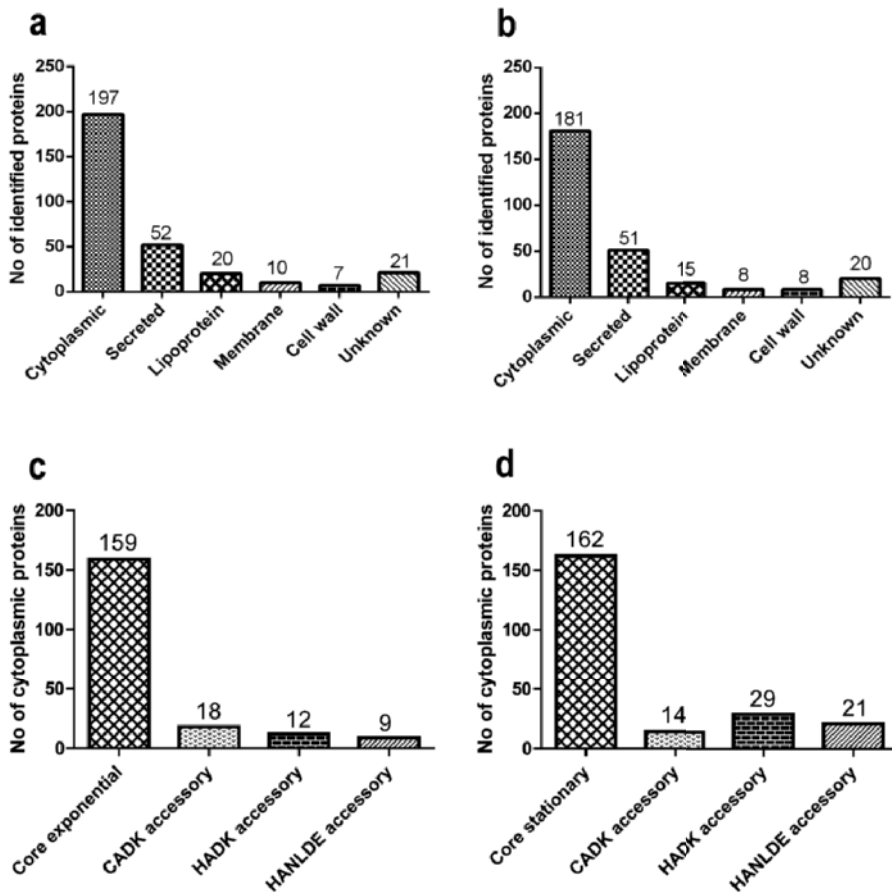


Fig. 3. Predicted subcellular localization of identified extracellular proteins. The predicted subcellular localization of all 494 identified extracellular proteins is shown for cells in the exponential (a) and stationary (b) growth phases. Panels (c) and (d), respectively, highlight the appearance of predicted cytoplasmic core and accessory cytoplasmic proteins in the growth medium of the CA<sup>DK</sup>, HA<sup>DK</sup> and HA<sup>NL-DE</sup> isolates in the exponential and stationary growth phases. The numbers of proteins identified in each category are indicated at the top of the bars.

both growth phases. Altogether, these data imply that the investigated CA and HA isolates are similar in terms of the predicted localization of their exoproteins. Nonetheless, the main distinction among these groups was the time point at which cytoplasmic proteins are liberated from the cells.

## Relative extracellular abundance of known and putative virulence factors

To obtain more comprehensive insights in the possible differences in the levels of known extracellular virulence factors, we assessed their relative abundance for the different investigated isolates. Detailed evaluation of the normalized spectral counts showed differential and similar expression levels for 24 virulence factors among the three groups of isolates both in the exponential growth phase (Fig. 4a), and in the stationary growth phase (Fig. 4b). Of note, neither PVL nor enterotoxins that were identified as potentially distinguishing features for CA and HA isolates based on the genome sequence were detectable in the extracellular proteome. On the other hand, statistically significantly different levels of the IsdA, IsdB, SCIN and Vwb proteins were identified in the growth media of exponentially growing isolates, and the same was true for the Ebps, IsdB, SCIN and Vwb proteins in the growth media of stationary growing isolates (Fig. 4a,b, Supplementary Table 4).

The relative amounts of individual secreted exoproteins are likely important for the behavior of the respective *S. aureus* isolate, especially where this concerns secreted toxins or immune evasion factors. Therefore, we determined the relative abundance of proteins in the three groups of isolates from the normalized spectral counts of proteins. A volcano plot was used to present the proteins that were detectable at statistically significantly higher or lower levels among the three groups of isolates during both the exponential and stationary growth phases. From the total of 283 proteins identified in samples collected in the exponential growth phase, a relatively large number of proteins was present at statistically significantly different levels when the CA<sup>DK</sup> and the two HA isolate groups (*i.e.* HA<sup>DK</sup> and HA<sup>NL-DE</sup>) were compared, and this difference was larger than the difference between the HA<sup>DK</sup> and HA<sup>NL-DE</sup> isolates (Fig. 5a; Supplementary Table 4). A similar pattern was observed for the samples harvested during the stationary

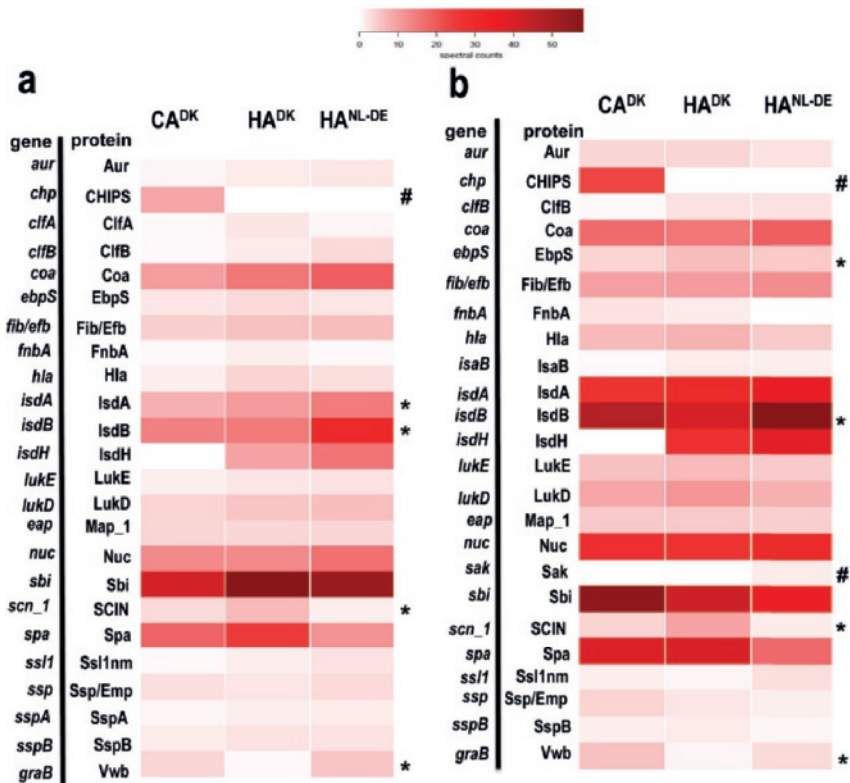


**Fig. 4. Heat map analysis of quantified extracellular virulence factors.** The normalized spectral counts of known extracellular virulence factors identified by Mass Spectrometry in growth media of the three groups of isolates are graphically represented as colored heat maps. Each heat map includes three columns representing each of the three groups of the isolates. Of note, each column of CA<sup>DK</sup> and HA<sup>DK</sup> isolates is based on the average of six different isolates each analyzed in duplicate, and the HA<sup>NL-DE</sup> column is based on the average of three different isolates each analyzed in duplicate. Each row represents a particular protein. Panels (a) and (b) represent known virulence factors of *S. aureus* as identified in the growth medium fractions of cells in the exponential and stationary growth phases, respectively. \*Statistically significant differences in relative abundance of the proteins marked between the groups; # Proteins present in one group of isolates only.

phase (Fig. 5b). Additionally, some proteins were exclusively present in one group of isolates, e.g. the chemotaxis inhibitory protein (CHIPS) was identified only in CA<sup>DK</sup>, the enterotoxin type D only in HA<sup>DK</sup>, and the enterotoxin type A only in HA<sup>NL-DE</sup> isolates, and this applied both to exponential and stationary phase growth

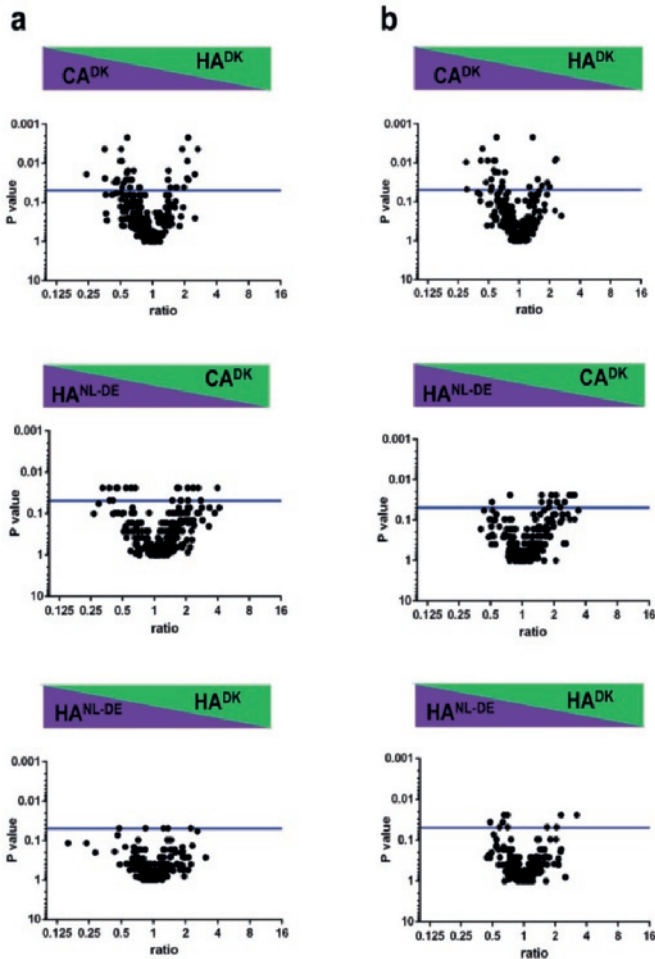


Fig. 5. Differences in relative extracellular protein abundance in CA<sup>DK</sup>, HA<sup>DK</sup> and HA<sup>NL-DE</sup> isolates. Statistically significant differences in the relative abundance of identified extracellular proteins are presented in volcano plots for samples collected in the exponential (a) and stationary (b) growth phases. Horizontal blue lines indicate a p-value threshold of 0.05.

medium samples (Supplementary Table 5). Together, these data show differences in the relative abundance

of extracellular proteins at statistically significant levels in all the three groups of isolates, but especially for the CA and HA isolates.

### Levels of mRNA for selected exoproteins

The abundance of a bacterial exoprotein reflects the net result of transcription of the respective gene, mRNA translation, translocation of the precursor protein across the membrane, post-translocational folding of the protein into a stable conformation, cell wall passage and the protein's stability in the bacterial extracellular milieu. This implies that extracellular protein abundance is not

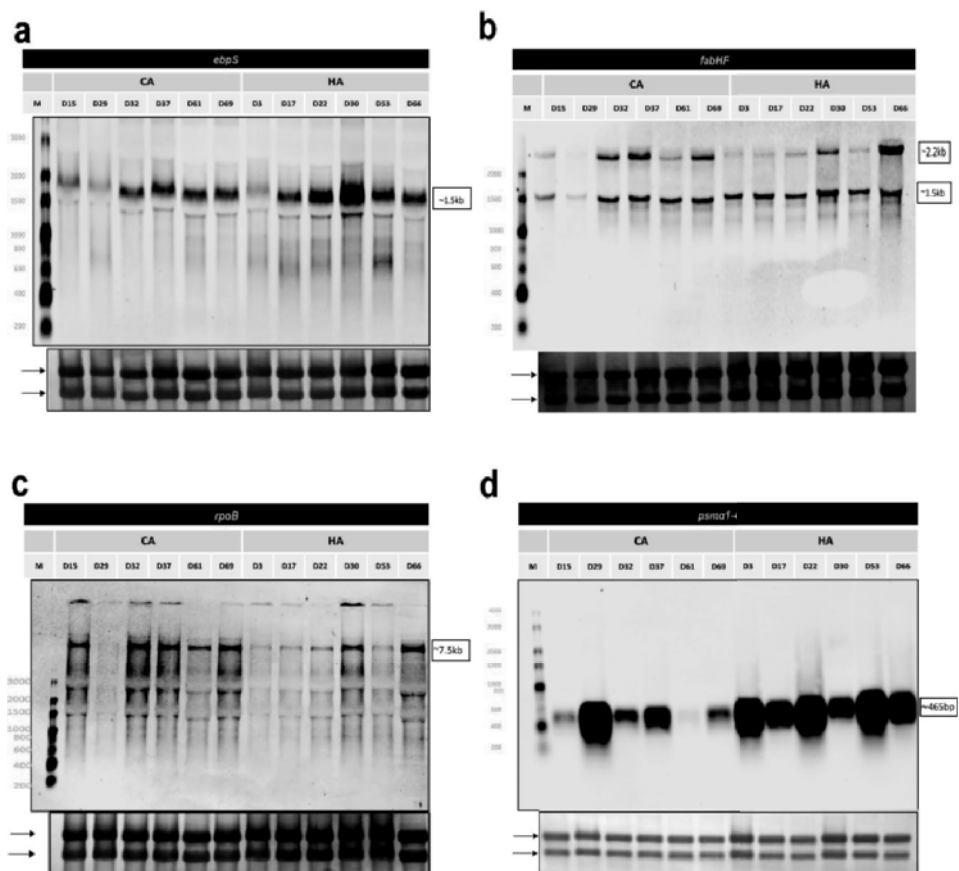


**Fig. 6. Northern blotting analysis of selected genes.** Arrows mark the positions of 23S- and 16S-rRNA bands on the methylene blue stained membranes. Sizes of specific transcripts are indicated on the right side of each display. In case of *fabHF* two bands were detected, the larger band of ~2.2 kb representing a *fabHF* transcript and the lower band of ~1.5 kb only *fabF*. (a) *ebpS*, (b) *fabHF*, (c) *rpoB*, and (d) *psma1-4*.

always linearly correlated with the transcript levels. Yet, mRNA levels are major determinants for protein expression levels. Therefore, a Northern blotting analysis was performed to assess whether there is a possible correlation between transcript levels and extracellular protein abundance. Specifically, we compared the transcript levels for a secreted virulence factor (*ebpS*) and two cytosolic proteins (*fabF* and *rpoB*). Consistent with the MS data, in the stationary phase, the mRNA level of *ebpS* was higher in HA isolates than in the CA isolates (Fig. 6a), whereas

the mRNA levels of *fabF* and *rpoB* were higher in the CA isolates compared to the HA isolates (Fig. 6b,c). Of note, the *fabF* and *rpoB* mRNA levels in the CA<sup>DK</sup> isolate D29 were more similar to the respective mRNA levels in HA<sup>DK</sup> isolates than to those in the CA<sup>DK</sup> isolates. On the other hand, two of HA<sup>DK</sup> isolates (D30 and D66), displayed *fabF* and *rpoB* mRNA levels comparable to those observed for the CA<sup>DK</sup> isolates.

Northern blotting analyses can also provide information on the expression of genes for which the encoded proteins were not covered by the proteome analysis. Since phenol-soluble modulins (PSMs) are particularly relevant for virulence, but notoriously difficult to identify by proteomics due to their small size, we investigated the *psmA1-4* mRNA levels by Northern blotting. In the stationary growth phase, the *psmA1-4* mRNA levels were higher in most of the HA<sup>DK</sup> isolates than in the CA<sup>DK</sup> isolates (Fig. 6d). However, also the CA<sup>DK</sup> isolate D29 showed a relatively high level of *psmA1-4* mRNA that was comparable to the *psmA1-4* mRNA levels in the HA<sup>DK</sup> isolates (Fig. 6d). Based on these Northern blotting data, the proteomics data were reassessed with less stringent criteria where we considered also proteins identified with only one peptide. Thus, we were able to identify both the PSM $\beta$ 1 and PSM $\beta$ 2 proteins in medium fractions of five out of the six HA<sup>DK</sup> isolates grown to stationary phase. Of note, the same was true for the D29 CA<sup>DK</sup> isolate. These findings are fully consistent with the relative mRNA levels detected by Northern blotting.

## Clustering of CA and HA isolates based on exoproteome abundance signatures

Principal component analysis (PCA) was performed to assess the overall relationships between the different investigated isolates in terms of their exoproteome profiles. Of note, this PCA was based on the normalized spectral

counts of proteins that were produced by all three groups of isolates, specifically 283 proteins from exponentially growing bacteria, and 308 proteins from bacteria in the stationary growth phase. Importantly, the PCA analysis revealed that the CA- and HA-MRSA isolates clustered in two distinct groups based on the 'exoprotein abundance signatures' where the HA cluster included both the HA<sup>NL-DE</sup> and the HA<sup>DK</sup> isolates (Fig. 7a, b) irrespective of their geographical origin. Yet, the HA cluster included two CA<sup>DK</sup> isolates (D29 and D61), whose exoprotein abundance signatures apparently resemble those of the analyzed HA isolates.

The PCA analysis in Figure 7 was based on all identified extracellular proteins, including proteins with different predicted subcellular localizations. To assess whether the discriminating information relates to proteins with a particular predicted localization site, PCA analysis was performed on: i, predicted cytoplasmic proteins alone, ii, all identified proteins except the predicted cytoplasmic proteins, and iii, all identified proteins except the predicted cytoplasmic proteins and the proteins of unknown localization. Unexpectedly, the

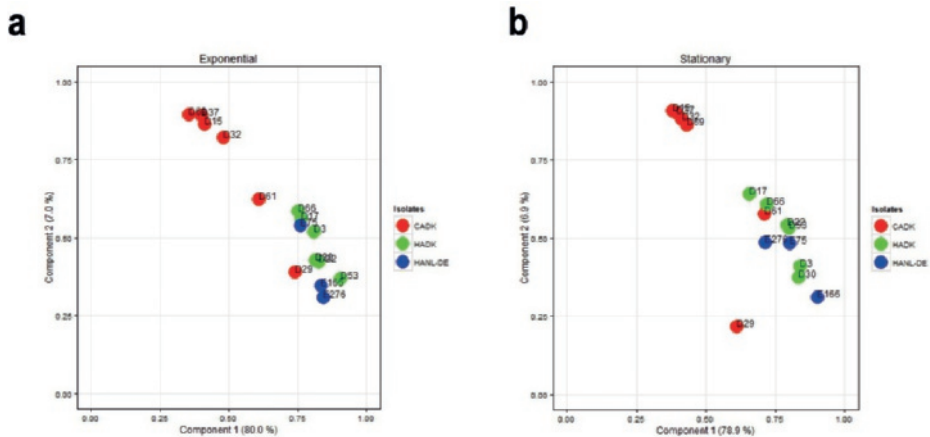


**Fig. 7. Principal component analysis (PCA) of the normalized spectral counts of identified extracellular proteins.** Two-dimensional PCA plots are displayed for growth medium samples from the 15 CA<sup>DK</sup>, HA<sup>DK</sup> and HA<sup>NL-DE</sup> isolates in the (a) exponential growth phase and (b) stationary growth phase.



distinguishing information was primarily associated with the predicted cytoplasmic proteins (Supplementary Table 6).

Voronoi treemaps can be applied to link quantitative proteomic data and functional classifications. Thus, we used Voronoi treemaps to characterize the extracellular proteins identified for the three groups of isolates. The biological functions of the identified proteins were mainly related to protein biosynthesis, carbohydrate and carbon metabolism, oxidative stress, and adhesion (Supplementary Figure 1a, b). Of note, adhesion-associated extracellular proteins were somewhat more pronounced among the HA- than the CA isolates in the exponential growth phase (Supplementary Figure 1a). Conversely, adhesion-related extracellular proteins were more prominently present in CA- than in HA isolates in the stationary growth phase (Supplementary Figure 1b). Despite the fact that there were unique proteins identified in each of the three groups of isolates, no major differences in the overall functions of the identified extracellular proteins were observed.

## Differences in staphylococcal survival within epithelial cells

Since the PCA analysis of exoproteins grouped the studied *S. aureus* isolates into two distinct clusters, we asked the question whether these groups might interact differently with human host cells. A bronchial epithelial cell line (16HBE14o-) was selected for this purpose, because CA-MRSA isolates have been implicated in severe respiratory infections among healthy individuals from the community. This fact might indicate a superior ability of this group of bacteria to interact with airway cells. Furthermore, the 16HBE14o- epithelial cell line forms a confluent layer that allows the monitoring of infecting bacteria over several days. Thus, *in vitro* cultured 16HBE14o- epithelial cells were infected with the CA<sup>DK</sup>, HA<sup>DK</sup> and

HA<sup>NL-DE</sup> isolates, and the subsequent binding, internalization and intracellular survival of staphylococci were assessed through counting by flow cytometry. While the staphylococcal isolates did not show major differences in the internalization rate into the epithelial cells, there was a marked difference in post-internalization growth and survival. As shown in Figure 8 and Supplementary Figure 2, four CA<sup>DK</sup> isolates (D15, D32, D37, D69) were able to multiply inside the epithelial cells during the first two days post infection, after which the population size decreased. In contrast, the HA<sup>DK</sup> isolates did not multiply with the exception of isolate D17, which showed a slight increase, comparable to the CA<sup>DK</sup> isolate D69 (Fig. 8). Of note, the CA<sup>DK</sup> isolates D29 and D61, which were grouped with the HA<sup>DK</sup> isolates in the exoproteome PCA analysis (Fig. 7), displayed similar intracellular behavior as the five HA<sup>DK</sup> isolates D03, D22, D30, D53 and D66. Notably, all the three HA<sup>NL-DE</sup> isolates showed a similar intracellular behavior as the HA<sup>DK</sup> isolates. These findings imply that the distinction of the investigated HA and CA isolates based on differences in their exoproteomes, is reflected in their growth and survival behavior upon internalization of human bronchial epithelial cells.

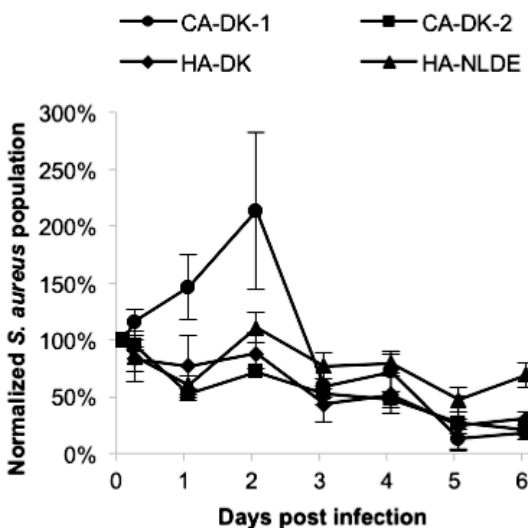


**Fig. 8. Survival of CA and HA isolates internalized by 16HBE14o- bronchial epithelial cells.** Averaged survival curves are shown for the CA<sup>DK</sup>, HA<sup>DK</sup> and HA<sup>NL-DE</sup> isolates, where the CA<sup>DK</sup> isolates are separated into two groups in accordance with their exoprotein abundance signatures in Fig. 8 (CA-DK-1 includes isolates D15, D32, D37 and D69; CA-DK-2 includes isolates D29 and D61).

## Discussion

The serious threat that MRSA represents for hospitalized patients demands an accurate and reliable method of distinction between CA- and HA-MRSA isolates for the purpose of prevention and control of outbreaks. In the present study, we explored the feasibility of applying a combined genome and proteomics-based approach to distinguish MRSA isolates with different epidemiological behavior. To facilitate the interpretation of the complex data, we used a set of genetically closely related CA- and HA-MRSA isolates with the sequence type ST8. Altogether, our findings revealed several distinguishing features between the investigated CA and HA isolates at the levels of the accessory genome and the exoproteome.

Since exoproteins have major roles in staphylococcal colonization of the host and virulence, we compared the exoproteome profiles of three genetically similar, but epidemiologically unrelated groups of MRSA isolates, i.e. the CA<sup>DK</sup>, HA<sup>DK</sup> and HA<sup>NL-DE</sup> isolates. Noticeably, the vast majority of identified exoproteins was shared by all the three groups of isolates. However, some of the identified exoproteins were unique for a particular group of isolates, while the abundance of several common proteins varied among the three groups of isolates. This probably reflects the fact that the *S. aureus* exoproteome is heterogeneous due to this organism's genomic plasticity <sup>26,27</sup>. Nonetheless, the investigated HA<sup>NL-DE</sup> isolates shared more similarities with respect to accessory virulence genes and actually detected exoproteins with the HA<sup>DK</sup> isolates than with the CA<sup>DK</sup> isolates, even though their core genome was more closely related to that of the CA<sup>DK</sup> isolates. The latter finding is in line with previously reported observations that genetically closely related *S. aureus* isolates may reveal heterogeneous exoproteome profiles <sup>38,39</sup>. Taken together, our combined observations imply that both qualitative and quantitative differences in the exoproteome profile might serve as markers to

discriminate the three groups of *S. aureus* isolates with different epidemiological backgrounds. Of note, some observed differences for accessory virulence genes that are apparently distinctive for the CA and HA isolates at the genome level, such as the genes for PVL and enterotoxins, were not reflected in the present proteomics analyses, because the respective proteins were not detected. This lack of detection may relate to their actual expression levels under the investigated conditions, or to the fact that the actual identification of proteins by MS depends on various factors, including the method of sample preparation, or the acquisition and analysis of the MS data. Yet, it should be noted that these proteins were identified in some other proteomic studies <sup>40,41</sup>.

Knowledge of the sub-cellular localization of bacterial proteins can provide valuable insights into protein functions, especially in relation to colonization of the host, fitness and virulence <sup>26</sup>. In this respect, the attention is usually focused on actively secreted proteins that are synthesized with N-terminal signal peptides, because these include the major known virulence factors <sup>26,27</sup>. However, our proteomic analysis revealed only few significant differences in the detection of actively secreted proteins in the CA and HA groups that could be related to virulence (i.e. IsdA and IsdB), adhesion to host tissues (i.e. Ebps, Vwb), or immune evasion (i.e. SCIN). In addition, some other known virulence factors, such as CHIPS, the enterotoxin type D and the enterotoxin type A were uniquely identified in the CA<sup>DK</sup>, HA<sup>DK</sup>, and HA<sup>NLDE</sup> isolates, respectively, irrespective of the growth phase. On the other hand, we observed major differences in the appearance of predicted cytoplasmic proteins in the exoproteomes of the investigated CA and HA isolates, where a higher number of cytoplasmic proteins was identified in the growth medium of the CA group than in the medium of the two HA groups during the exponential growth phase. Conversely, a higher number of cytoplasmic proteins was identified in the HA group than the CA group during the stationary growth phase. This difference can be interpreted in at least three ways. Firstly,

there may be a difference in the timing of autolysis of cells <sup>36,37</sup> resulting in the early release of cytoplasmic proteins into the extracellular milieu by cells from the CA group. On the other hand, it is known that cell wall-associated and secreted proteases can degrade cytoplasmic proteins released into the growth medium <sup>36</sup>. Hence a second possible explanation for the observed differences would be that the HA isolates are more proteolytic in the exponential growth phase than the CA isolates, leading to the observed differences due to degradation of liberated cytoplasmic proteins. In a third possible scenario, 'cytoplasmic' proteins are actively delivered into the growth medium via non-classical secretion mechanisms that are as yet ill-defined <sup>33,34,37</sup>. In this case, one would have to assume that the timing of non-classical secretion differs for CA and HA isolates. Inspection of the genome sequences of the investigated MRSA isolates showed that the genes for known autolysins (*atl*, *isaA*, *lytM*), proteases (*aur*, *sspA*, *sspB*, *sspC*, *spiA*, *spiB*, *spiC*, *spiD*, *spiE*, *spiF* and *IsaA*) and secretion pathways (*sec*, *tat* and type VII secretion) are intact with only few SNPs detectable in the coding and intergenic regions, as was the case for major gene regulators. None of the observed SNPs causes a premature stop of translation or a mutation that is known to be important for activity (data not shown). Of note, our comparative genome analysis suggests that the distinctive features of CA- and HA-MRSA isolates relate predominantly to the accessory genome, which might suggest a role of the respective genes at least in the timing of the extracellular appearance of predicted cytoplasmic proteins.

The principal component analysis (PCA) on the exoproteome data based on normalized spectral counts grouped the 15 investigated *S. aureus* isolates into two distinct groups. Herein, all the HA isolates formed a distinct cluster, whereas four of the six CA isolates formed a separate cluster. Importantly, the clustering of all HA<sup>DK</sup> and HA<sup>NL-DE</sup> isolates in one group implies that our proteomics approach identifies a common signature of all investigated HA-MRSA isolates. Intriguingly, two isolates designated as CA grouped with the HA isolates, suggesting that these

two “CA isolates” (D29, D61) may actually be hospital-adapted isolates that could have been propagated in the community. Consistent with this idea, our Northern blotting analysis showed that the transcript levels for exoproteins like FabF, RpoB and PSM $\alpha$ 1-4 in the CA isolate D29 resembled more closely the respective profiles in the HA isolates. Yet, this was not the case for isolate D61, whose *fabF* and *rpoB* transcript levels matched with those of the CA isolates, while the *psma1-4* transcript level was very low. An alternative possibility is that the CA isolates D29 and D61 are genuine CA isolates, in which case our proteome analyses might highlight another distinguishing feature of the two clusters. Indeed, the distinction of CA and HA groups based on our PCA analysis seems to have predictive value for the growth behavior and survival of *S. aureus* in non-professional phagocytic epithelial cells. Clearly, the CA isolates displayed an increase in net cell number after internalization by epithelial cells compared with the HA isolates, whose bacterial count did not substantially increase following internalization. This finding would be fully in line with an earlier study that suggested better survival of CA-MRSA than of HA-MRSA inside human neutrophils <sup>42</sup>. Together, these findings imply that the cytoplasmic proteins identified in the exoproteome are indicative not only for the epidemiological behavior, but also could have an impact on the intracellular behavior of *S. aureus* within epithelial cells influencing their survival or replication capabilities. Of course, this does not exclude the possible involvement of known virulence factors with a clear role in virulence, such as phenol-soluble modulins, which were previously implicated in epidemiological behavior and intracellular survival <sup>29,43-45</sup>, or the leukocidins PVL or LukAB/ED <sup>46</sup>.

In recent years, increasing evidence has been obtained that particular cytoplasmic proteins may have different functions at intracellular and extracellular locations <sup>47,48</sup>. Such proteins are often regarded as ‘moonlighting’ proteins. Of note, the cytoplasmic proteins which we could consider here as potential moonlighting

proteins are mostly proteins that are constitutively expressed at relatively high levels, and that have previously identified roles in processes such as sugar metabolism, adherence to host tissues, pathogenesis, and/or immune evasion <sup>49-52</sup>. Of note, a number of these potentially moonlighting proteins do not only occur in prokaryotes but also in eukaryotes, which could be suggestive of molecular mimicry where pathogens disguise themselves with a corona of factors that the human immune system does not recognize as non-self <sup>50,53,54</sup>. Altogether, the possible roles of moonlighting cytoplasmic proteins in the different epidemiology and intracellular survival of CA and HA USA300 isolates as highlighted in our present study would be fully in line with recent studies where it was proposed that such proteins contribute to staphylococcal virulence <sup>33,35,55,56</sup>.

We conclude that our present proteomics approach to identify exoproteome signatures, and the results obtained with this approach, open up novel avenues to study and predict the epidemiological behavior of clinical MRSA isolates. Clearly, our study is built on genetically closely related MRSA isolates with distinct epidemiological behavior. It will be an important challenge for future research to assess whether a similar distinction can be achieved when this approach is applied to genetically distantly related MRSA isolates with different epidemiological behavior in hospitals and the community.

## Materials and Methods

### Bacterial isolates

Relevant properties of the 15 MRSA isolates used for exoproteome analyses are listed in Supplementary Table 7. 12 isolates with the PFGE profile USA300 were collected by the Statens Serum Institut (Copenhagen, Denmark) in the period between 1999 and 2006 <sup>21</sup>. These 12 isolates included six CA-MRSA isolates with *spa* type t008 (referred to as CA<sup>DK</sup>), and six HA-MRSA isolates with *spa* type t024

(referred to as HA<sup>DK</sup>)<sup>18,21</sup>. The remaining three HA-MRSA isolates with *spa* types t008 or t024 (referred to as HA<sup>NL-DE</sup> isolates) were collected in the period between 1996 to 2010 in hospitals located within the Dutch-German border region (EUREGIO)<sup>19</sup>.

## Whole genome sequencing of isolates and analysis

Whole genome sequencing of the investigated *S. aureus* isolates was performed on an Illumina MiSeq instrument and the Nextera<sup>®</sup> XT, 2x 250bp kit using the manufacturer's standard protocols (Illumina, Inc, USA). DNA for the sequencing was extracted using the DNeasy Blood and Tissue kit (Qiagen, Valencia, CA, USA). The WGS datasets generated and/or analysed in the current study are available in the European Nucleotide Archive (ENA) repository under accession number ERP018940 (<http://www.ebi.ac.uk/ena/data/view/PRJEB17079>). Reads from the isolates were assembled using SPAdes<sup>57</sup>, annotated using PROKKA<sup>58</sup>, and the core and pan-genome of the isolates was estimated using ROARY<sup>59</sup>. The alignment of the core genome from ROARY was used as input to create a phylogenetic tree using RAxML<sup>60</sup> with 100 bootstrap supports. The phylogenetic tree and accessory genome heatmap were visualized using ggtree. Specifically, the phylogenetic tree was based on the variable positions in the core genome of the 15 isolates (2,334 genes). The accessory genome was defined as genes present in at most 70% of the isolates resulting in 992 accessory genes. Virulence genes were identified using VirulenceFinder<sup>61</sup>. The analysis of potential antimicrobial resistance genes was performed with the web-based ResFinder tool<sup>62</sup>.

## Bacterial cultivation for proteome sampling

Bacteria were grown overnight (14-16 h) at 37°C in 25 mL Trypton Soy Broth (TSB) under vigorous shaking (115 rpm). The cultures were then diluted into 25 mL pre-warmed RPMI 1640 medium supplemented with 2 mM glutamine (GE



Healthcare/PAA, Little Chalfont, United Kingdom) to an OD<sub>600</sub> of 0.05 and cultivation was continued under the same conditions. Exponentially growing cells with an OD<sub>600</sub> of ~0.5 were re-diluted into 120 mL fresh, pre-warmed RPMI medium to a final OD<sub>600</sub> of 0.05. The cultivation was continued until the cultures had reached 90 min within the stationary growth phase. Within this period, two time points were selected for sample collection. The first one was set at OD<sub>600</sub> of ~0.5, corresponding to the exponential growth phase, and the second one was set at ~OD<sub>600</sub> of 1.3, corresponding to approx. 90 min after entry into the stationary phase. At these two time points, 1.5 ml culture aliquots were collected. In brief, the collected aliquots were centrifuged for 10 min at 4°C and 8000×g with the subsequent application of a 0.22 µM filter step (GE Healthcare Systems, Little Chalfont, United Kingdom) to remove the remaining bacterial cells. The extracellular proteins in the supernatant were precipitated with 10 % w/v TCA on ice at 4°C overnight. Finally, the precipitates were collected by centrifugation for 20 min at 4°C and 8000×g, washed with ice-cold acetone, and dried at room temperature. The dried protein pellets were stored at -20°C until further use. For each isolate two biological replicates were analyzed, which adds up to 24 exponential phase and 24 stationary phase samples for the CA<sup>DK</sup> and HA<sup>DK</sup> strains, respectively, and to 6 exponential phase and 6 stationary phase samples for the HA<sup>NL-DE</sup> strains.

## Sample preparation for proteome analysis

Dried protein samples were processed as described previously<sup>54</sup>. Briefly, protein pellets were dissolved in 50 mM ammonium bicarbonate buffer (Fluka, Buchs, Switzerland), reduced with 10 mM dithiothreitol (DuchefaBiochemie, Haarlem, the Netherlands) for 30 min, and alkylated with 10 mM iodoacetamide (Sigma-Aldrich, St. Louis, USA) for 30 min in the dark. To digest complex protein samples, 80 ng trypsin (Promega, Madison, USA) was added and the samples

were incubated overnight at 37°C under static conditions. To stop the digestion, the samples were acidified with a final concentration of 0.1 % trifluoroacetic acid (TFA, Sigma-Aldrich, St. Louis, USA) and subsequently purified using ZipTips (Millipore, Billerica, USA). For this purpose, the tips were stepwise equilibrated with 30 µL acetonitrile (ACN, Fluka, Buchs, Switzerland), 30 µL 80 % ACN/0.1 % TFA, 50 % ACN/0.1 % TFA, 30 µL 30 % ACN/0.1 % TFA and finally 30 µL 0.1 % TFA. Peptides were bound to ZipTips by pipetting 10 times 10 µL of the sample. Impurities were removed by washing with 50 µL 0.1 % TFA and finally peptides were eluted with 20 µL 50 % ACN/0.1 % TFA and 20 µL 80 % ACN/0.1 % TFA. The final eluates were concentrated using a vacuum centrifuge (Eppendorf, Hamburg, Germany) and stored at 4°C until further use.

## Mass spectrometry

Tryptic peptides were separated by reversed phase liquid chromatography (LC) coupled online to electrospray ionization mass spectrometry (ESI-MS) using an LTQ Orbitrap as described by Stobernack *et al.*<sup>63</sup>. Database searching was done with Sorcerer-SEQUEST 4 (Sage-N Research, Milpitas, USA). After extraction from the raw files, \*.dta files were searched with Sequest against a target-decoy database with a set of common laboratory contaminants. The databases for the respective peptide/protein search were created from the genome sequences of the 15 investigated MRSA isolates. The RAST annotation file of these 15 MRSA isolates was used to create a non-redundant database comprising protein sequences of all isolates. Protein sequences that differed in only one amino acid were included in this database. Finally, validation of MS/MS-based peptide and protein identifications was performed with Scaffold v4.3.4 (Proteome Software, Portland, USA). Peptide identifications were accepted if they exceeded specific database search engine thresholds. SEQUEST identifications required at least deltaCn scores of greater than 0.1 and XCorr scores of greater than 2.2, 3.3 and 3.75

for doubly, triply and quadruply charged peptides, respectively. With these filter parameters, no false-positive hits were obtained, which was verified by a search against a concatenated target-pseudo reversed decoy database. Normalized spectral counts were obtained from the Scaffold file by considering a 99 % protein threshold, and a minimum of two peptides for each protein. The normalized spectral count data were exported from Scaffold and curated in Microsoft Excel before further analysis. The filtered MS data associated with this manuscript can be downloaded from the PRIDE partner repository of the ProteomeXchange Consortium using the following link: <http://www.ebi.ac.uk/pride/archive/login> (Username: reviewer84128@ebi.ac.uk, and Password: fzzQQiRF).

## Prediction of protein localization, biological processes and molecular functions

Prediction of the subcellular localization of proteins that were identified by LC-MS/MS was performed using different bioinformatics tools. Since individual bioinformatics tools are not able to specifically predict all possible localization sites of bacterial proteins <sup>64</sup>, we used eight different computer programs, namely SignalP4.1 (<http://www.cbs.dtu.dk/Services/SignalP/>) <sup>65</sup>, Phobius (<http://www.ebi.ac.uk/Tools/pfa/phobius/>) <sup>66</sup>, Predisi (<http://www.predisi.de/>) <sup>67</sup>, LipoP1.0 (<http://www.cbs.dtu.dk/services/LipoP/>) <sup>68</sup>, ProtComp9.0 (<http://linux1.softberry.com/berry.phtml?topic=protcompan&group=programs&subgroup=proloc>) <sup>69</sup>, PSort 3.0.3b (<http://www.psort.org/psortb/index.html>) <sup>70</sup>, TMHMM2.0c (<http://www.cbs.dtu.dk/services/TMHMM/>) <sup>71</sup>, and PScan (<http://prosite.expasy.org/scanprosite/>) <sup>72</sup>. The settings used for of each program are specified in Supplementary Table 8. A detailed description of output parameters, scores and thresholds for each tag is presented in Supplementary Table 9. Voronoi treemaps to link quantitative proteomic data and functional classifications were created using the Paver software (DECODON GmbH,

Greifswald, Germany) with the latest functional categorization of SEED database of *S. aureus* USA300\_FPR3757<sup>73</sup>.

## RNA isolation

Bacterial isolates were grown under the same condition as for the proteomics sample collection. 25 ml culture aliquots were collected for RNA isolation 90 min after entry into the stationary growth phase, corresponding to an OD<sub>600</sub> of approx. 1.3. RNA was isolated from bacteria as described previously<sup>74</sup>. Briefly, ½ volume of frozen killing buffer (20 mM Tris/HCl [pH 7.5], 5 mM MgCl<sub>2</sub>, 20mM NaN<sub>3</sub>) was added to the bacterial culture, and bacterial cells were collected by centrifugation for 3 minutes, 8000 rpm at 4°C. The supernatant was discarded, and pellets were frozen in liquid nitrogen and stored at -80°C until further processing. Cell pellets were re-suspended in ice-cold killing buffer and transferred into Teflon vessels filled with liquid N<sub>2</sub> for disruption. Cells were then mechanically disrupted with a Mikro-Dismembrator S (Sartorius) for 2 min, 2600 rpm. The resulting powder was re-suspended in lysis solution that was pre-warmed at 50°C (4 M guanidine thiocyanate, 25 mM sodium acetate [pH 5.2], 0.5% N-laurylsarcosinate 40 [wt/vol]) by repeated up- and down-pipetting. Then, lysates were transferred into pre-cooled micro-centrifuge tubes, and frozen at -80°C.

Total RNA was isolated by phenol-chloroform extraction as described previously<sup>74</sup>. Samples were processed twice with an equal volume of acid phenol solution (Sigma-Aldrich, Zwijndrecht, the Netherlands), and mixed thoroughly on an Eppendorf tube shaker until completely thawed. The resulting suspension was then centrifuged for 5 min, 12000 rpm, and the supernatant was transferred into a fresh microcentrifuge tube. Next, samples were processed once with one volume of Chloroform/isoamyl alcohol, mixed well, and centrifuged for 5 min, 12000 rpm. RNA was precipitated from the supernatant by the addition of 1/10 volume of 3 M

Na-Acetate, pH 5.2, and 0.8 ml of isopropanol. The precipitated RNA was washed once with 70 % RNase-free ethanol and dissolved in RNase-free water.

## Northern blot analysis

Northern blot analysis was performed as described previously <sup>75</sup>. Specific biotin-labelled RNA probes were generated by *in vitro* synthesis using a T7 RNA polymerase and Bio-16-UTP (Life Technologies). 3-10 µg of total RNA per lane was separated on 1.2 % denaturing agarose gels. Gene-specific transcripts were detected with the aid of biotin-labeled anti-sense RNA-probes. Fluorescent detection of the biotin- labelled probes was carried out using IRDye® 800CW Streptavidin (LI-COR Biosciences - GmbH) and the Odyssey Clx Imaging System (LI-COR Biosciences - GmbH) according to the instructions of the manufacturer. Primer sequences are listed in Supplementary Table 10.

## Survival of bacteria upon epithelial cell infection

### *Cell lines and culture conditions*

The human bronchial epithelial cell line 16HBE14o- was used to investigate the survival of MRSA isolates upon internalization. The epithelial cells were cultured in eukaryotic minimal essential medium (eMEM; 1x MEM without arginine and lysine; Costumer formulation, PromoCell GmbH, Heidelberg, Germany) supplemented with 10 % (v/v) fetal calf serum (FCS; Biochrom AG, Berlin, Germany), 2 % (v/v) L-glutamine 200 mM (PAN-Biotech GmbH, Aidenbach, Germany) and 1 % (v/v) non-essential amino acids 100x (PAN-Biotech GmbH). The cells were seeded at a density of  $1 \times 10^5$  cells/cm<sup>2</sup> in CellStar® 12-well plates (Greiner Bio-One, Frickenhausen, Germany) and cultured for three days at 37°C, 5 % CO<sub>2</sub> in a humidified atmosphere after which they were ready for infection experiments.

### *Bacterial culture conditions*

The bacteria were cultured in prokaryotic minimal essential medium (pMEM; 1x MEM without sodium bicarbonate; Invitrogen, Karlsruhe, Germany) supplemented with 1x non-essential amino acids (PAN-Biotech GmbH), 4 mM L-glutamine (PAN-Biotech GmbH), 10 mM HEPES (PAN-Biotech GmbH), 2 mM L-alanine, 2 mM L-leucine, 2 mM L-isoleucine, 2 mM L-valine, 2 mM L-aspartate, 2 mM L-glutamate, 2 mM L-serine, 2 mM L-threonine, 2 mM L-cysteine, 2 mM L-proline, 2 mM L-histidine, 2 mM L-phenyl alanine and 2 mM L-tryptophan (Sigma-Aldrich, Munich, Germany), adjusted to pH 7.4 and sterilized through filtration. Notably, for the overnight pre-culture 0.01 % of yeast extract was added.

### *Internalization procedure*

The internalization of MRSA into epithelial cells was carried out as described previously by Pfortner *et al.*<sup>76</sup>. Briefly, bacterial cultures were inoculated from exponentially growing overnight cultures, starting at an inoculation OD<sub>600</sub> of 0.05 and permitting growth until the mid-exponential phase at 37°C, 150 rpm in a shaking water bath. The bacterial numbers were determined by flow cytometry with a Guava easyCyte™ flow cytometer (MilliporePrior Billerica, MA, USA). Prior to infection, the numbers of epithelial cells were assessed by detaching them from the plates with trypsin-EDTA 0.25 % (Thermo Fisher Scientific, Waltham, USA), mixing with Trypan blue dye, and counting with a Countess® cell counter (Invitrogen, Karlsruhe, Germany). In order to infect epithelial cells with MRSA at a multiplicity of infection (MOI) of 1:25, the host cell medium was exchanged with the infection mix (MRSA diluted on eMEM, buffered with 2.9 µl sodium hydrogen carbonate [7.5 %] per ml of bacterial culture added) and incubated for one hour at 37°C, 5 % CO<sub>2</sub> in an incubator. Afterwards, the cell culture medium was exchanged with fresh eMEM containing 10 µg/ml lysostaphin, and this medium was exchanged every two days for long-term experiments.

Sampling of the 16HBE14o- cells was performed by detaching of the cells from the plate with trypsin-EDTA 0.25 %, and the collection of internalized bacteria was carried out through incubation of the plate with 0.05 % SDS for 5 min. Quantification of the intracellular MRSA isolates was performed by flow cytometry with a GUAVA®easyCyte (Merck Millipore, Darmstadt, Germany). To this end, the bacteria were stained with 0.2 µg/ml Vancomycin BODIPY FL (Thermo Fisher Scientific, Waltham, USA), and detected using a 488 nm laser for excitation as described <sup>77</sup>. The intracellular survival of each isolate was analyzed in independent duplicate experiments.

## Graphical and statistical analyses

Volcano plot analyses were performed using GraphPad Prism version 6. Statistical analyses were performed using the Wilcoxon signed-rank test. A P-value of less than or equal to 0.05 was considered statistically significant. Principal component analysis (PCA) was performed using the Statistical Package for Social Science (SPSS) version 22. The component loading of the extracellular proteins from the 15 CA<sup>DK</sup>, HA<sup>DK</sup> and HA<sup>NL-DE</sup> isolates was calculated both for growth medium fractions of cells in the exponential and stationary growth phases based on normalized spectral count. The Venn diagram was constructed using Venny version <sup>78</sup>.

## Ethics.

The present research has no particular ethical implications.

## Funding

This work was supported by the Graduate School of Medical Sciences of the University of Groningen [to S.A.M., L.M.P.M. and C.G], Deutsche Forschungsgemeinschaft Grant GRK1870 [to L.M.P. M. and U.V.], the People

Programme (Marie Skłodowska-Curie Actions) of the European Union's Horizon 2020 Programme under REA grant agreement no. 642836 [to S.G., D.B. and J.M.v.D.], and Deutsche Forschungsgemeinschaft (SFB/TRR 34 framework) [to D.B. and A.O.].

#### Disclosure of Potential Conflicts of Interest

The authors declare that they have no financial and non-financial competing interests in relation to the documented research.

## Acknowledgements

We thank Eliane Popa for critically reading the manuscript, and Alex Reder, Alex Friedrich and Girbe Buist for helpful discussions.

## References

1. Kriegeskorte A, Peters G. Horizontal gene transfer boosts MRSA spreading. *Nat Med.* 2012; 18:662–3.
2. Wertheim HF, Melles DC, Vos MC, van Leeuwen W, van Belkum A, Verbrugh H a, Nouwen JL. The role of nasal carriage in *Staphylococcus aureus* infections. *Lancet Infect Dis* 2005; 5:751–62.
3. Lowy FD. Antimicrobial resistance: The example of *Staphylococcus aureus*. *J. Clin. Invest.* 2003; 111:1265–73.
4. Chambers HF, Deleo FR. Waves of resistance: *Staphylococcus aureus* in the antibiotic era. *Nat Rev Microbiol* 2009; 7:629–41.
5. De Kraker ME, Wolkewitz M, Davey PG, Grundmann H. Clinical impact of antimicrobial resistance in European hospitals: Excess mortality and length of hospital stay related to methicillin-resistant *Staphylococcus aureus* bloodstream infections. *Antimicrob Agents Chemother* 2011; 55:1598–605.
6. De Kraker ME, Davey PG, Grundmann H. Mortality and hospital stay associated with resistant *Staphylococcus aureus* and *Escherichia coli* bacteremia: Estimating the burden of antibiotic resistance in Europe. *PLoS Med* 2011; 8.



7. Sun H, Wei C, Liu B, Jing H, Feng Q, Tong Y, Yang Y, Yang L, Zuo Q, Zhang Y, et al. Induction of systemic and mucosal immunity against methicillin-resistant *Staphylococcus aureus* infection by a novel nanoemulsion adjuvant vaccine. *Int J Nanomedicine* 2015; 10:7275–90.
8. Olaniyi R, Pozzi C, Grimaldi L, Bagnoli F. *Staphylococcus aureus*-associated skin and soft tissue infections: anatomical localization, epidemiology, therapy and potential prophylaxis. *Curr Top Microbiol* 2016; 409:199-227.
9. Missiakas D, Schneewind O. *Staphylococcus aureus* vaccines: Deviating from the carol. *J Exp Med* 2016; 213:1645–53.
10. Weber JT. Community-associated methicillin-resistant *Staphylococcus aureus*. *Clin Infect Dis* 2005; 41 Suppl 4:S269-72.
11. DeLeo FR, Otto M, Kreiswirth BN, Chambers HF. Community-associated methicillin-resistant *Staphylococcus aureus*. *Lancet* 2010; 375:1557–68.
12. Wang R, Braughton KR, Kretschmer D, Bach T-HL, Queck SY, Li M, Kennedy AD, Dorward DW, Klebanoff SJ, Peschel A, et al. Identification of novel cytolytic peptides as key virulence determinants for community-associated MRSA. *Nat Med* 2007; 13:1510–4.
13. David MZ, Daum RS. Community-associated methicillin-resistant *Staphylococcus aureus*: Epidemiology and clinical consequences of an emerging epidemic. *Clin. Microbiol. Rev.* 2010; 23:616–87.
14. Lindsay JA, Holden MTG. *Staphylococcus aureus*: Superbug, super genome? *Trends Microbiol.* 2004; 12:378–85.
15. Sabat AJ, Budimir A, Nashev D, Sá-Leão R, van Dijk J m, Laurent F, Grundmann H, Friedrich AW, ESCMID Study Group of Epidemiological Markers (ESGEM). Overview of molecular typing methods for outbreak detection and epidemiological surveillance. *Euro Surveill* 2013;18:20380.
16. Thurlow LR, Joshi GS, Clark JR, Spontak JS, Neely CJ, Maile R, Richardson AR. Functional modularity of the arginine catabolic mobile element contributes to the success of USA300 methicillin-resistant *Staphylococcus aureus*. *Cell Host Microbe* 2013; 13:100–7.
17. Diep BA, Gill SR, Chang RF, Phan TH, Chen JH, Davidson MG, Lin F, Lin J, Carleton HA, Mongodin EF, et al. Complete genome sequence of USA300, an epidemic clone of community-acquired methicillin-resistant *Staphylococcus aureus*. *Lancet* 2006; 367:731–9.

18. Larsen AR, Goering R, Stegger M, Lindsay JA, Gould KA, Hinds J, Sørum M, Westh H, Boye K, Skov R. Two distinct clones of methicillin-resistant *Staphylococcus aureus* (MRSA) with the same USA300 pulsed-field gel electrophoresis profile: A potential pitfall for identification of USA300 community-associated MRSA. *J Clin Microbiol* 2009; 47:3765–8.
19. Glasner C, Sabat AJ, Dreisbach A, Larsen AR, Friedrich AW, Skov RL, van Dijl JM. Rapid and high-resolution distinction of community-acquired and nosocomial *Staphylococcus aureus* isolates with identical pulsed-field gel electrophoresis patterns and *spa* types. *Int J Med Microbiol* 2013; 303:70–5.
20. Stam-Bolink EM, Mithoe D, Baas WH, Arends JP, Möller AVM. Spread of a methicillin-resistant *Staphylococcus aureus* ST80 strain in the community of the northern Netherlands. *Eur J Clin Microbiol Infect Dis* 2007; 26:723–7.
21. Larsen AR, Stegger M, Böcher S, Sørum M, Monnet DL, Skov RL. Emergence and characterization of community-associated methicillin-resistant *Staphylococcus aureus* infections in Denmark, 1999 to 2006. *J Clin Microbiol* 2009; 47:73–8.
22. Otter JA, French GL. Community-associated methicillin-resistant *Staphylococcus aureus* strains as a cause of healthcare-associated infection. *J. Hosp. Infect.* 2011; 79:189–93.
23. Francois P, Scherl A, Hochstrasser D, Schrenzel J. Proteomic approach to investigate MRSA. *Methods Mol Biol* 2007; 391:179–99.
24. Mäder U, Nicolas P, Depke M, Pané-Farré J, Debarbouille M, van der Kooi-Pol MM, Guérin C, Dérozier S, Hiron A, Jarmer H, et al. *Staphylococcus aureus* Transcriptome Architecture: From Laboratory to Infection-Mimicking Conditions. *PLOS Genet* 2016; 12:e1005962.
25. Muers M. Gene expression: Transcriptome to proteome and back to genome. *Nat Rev Genet* 2011; 12:518.
26. Sibbald MJ, Ziebandt AK, Engelmann S, Hecker M, de Jong A, Harmsen HJM, Raangs GC, Stokroos I, Arends JP, Dubois JYF, et al. Mapping the pathways to staphylococcal pathogenesis by comparative secretomics. *Microbiol Mol Biol Rev* 2006; 70:755–88.
27. Ziebandt AK, Kusch H, Degner M, Jaglitz S, Sibbald MJJB, Arends JP, Chlebowicz MA, Albrecht D, Pantuček R, Doškar J, et al. Proteomics uncovers extreme heterogeneity in the *Staphylococcus aureus* exoproteome

- due to genomic plasticity and variant gene regulation. *Proteomics* 2010; 10:1634–44.
28. Koymans KJ, Vrieling M, Gorham RD, van Strijp JAG. Staphylococcal Immune Evasion Proteins: Structure, Function, and Host Adaptation. *Curr Top Microbiol Immunol* 2016; 409:441–489.
  29. Spaan AN, Surewaard BG, Nijland R, van Strijp JA. Neutrophils versus *Staphylococcus aureus*: a biological tug of war. *Annu Rev Microbiol* 2013; 67:629–50.
  30. He QY, Chiu JF. Proteomics in biomarker discovery and drug development. *J Cell Biochem* 2003; 89:868–86.
  31. Tenover FC, Goering R V. Methicillin-resistant *Staphylococcus aureus* strain USA300: Origin and epidemiology. *J. Antimicrob. Chemother.* 2009; 64:441–6.
  32. Antelmann H, Tjalsma H, Voigt B, Ohlmeier S, Bron S, Van Dijl JM, Hecker M. A proteomic view on genome-based signal peptide predictions. *Genome Res* 2001; 11:1484–502.
  33. Ebner P, Rinker J, Götz F. Excretion of cytoplasmic proteins in *Staphylococcus* is most likely not due to cell lysis. *Curr Genet* 2016; 62:19–23.
  34. Wang G, Xia Y, Song X, Ai L. Common Non-classically Secreted Bacterial Proteins with Experimental Evidence. *Curr. Microbiol.* 2016; 72:102–11.
  35. Götz F, Yu W, Dube L, Prax M, Ebner P. Excretion of cytosolic proteins (ECP) in bacteria. *Int. J. Med. Microbiol.* 2015; 305:230–7.
  36. Krishnappa L, Dreisbach A, Otto A, Goosens VJ, Cranenburgh RM, Harwood CR, Becher D, Van Dijl JM. Extracytoplasmic proteases determining the cleavage and release of secreted proteins, lipoproteins, and membrane proteins in *Bacillus subtilis*. *J Proteome Res* 2013; 12:4101–10.
  37. Bendtsen JD, Kiemer L, Fausbøll A, Brunak S. Non-classical protein secretion in bacteria. *BMC Microbiol* 2005; 5:58.
  38. Liew YK, Hamat RA, Belkum A Van, Chong PP, Neela V. Comparative exoproteomics and host inflammatory response in *Staphylococcus aureus* skin and soft tissue infections, bacteremia, and subclinical colonization. *Clin Vaccine Immunol* 2015; 22:593–603.

39. Liew YK, Hamat RA, Nordin SA, Chong PP, Neela V. The exoproteomes of clonally related *Staphylococcus aureus* strains are diverse. *Ann Microbiol* 2015; 65:1809–1813.
40. Cassat JE, Hammer ND, Campbell JP, Benson MA, Perrien DS, Mrak LN, Smeltzer MS, Torres VJ, Skaar EP. A secreted bacterial protease tailors the *Staphylococcus aureus* virulence repertoire to modulate bone remodeling during osteomyelitis. *Cell Host Microbe* 2013; 13:759–72.
41. Monteiro R, Hébraud M, Chafsey I, Chambon C, Viala D, Torres C, Poeta P, Igrejas G. Surfaceome and exoproteome of a clinical sequence type 398 methicillin resistant *Staphylococcus aureus* strain. *Biochem Biophys Reports* 2015; 3:7–13.
42. Voyich JM, Braughton KR, Sturdevant DE, Whitney AR, Saïd-Salim B, Porcella SF, Long RD, Dorward DW, Gardner DJ, Kreiswirth BN, et al. Insights into mechanisms used by *Staphylococcus aureus* to avoid destruction by human neutrophils. *J Immunol* 2005; 175:3907-19.
43. Geiger T, Francois P, Liebeke M, Fraunholz M, Goerke C, Krismer B, Schrenzel J, Lalk M, Wolz C. The stringent response of *Staphylococcus aureus* and its impact on survival after phagocytosis through the induction of intracellular PSMs expression. *PLoS Pathog* 2012; 8.
44. Cheung GYC, Joo HS, Chatterjee SS, Otto M. Phenol-soluble modulins - critical determinants of staphylococcal virulence. *FEMS Microbiol. Rev.*2014; 38:698–719.
45. Surewaard BGJ, De Haas CJC, Vervoort F, Rigby KM, Deleo FR, Otto M, Van Strijp JAG, Nijland R. Staphylococcal alpha-phenol soluble modulins contribute to neutrophil lysis after phagocytosis. *Cell Microbiol* 2013; 15:1427–37.
46. Dumont AL, Yoong P, Surewaard BGJ, Benson MA, Nijland R, van Strijp JAG, Torres VJ. *Staphylococcus aureus* elaborates the leukotoxin LukAB to mediate escape from within human neutrophils. *Infect Immun* 2013; 81:1830–41.
47. Radisky DC, Stallings-Mann M, Hirai Y, Bissell MJ. Single proteins might have dual but related functions in intracellular and extracellular microenvironments. *Nat Rev Mol Cell Biol* 2009; 10:228–34.
48. Huberts DH, van der Klei IJ. Moonlighting proteins: An intriguing mode of multitasking. *Biochim Biophys Acta - Mol Cell Res* 2010; 1803:520–5.

49. Bonar E, Wójcik I, Władyka B. Proteomics in studies of *Staphylococcus aureus* virulence. *Acta Biochim. Pol.*2015; 62:367–81.
50. Kainulainen V, Korhonen TK. Dancing to another tune-adhesive moonlighting proteins in bacteria. *Biology* 2014; 3:178–204.
51. Wang G, Xia Y, Cui J, Gu Z, Song Y, Chen YQ, Chen H, Zhang H, Chen W. The roles of moonlighting proteins in bacteria. *Curr. Issues Mol. Biol.*2014; 16:15–22.
52. Otto A, van Dijl JM, Hecker M, Becher D. The *Staphylococcus aureus* proteome. *Int. J. Med. Microbiol.*2014; 304:110–20.
53. Wang W, Jeffery CJ. An analysis of surface proteomics results reveals novel candidates for intracellular/surface moonlighting proteins in bacteria. *Mol Biosyst* 2016; 12:1420–31.
54. Dreisbach A, Hempel K, Buist G, Hecker M, Becher D, Van Dijl JM. Profiling the surfacome of *Staphylococcus aureus*. *Proteomics* 2010; 10:3082–96.
55. Henderson B, Martin A. Bacterial moonlighting proteins and bacterial virulence. *Curr Top Microbiol Immunol* 2013; 358:155–213.
56. Ebner P, Rinker J, Nguyen MT, Popella P, Nega M, Luqman A, Schitteck B, Di Marco M, Stevanovic S, Götza F. Excreted cytoplasmic proteins contribute to pathogenicity in *Staphylococcus aureus*. *Infect Immun* 2016; 84:1672–81.
57. Bankevich A, Nurk S, Antipov D, Gurevich AA, Dvorkin M, Kulikov AS, Lesin VM, Nikolenko SI, Pham S, Prjibelski AD, et al. SPAdes: A New Genome Assembly Algorithm and Its Applications to Single-Cell Sequencing. *J Comput Biol* 2012; 19:455–77.
58. Seemann T. Prokka: Rapid prokaryotic genome annotation. *Bioinformatics* 2014; 30:2068–9.
59. Page AJ, Cummins CA, Hunt M, Wong VK, Reuter S, Holden MTG, Fookes M, Falush D, Keane JA, Parkhill J. Roary: Rapid large-scale prokaryote pan genome analysis. *Bioinformatics* 2015; 31:3691–3.
60. Stamatakis A. RAxML version 8: A tool for phylogenetic analysis and post-analysis of large phylogenies. *Bioinformatics* 2014; 30:1312–3.

61. Joensen KG, Scheutz F, Lund O, Hasman H, Kaas RS, Nielsen EM, Aarestrup FM. Real-time whole-genome sequencing for routine typing, surveillance, and outbreak detection of verotoxigenic *Escherichia coli*. *J Clin Microbiol* 2014; 52:1501–10.
62. Zankari E, Hasman H, Cosentino S, Vestergaard M, Rasmussen S, Lund O, Aarestrup FM, Larsen MV. Identification of acquired antimicrobial resistance genes. *J Antimicrob Chemother* 2012; 67:2640–4.
63. Stobernack T, Glasner C, Junker S, Gabarrini G, de Smit M, de Jong A, Otto A, Becher D, van Winkelhoff AJ, van Dijk JM. The Extracellular Proteome and Citrullinome of the Oral Pathogen *Porphyromonas gingivalis*. *J Proteome Res* 2016; 15:4532–4543.
64. Gardy JL, Brinkman FSL. Methods for predicting bacterial protein subcellular localization. *Nat Rev Microbiol* 2006; 4:741–51.
65. Petersen TN, Brunak S, von Heijne G, Nielsen H. SignalP 4.0: discriminating signal peptides from transmembrane regions. *Nat Methods* 2011; 8:785–6.
66. Käll L, Krogh A, Sonnhammer ELL. A combined transmembrane topology and signal peptide prediction method. *J Mol Biol* 2004; 338:1027–36.
67. Hiller K, Grote A, Scheer M, Münch R, Jahn D. PrediSi: Prediction of signal peptides and their cleavage positions. *Nucleic Acids Res* 2004; 32:W375–9.
68. Juncker AS, Willenbrock H, Von Heijne G, Brunak S, Nielsen H, Krogh A. Prediction of lipoprotein signal peptides in Gram-negative bacteria. *Protein Sci* 2003; 12:1652–62.
69. Clark HF, Gurney AL, Abaya E, Baker K, Baldwin D, Brush J, Chen J, Chow B, Chui C, Crowley C, et al. The secreted protein discovery initiative (SPDI), a large-scale effort to identify novel human secreted and transmembrane proteins: A bioinformatics assessment. *Genome Res* 2003; 13:2265–70.
70. Yu NY, Wagner JR, Laird MR, Melli G, Rey S, Lo R, Dao P, Cenk Sahinalp S, Ester M, Foster LJ, et al. PSORTb 3.0: Improved protein subcellular localization prediction with refined localization subcategories and predictive capabilities for all prokaryotes. *Bioinformatics* 2010; 26:1608–15.
71. Kahsay RY, Gao G, Liao L. An improved hidden Markov model for transmembrane protein detection and topology prediction and its applications to complete genomes. *Bioinformatics* 2005; 21:1853–8.

72. de Castro E, Sigrist CJA, Gattiker A, Bulliard V, Langendijk-Genevaux PS, Gasteiger E, Bairoch A, Hulo N. ScanProsite: Detection of PROSITE signature matches and ProRule-associated functional and structural residues in proteins. *Nucleic Acids Res* 2006; 34:W362-5.
73. Bernhardt J, Michalik S, Wollscheid B, Völker U, Schmidt F. Proteomics approaches for the analysis of enriched microbial subpopulations and visualization of complex functional information. *Curr. Opin. Biotechnol.* 2013; 24:112–9.
74. Nicolas P, Mäder U, Dervyn E, Rochat T, Leduc A, Pigeonneau N, Bidnenko E, Marchadier E, Hoebeke M, Aymerich S, et al. Condition-dependent transcriptome reveals high-level regulatory architecture in *Bacillus subtilis*. *Science* 2012; 335:1103–6.
75. Homuth G, Masuda S, Mogk A, Kobayashi Y, Schumann W. The dnaK operon of *Bacillus subtilis* is heptacistronic. *J Bacteriol* 1997; 179:1153–64.
76. Pförtner H, Wagner J, Surmann K, Hildebrandt P, Ernst S, Bernhardt J, Schurmann C, Gutjahr M, Depke M, Jehmlich U, et al. A proteomics workflow for quantitative and time-resolved analysis of adaptation reactions of internalized bacteria. *Methods* 2013; 61:244–50.
77. Hildebrandt P, Surmann K, Salazar MG, Normann N, Völker U, Schmidt F. Alternative fluorescent labeling strategies for characterizing gram-positive pathogenic bacteria: Flow cytometry supported counting, sorting, and proteome analysis of *Staphylococcus aureus* retrieved from infected host cells. *Cytom Part A* 2016;89:932-940.
78. Oliveros JC. VENNY. An interactive tool for comparing lists with Venn Diagrams. [Internet]. BioinfoGP of CNB-CSIC2007; :<http://bioinfogp.cnb.csic.es/tools/venny/index.ht>. Available from: <http://bioinfogp.cnb.csic.es/tools/venny/index.html>.

## Chapter 5

# **Metabolic niche adaptation of community- and hospital-associated methicillin-resistant *Staphylococcus aureus***

---

Solomon A. Mekonnen<sup>#</sup>, Laura M. Palma Medina<sup>#</sup>, Stephan Michalik, Marco G. Loreti, Manuela Gesell Salazar, Jan Maarten van Dijk<sup>§</sup>, and Uwe Völker<sup>§</sup>

<sup>#</sup>: These authors contributed equally to this work

<sup>§</sup>: Corresponding authors

*Journal of Proteomics* 193, 154–161 (2019)

Supplementary Material is available at [http://bit.ly/Thesis\\_Palma\\_Medina](http://bit.ly/Thesis_Palma_Medina)





## Abstract

Methicillin-resistant *Staphylococcus aureus* (MRSA) originally emerged in nosocomial settings and has subsequently spread into the community. In turn, community-associated (CA) MRSA lineages are nowadays introduced from the community into hospitals where they can cause hospital-associated (HA) infections. This raises the question of how the CA-MRSA lineages adapt to the hospital environment. Previous studies implicated particular virulence factors in the CA-behaviour of MRSA. However, we hypothesized that physiological changes may also impact staphylococcal epidemiology. With the aim to identify potential metabolic adaptations, we comparatively profiled the cytosolic proteomes of CA- and HA-isolates from the USA300 lineage that was originally identified as CA-MRSA. Interestingly, enzymes for gluconeogenesis, the tricarboxylic acid cycle and biosynthesis of amino acids are up-regulated in the investigated CA-MRSA isolates, while enzymes for glycolysis and the pentose phosphate pathway are up-regulated in the HA-MRSA isolates. Of note, these data apparently match with the clinical presentation of each group. These observations spark interest in central carbon metabolism as a key driver for adaptations that streamline MRSA for propagation in the community or the hospital.

## Introduction

*Staphylococcus aureus* is a Gram-positive bacterium frequently colonizing the human body. However, it is also a dangerous pathogen capable of causing a wide array of diseases ranging from skin to soft tissue infections and ultimately life-threatening invasive disease [1]. The ability of *S. aureus* to colonize certain niches of the host, and to cause particular diseases is dependent on both its virulence factor repertoire and its adaptation capability. Omics profiling approaches provide new insights into both the virulence factors expressed in specific host niches and the adaptive responses mounted by *S. aureus* [2–4]. Thus, it is well established that *S. aureus* expresses a whole arsenal of virulence factors, such as toxins, degradative enzymes, adhesins, and other surface-associated proteins that allow this pathogen to establish infection and to survive in the host [5–7]. *S. aureus* has also evolved resistance to many antibiotics including penicillin, methicillin, oxacillin, and last resort antibiotics, such as linezolid and daptomycin. Two major methicillin-resistant *Staphylococcus aureus* (MRSA) classes are distinguished based on epidemiology, namely community-associated (CA) and hospital-associated (HA) MRSA [8]. Risk factors for infection by HA-MRSA are recent hospitalization, dialysis, nursing-home residence, and other co-morbidities such as diabetes, chronic renal failure, and chronic pulmonary diseases that bring individuals in contact with healthcare settings [9]. In contrast, the main risk factor for attracting CA-MRSA is close interaction with many different individuals which can occur in nurseries, sport centres, and the army.

We have recently shown that closely related CA- and HA-MRSA isolates of the USA300 lineage can be distinguished based on their whole genome sequences (WGS) and exoproteome profiles [10]. Importantly, the comparative genome analysis revealed that the distinctive features of these two groups of isolates relate predominantly to the accessory genome. Interestingly, particular virulence genes

encoded on mobile genetic elements, such as the PVL-encoding genes *lukF* and *lukS*, were exclusively present in the CA-isolates, while enterotoxin-encoding genes such as *sea*, *sed*, *sej*, and *ser* were found only in the HA-isolates [10]. Exoproteome data showed that the investigated CA- and HA-MRSA isolates can be distinguished by two distinct extracellular protein abundance clusters that are predictive not only for the epidemiologic behaviour of USA300 isolates, but also for their growth and survival within lung epithelial cells. This was indicative of adaptations of these USA300 isolates, which are generally considered as CA-MRSA, to the hospital environment. Such adaptations are of interest, because the current rise of MRSA infections in the community inevitably leads to the introduction of CA-MRSA into the hospital environment. Notably, adaptive mechanisms often relate to alterations in the metabolic status of a bacterium. In the case of *S. aureus*, such alterations are known to influence the expression of virulence factors. However, the particular carbon and nitrogen sources that are available to *S. aureus* in specific host niches also require specific adaptation [11]. Importantly, the respective metabolic pathways are essential for bacterial proliferation within the host. Therefore, we hypothesised that the investigated HA-USA300 isolates have also adapted to the hospital environment, at least in part, by changes in their metabolic pathways.

The present study was aimed at identifying potential metabolic adaptations in the, originally community-associated, USA300 lineage to the hospital environment. To this end, we employed a proteomics approach with a focus on the cytosolic protein complement. As anticipated, the data obtained highlight differences between the investigated CA- and HA-isolates in the protein abundance of several major metabolic pathways. These include glycolysis, gluconeogenesis, pentose phosphate pathway, TCA cycle, and amino acid biosynthesis. Importantly, the observed adaptations have biomedically relevant implications for virulence, stress tolerance, and antibiotic resistance.

## Methods

### Bacterial strains

The CA- and HA-MRSA strains examined in this study were collected in Denmark by the Statens Serum Institut (Copenhagen, Denmark) in the period between 1999 and 2006 [12]. They share the pulsed-field gel electrophoresis profile USA300, but differ in *spa*-type. While the three investigated CA-MRSA isolates D15, D32 and D37 share the *spa*-type t008, the three investigated HA-MRSA isolates D17, D22 and D53 share the *spa*-type t024 [12,13]. Genome sequences and the exoproteome profiles of these strains were previously described [12,13,10].

### Cultivation of bacteria and sample preparation

The cultivation of bacteria was carried out as described before [10]. Briefly, bacteria were grown overnight in Tryptone Soy Broth (TSB) at 37°C. Exponentially growing cultures were used to inoculate Roswell Park Memorial Institute-1640 (RPMI) medium supplemented with 2 mM glutamine (GE Healthcare/PAA, Little Chalfont, United Kingdom) to a final optical density at 600 nm (OD<sub>600</sub>) of 0.05, and growth was continued until mid-exponential phase. Exponentially growing cells were then used to inoculate fresh RPMI medium to a final OD<sub>600</sub> of 0.05. Samples from three independent biological replicates were taken in the transition phase between the exponential and stationary growth phases, and two hours after entry into the stationary growth phase. Cells were collected by centrifugation of 13 ml of culture at 13,000 × g, 10 min, at 4°C. The cell pellets were immediately frozen in liquid nitrogen, and stored at -80°C until further processing. To extract the cytosolic protein fraction, cells were disrupted using FastPrep®. Briefly, bacterial cell pellets were re-suspended with an appropriate volume of 1 × urea/ thiourea buffer, and transferred to 2 ml screw-cap tubes pre-filled with glass beads (Sigma-Aldrich, St. Louis, USA) in half the volume of the suspension. The mixture was

disrupted in a FastPrep FP120 (Thermo Fischer Scientific Inc., MA, USA) by shaking at maximal speed for 30 s followed by 3 min cooling on ice. After repeating the disruption three times, the protein extract was collected by centrifugation at 4°C, 10,000 x g for 30 min. The supernatant was collected in a new reaction tube. Determination of protein concentrations was performed with a Bradford assay (Biorad, München, Germany). Four µg of protein extract were digested with trypsin (Promega, Madison, WI, US; ratio of 1:25 trypsin to protein) at 37°C overnight. To stop the digestion, a final concentration of 1% v/v trifluoroacetic acid (TFA; Merck, Darmstadt, Germany) was added. Finally, peptide samples were purified using ZipTip®µ-C18 columns (Merck Millipore, Darmstadt, Germany) and eluted in 5 µl of 50% acetonitrile (ACN; Sigma-Aldrich, St. Louis, USA) followed by elution with 5 µl of 80% ACN. The 10 µl eluate was first frozen at -80 °C overnight and then dried by vacuum centrifugation. Finally, the dried peptides were reconstituted in 10 µl buffer A [2% (v/v) ACN and 0.1% (v/v) acetic acid in HPLC-grade water (Baker)].

## Acquisition and processing of mass spectrometry data

Acquisition of mass spectrometry (MS) data was performed in data-independent mode (DIA) mode by shotgun nano-liquid chromatography (LC)-MS/MS on a Q Exactive™ Plus (Thermo-Fisher Scientific, Waltham, MA, USA) connected to an Ultimate® 3000 Nano LC as described before [14]. DIA measurement parameter settings are provided in Supplementary Table 1. Prior to the separation of samples by nano-HPLC, an iRT-spike-in-mix (Biognosys AG, Schlieren, Switzerland) was added to the samples. To construct strain-specific ion libraries, samples were measured in data-dependent mode (DDA) as described before [15]. DDA measurement parameter settings are provided in Supplementary Table 2. Specific sequences of the respective isolates were used to search for the database by MaxQuant [16], and the MaxQuant parameter settings are provided in

Supplementary Table 3. The Spectronaut™ Pulsar software package (v 11.0.15038.12.32941, Biognosys AG 2013) was used to analyse the samples in a strain-dependent manner. The Spectronaut™ settings are provided in Supplementary Table 4. The raw MS data and other associated files of the present study can be downloaded from the MassIVE repository using the following link: <https://massive.ucsd.edu/ProteoSAFe/jobs.jsp>.

## Analysis of data

To compare the different strains, a blastP analysis (default parameters, BLAST 2.6.0+) was performed to the closely related and well-annotated *S. aureus* USA300\_FPR3757 strain. The protein annotation of this strain was retrieved from AureoWiki (<http://aureowiki.med.uni-greifswald.de/>) [17]. The results were filtered for the top hit for each individual protein in the BLASTp analysis. Only proteins with a minimum overall amino acid sequence identity of 70% were considered for quantification. Importantly, this led to the exclusion of only 12 identified proteins that were not mapped to USA300\_FPR3757 protein sequences but were uniquely mapped to CA-isolates.

To quantify protein amounts, the ion intensity areas under the respective curves from the individual strain reports were used for a global median normalization. Peptide intensities were calculated by summing up the normalized ion data for each peptide. To compare differences in protein abundance between the investigated CA- and HA-MRSA isolates, the mean of the biological replicates per peptide and strain was calculated. Only peptides present in both CA- and HA-isolates as well as in a minimum of two out of three isolates per group were used for statistical testing. Ratios for each peptide were calculated by generating pairwise ratios from each HA- versus CA-isolate at the peptide level in all combinations as described previously [15]. The obtained values were tested per

protein using the Wilcoxon rank sum test against an absolute fold change of 1.3. Proteins with p-values below 0.05 were considered to be present in significantly different abundance. Protein annotation and pangene symbols were extracted from AureoWiki [17]. A table with all the analyses is provided as Supplementary Table 5. Of note, proteins that did not fulfil our inclusion criterion for analysis, i.e. presence of a particular protein in a minimum of two out of three isolates led to the exclusion of 46 and 47 proteins that were uniquely identified in the CA- or HA-isolates, respectively (Supplementary Table 6).

## Visualization of proteome data in Voronoi treemaps

Voronoi treemaps were generated using the Paver 2.0 software (Decodon GmbH, Greifswald, Germany) [18]. The regulon assignments of the genes that encoded proteins of interest was extracted from AureoWiki in order to generate a treemap. The template treemap calculation for each isolate was performed using the free swarm algorithm as previously described [15].

## Extraction of carotenoid

Carotenoid extraction was done as described previously, with slight modifications [19]. Briefly, CA- and HA-isolates were cultured in TSB shaking at 220 rpm at 37° for 24 h. The cell densities were adjusted by measuring OD<sub>600</sub> to obtain comparable cell amounts with a total volume of 1 ml culture, and the cells were collected by centrifugation at 10,000 × g, 2 min followed by washing with PBS. Cell pellets were suspended in 500 µl of methanol and heated to 55°C for 5 min, followed by a centrifugation at 10,000 × g for 2 min. The extraction was repeated until no further pigment could be extracted. The extracts were collected, and absorption spectra were recorded at 465 nm.



## Results

### Distinction of CA- and HA-MRSA isolates based on cellular proteome profiles

In a recent study, we performed a comparative genome and exoproteome analysis on CA- and HA-MRSA isolates of the USA300 lineage to pinpoint epidemiologically relevant distinctive features in these closely related bacteria [10]. In particular, a PCA analysis of the exoproteome data identified core isolates of each group. For the CA-MRSA group, the core isolates were D15, D32 and D37, and for the HA-MRSA group these were isolates D17, D22 and D53. We therefore decided to focus the present comparative analysis of the cytosolic proteome on these six isolates. To this end, the different isolates were cultured in RPMI medium, because a previous transcriptome analysis with tiling arrays had shown that the transcript profiles of *S. aureus* grown in RPMI closely resembled those of *S. aureus* grown in human plasma [2]. The RPMI growth condition thus reflects the particular nutritional challenges encountered by *S. aureus* when the bacteria have become invasive and entered the bloodstream of a patient with bacteraemia. Further, we addressed bacteria in the transition phase between the exponential and stationary growth phases, where most virulence factors start to be expressed, and two hours after entry into the stationary phase as these growth stages are of the highest clinical relevance. Altogether, 1000 proteins were identified in our MS analysis where the criterion for protein identification was the detection of minimally two peptides in at least two out of three isolates per CA- or HA-isolate group. As expected, per isolate group, rather extensive differences in protein composition were detectable between the two time points of sampling (Supplementary Table 5) which also resulted in clear separation of transient and stationary phase samples of each strain in the first and strongest component of a principal component analysis (PCA, Fig. 1). However, it was a surprise that the

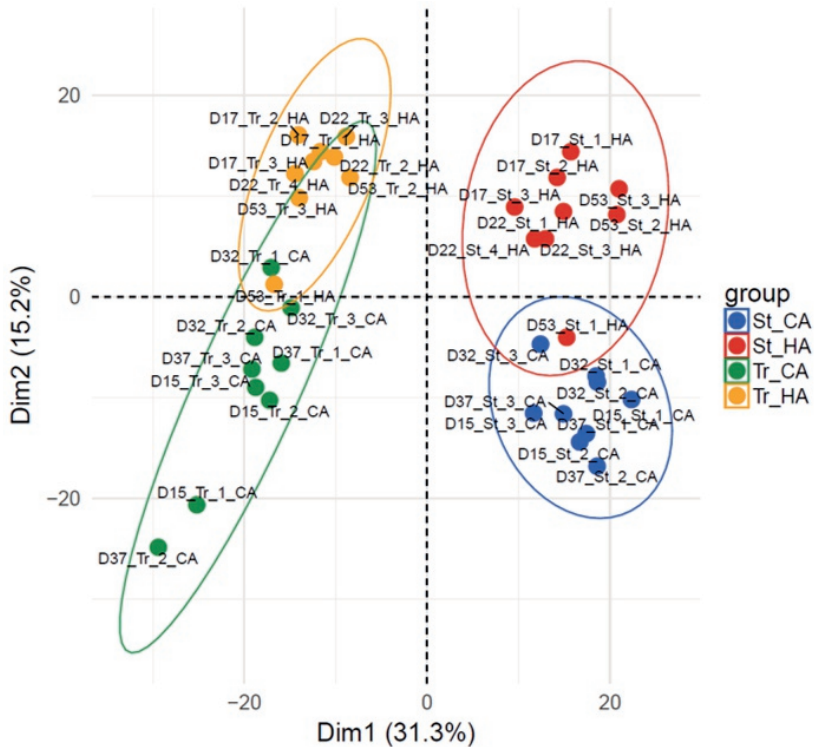


**Figure 1. Principal component analysis of cytosolic protein intensities in CA- and HA-MRSA isolates.** A principal component analysis (PCA) was performed on the intensity of proteins identified by mass spectrometry using R (version 3.4.3) and the factomineR package (version 1.39). Missing values were removed. Data centering was performed by subtracting the column means of the data from their corresponding columns, and protein intensities with no protein identification were omitted. To unify the variance scaling of data, the (centered) columns of the data were divided by their standard deviations. For each isolate three biological replicates were analysed in both transient and stationary phase samples. Dimensions 1 and 2 were used to plot the graph. Green and blue circles represent transient (Tr) phase and stationary (St) phase samples from CA-MRSA isolates, whilst yellow and red circles represent transient (Tr) and stationary (St) samples from HA-MRSA isolates, respectively.

unbiased PCA analysis also uncovered a sharp distinction between the investigated CA- and HA-isolates, irrespective of the time point of sampling (Fig. 1). A further inspection of the data revealed that 239 proteins were differentially expressed ( $p \leq 0.05$ ) between the CA- and HA-isolates in the transition phase, and 186 proteins in the stationary phase as graphically represented in the Volcano

plots in Figure 2. These observations show that cells of these two isolate groups with different epidemiological behaviour have a distinct protein composition.

The observed differences in the protein levels between the two groups of isolates could potentially relate to differences in gene expression or differences e.g. in protein stability due to differences in protein sequences. We, therefore, performed blastP comparisons, which showed sequence differences for 38 proteins, whereas the remainder of the proteins with differential abundance in the CA- and HA-isolates showed identical amino acid sequences in both isolate groups

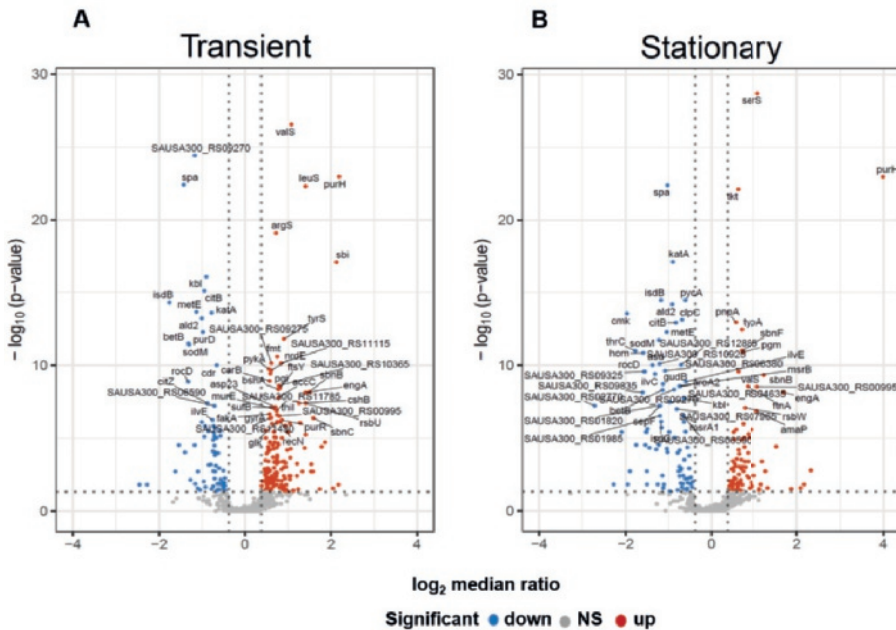


Figure 2. Volcano plots presenting proteins with differential abundance in CA- and HA-MRSA isolates. A Wilcoxon rank sum test against a fold change of 1.3 was used to compute the significance level of differentially abundant proteins in the cytosolic fractions of CA- and HA-MRSA isolates. (A) transition phase samples, (B) stationary phase samples. Each dot represents a particular protein. Red marks a significantly higher abundance in HA-isolates, and blue a significantly higher abundance in CA-isolates. Grey marks the absence of a significant difference in protein abundance. Top 50 proteins with the highest P-values were marked with their corresponding pangene identifier, otherwise with locus ID.

(Supplementary Fig. 1). This implies that the majority of proteins with differential abundance in CA- and HA-isolates are differentially regulated and that only a minor fraction may show differential behaviour based on structural differences.

## Regulator-based stratification of differential protein abundance

Proteins that showed statistically significant different levels in CA- and HA-MRSA were categorised based on the known regulators of the respective genes. This revealed that proteins encoded by genes under control of the alternative RNA polymerase sigma factor B (SigB) and the putative transcriptional regulator (MtlR) were up-regulated among the HA-isolates (Figure 3A, B; Supplementary Fig. 2). Notably, this does not only apply to the strictly SigB-controlled proteins Asp23, RsbV and RsbW, but also to proteins that are controlled by SigB and other regulators (Fig. 3B, D). In contrast, proteins encoded by genes that are controlled by the regulator of branched-chain amino acid synthesis (CodY) and the catabolite control protein A (CcpA) were up-regulated among the CA-isolates (Fig. 3C, D; Supplementary Fig. 1).

## Differential protein abundance in metabolic pathways

To better understand the physiological changes potentially underlying differences in epidemicity, the identified proteins were categorised based on their assignment to different metabolic pathways. Interestingly, proteins involved in glycolysis, such as the triosephosphate isomerase TpiA, the aldehyde dehydrogenase GapA, the phosphoglycerate kinase Pfkfb3 and the 2,3-bisphosphoglycerate-independent phosphoglycerate mutase Pgm were significantly more abundant in the HA-isolates (Fig. 4A, B). Similarly, proteins involved in the pentose phosphate pathway such as transketolase (Tkt) were more abundant in the HA-isolates (Fig.

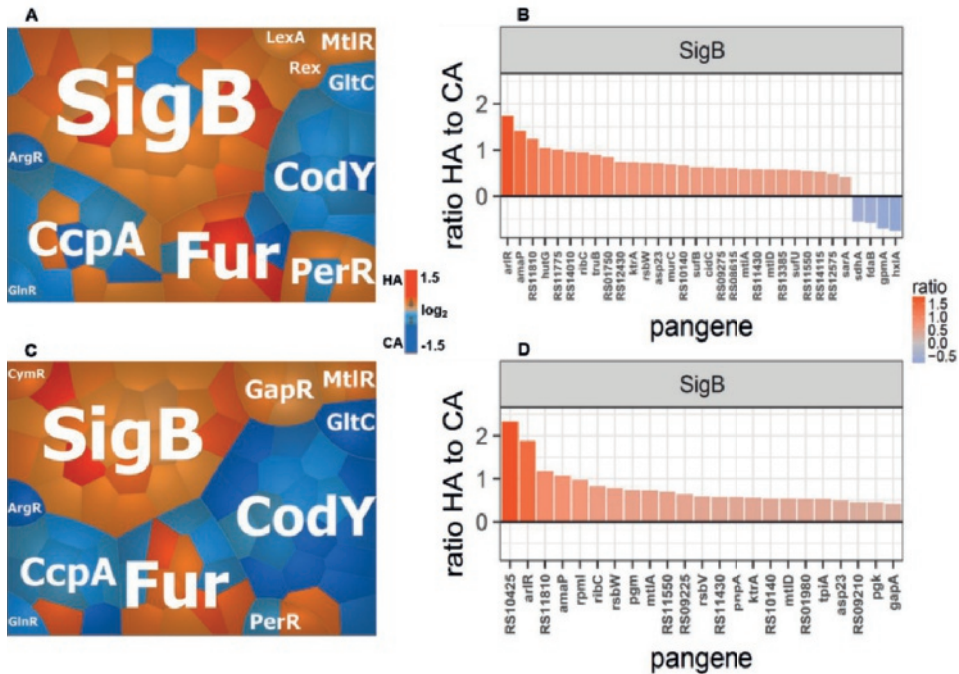


**Figure 3. Regulon-based stratification of genes encoding proteins present at statistically significantly different levels in the CA- and HA-MRSA isolates.** (A) Voronoi treemap of regulon-based stratification of proteins present at statistically significantly different levels in the transient phase samples. (B) Bar plot of SigB-regulated proteins present at statistically significantly different levels in the transient phase samples. (C) Voronoi treemap of regulon-based stratification of proteins present at statistically significantly different levels in the stationary phase samples. (D) Bar plot of SigB-regulated proteins present at statistically significantly different levels in the stationary phase samples. Ratios of protein intensities in HA- and CA-isolates in  $\log_2$  were used to create both the Voronoi treemaps and the bar graphs. Individual cells in the Voronoi treemaps (A, C) represent particular significantly differentially regulated proteins. Blue cells represent proteins up-regulated in CA-isolates, and orange cells represent proteins up-regulated in HA-isolates. In the bar graphs (B, D), the Y-axis indicates the HA/CA protein ratios in  $\log_2$ , and the X-axis shows the respective pangene names or locus IDs of the USA300\_FPR3757 strain for the corresponding proteins. The 'SAUSA300\_' prefix was omitted for names starting with 'RS' for a better graphical representation of the Figure.

4C, D) On the other hand, proteins involved in gluconeogenesis, such as the pyruvate carboxylase PycA (Fig. 4E, F), and the tricarboxylic acid (TCA) cycle, such as CitB and CitZ (Fig. 4G, H), were more abundant in the CA-isolates. The

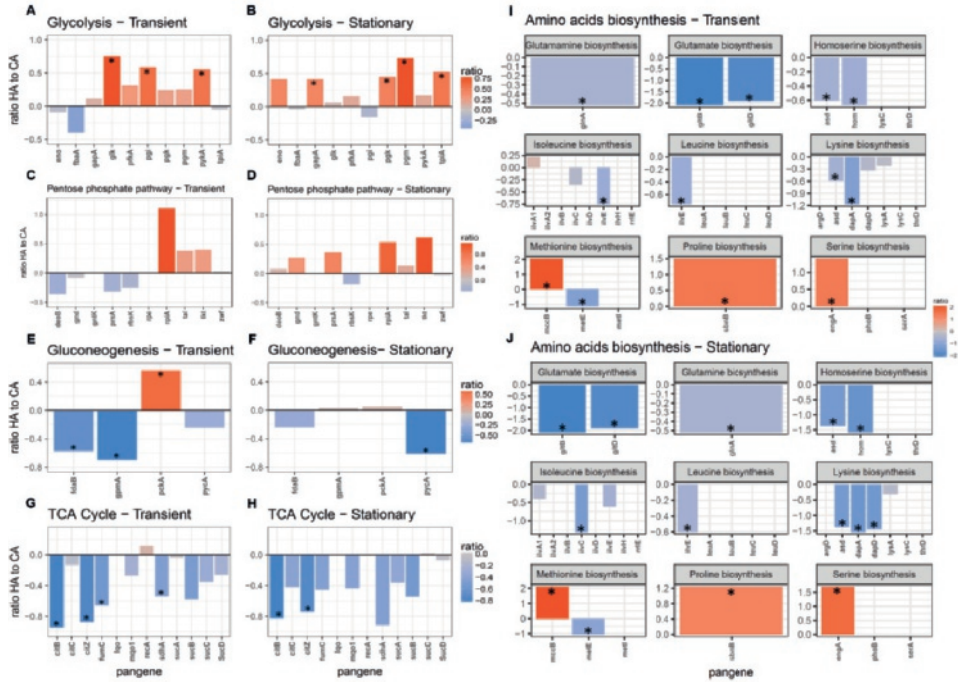


**Figure 4. Assignment of identified proteins according to their roles in metabolic pathways.** Ratios of proteins implicated in the glycolysis (A, B), pentose phosphate pathway (C, D), gluconeogenesis (E, F), TCA cycle (G, H) and different amino acid biosynthetic pathways (I, J) are presented. Panels A, C, E, G and I relate to transition phase samples, and panels B, D, F, H and J relate to stationary phase samples. \* Statistically significant differences in protein intensity; empty boxes relate to proteins involved in the specified pathway that were not identified in the analysis.

latter also applied to proteins involved in the biosynthesis of several amino acids, including glutamate, glutamine, homoserine, isoleucine, leucine and lysine (Fig. 4I, J), whereas proteins involved in the synthesis of proline were less abundant in the CA-isolates. A further potentially important metabolic difference was observed for proteins involved in the purine biosynthesis. Interestingly, in the HA-isolates we observed an up-regulation of the purine synthesis repressor PurR, and a corresponding down-regulation of PurR-regulated proteins PurS, PurL, PurN, and PurD (Fig. 5A). Of note, only PurH was up-regulated in the HA-isolates, but this may relate to an amino acid substitution as PurH is one of the 38

differentially expressed proteins with an amino acid substitution (Supplementary Fig. 1).

## Impact of metabolic differences on the production of staphyloxanthin

SigB is known to positively regulate the expression of the *crtM* gene, which plays a crucial role in the biosynthesis of the carotenoid staphyloxanthin, the pigment that gives *S. aureus* its golden appearance [20,21]. In addition, Lan and colleagues have shown that inactivation of the *citZ* gene, which encodes the first enzyme in the TCA cycle, or inactivation of the *purH* gene involved in purine biosynthesis, both lead to increased staphyloxanthin production [22]. Since CitZ and several proteins in purine biosynthesis are down-regulated in the HA-isolates, while PurH contains an amino acid substitution in these isolates, we hypothesized that the HA-isolates might display higher-levels of staphyloxanthin than the CA-isolates. Indeed, inspection of HA- and CA-isolates grown in TSB showed that the HA-MRSA isolates displayed a stronger pigmentation than the CA-isolates, and this qualitative observation was subsequently validated by quantification of extracted staphyloxanthin (Fig. 5B, C).

## Discussion

The Gram-positive bacterium *S. aureus* requires 13 biosynthetic intermediates [23] to synthesize all macromolecules that it needs to be a successful pathogen that conquers different niches on and in the human body. These biosynthetic intermediates are derived from only three metabolic pathways in central carbon metabolism, namely glycolysis, the pentose phosphate pathway and the TCA cycle [23]. This focuses attention on the relationships between metabolism and the particular behaviour of this pathogen. In the present study, we analysed differences in the cellular protein profiles of two groups of genetically closely

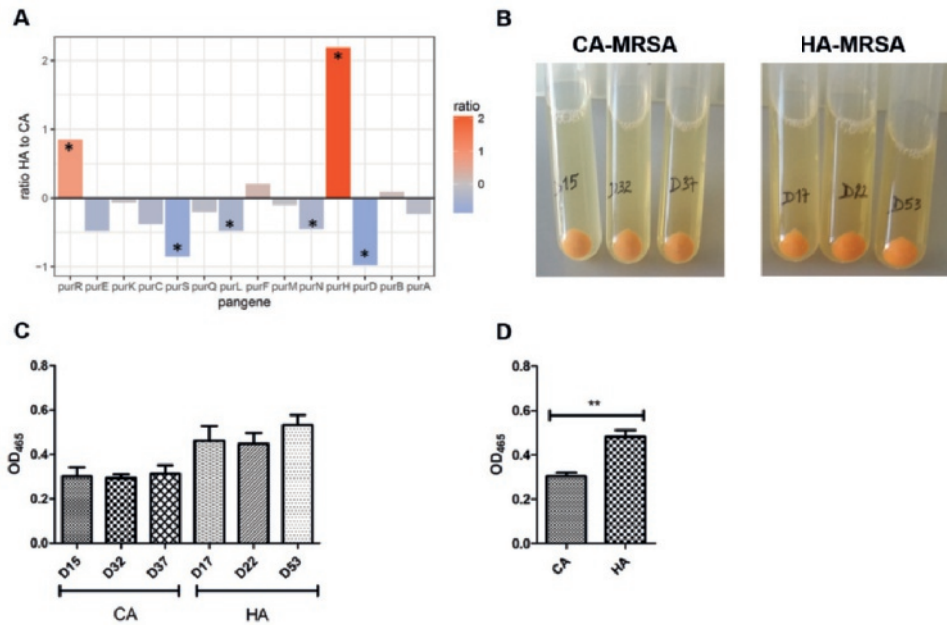


**Figure 5. Correlation between protein levels of purine biosynthesis and isolate pigmentation.** (A) The HA/CA ratios of proteins involved in purine metabolism are represented in a bar graph. (B) Yellow pigmentation of CA- and HA-isolates was assessed upon growth in TSB medium and subsequently pelleting the cells by centrifugation. (C) Carotenoids were extracted from pelleted cells by methanol extraction and the yellow coloration of the extracted pigment was assessed by OD<sub>465</sub> readings. (D) averaged values of the OD<sub>465</sub> readings for pigment extracted from CA- or HA-isolates. \*, Statistically significant differences in protein abundance or intensity of extracted pigment.

related, but epidemiologically distinct, isolates of the USA300 lineage that had been collected from Danish hospitals or the community in the Copenhagen area. A total of 1000 proteins were identified through mass spectrometry analysis of the cytosolic fractions of the isolates, many of which have prominent roles in metabolism and physiology. Importantly, our data analysis uncovers significant differences in the levels of proteins involved in glycolysis, the pentose phosphate pathway and the TCA cycle showing that central carbon metabolism is key to understanding staphylococcal epidemicity.



Glycolysis is the main pathway that converts glucose internalized by *S. aureus* in a cascade of ten consecutive steps to pyruvate under aerobic conditions [24]. Intriguingly, the here investigated HA-MRSA isolates displayed significantly higher levels of glycolytic enzymes such as TpiA, GapA, Pgc and Pgm than the CA-MRSA isolates. This implies that the repression of the respective genes by the glycolytic operon regulator GapR is less tight in the HA-isolates. In contrast, the HA-isolates contained relatively lower levels of the gluconeogenesis enzymes GpmA, FdaB and PycA. These findings imply that, under exactly the same growth conditions, the HA-isolates have the 'notion' that there is sufficient glucose available, while the CA-isolates perceive a shortage in glucose. It thus seems that the HA-isolates are geared towards high glucose consumption while the CA-isolates anticipate glucose deprivation. This may provide the HA- or the CA-isolates with selective advantages depending on the availability of glucose in a particular niche of the human body.

The pentose phosphate pathway and TCA cycle are important pathways to maintain carbon homeostasis, and provide precursors for amino acid biosynthesis [25]. The observed up-regulation of the pentose phosphate pathway of HA-isolates suggests that these isolates are better prepared to regenerate fructose-6-P and glyceraldehyde-3-P to prime glycolysis, which would be in line with the up-regulation of the glycolytic pathway. Consistent with this idea, the HA-MRSA isolates showed a significantly higher level of the Tkt protein.

The TCA cycle and the production of virulence factors are both regulated by CodY [23]. Therefore, alterations in bacterial metabolism can be directly correlated to bacterial survival and virulence [26,27]. Interestingly, the HA-MRSA isolates contained lower levels of the CcpA-regulated TCA cycle enzymes CitB and CitZ than the CA-MRSA isolates. In this respect, it is noteworthy that Somerville *et al.* showed that inactivation of the TCA cycle significantly reduces the production of

several important virulence factors, such as  $\alpha$ - and  $\beta$ -toxins, a glycerol ester hydrolase (lipase), and Sec [27]. Further, especially the lowered CitZ level could lead to the production of higher staphyloxanthin levels and, consequently, improved oxidative stress management. Thus, the hospital-adapted isolates of the USA300 lineage could display enhanced fitness and be less virulent than the original CA-type, which is an idea that matches well with the clinical presentation of infections caused by CA-MRSA. It is also interesting to speculate that this adaptive behaviour relates to higher numbers of frail individuals in the hospital setting compared to the community. In addition, it has been proposed that down-regulation of TCA cycle enzymes could be a consequence of iron starvation [27,28]. Consistent with this idea, the here investigated HA-isolates with relatively low levels of TCA cycle enzymes display increased levels of the Fur-regulated cytoplasmic SbnABCFGH (Supplementary Fig. 2) proteins involved in siderophore-dependent iron uptake. On the other hand, the HA-isolates display relatively low levels of proteins belonging to the IsdABC system for iron acquisition. This would suggest that HA- and CA-isolates preferentially employ different systems for iron acquisition, which might be related to a preference for different sources of iron available in different host niches. However, in this respect, one should bear in mind that molecular iron may also represent a source of oxidative stress through Fenton-related chemistry [29]. Accordingly, the apparently differential regulation of iron acquisition systems could also relate to the evasion of oxidative stress.

Amino acids are used for protein biosynthesis, but they can also be applied as an alternative source of carbon and nitrogen if these essential elements are insufficiently available. Though the RPMI medium used to culture bacteria in the present study is supplemented with all 20 essential amino acids, compared to the HA-isolates, the CA-isolates were found to up-regulate proteins needed in the metabolism of several amino acids, such as glutamate, homoserine, isoleucine, and

lysine. In terms of host adaptation, this may indicate that in their preferred niche the CA-isolates are limited in free amino acids. This is a plausible assumption as CA-isolates are mostly implicated in skin and soft tissue infections.

Previous studies have shown the role of purine biosynthesis in processes that are important for adaptation and fitness. Clearly, purine biosynthesis contributes to the synthesis of DNA and RNA which, in turn, drives the synthesis of proteins. Furthermore, purine contributes to *S. aureus* resistance to lysostaphin [30], fitness and virulence [22]. In the current study, we observed that enzymes contributing to purine metabolism were down-regulated in the HA- isolates compared to the CA-isolates. In relation to purine metabolism, it is noteworthy that the HA-isolates displayed up-regulation of proteins controlled by SigB, because Lan *et al.* [22] and Li *et al.* [31] have shown that limited purine biosynthesis leads to SigB activation. Thus, reduced level of purine biosynthetic proteins in the HA-isolates would be sufficient to explain the observed up-regulation of SigB-dependent proteins in these isolates. Like for the amino acid biosynthetic proteins, also the adjustment of the purine biosynthetic pathway in HA-isolates may reflect their preference for certain niches in the human host where purine is abundantly available. Of note, high purine levels are encountered in blood and our proteome data may thus reflect the fact that HA-MRSA is mostly implicated in invasive diseases, bacteraemia in particular. Importantly, the down-regulation of the purine metabolism in HA-isolates is not only reflected in the levels of purine biosynthetic proteins, but also in the elevated levels of staphyloxanthin, the 'golden' pigment. As shown by Lan *et al.* the up-regulation of staphyloxanthin is one of the consequences of a deficiency in purine biosynthesis [22].

## Conclusion

Altogether, the present analysis of the cytosolic proteome complement of HA- and CA-isolates of the USA300 lineage shows that part of the adaptation of this CA-

lineage to the hospital environment takes place at the level of central carbon metabolism. The specific changes observed match well with the clinical manifestations of the two different groups. CA-MRSA is notorious for skin and soft tissue infections and, accordingly, bacteria belonging to this group need to be prepared for propagation and survival in an environment where glucose, free amino acids, and purines are limiting resources. On the other hand, HA-MRSA has a higher tendency to cause invasive disease and bacteraemia in frail patients, which leads the bacteria to niches where there is potentially a reduced need for them to synthesize their own glucose, amino acids, and purines. These observations spark interest in central carbon metabolism as a key driver for adaptations that streamline MRSA for propagation in the community or the hospital.

## Funding

Funding for this project was received from the Graduate School of Medical Sciences of the University of Groningen [to S.A.M., L.M.P.M., and J.M.v.D.], and the Deutsche Forschungsgemeinschaft Grant GRK1870 [to S.A.M., L.M.P.M., and U.V.]. The funders had no role in study design, data collection and analysis, decision to publish, or preparation of the manuscript.

## Disclosure of Potential Conflicts of Interest

The authors declare that they have no financial and non-financial competing interests in relation to the documented research.

## Acknowledgments

We thank Michael Lalk and Anne Leonard for helpful discussion, and Manuela Gesell-Salazar for critically reading the manuscript.

## References

1. H.F. Wertheim, D.C. Melles, M.C. Vos, W. van Leeuwen, A. van Belkum, H. a Verbrugh, J.L. Nouwen, The role of nasal carriage in *Staphylococcus aureus* infections, *Lancet Infect. Dis.* 5 (2005) 751–762.
2. U. Mäder, P. Nicolas, M. Depke, J. Pané-Farré, M. Debarbouille, M.M. van der Kooi-Pol, C. Guérin, S. Dérozier, A. Hiron, H. Jarmer, A. Leduc, S. Michalik, E. Reilman, M. Schaffer, F. Schmidt, P. Bessières, P. Noirot, M. Hecker, T. Msadek, U. Völker, J.M. van Dijl, *Staphylococcus aureus* Transcriptome Architecture: From Laboratory to Infection-Mimicking Conditions, *PLOS Genet.* 12 (2016) e1005962.
3. M. Hecker, U. Mäder, U. Völker, From the genome sequence via the proteome to cell physiology - Pathoproteomics and pathophysiology of *Staphylococcus aureus*, *Int. J. Med. Microbiol.* 308 (2018) 545-557.
4. P. François, A. Scherl, D. Hochstrasser, J. Schrenzel, Proteomic approaches to study *Staphylococcus aureus* pathogenesis, *J. Proteomics.* 73 (2010) 701–708.
5. C. Kong, H.M. Neoh, S. Nathan, Targeting *Staphylococcus aureus* toxins: A potential form of anti-virulence therapy, *Toxins (Basel).* 8 (2016) E72.
6. M. Otto, *Staphylococcus aureus* toxins, *Curr. Opin. Microbiol.* 17 (2014) 32–37.
7. D. Ribet, P. Cossart, How bacterial pathogens colonize their hosts and invade deeper tissues, *Microbes Infect.* 17 (2015) 173–183.
8. M.F.Q. Kluytmans-Vandenbergh, J.A.J.W. Kluytmans, Community-acquired methicillin-resistant *Staphylococcus aureus*: current perspectives., *Clin. Microbiol. Infect.* 12 Suppl 1 (2006) 9–15.
9. J.M. Buck, K. Como-Sabetti, K.H. Harriman, R.N. Danila, D.J. Boxrud, A. Glennen, R. Lynfield, Community-associated methicillin-resistant *Staphylococcus aureus*, Minnesota, 2000-2003, *Emerg.Infect.Dis.* 11 (2005) 1532–1538.
10. S.A. Mekonnen, L.M. Palma Medina, C. Glasner, E. Tsompanidou, A. de Jong, S. Grasso, M. Schaffer, U. Mäder, A.R. Larsen, H. Gumpert, H. Westh, U. Völker, A. Otto, D. Becher, J.M. van Dijl, Signatures of cytoplasmic proteins in the exoproteome distinguish community- and hospital-associated methicillin-resistant *Staphylococcus aureus* USA300 lineages, *Virulence.* 8 (2017) 891-907.

11. C.R. Halsey, S. Lei, J.K. Wax, M.K. Lehman, A.S. Nuxoll, L. Steinke, M. Sadykov, R. Powers, P.D. Fey, Amino acid catabolism in *Staphylococcus aureus* and the function of carbon catabolite repression, *MBio*. 8 (2017) e01434-16.
12. A.R. Larsen, M. Stegger, S. Böcher, M. Sørnum, D.L. Monnet, R.L. Skov, Emergence and characterization of community-associated methicillin-resistant *Staphylococcus aureus* infections in denmark, 1999 to 2006, *J. Clin. Microbiol.* 47 (2009) 73–78.
13. A.R. Larsen, R. Goering, M. Stegger, J.A. Lindsay, K.A. Gould, J. Hinds, M. Sørnum, H. Westh, K. Boye, R. Skov, Two distinct clones of methicillin-resistant *Staphylococcus aureus* (MRSA) with the same USA300 pulsed-field gel electrophoresis profile: A potential pitfall for identification of USA300 community-associated MRSA, *J. Clin. Microbiol.* 47 (2009) 3765–3768.
14. R. Bruderer, O.M. Bernhardt, T. Gandhi, S.M. Miladinović, L.-Y. Cheng, S. Messner, T. Ehrenberger, V. Zanotelli, Y. Butscheid, C. Escher, O. Vitek, O. Rinner, L. Reiter, Extending the Limits of Quantitative Proteome Profiling with Data-Independent Acquisition and Application to Acetaminophen-Treated Three-Dimensional Liver Microtissues, *Mol. Cell. Proteomics*. 14 (2015) 1400–1410.
15. S. Michalik, M. Depke, A. Murr, M. Gesell Salazar, U. Kusebauch, Z. Sun, T.C. Meyer, K. Surmann, H. Pförtner, P. Hildebrandt, S. Weiss, L.M. Palma Medina, M. Gutjahr, E. Hammer, D. Becher, T. Pribyl, S. Hammerschmidt, E.W. Deutsch, S.L. Bader, M. Hecker, R.L. Moritz, U. Mäder, U. Völker, F. Schmidt, A global *Staphylococcus aureus* proteome resource applied to the *in vivo* characterization of host-pathogen interactions, *Sci. Rep.* 7 (2017) 9718.
16. J. Cox, N. Neuhauser, A. Michalski, R.A. Scheltema, J. V. Olsen, M. Mann, Andromeda: A peptide search engine integrated into the MaxQuant environment, *J. Proteome Res.* 10 (2011) 1794–1805.
17. S. Fuchs, H. Mehlan, J. Bernhardt, A. Hennig, S. Michalik, K. Surmann, J. Pané-Farré, A. Giese, S. Weiss, L. Backert, A. Herbig, K. Nieselt, M. Hecker, U. Völker, U. Mäder, AureoWiki - The repository of the *Staphylococcus aureus* research and annotation community, *Int. J. Med. Microbiol.* 308 (2017) 558-568.
18. J. Bernhardt, S. Funke, M. Hecker, J. Siebourg, Visualizing gene expression data via voronoi treemaps, in: 6th Int. Symp. Vor. Diagrams Sci. Eng. ISVD 2009, 2009: pp. 233–241.

19. K. Morikawa, a Maruyama, Y. Inose, M. Higashide, H. Hayashi, T. Ohta, Overexpression of sigma factor, sigma(B), urges *Staphylococcus aureus* to thicken the cell wall and to resist beta-lactams., *Biochem. Biophys. Res. Commun.* 288 (2001) 385–389.
20. A. Pelz, K.P. Wieland, K. Putzbach, P. Hentschel, K. Albert, F. Götz, Structure and biosynthesis of staphyloxanthin from *Staphylococcus aureus*, *J. Biol. Chem.* 280 (2005) 32493–32498.
21. S. Katzif, E.H. Lee, A.B. Law, Y.L. Tzeng, W.M. Shafer, CspA regulates pigment production in *Staphylococcus aureus* through a SigB-dependent mechanism, *J. Bacteriol.* 187 (2005) 8181–8184.
22. L. Lan, A. Cheng, P.M. Dunman, D. Missiakas, C. He, Golden pigment production and virulence gene expression are affected by metabolisms in *Staphylococcus aureus*, *J. Bacteriol.* 192 (2010) 3068–3077.
23. G.A. Somerville, R.A. Proctor, At the Crossroads of Bacterial Metabolism and Virulence Factor Synthesis in Staphylococci, *Microbiol. Mol. Biol. Rev.* 73 (2009) 233–248.
24. M. Liebeke, H. Meyer, S. Donat, K. Ohlsen, M. Lalk, A metabolomic view of *Staphylococcus aureus* and its ser/thr kinase and phosphatase deletion mutants: Involvement in cell wall biosynthesis, *Chem. Biol.* 17 (2010) 820–830.
25. A. Stincone, A. Prigione, T. Cramer, M.M.C. Wamelink, K. Campbell, E. Cheung, V. Olin-Sandoval, N.M. Grüning, A. Krüger, M. Tauqeer Alam, M.A. Keller, M. Breitenbach, K.M. Brindle, J.D. Rabinowitz, M. Ralser, The return of metabolism: Biochemistry and physiology of the pentose phosphate pathway, *Biol. Rev.* 90 (2015) 927–963.
26. C. Massilamany, A. Gangaplara, D.J. Gardner, J.M. Musser, D. Steffen, G.A. Somerville, J. Reddy, TCA cycle inactivation in *Staphylococcus aureus* alters nitric oxide production in RAW 264.7 cells, *Mol. Cell. Biochem.* 355 (2011) 75–82.
27. G.A. Somerville, M.S. Chaussee, C.I. Morgan, J.R. Fitzgerald, D.W. Dorward, L.J. Reitzer, J.M. Musser, *Staphylococcus aureus* aconitase inactivation unexpectedly inhibits post-exponential-phase growth and enhances stationary-phase survival, *Infect. Immun.* 70 (2002) 6373–6382.

28. D.B. Friedman, D.L. Stauff, G. Pishchany, C.W. Whitwell, V.J. Torres, E.P. Skaar, *Staphylococcus aureus* redirects central metabolism to increase iron availability, *PLoS Pathog.* 2 (2006) 0777–0789.
29. R. Gaupp, N. Ledala, G.A. Somerville, Staphylococcal response to oxidative stress, *Front. Cell. Infect. Microbiol.* 2 (2012) 33.
30. A. Gründling, D.M. Missiakas, O. Schneewind, *Staphylococcus aureus* mutants with increased lysostaphin resistance, *J. Bacteriol.* 188 (2006) 6286–6297.
31. L. Li, W. Abdelhady, N.P. Donegan, K. Seidl, A. Cheung, Y.-F. Zhou, M.R. Yeaman, A.S. Bayer, Y.Q. Xiong, Role of Purine Biosynthesis in Persistent Methicillin-Resistant *Staphylococcus aureus* (MRSA) Infection, *J. Infect. Dis.* 218 (2018) 1367-1377.





## Chapter 6

### **Summary and future perspectives**

---



*Staphylococcus aureus* is one of the commonly encountered bacteria of the human microbiome. Although mostly a seemingly harmless commensal microbe, *S. aureus* can act as an invasive pathogen with seriously devastating effects on its host's health and wellbeing. A wide range of infections caused by this bacterium has been reported to affect diverse parts of the human body, including the skin, soft tissues and bones, as well as important organs like the heart, kidneys and lungs. Particularly, *S. aureus* is infamous for being a major causative agent of respiratory tract infections that may escalate up to necrotizing pneumonia. Due to its clinical relevance, this pathogen has been intensively studied for many years. Nonetheless, further research in this field is still needed, because of the high capacity of *S. aureus* to evolve drug resistance, its high genomic plasticity and adaptability and, not in the last place, the plethora of niches within the human body where it can thrive and survive. In this regard, there are still many uncertainties concerning the specific adaptations carried out by *S. aureus* during colonization and infection of the human body, the transition between both stages, and upon the invasion of different types of host cells. To shed more light on some of these adaptations, the research described in this thesis has employed *in vitro* models of infection that mimic particular conditions during the infectious process with special focus on the lung epithelium. The adaptations displayed by *S. aureus* were monitored using advanced proteomics. Furthermore, the analyses documented in this thesis included *S. aureus* strains with diverse backgrounds and epidemiology to take into account the genetic diversity encountered in this species.

A general introduction to the current status of the field is presented in **chapter 1**, which highlights the genomic plasticity of *S. aureus* and its capability to optimally regulate its gene expression for propagation and survival in the challenging ecological niches of the human body. Of note, the genomic variability of *S. aureus* is based on its capability to acquire mobile genetic elements, which often carry

genes granting antibiotic resistances and encoding virulence factors. In particular, chapter 1 showcases the virulence factors and regulatory mechanisms employed by *S. aureus* to conquer and corrupt the cells, tissues and immune defenses of the human host. Additionally, the distinction between community- and hospital-acquired Methicillin resistant *S. aureus* (CA- and HA-MRSA) is introduced.

The adaptive behavior of *S. aureus* during infection in specific niches of the human body is still not completely understood, and this applies particularly to its intracellular residence over extended periods of time. For this reason, the research described in **chapter 2** was undertaken with a focus on the dynamic relationship between *S. aureus* and lung epithelial cells. Over 4 days post internalization the proteomes of host cells and the invading pathogen were monitored, revealing a continuous bidirectional interaction. Of note, during the infection, two subpopulations of *S. aureus* displaying differential rates of replication and intracellular localization were observed. A replicating subpopulation was more abundant during the first 24 h of infection, remained enclosed in vesicles, and displayed a rapid increase in numbers, which culminated in the lysis of the host cells. The proteomics analyses illustrated that this lytic event was an apoptotic reaction, most likely caused by the presence of the pathogen intracellularly. The other subpopulation of internalized *S. aureus*, which displayed a dormant phenotype, was found to reside predominantly in the host cytosol. By the end of the experimental time window of four days, the presence of this dormant *S. aureus* population correlated with the expression of inflammatory host proteins. Furthermore, the simultaneous proteomic inspection of host and pathogen revealed a continuous interplay at the metabolic level, which potentially determines the outcome of the infection. In this regard, the pathogen was found to regulate expression of proteins related to an exposure to nutrient- and oxygen-deprived environments. For example, the presumably microaerobic intracellular conditions triggered an increase in the production of proteins related to

fermentation. Further significant changes involved the central carbon metabolism, where an increase in proteins related to the TCA cycle and amino acid degradation was observed. These proteomic changes relating to metabolic pathways reflect the pathogen's efforts to optimize energy production from alternative carbon and nitrogen sources. Moreover, the presumptive depletion of amino acids by the pathogen will have an impact on the host metabolism, in particular the arginine and asparagine biosynthetic pathways, as previously reported (1). Importantly, the investigations detailed in chapter 2 show that also other amino acid metabolic pathways may have an impact on host-pathogen interactions, especially those for proline, glutamate and alanine. Taken together, the documented results highlight the interplay between host and pathogen at the metabolic level and their reciprocal adaptations. Ultimately, the host cells that survived the infection carried a non-replicating persistent population of *S. aureus* in their cytoplasm. These findings show that the final outcome of an intracellular *S. aureus* infection is not only determined by the production of virulence factors, but also by the usage of intracellular resources, and the subsequent metabolic adaptations by the host and its intracellular bacteria.

The analyses described in chapter 2 do not consider the potential variations occurring when there is an underlying disease condition. For this reason, the implemented lung epithelial model was adapted to represent two regenerative stages of the lung epithelium, namely the initial stage of migration and repair, and the subsequent stage of fibrogenesis. As described in **chapter 3**, the results from this study demonstrated that initial stages in the regeneration of the host epithelium have a significant impact on the infection dynamics. The low polarization level observed during the migratory state of the epithelial cells permitted higher internalization and intracellular replication rates of *S. aureus*, which led to reduced host cell survival. In contrast, the fibrogenesis stage displayed a strengthening of the tight junctions, thereby reducing internalization

of the pathogen and leading to low bacterial replication rates upon internalization. Regardless of the differences observed for these two infection settings, the adaptations of the bacterial proteomes to the intracellular conditions were found to be very similar. Nevertheless, differences were detected for *S. aureus* proteins regulated by the Rex regulon. Rex senses imbalances in the redox state of the bacteria, which could be caused by the levels of available oxygen, activation of the TCA cycle, or an abundance of NO. Further analyses showed that only the NO levels were different between the two infection settings, and that this was a consequence of the overproduction of the NO synthetase of *S. aureus*, a phenotype that can be correlated with high colonization rates (2). These observations imply a NO-dependent modulation of the bacterial cytoplasmic redox state to maintain homeostasis prior to internalization. Altogether, the studies described in chapter 3 provide a deeper insight into how *S. aureus* takes advantage of a breached epithelial barrier, and how infected epithelial cells have a limited ability to respond adequately to staphylococcal insults.

To expand the analysis of *S. aureus* adaptability to the host environment, the last two experimental chapters of this thesis address MRSA isolates from different epidemiological backgrounds. **Chapter 4** documents genomics and proteomics analyses to characterize and differentiate two groups of 6 isolates each, representing CA- and HA-MRSA variants of the *S. aureus* USA300 lineage collected in Denmark (DK). Additionally, this study included three *S. aureus* HA isolates from the Dutch-German border region (NL-DE) as benchmark. At the genetic level, the core genome of CA<sup>DK</sup>-isolates presented more similarity to HA<sup>NL-DE</sup>-isolates, while the accessory genome presented more similarities between the HA<sup>DK</sup> and HA<sup>NL-DE</sup>-isolates. At the exoproteome level, however, most identified proteins were shared among all groups. Nonetheless, differences were found in the amounts of proteins expressed by the different groups and in group-specific proteins. The vast majority of such differences was found to involve secreted

proteins with a predicted cytoplasmic localization, now referred to as extracellular cytoplasmic proteins or ECP (3). Most likely, at least some of these proteins have a moonlighting nature, serving not only their well-defined functions in the bacterial cytoplasm, but also extracellular functions in the colonization and infection of the host. Interestingly, a higher abundance of such proteins was observed for CA-isolates during the exponential growth phase and for HA-isolates during the stationary phase. This difference might be related to differential timing of ECP secretion events in the two epidemiologically distinct groups. Lastly, a comparison of exoproteome abundance signatures showed that, regardless of the distinct geographical origin of the investigated isolates, the two HA-groups cluster together. Subsequent internalization experiments using lung epithelial cells mirrored the clustering based on the exoproteome analyses. These findings focus special attention on possible roles of 'liberated' ECPs in the epidemiology and intracellular survival of CA- and HA-MRSA isolates. ECPs were already invoked in the virulence of *S. aureus*, but a possible role in the epidemiology of MRSA is new. Further, this study implies that proteomics could become a useful tool for characterizing *S. aureus* isolates and predicting their epidemiological behavior.

As concluded in chapter 2, metabolic adaptations of isolates play an important role as drivers of virulence. Accordingly, **chapter 5** presents an extended analysis of a subset of the clinical HA- and CA-MRSA isolates from Denmark investigated in the studies described in chapter 4. The cytosolic proteomes of this subset displayed significant differences between the two groups of isolates. The CA-MRSA group presented higher amounts of proteins related to the TCA cycle, amino acid metabolism and gluconeogenesis. This disposition of the CA-isolates towards these pathways underlines their preparedness to encounter nutrient-deficient environments, consistent with their clinical presentation in skin and soft tissue infections. Conversely, the HA-isolates displayed higher levels of proteins related to glycolysis, and the pentose phosphate pathway and lower levels of



proteins belonging to the purine biosynthetic pathway. This indicates that the HA-isolates may prefer niches with abundant resources, such as blood. Altogether, these observations support the view that adaptations in central carbon metabolism are key drivers that streamline the investigated MRSA isolates for infection of healthy individuals in the community or frail patients in the hospital.

In conclusion, the studies detailed in this dissertation highlight the importance of staphylococcal metabolism and fitness as pertinent drivers of virulence. Although metabolic pathways are frequently ignored in infection research, in fact, they influence the capability of *S. aureus* isolates to thrive and survive in a plethora of different host environments. Moreover, across the different studies presented in the current thesis, proteomics proved to be an invaluable tool to explore the adaptations of both *S. aureus* and its host during infection conditions, and to deepen our understanding of the differences among CA- and HA-MRSA isolates. The primary characterization of the investigated CA- and HA-MRSA isolates on a proteome level was based on cultures in RPMI medium, which represents a condition that mimics nutrient supply during blood stream infections (4). Nonetheless, this setting lacks the presence of human host cells, and it will therefore be of interest to continue the characterization of MRSA isolates with different epidemiological backgrounds by using infection models that are even more realistic representations of infection, such as the lung epithelial cell model used for the studies described in chapters 2 and 3 of this dissertation. Moreover, the human immune system comprises several types of cells and defense mechanisms that *S. aureus* must evade or eliminate in the course of an infection. Therefore, further studies should also consider models that include a more complex representation of the host, for example by the inclusion of both epithelial and immune cells in the infection model. Such multi-cell type infection models are likely to play increasingly prominent roles in infection research in the years to come, and they will provide us with a deeper understanding of the complex

networks of interactions between the human host and commensal pathogens like *S. aureus*.

## References

1. Ren, W., Rajendran, R., Zhao, Y., Tan, B., Wu, G., Bazer, F. W., Zhu, G., Peng, Y., Huang, X., Deng, J., and Yin, Y. (2018) Amino Acids As Mediators of Metabolic Cross Talk between Host and Pathogen. *Front. Immunol.* 9, 319
2. Kinkel, T. L., Ramos-Montañez, S., Pando, J. M., Tadeo, D. V., Strom, E. N., Libby, S. J., and Fang, F. C. (2016) An Essential Role for Bacterial Nitric Oxide Synthase in *Staphylococcus aureus* Electron Transfer and Colonisation. *Nat. Microbiol.* 2, 16224
3. Ebner, P., and Götz, F. (2019) Bacterial Excretion of Cytoplasmic Proteins (ECP): Occurrence, Mechanism, and Function. *Trends Microbiol.* 27, 176–187
4. Mäder, U., Nicolas, P., Depke, M., Pané-Farré, J., Debarbouille, M., Kooi-Pol, M. M. van der, Guérin, C., Dérozier, S., Hiron, A., Jarmer, H., Leduc, A., Michalik, S., Reilman, E., Schaffer, M., Schmidt, F., Bessières, P., Noirot, P., Hecker, M., Msadek, T., Völker, U., and Dijk, J. M. van (2016) *Staphylococcus aureus* Transcriptome Architecture: From Laboratory to Infection-Mimicking Conditions. *PLOS Genet.* 12, e1005962



## Chapter 7

### **Nederlandse samenvatting**

---



*Staphylococcus aureus* is een bacterie die regelmatig aangetroffen wordt in het microbioom van de mens. Hoewel *S. aureus* zich overwegend als een onschuldige commensaal gedraagt kan hij zich ook manifesteren als een invasieve ziekteverwekker die een desastreus effect heeft op de gezondheid van zijn gastheer. Infecties veroorzaakt door *S. aureus* kunnen zich vrijwel overal op en in ons lichaam voordoen. Zo kunnen niet alleen de huid, zachte weefsels en onze botten door deze bacterie aangetast worden, maar ook belangrijke organen zoals het hart, de nieren en de longen. *S. aureus* is met name een beruchte veroorzaker van luchtweginfecties die kunnen escaleren tot een zogenaamde necrotiserende pneumonie die veelal fataal is voor de getroffen patiënt. Vanwege deze klinische relevantie wordt *S. aureus* al sinds vele jaren bestudeerd. Desondanks is onderzoek naar deze gevaarlijke ziekteverwekker nog steeds nodig, met name omdat hij snel resistent wordt tegen antibiotica, zich gemakkelijk aanpast aan nieuwe omstandigheden en omdat hij zich op veel plekken in ons lichaam kan verstoppen. Zo is er nog erg veel onduidelijkheid over de specifieke adaptaties die *S. aureus* in staat stellen het menselijke lichaam te koloniseren, te infecteren en zich aansluitend zelfs te verbergen binnen in onze eigen cellen. Om dergelijke aanpassingen beter te kunnen begrijpen werd bij het onderhavige promotie-onderzoek gebruik gemaakt van infectiemodellen, waarbij de condities in ons lichaam zo nauwgetrouw mogelijk werden nagebootst in een experimentele setting. Hierbij werd de aandacht met name gelegd op infectie van het long-epitheel. De aanpassingen die *S. aureus* onder dergelijke infectie-simulerende condities laat zien werden bestudeerd met behulp van geavanceerde proteomics-technieken. Daarnaast werd gebruik gemaakt van *S. aureus* stammen die geïsoleerd zijn op verschillende geografische locaties en die een voorkeur vertonen voor het veroorzaken van infecties in zwakke patiënten in een ziekenhuis of in gezonde individuen. Hiermee werd recht gedaan aan de

genetische diversiteit en het uiteenlopende epidemiologische gedrag van de bacteriesoort *S. aureus*.

In **hoofdstuk 1** van dit proefschrift wordt het onderhavige onderzoek geïntroduceerd met een overzicht van de mechanismen die *S. aureus* inzet om zich aan te passen aan veranderende omstandigheden binnen en buiten het menselijke lichaam. Dit gebeurt niet alleen door regulatie van de gen-expressie, maar ook door het verwerven van 'nieuwe' genen die bijvoorbeeld coderen voor antibioticumresistentie of voor zogenaamde virulentiefactoren. Deze virulentiefactoren zijn veelal eiwitten, waarvan de bacterie gebruik maakt om onze weefsels en cellen te koloniseren, binnen te dringen en te corrumperen, of om ons afweersysteem te ontwijken en uit te schakelen. In hoofdstuk 1 worden tevens de verschillen tussen de *S. aureus* varianten die in ziekenhuizen gevonden worden, ook bekend als 'hospital-associated' ofwel 'HA-*S. aureus*', en de varianten die overwegend bij gezonde personen ziekte veroorzaken en die bekend staan als 'community-associated' ofwel 'CA-*S. aureus*' uiteengezet.

Het onderzoek beschreven in **hoofdstuk 2** werd uitgevoerd om beter te begrijpen welke aanpassingen *S. aureus* ondergaat gedurende het verblijf van deze bacterie in het binnenste van onze cellen, met name het long-epitheel. Hiertoe werden gedurende een periode van vier dagen de proteomen van de gastheercellen en de binnengedrongen ziekteverwekkers simultaan bestudeerd. Dit bracht een sterke wisselwerking tussen de bacteriën en de gastheercellen aan het licht. Opvallend was dat in de longepitheelcellen twee *S. aureus* subpopulaties aangetoond konden worden. Enerzijds was er een snel groeiende subpopulatie gedurende de eerste 24 uur na de start van de infectie detecteerbaar. Deze populatie was prominent aanwezig, maar bleef geëncapsuleerd in membraanvesicles van de gastheercellen. Uiteindelijk veroorzaakte deze subpopulatie van de bacteriën lysis van de gastheercel. De proteoomanalyses lieten duidelijk zien, dat de gastheercel-lysis het

gevolg was van een apoptotische reactie die getriggered werd door de intracellulaire ziekteverwekker. De andere sub-populatie van geïnternaliseerde *S. aureus* bacteriën verkeerde in een soort slaapstand en bevond zich voornamelijk in het cytoplasma van de gastheercellen. Vier dagen na aanvang van de infectie viel de aanwezigheid van deze slapende *S. aureus* subpopulatie samen met de expressie van ontstekings-gerelateerde gastheereiwitten. Een belangrijke conclusie die uit dit onderzoek getrokken kan worden is dat de gastheer en de geïnternaliseerde ziekteverwekker continu hun metabolisme aanpassen aan de klaarblijkelijk veranderende omstandigheden binnen in de gastheer cel. De richting waarin deze aanpassingen plaatsvinden is bepalend voor de uitkomst van de infectie. *S. aureus* bleek vooral de expressie van eiwitten aan te passen die nodig zijn om te overleven in milieus waar voedsel en zuurstof in beperkte mate aanwezig zijn. De lage zuurstofspanning in de gastheercellen was bijvoorbeeld aanleiding voor de bacterie om vooral eiwitten aan te maken die nodig zijn voor fermentatieve groei. Andere significante aanpassingen betroffen het centrale koolstofmetabolisme, waarbij een toename van eiwitten betrokken bij de citroenzuurcyclus en aminozuuraafbraak waargenomen werd. Deze aanpassingen reflecteren de inspanningen van *S. aureus* om energie te genereren uit alternatieve koolstof- en stikstof-bronnen. Daarnaast zal het vermoede verbruik van aminozuren van invloed zijn op het metabolisme van de gastheer cel, met name de biosynthetische routes voor arginine en asparagine (1). Het onderzoek beschreven in hoofdstuk 2 laat echter ook zien dat het metabolisme voor andere aminozuren, met name proline, glutamaat en alanine ook een rol kan spelen tijdens intracellulaire infectie. Alles tezamen beschouwd maken de beschreven experimenten een dynamische metabole wisselwerking tussen bacterie- en gastheercellen zichtbaar. De gastheercellen die de infectie overleven dragen een niet-replicerende populatie van persistente *S. aureus* bacteriën in hun cytoplasma. Deze waarnemingen laten duidelijk zien, dat de uiteindelijke uitkomst van een



intracellulaire *S. aureus* infectie niet alleen bepaald wordt door de productie van virulentiefactoren, maar ook door de manier waarop intracellulair aanwezige nutriënten benut en uitgeput worden. De uitputting van nutriënten geeft vervolgens weer aanleiding tot verdere metabole adaptaties bij zowel de gastheer als de intracellulaire bacteriën.

De analyses beschreven in hoofdstuk 2 houden geen rekening met de mogelijke variaties die zich kunnen voordoen in geval van andere aandoeningen voorafgaand aan de infectie. Daarom werd het longepitheel-infectiemodel zodanig aangepast, dat het twee regeneratieve stadia van beschadigd longepitheel simuleert, te weten het initiële stadium van celmigratie en herstel van de barrière en het vervolgstadium waarbij fibrogenese optreedt. De resultaten die op grond van deze aanpassingen in het infectiemodel verkregen werden zijn beschreven in **hoofdstuk 3**. Ze laten zien, dat de initiële stadia van barrièreherstel bepalend zijn voor het verdere verloop van de infectie. Het geringe polarisatieniveau van het longepitheel tijdens de fase van epitheelcelmigratie gaf aanleiding tot internalisatie van grotere aantallen bacteriën en snelle replicatie van de geïnternaliseerde bacteriën, hetgeen de overlevingskansen van de geïnfecteerde gastheercellen aanzienlijk verlaagde. In het stadium van fibrinogese was de internalisatie van bacteriën veel geringer wat te verklaren is door de vorming van een 'zonula occludens' (zogenaamde 'tight junctions' in het Engels), waarbij de membranen van de longepitheelcellen samenkomen en een barrière vormen. Ongeacht de verschillen in de twee infectie-scenario's, bleken de aanpassingen in het proteoom van de bacteriën na internalisatie grotendeels overeen te komen. De belangrijkste verschillen werden waargenomen voor eiwitten die deel uit maken van het zogenaamde Rex-regulon. Rex is een sensor die veranderingen in de interne redoxpotentiaal van de bacterie meet die veroorzaakt kunnen worden door veranderingen in de zuurstofspanning, activatie van de citroenzuurcyclus of een verhoogde concentratie van stikstofmonoxide (NO). Nader onderzoek liet zien dat

de NO-niveaus inderdaad verschilden in de beide infectie-scenarios en dat dit het gevolg was van overproductie van de NO-synthase van *S. aureus*. Dit fenotype is reeds eerder als kenmerk van *S. aureus* beschreven tijdens de kolonisatie van gastheerweefsels (2). Deze waarnemingen impliceren dat *S. aureus* de redox-staat van zijn cytoplasma moduleert met behulp van NO om de homeostase te garanderen voorafgaand aan internalisatie door gastheercellen. Tezamen verschaffen de resultaten beschreven in hoofdstuk 3 een beter inzicht in de manier waarop *S. aureus* op slinkse wijze misbruik maakt van beschadigd longepitheel en hoe de geïnfecteerde epitheelcellen slechts weinig adequaat hierop kunnen reageren.

Om een dieper inzicht te krijgen in het vermogen van *S. aureus* om zich aan te passen aan andere milieus werd het onderzoek beschreven in de laatste twee experimentele hoofdstukken van dit proefschrift gewijd aan meticilline-resistente *S. aureus* (MRSA) isolaten met een verschillende epidemiologische achtergrond. **Hoofdstuk 4** beschrijft de genom- en proteoomanalyse van zes CA- en zes HA-MRSA-isolaten die behoren tot de *S. aureus* USA300 lijn en allemaal van patiënten in Denemarken (DK) afkomstig zijn. Tevens werden drie *S. aureus* HA-isolates uit het Nederlands-Duitse grensgebied (NL-DE) als controle in het onderzoek meegenomen. Bij vergelijking van het kerngenoom van al deze isolaten vertoonden de CA<sup>DK</sup>-isolaten meer gelijkenis met de HA<sup>NL-DE</sup>-isolaten, terwijl het variabele gedeelte van het genoom meer overeenkomsten tussen de HA<sup>DK</sup>- en de HA<sup>NL-DE</sup>-isolaten liet zien. Bij de analyse van het exoproteoom bleek, dat de meeste uitgescheiden eiwitten van de drie groepen overeenkwamen. Er werden desalniettemin heel duidelijke verschillen waargenomen in de hoeveelheden van deze uitgescheiden eiwitten en er bleken ook groep-specifieke eiwitten te zijn. Een opmerkelijke bevinding was dat de meeste uitgescheiden eiwitten op grond van hun eigenschappen en bekende functie eigenlijk in het cytoplasma van de bacteriën gelokaliseerd zouden moeten zijn en niet in het extracellulaire milieu.

Dergelijke eiwitten worden tegenwoordig vaak extracellulaire cytoplasmatische eiwitten of ECPs genoemd (3). Waarschijnlijk heeft een aantal van deze eiwitten een zogenaamde ‘moonlighting’ functie. Dit wil zeggen dat ECPs naast hun bekende en goed-gekaracteriseerde functie in het cytoplasma nog een tweede functie buiten de bacteriecel vervullen, bijvoorbeeld in de kolonisatie en infectie van de gastheer. Dergelijke eiwitten werden in grotere hoeveelheden door de CA-isolaten in de exponentiële groeifase uitgescheiden, terwijl dit voor de HA-isolaten het geval was tijdens de stationaire groeifase. Dit verschil duidt er op, dat er een verschil in de timing van ECP secretie is in de CA- en HA-isolaten. Tenslotte liet een vergelijking van de exoproteoom-abundantie-signaturen zien dat, onafhankelijk van de geografische oorsprong van de onderzochte isolaten, de twee groepen van HA-isolaten een cluster vormen die verschilt van het cluster dat gevormd wordt door de CA-isolaten. Deze verschillen werden weerspiegeld in de resultaten van een experiment, waarbij de internalisatie van de diverse isolaten in longepitheelcellen werd onderzocht. In dit geval vertoonden de CA-isolaten intracellulaire groei, terwijl de HA-isolaten dit niet deden. Deze bevindingen suggereren dat de ECPs mogelijk bepalend zijn voor het verschil in de epidemiologie van de onderzochte isolaten en hun intracellulaire groei en overleving. ECPs waren al eerder geassocieerd met de virulentie van MRSA-isolaten, maar een mogelijke rol van ECPs in de epidemiologie van MRSA is een compleet nieuwe bevinding. De resultaten beschreven in hoofdstuk 4 laten verder zien, dat proteoomanalyses een geschikt hulpmiddel kunnen vormen bij de karakterisatie van *S. aureus* isolaten en het voorspellen van hun epidemiologische gedrag.

In hoofdstuk 2 werd reeds geconcludeerd dat metabole aanpassingen een sturende rol kunnen hebben in het vermogen van *S. aureus* om ziekte te veroorzaken. **Hoofdstuk 5** beschrijft een uitgebreide analyse van een subset van de klinische HA- en CA-MRSA isolaten uit Denemarken die in hoofdstuk 4

geïntroduceerd zijn. Het cellulaire proteoom van deze isolaten liet, net als het exoproteoom, aanzienlijke verschillen zien die specifiek waren voor de HA- en CA-MRSA-isolaten. In de CA-MRSA-groep werden hogere hoeveelheden aangetroffen van eiwitten die betrokken zijn bij de citroenzuurcyclus, het aminozuurmetabolisme en de gluconeogenese. De voorprogrammering van de CA-isolaten voor gebruik van deze metabole routes suggereert, dat ze ingesteld zijn op voedselarme milieus. Dit is in overeenstemming met het gegeven, dat deze isolaten veelal betrokken zijn bij infecties van de huid en zachte weefsels die relatief voedselarm zijn. Omgekeerd werden in de HA-isolaten grotere hoeveelheden van eiwitten gevonden die een rol spelen bij de glycolyse en de pentosefosfaatroute en lagere hoeveelheden van eiwitten die betrokken zijn bij de biosynthese van purines. Dit suggereert dat de HA-isolaten een voorkeur hebben voor voedselrijke niches, zoals ons bloed. Tezamen ondersteunen deze waarnemingen het idee, dat aanpassingen in het centrale koolstofmetabolisme de onderzochte MRSA-isolaten optimaal geschikt maken voor het veroorzaken van infecties in zwakke patiënten in een ziekenhuisomgeving of in de gemeenschap van gezonde individuen.

Alle resultaten beschreven in dit proefschrift tezamen onderstrepen het idee, dat het metabolisme een sleutelrol speelt bij de virulentie van de *S. aureus* bacterie. Tot dusver werd de rol van metabole routes eigenlijk stelselmatig onderschat in infectie-gerelateerd onderzoek, maar op grond van de onderhavige studies moet geconcludeerd worden, dat ze eigenlijk een sleutelrol spelen bij het vermogen van *S. aureus* om te groeien en te overleven in de verschillende niches van het menselijke lichaam. Tevens kan geconcludeerd worden, dat proteomics een waardevolle benadering is om de aanpassingen van *S. aureus* en zijn humane gastheer onder infectie-condities in kaart te brengen en om onze kennis over de verschillen tussen CA- en HA-MRSA-isolaten te verdiepen. De hier beschreven karakterisering van CA- en HA-MRSA-isolaten op proteoom-niveau was

gebaseerd op cultures in het zogenaamde RPMI medium, dat de condities nabootst die *S. aureus* ondervindt gedurende bloedbaaninfecties (4). In deze setting ontbreken echter de humane gastheercellen en het is daarom van belang om in toekomstige studies de MRSA-isolaten met verschillende epidemiologische achtergrond verder te karakteriseren door gebruik te maken van infectiemodellen die de condities van een echte infectie in de mens nog realistischer weergeven. Dit zou bijvoorbeeld kunnen met behulp van het long-epitheel-infectiemodel, zoals beschreven in de hoofdstukken 2 en 3 van dit proefschrift. Het humane immuunsysteem omvat tevens meerdere celtypes en afweermechanismen, waaraan *S. aureus* moet ontsnappen, of die de bacterie moet uitschakelen gedurende het verloop van een infectie. Toekomstige studies zouden daarom ook in staat moeten zijn om een nog completere simulatie van de condities in de gastheer na te bootsen. Dit zou bijvoorbeeld gerealiseerd kunnen worden door de aanwezigheid van zowel epitheelcellen als immuuncellen in één infectiemodel. Dergelijke multi-celtype infectiemodellen zullen zeer waarschijnlijk een prominente rol spelen bij toekomstig onderzoek naar infectieziektes en ze zullen ongetwijfeld leiden tot een beter begrip van de complexe en dynamische interacties tussen de humane gastheer en commensale ziekteverwekkers zoals *S. aureus*.

## Referenties

1. Ren, W., Rajendran, R., Zhao, Y., Tan, B., Wu, G., Bazer, F. W., Zhu, G., Peng, Y., Huang, X., Deng, J., and Yin, Y. (2018) Amino Acids As Mediators of Metabolic Cross Talk between Host and Pathogen. *Front. Immunol.* 9, 319
2. Kinkel, T. L., Ramos-Montañez, S., Pando, J. M., Tadeo, D. V., Strom, E. N., Libby, S. J., and Fang, F. C. (2016) An Essential Role for Bacterial Nitric Oxide Synthase in *Staphylococcus aureus* Electron Transfer and Colonisation. *Nat. Microbiol.* 2, 16224
3. Ebner, P., and Götz, F. (2019) Bacterial Excretion of Cytoplasmic Proteins (ECP): Occurrence, Mechanism, and Function. *Trends Microbiol.* 27, 176–187

4. Mäder, U., Nicolas, P., Depke, M., Pané-Farré, J., Debarbouille, M., Kooi-Pol, M. M. van der, Guérin, C., Dérozier, S., Hiron, A., Jarmer, H., Leduc, A., Michalik, S., Reilman, E., Schaffer, M., Schmidt, F., Bessières, P., Noirot, P., Hecker, M., Msadek, T., Völker, U., and Dijn, J. M. van (2016) *Staphylococcus aureus* Transcriptome Architecture: From Laboratory to Infection-Mimicking Conditions. *PLOS Genet.* 12, e1005962



## Appendices

---





## Biography

Laura Marcela Palma Medina was born on the 27<sup>th</sup> of September 1988 in Ibagué, Colombia. She studied Chemical Engineering at Universidad de los Andes in Bogotá, Colombia from 2006 to 2011, while minoring in Bioengineering. Afterwards, she continued her studies at the same institution and received her master's degree in Engineering in 2012. The topic of her dissertation was the kinetic and bioinformatics characterization of cellulases from a metagenomic library of soil specific to african oil palm empty fruit bunch, a work supervised by Prof. Andrés González-Barrios. Additionally, she carried out an international internship at Texas A&M University in the summer 2011, where she focused on the study of a mutant of *Pseudomonas aeruginosa* PA14 resistant to Gallium due to transposon Tn5 *luxAB*-Tc insertion in *hitABC* operon. This last experience motivated her to pursue, later in life, a PhD in infectious diseases.

After one year working as a research and development engineer in food industry, she moved to Europe in 2014 to start her doctoral studies under the co-supervision of Prof. Jan Maarten van Dijk at the Department of Medical Microbiology at the University Medical Center Groningen and Prof. Uwe Völker at the department of Funcional Genomics in the University Medicine Greifswald. Consequently, she obtained a dual PhD degree from both Universities. Since 2019 she works as post-doctoral researcher at the Karoliska Institute, Sweden in the Center for Infectious Medicine in the research group of Prof. Anna Norrby-Teglund.



## List of publications

### Journal articles (peer reviewed)

1. **L.M. Palma Medina**, A-K. Becker, S. Michalik, P. Hildebrandt, M. Gesell Salazar, K. Surmann, S. A. Mekonnen, L. Kaderali, J. M. van Dijnl, U. Völker. *Distinct adaptive responses of Staphylococcus aureus upon infection of bronchial epithelium during different stages of regeneration*. In preparation for submission.
2. T. Stobernack, **L.M. Palma Medina**, M. du Teil Espina, D. R. Piebenga, A. Otto, T. Sura, D. Becher, A. de Jong, A. J. van Winkelhoff, E. Brouwer, J. Westra, P. Heeringa and J. M. van Dijnl. *Porphyromonas gingivalis and its secreted peptidylarginine deiminase modulate the proteome of human neutrophils and macrophages*. In preparation for submission.
3. S.A. Mekonnen, E. Tsompanidou, A. de Jong, A. Anaya Sánchez, L. Berentsen, E.J.M. Raineri, M. Bispo, **L.M. Palma Medina**, T.K. Prajsnar, A.H. Meijer, A.R. Larsen, H. Westh, A. Reder, U. Mäder, A.W. Friedrich, U. Völker, J.M. van Dijnl. *Prolonged intra-neutrophil survival as an adaptive strategy of Staphylococcus aureus USA300 in the hospital environment*. In preparation for submission.
4. **L.M. Palma Medina**, A.-K. Becker, S. Michalik, H. Yedavally, E.J.M. Raineri, P. Hildebrandt, M. Gesell Salazar, K. Surmann, H. Pförtner, S.A. Mekonnen, A. Salvati, L. Kaderali, J.M. van Dijnl, U. Völker, *Metabolic cross-talk between human bronchial epithelial cells and internalized Staphylococcus aureus as a driver for infection*, Mol. Cell Proteomics. 18 (2019) mcp.RA118.001138.
5. X. Zhao\*, **L.M. Palma Medina\***, T. Stobernack, C. Glasner, A. de Jong, P. Utari, R. Setroikromo, W.J. Quax, A. Otto, D. Becher, G. Buist, J.M. van Dijnl, *Exoproteome heterogeneity among closely related Staphylococcus aureus t437 isolates and possible implications for virulence*, J. Proteome Res. (2019).
6. S.A. Mekonnen\*, **L.M. Palma Medina\***, S. Michalik, M.G. Loreti, M.G. Salazar, J.M. van Dijnl, U. Völker, *Metabolic niche adaptation of community- and hospital-associated methicillin-resistant Staphylococcus aureus*, Journal of Proteomics. 193 (2019) 154–161.
7. T.Stobernack, M.du Teil Espina, L.M. Mulder, **L.M. Palma Medina**, D.R. Piebenga, G.Gabarrini, X.Zhao, K.M.J.Janssen, J.Hulzebos, E.Brouwer,

- T.Sura, D.Becher, A.J.van Winkelhoff, F.Götz, A.Otto, J.Westra, J.M.van Dijn. *A secreted bacterial peptidylarginine deiminase can 'neutralize' human innate immune defense*. MBio. 9(5) (2018) e01704-18.
8. G. Gabarrini, **L.M. Palma Medina**, T. Stoberneck, R.C. Prins, M. du Teil Espina, J. Kuipers, M.A. Chlebowicz, J.W.A. Rossen, A.J. van Winkelhoff, J.M. van Dijn, *There's no place like OM: Vesicular sorting and secretion of the peptidylarginine deiminase of Porphyromonas gingivalis*, Virulence. 9 (2018) 456–464.
  9. S.A. Mekonnen, **L.M. Palma Medina**, C. Glasner, E. Tsompanidou, A. de Jong, S. Grasso, M. Schaffer, U. Mäder, A.R. Larsen, H. Gumpert, H. Westh, U. Völker, A. Otto, D. Becher, J.M. van Dijn. *Signatures of cytoplasmic proteins in the exoproteome distinguish community- and hospital-associated methicillin-resistant Staphylococcus aureus USA300 lineages*, Virulence. 0 (2017) 1–17.
  10. S. Michalik, M. Depke, A. Murr, M. Gesell Salazar, U. Kusebauch, Z. Sun, T.C. Meyer, K. Surmann, H. Pförtner, P. Hildebrandt, S. Weiss, **L.M. Palma Medina**, M. Gutjahr, E. Hammer, D. Becher, T. Pribyl, S. Hammerschmidt, E.W. Deutsch, S.L. Bader, M. Hecker, R.L. Moritz, U. Mäder, U. Völker, F. Schmidt, *A global Staphylococcus aureus proteome resource applied to the in vivo characterization of host-pathogen interactions*, Scientific Reports 7 (2017) 9718
  11. **L.M. Palma Medina\***, D.C. Ardila\*, M.M. Zambrano, S. Restrepo, A.F. Gonzalez Barrios, *In vitro and in silico characterization of metagenomic soil-derived cellulases capable of hydrolyzing oil palm empty fruit bunch*, Biotechnology Reports 15 (2017) 55–62.

## Book Chapters

1. D.C. Ardila Montoya\*, **L.M. Palma Medina\***, M.M. Zambrano, S. Restrepo, A.F. González-Barrios. *Bioprospección de estudios de celulasas en ambientes extremos colombianos*, in: Aprovechamiento de biomasa lignocelulósica: algunas experiencias de investigación en Colombia, 1st ed. Universidad Jorge Tadeo Lozano, Bogotá, Colombia (2015): pp. 117–144. ISBN: 978-958-725-152-4

## Acknowledgements.

Nothing anyone would have said to me could have prepared me for the amazing experience that was the PhD. Every day I am grateful for all the memories, good and bad, that I collected during these years. This great adventure would have never been written if Jan Maarten van Dijl would have not accepted to meet me over skype and later host me for an internship five years ago. So first, I thank Jan Maarten for allowing me to pursue my dream career and for believing in my potential at every step of the way. Thank you for the great scientific conversations during working hours but also for all the great meetings over beer. And of course, this PhD would have also not been possible without the support of Uwe Völker. Thank you so much Uwe for the great scientific support, I must say that I hold a great admiration for your capacity to connect ideas and keep developing science. To you both, I thank you for all the professional and personal teachings.

I would like to express my gratitude to the members of my thesis assessment committee Prof. Friedrich Götz, Prof. Sven Hammerschmidt, Prof. Matthias Heinemann, and Prof. Oscar P. Kuipers. I thank you for taking the time to read and approve my thesis.

Of course, every experience was built conjunctively with all the people surrounding me. For convenience, I would like to thank you all in a chronological order.

People do not tend to think of Greifswald as a great city, but I must say that that little town in the north of Germany will always be my second home and I am really grateful for the more than two years that I lived there. First, I want to thank all my colleagues from the Functional Genomics Department in Greifswald, which not only helped me to get the results of the publications enclosed in this thesis but with whom I also shared great moments in the office. Thank you Alex, Anna, Dhople, Elke, Eric, Frank, Georg, Henrike, Hermann, Kristen, Lars, Leif, Manu,

Marc, Maren, Petra, Praveen, Rasmita, Sascha, Sabine, Sophie, Stefan, Stephan, Tanja, Ulrike M., and Ulrike L. I also would like to thank my cooperators at the institute of Bioinformatics Ann-Kristin and Lars Kaderali for their support in the data analysis. Especially, I want to thank Kristin Surmann, for all the daily discussions, for always being available and for giving me a lot of perspective on the way of doing my PhD. I very much appreciate all the time with you, in and out of the lab.

Science was not only done inside the lab, but I had the luck to belong to the Research Training Group (GRK) 1870, which promoted activities for active discussion and growth in Science. I would like to thank all my colleagues, in particular Anica, Claudia, Franzi, Johannes, Juliane, Karolin, Maria, Patricia, and Tom. In this context, I would also like to thank all the professors from the GRK, but especially Sven Hammerschmidt. I also want to thank Sylvia Kohler, Katherine Stark, and Imme Burkart-Jürgens for all their support with the administrative tasks.

I feel very lucky that I was one of the sandwich PhDs that were part of the training group. I shared this international experience with Jolien and Solomon, and without their company along the way, the PhD would have not been the same. Jolien, thank you so much for all your emotional support and for all the nice talks. Solomon, I very much enjoyed working side by side with you. Thank you, for all the scientific discussions and all the nice time outside the lab.

In 2016 and after all the hard work in Greifswald, I moved to another northern city: Groningen. There, I did the data analysis and all the writing. I must say that this was a great change that challenged me in many new ways. Thank you MolBac for welcoming me halfway into my PhD, and for all the fun that we had together. First, I would like to recognize my editor: Giorgio, thank you so much for checking the text from this thesis, and for supporting me in the last years

regardless of all the ups and downs. To my officemates: Andrea, Suruchi, and Tim. Thank you for the countless hours of support and laughs, we really made up the coolest office. To my friends, Bimal, Elisa, Mafalda, Marina, Marines, and Margarita. I am grateful for every day that I had you in the lab, but even more for all the time we spent outside it. Of course, it would have not been the same without all the team, so thank you also to all the other members of the lab: Andrea A., Dennis, Eleni, Francis, Francisco, Gaby, Girbe, Harita, Hermie, Jolanda, Lisanne, Lise, Lu, Marjolein, Min, Paola, Rense, Rita, Rocio, Sjouke, Stefano, Usma, Xin, and Yare. Thank you for contributing to the great environment in the lab.

I must say that I had great times in both research groups and that they were decisive for the culmination of this thesis. However, on the way, I have also shared many moments with my non-academic friends. First, I deeply want to thank my great friends from Greifswald: Alejo, Ela, Daniel, Fabio, Fibi, Leo, Maike, Maria I., and Maria P. My life there would have never been the same without your daily presence. Thank you for all the laughs, the dancing, the food, the chocolate, the wine, and for just been there. I also want to thank Laura N., Mila, Ruby, Yadwi, and the Alemañoles for the nice time shared together. From Groningen I would like to thank Anika, Amritapurna, Bart, Charlotte, Linda, Siebe, and Silavadin, for enriching my life in this city, and making it a whole experience.

Por supuesto, nunca habría llegado tan lejos de no ser por el apoyo constante de aquellas personas que están en Colombia. Entre más pasa el tiempo, más me doy cuenta de todos los detalles que todos ustedes imprimieron en mí. Querida familia, desde la distancia no ha pasado un día en el que no los piense. Gracias papá por inculcarme un profundo amor por la ciencia y el saber, por mostrarme que hacer un trabajo a medias nunca será un trabajo bien hecho y que hay que ser *siempre excelente*. Gracias mamá por apoyarme emocionalmente y por todos tus detalles de amor. No conozco mujer más berraca que tú, y de tí aprendí a guerrear y a nunca darme por vencida. Julián, la admiración que tengo por ti es más grande



de la que puedo expresar con palabras, los retos que tu has tenido que enfrentar han sido mucho mayores de los que yo jamás he tenido. Por llegar hasta donde has llegado, y después de todo lo caminado, no me queda más que decirte que eres una gran fuente de inspiración. Juan Diego, gracias por ampliar mi perspectiva de la vida, creo que haber crecido contigo a mi lado me hizo una persona más humilde y comprensiva, gracias. Tía Marlén, gracias por todos tus mensajes de apoyo desde Colombia, siempre sentí tus oraciones presentes en mi vida. También quiero agradecer a todos mis amigos en Colombia por haberme apoyado a dar este salto, su apoyo fue indispensable.

Men inte bara min biologiska familj har hjälpt mig från avståndet. Jag är den lyckligaste tjejen eftersom jag här en europeisk familj. Tack så mycket pappa Kenneth, mamma Annelie, Linda och mormor för att välkomna mig i er familj. Ni är allt i mitt hjärta. Min svenska räcker inte för att berätta hur mycket jag älskar er alla. Tack för att du öppnar ditt hem för mig varje år. Jag kan inte vänta tills vi kan spendera mer tid tillsammans. Bland alla de fantastiska människor jag har nämnt i detta erkännande, förtjänar ingen större tack än Patric Holmvall. Patric, tusen tusen tusen tack så mycket för ditt stöd. Jag är glad att vi tog risken att fortsätta detta galna äventyr. Ditt stöd och förståelse utan gränser hållde mig levande även i de svåraste stunderna. Tack för att du följer all min galskap och för att visa mig vad ren kärlek är.

Lastly, and as weird as this might sound, I deeply would like to thank all the amazing musicians that have made the music that constitutes the amazing soundtrack of this adventure. They are way too many to mention, and too far to even ever read this. From the bottom of my soul, thank you for every note that you wrote reminding me of how joyful life is.

Muchas gracias... Vielen Dank... Hartelijk Dank... Tack så mycket...

Laura Marcela Palma Medina, 2019



